Studies in *(S)*-Lysine Biosynthesis via the Diaminopimelate Pathway

A thesis submitted in partial fulfilment
of the requirements for the degree of
Doctor of Philosophy
in Chemistry
at the University of Canterbury,
Christchurch, New Zealand
by

Carolyn V. Coulter B.Sc. (Hons)

December 1997

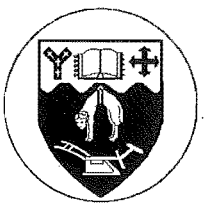

Contents

Acknowledgements

I would like to acknowledge:

Dr A.J. Pratt for his supervision during this research.

Dr A.D. Abell, Dr O.J. Curnow, Dr J.A. Gerrard, Professor M.P. Hartshorn, and Professor D.A. House for their assistance with the chemistry in this research.

Dr H.K. Mahanty and the members of his research group for their expertise in molecular biology.

The University of Canterbury Scholarships for funding.

My fellow students, especially J. Dyer, D. Hoult, R. Lill, S. Meade, and P. Rendle.

C. Brown and D. Hoult for proof-reading this thesis.

Abstract

The enzymes of the diaminopimelate (dap) pathway, which is responsible for the biosynthesis of *(S)*-lysine in plants and micro-organisms, are of interest as potential targets for herbicide and antibacterial research. This thesis has investigated two key enzymes of this pathway: dihydrodipicolinate synthase (DHDPS) and dihydrodipicolinate reductase (DHDPR). DHDPS, the first enzyme committed specifically to *(S)*-lysine biosynthesis, catalyses the condensation of pyruvate and *(S)*-aspartate β-semialdehyde (*(S)*-ASA) to form an unstable heterocycle. Dihydrodipicolinate reductase (DHDPR), the next enzyme in the pathway, mediates the reduction of this product to tetrahydro-dipicolinate.

A coupled assay measuring the activities of DHDPS and DHDPR was optimised. Both DHDPS and DHDPR were purified from *E. coli* strains that had been genetically engineered to overproduce these enzymes. This assay monitored the utilisation of NADPH, at 340 nm, by DHDPR.

Kinetic studies were performed on DHDPS, giving K_m and V_{max} parameters for both substrates, *(S)*-aspartate β-semialdehyde (synthesised from *(S)*-allylglycine) and pyruvate. It was shown that *(S)*-aspartate β-semialdehyde did not inhibit the DHDPS enzyme even at high substrate concentrations, although *(S)*-lysine was found to be a feedback inhibitor, acting in a reversible uncompetitive manner with respect to both substrates, thus, binding at an allosteric site.

Kinetic studies were performed on DHDPR, giving K_m and V_{max} values for the substrate. DHDPR was shown to utilise either NADPH or NADH as a redox coenzyme. Of these NADPH is generally used in the assay due to its greater chemical stability, even though the K_m for NADH is lower.

Structural and enzymatic inhibition studies on DHDPS revealed that *(S)*-aspartate β-semialdehyde exists predominantly as a linear hydrate in solution at physiological pH. Inhibition studies on DHDPS showed that the cyclic molecule homoserine lactone and related compounds, such as 2-aminocyclopentanone, which mimic a possible cyclic form of *(S)*-aspartate β-semialdehyde are allosteric site inhibitors acting in a reversible noncompetitive manner. Analogues of the hydrate form of *(S)*-aspartate β-semialdehyde such as the amino acids *(R)*-cysteine sulfinic acid, and *(S)*-glutamic acid inhibited in a reversible uncompetitive manner. *(S)*-Aspartic acid also inhibited DHDPS, but was a reversible mixed type inhibitor.

NMR studies were used to investigate the structure of the product of the DHDPS catalysed reaction, and the data was consistent with it being 4-hydroxy-2,3,4,5-tetrahydrodipicolinic acid. Various mimics of this compound were tested as possible product inhibitors of DHDPS, and as possible substrate inhibitors of DHDPR. The most potent inhibitors of DHDPR evaluated were dipicolinic acid and isophthalic acid which both inhibited in a reversible competitive manner. Tetrahydroisophthalic acid analogues were tested for inhibition of DHDPS and DHDPR. Δ^3-Tetrahydroisophthalic acid showed moderate inhibition of both enzymes, while Δ^2-tetrahydroisophthalic acid showed only very slight inhibition.

Abbreviations

$[\alpha]_D^t$	specific rotation at t °C as measured at the sodium D line (589.3 nm).
ΔA_{340}	change in absorbance at 340 nm
a	axial
amp R	ampicillin resistance gene
Ar	aryl
(S)-ASA	*(S)*-aspartate β-semialdehyde
ATP	adenosine 5'-triphosphate
bd	broad doublet
Bis-Tris	Bis(2-hydroxyethyl)iminotris(hydroxymethyl)methane
bp	base pairs
bp	boiling point
bs	broad singlet
BSA	bovine serum albumin
c	concentration in g/100 ml (ORD spectra)
°C	degrees Celsius
CI	chemical ionisation
cm	centimetre
CoA	coenzyme A
COSY	proton proton coupling spectroscopy
δ	chemical shift in parts per million downfield from tetramethylsilane.
d	doublet
Da	Daltons
dap	diaminopimelate
dd	doublet of doublets
DEAE	diethylaminoethyl
DHDPA	dihydrodipicolinate
DHDPR	dihydrodipicolinate reductase
DHDPS	dihydrodipicolinate synthase
dH_2O	distilled/de-ionised water
dt	doublet of triplets
DMF	dimethylformamide
DNA	deoxyribonucleic acid
ε	extinction coefficient
e	equatorial
E. coli	*Escherichia coli*
Ed.	editor
Eds	editors

ed.	edition
EDTA	ethylenediaminetetraacetic acid
EI	electron ionisation
ESMS	electrospray mass spectrometry
FAB	fast atom bombardment
FMN	flavin mononucleotide
FT	Fourier transform
g	gram
G^+	Gram positive
G^-	Gram negative
gly	glycerol
Hepes	*N*-2-hydroxyethylpiperazine-*N'*-2-ethane sulfonic acid
HMBC	heteronuclear mutibond coupling spectroscopy
HSQC	heteronuclear single quantum coherence spectroscopy
HRMS	high resolution mass spectrometry
hr	hour
Hz	Hertz
I	inhibitor
[I]	inhibitor concentration
IC_{50}	inhibitor concentration giving 50% inhibition
IR	infra-red
J	coupling constant
kb	kilobase
kDa	kiloDalton
K_i	inhibition constant
K_m	Michaelis-Menten constant
kV	kilovolts
l	litre
LB	Luria-Bertani
µg	microgram
µl	microlitre
M	moles per litre ($mol \cdot l^{-1}$)
m	multiplet (NMR)
m	medium (IR)
m-	*meta-*
Mes	2-(*N*-Morpholino)ethanesulfonic acid
min	minute
mg	milligram
MHz	megaHertz
ml	millilitre

mm	millimetre
Mops	3-(*N*-Morpholino)propanesulfonic acid
M_r	relative molecular weight
mp	melting point
MS	mass spectrum
m/z	mass to charge ratio
NAD^+	nicotinamide adenine dinucleotide
NADH	nicotinamide adenine dinucleotide, reduced form
$NADP^+$	nicotinamide adenine dinucleotide phosphate
NADPH	nicotinamide adenine dinucleotide phosphate, reduced form
nm	nanometers
NMR	nuclear magnetic resonance
nOe	nuclear Overhauser effect
NOBA	nitrobenzylalcohol
o-	*ortho-*
ORD	optical rotation
Ori	origin of replication
p-	*para-*
PAGE	polyacrylamide gel electrophoresis
PCR	polymerised chain reation
ppm	parts per million
Q	quaternary ammonium
q	quartet
qu	quintet
R_f	retention factor
RNase	ribonuclease
rpm	revolutions per minute
R.T.	room temperature
S	substrate
[S]	substrate concentration
s	singlet (NMR)
s	strong (IR)
SDS	sodium dodecyl sulfate
sp.	species
spp.	species (plural)
suc	succinyl
t	triplet
TEMED	*N,N,N',N'*-tetramethylethylenediamine
tert	tertiary
tet R	tetracycline resistance gene

TFA	trifluoroacetic acid
THF	tetrahydrofuran
thio	thioglycerol
TLC	thin layer chromatography
TMS	tetramethylsilane
Tris	tris(hydroxymethyl)methylamine
U	unit of enzyme activity ($\mu mol \cdot ml^{-1}s^{-1}$)
UV	ultra-violet
υ_{max}	infra-red maximum
V_{max}	maximum rate
w	weak
wrt	with respect to
w/v	unit weight (g) per volume (100 ml)
*	denotes a kinetic reading that has not been included in the K_m and V_{max} calculations.

Introduction

Introduction

Background

Herbicide and antibacterial research focuses on inhibiting the growth of specific plants and bacteria. The advent of herbicides has greatly increased crop production, while antibacterial agents have revolutionised the treatment of bacterial infections. However, resistance to herbicides and antibacterial agents is becoming a crisis.[1,2] Plants that are resistant to traditional herbicides are now emerging and posing a threat to crop production. There are also new strains of bacteria that are resistant to many of the antibacterial agents currently in use. Thus, there is an ongoing challenge to produce new herbicides and antibacterial agents, preferably with novel modes of action, to overcome these problems of resistance.

Herbicides act by inhibiting the growth of plants. It is important that they selectively inhibit plants and that they are environmentally safe. Many herbicides act by inhibiting amino acid biosynthesis. For example chlorsulfuron (1)[3] blocks the synthesis of branched chain amino acids, while aminotriazole (2)[3] blocks histidine synthesis, phosphinothricin (3)[3] blocks glutamine synthesis, and glyphosate (4)[2,3] blocks the synthesis of aromatic amino acids, see figure I-1. Herbicide resistance may be caused by the uptake of the herbicide becoming impaired, the plant acquiring the ability to detoxify the herbicide, the target enzyme becoming insensitive to the herbicide by mutation, or by the plant adapting to overproduce the target enzymes.[2] New herbicides are required to overcome these problems of resistance.

Figure I-1: Herbicides that block amino acid biosynthesis

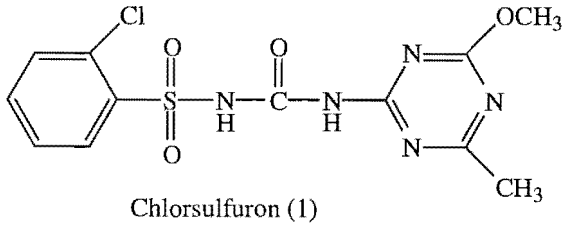

Chlorsulfuron (1)
Inhibits acetolactate synthetase.

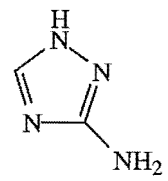

Aminotriazole (2)
Inhibits imidazole glycerol phosphate dehydratase.

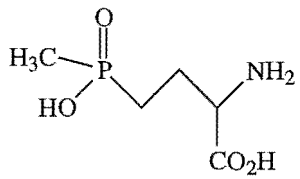

Phosphinothricin (3)
Inhibits glutamine synthetase.

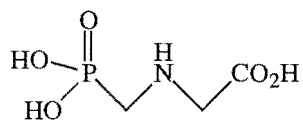

Glyphosate (4)
Inhibits 5-enolpyruvyl shikimate-3-phosphoric acid synthase.

Micro-organisms are also continually acquiring resistance to antibacterial agents. Thus, an ever increasing range of antibacterial agents is required. Not only is there the need to modify the drugs currently used, but also to find new drugs that have different modes of action. Antimicrobial agents are known to act against a number of targets.[4] Some act to inhibit bacterial cell wall synthesis, rendering growing bacteria osmotically sensitive. This class includes the classical β-lactam antibiotics—penicillins and cephalosporins, for example Penicillin G (5), see figure I-2. A second class of drugs affect the cell membrane, for example by disrupting the membrane. Amphotericin acts in this way. Two other classes of action are the inhibition of protein and nucleic acid synthesis. Common protein synthesis inhibitors include the tetracyclines and chloramphenicol (6), while common nucleic acid synthesis inhibitors include the sulfonamides, for example sulfanilamide (7), and the rifamycins.

Figure I-2: Examples of antimicrobial agents

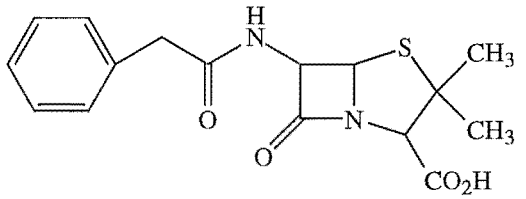

Penicillin G (5)

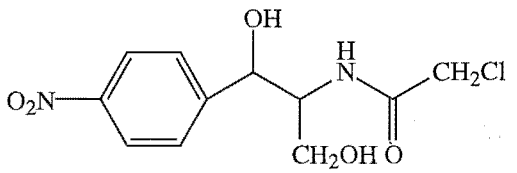

Chloramphenicol (6)

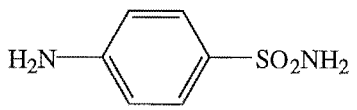

Sulfanilamide (7)

Mechanisms of bacterial drug resistance often involve the genetic spread of resistance via plasmids.[5] Modes of resistance include: alteration of the drug target; modification of metabolism of the drug leading to its detoxification; altered permeation and/or transport of the drug; the formation of a metabolic bypass; or overproduction of antagonistic metabolites and/or target enzymes.

(S)-Lysine and the aspartate family of amino acids

(S)-Lysine is part of the aspartate family of amino acids, which also includes *(S)*-methionine, *(S)*-threonine, and *(S)*-isoleucine. The aspartate family of amino acids are interesting subjects for research as their synthesis occurs via complex biochemical pathways which are incompletely understood. Many of the enzymes, their chemical substrates and products, as well as their regulation, are ill-characterised. All four aspartate family amino acids are essential (that is while they are required by animals their biosynthesis is carried out only by plants and micro-organisms) and their biosynthesis is of interest for two reasons. Firstly, inhibitors of these amino acids have the potential to be herbicides and/or antibacterial agents. Secondly, these essential amino acids are nutritionally important in foods.[6] By investigating the enzymology of their biosynthesis there is the potential to develop crops enriched in these nutritionally limiting amino acids. This is especially important for *(S)*-lysine which is a nutritionally limiting amino acid in many cereal crops.[7,8]

(S)-Lysine biosynthesis as a target for a new class of herbicides and/or antibacterial agents[9]

Since *(S)*-lysine is an essential amino acid, inhibitors of *(S)*-lysine biosynthesis would be selectively toxic to plant and micro-organisms but not to animals. This would create a new class of herbicides and/or antibacterial agents with a novel mode of action. As the lysine biosynthetic pathway in plants is analogous to that of bacteria, but not to that of fungi (fungi use a different pathway for the biosynthesis of *(S)*-lysine),[10] bacterial amino acid biosynthetic pathway can be used as a model to find inhibitors which could act as herbicides. While there are already herbicides that act by inhibiting amino acid biosynthesis at the enzymatic level there are no such antibacterial agents. The biosynthesis of *(S)*-lysine is an appropriate field for the search of herbicides and/or antibacterial agents since, as yet, no potent inhibitors have been found. Thus, the field of research is unbiased and further the biosynthetic genes have been well mapped in *Escherichia coli (E. coli)*, enabling a means of isolation of these enzymes.[11]

(S)-Lysine biosynthesis

The aspartate family of amino acids (*(S)*-methionine, *(S)*-threonine, *(S)*-isoleucine, and *(S)*-lysine) are synthesised from *(S)*-aspartate, itself derived from oxaloacetate (8) from the citric acid cycle, see figure I-3. Initially, *(S)*-aspartate (9) is phosphorylated by aspartokinase to give *(S)*-β-aspartyl phosphate (10), before being reduced to *(S)*-aspartate β-semialdehyde (11) by aspartate β-semialdehyde dehydrogenase. This is the branch point for the biosynthesis of the four aspartate derived amino acids, where *(S)*-aspartate β-semialdehyde (11) either enters the diamiopimelate (dap) pathway to produce *(S)*-lysine (12), or is reduced again to give *(S)*-homoserine (13), by homoserine dehydrogenase. *(S)*-Homoserine (13) is then used to produce *(S)*-methionine (14), *(S)*-threonine (15),

and *(S)*-isoleucine (16). Aspartokinase and homoserine dehydrogenase are the points of regulation in this pathway. In *E. coli* there are three isozymes of aspartokinase and two isozymes of homoserine dehydrogenase (the homoserine dehydrogenase activities being carried on the aspartokinase enzymes). *(S)*-Threonine (15) and *(S)*-isoleucine (16) regulate the expression of the aspartokinase-homoserine dehydrogenase I, and *(S)*-threonine (15) inhibits both activites. *(S)*-Methionine (14) represses the synthesis of aspartokinase-homoserine dehydrogenase II, while *(S)*-lysine (12) inhibits the activity and represses the synthesis of aspartokinase III.[12]

Figure I-3: Biosynthesis of the aspartate (9) family of amino acids

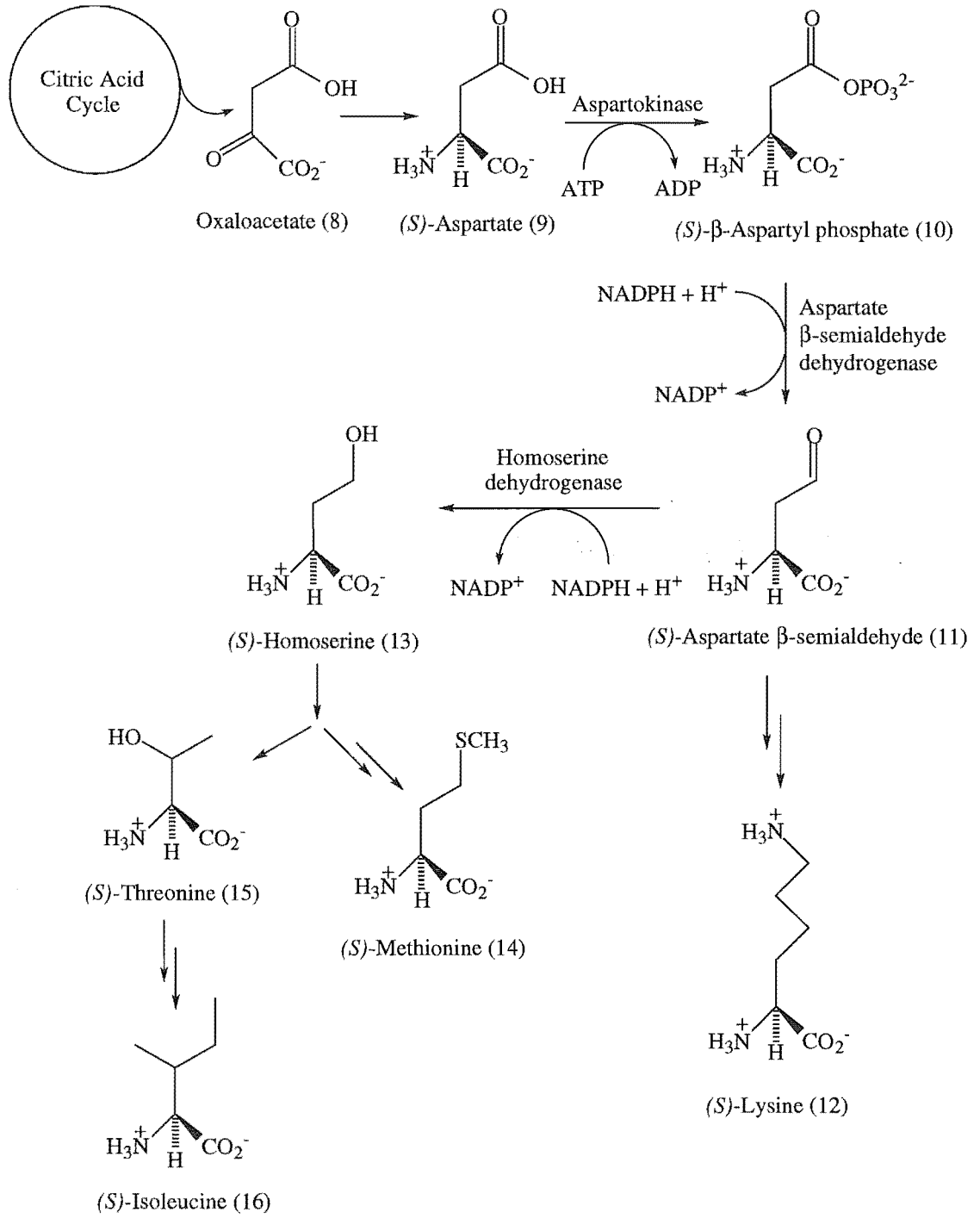

(*S*)-Lysine biosynthesis via the diaminopimelate pathway

(S)-Lysine (12) is synthesised via the diaminopimelate (dap) pathway in bacteria and plants, but via the α-aminoadipate pathway in fungi.[13] The genes of the enzymes of the diaminopimelate pathway have been well mapped in *E. coli*,[11] as have many other amino acid genes, providing a basis for the study of these enzymes.[14,15]

This research is limited to the biosynthetic pathway of lysine (12) in bacteria and plants via the diaminopimelate pathway, see figure I-4. The first committed step in the diaminopimelate pathway is the condensation of *(S)*-aspartate β-semialdehyde (*(S)*-ASA) (11) with pyruvate (17) to form an unstable heterocyclic molecule, thought to be dihydrodipicolinate (DHDPA) (18). Dihydrodipicolinate synthase (DHDPS)[16] is the enzyme that catalyses this reaction, and, as it undergoes feedback inhibition by the final product *(S)*-lysine (12), it is a key point in the regulation of *(S)*-lysine biosynthesis. DHDPS has been isolated from *E. coli*,[16,17,18] as well as other bacteria[19,20,21,22,23] and plant[24,25,26,27,28] sources. Dihydrodipicolinate (18) is then reduced to tetrahydro-dipicolinate (19), by dihydrodipicolinate reductase (DHDPR),[29] with concomitant oxidation of NAD(P)H. Feedback regulation by *(S)*-lysine (12) has not been observed for this enzyme. DHDPR has been isolated from *E. coli*,[29,30] other bacteria,[31,32] and also a plant source.[33]

The cyclic molecule, tetrahydrodipicolinate (19), is then ring opened via a succinylation to form an α-keto acid, succinyl-ε-keto-α-aminopimelate (20), in a reaction catalysed by tetrahydrodipicolinate succinylase.[34] Following this, succinyl-ε-keto-α-aminopimelate aminotransferase[35] performs a transamination to form succinyl diaminopimelate (21), which is then desuccinylated by succinyl diaminopimelate desuccinylase[36] to form *(S,S)*-diaminopimelate (22). Diaminopimelate epimerase[37] catalyses the epimerisation of *(S,S)*-diaminopimelate (22) to *meso*-diaminopimelate (23), which is then decarboxylated to yield *(S)*-lysine (12) by the enzyme, diaminopimelate decarboxylase.[38]

It has been observed that some bacteria use acetate ($-COCH_3$), rather than succinate ($-CO_2CH_2CO_2H$), in the ring opening step of the diaminopimelate pathway, while others may use both. A direct shunt from tetrahydrodipicolinate (19) to *meso*-diaminopimelate (23) has also been observed.[19] However, the extent to which this contributes to anabolism and/or catabolism is unclear. *E. coli* has been observed only to use succinate in the diaminopimelate pathway.

Many of the *(S)*-lysine (12) biosynthetic genes, which encode for the various enzymes, are regulated in their expression by the total *(S)*-lysine (12) pool. For example *dap B, dap D, dap E,* and *lys A* are regulated in this fashion,[39] however *dap A* is not. At

the enzymatic level only DHDPS, and the earlier enzyme aspartokinase, are feedback regulated by *(S)*-lysine (12).[40]

Figure I-4: The diaminopimelate pathway

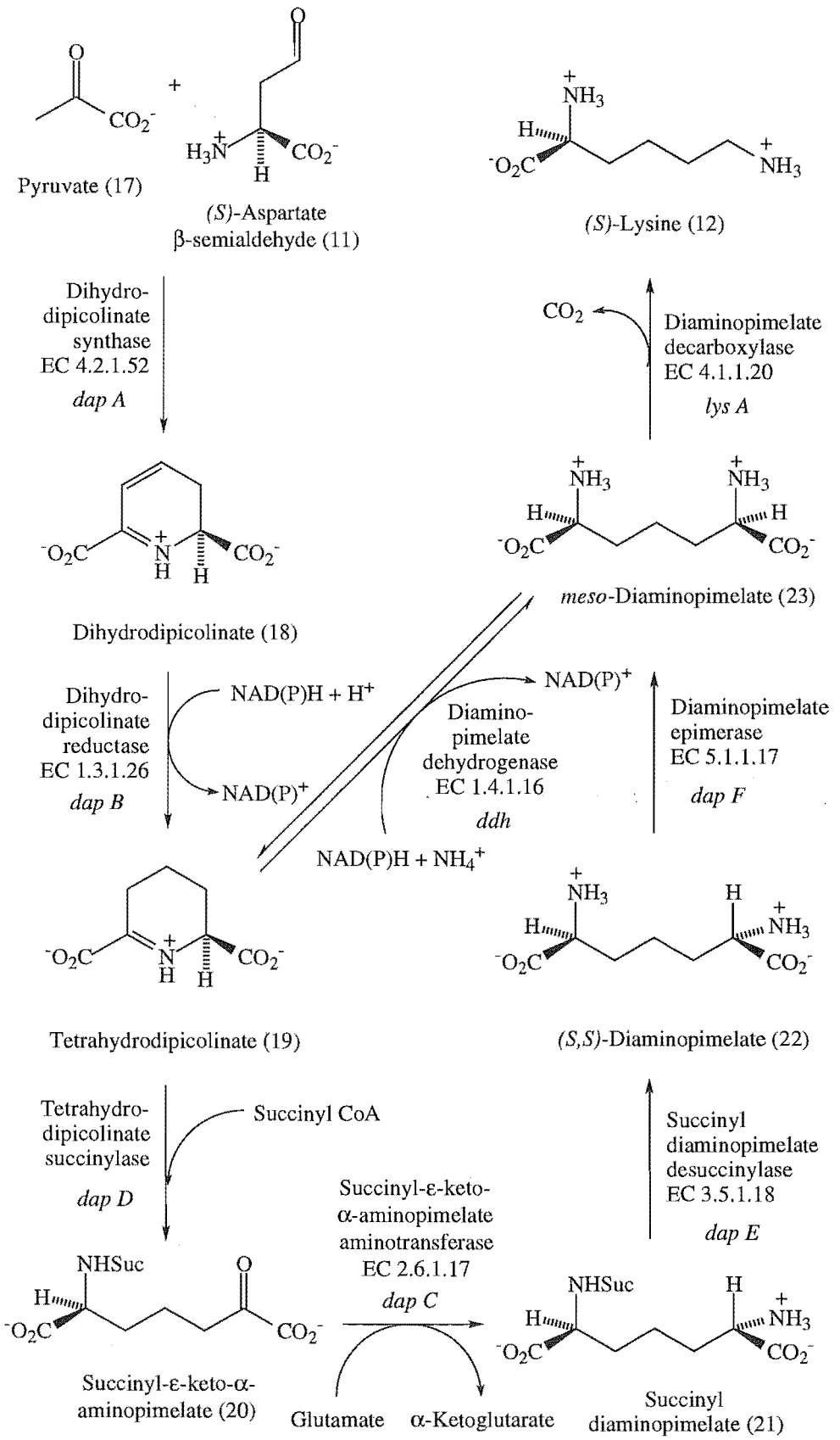

Although the diaminopimelate pathway generally leads to the production of *(S)*-lysine (12), it is also important as a source of *meso*-diaminopimelate (23), and as a source of dipicolinate (from dihydrodipicolinate (18)) in some organisms. *meso*-Diaminopimelate (23) is used in the peptidoglycan cell wall of Gram negative (G^-) bacteria, while Gram positive (G^+) bacteria use *(S)*-lysine (12).[41] Either *meso*-diaminopimelate (23) or *(S)*-lysine (12) is utilised in forming the cross links in the peptidoglycan, giving the cell wall its strength. Calcium dipicolinate is used in bacteria that produce endospores,[42,43] giving the spore cortex its heat resistance, while *meso*-diaminopimelate (23) is also present in the spores.

By blocking the *(S)*-lysine (12) biosynthetic pathway there are potentially three ways of producing antibacterial agents: by a lack of *(S)*-lysine (12) causing nutritional deficiency and leaving G^+ bacteria with an inferior cell wall leading to susceptibility to osmotic shock; by lack of *meso*-diaminopimelate (23) leaving G^- bacteria with an inferior cell wall leading to susceptibility to osmotic shock; and in certain organisms by lack of dipicolinate preventing spore formation.

Targets for inhibition[44]

In the search for enzyme inhibitors of *(S)*-lysine (12) biosynthesis we chose to concentrate our efforts on the first two enzymes specific to *(S)*-lysine (12) biosynthesis, that is DHDPS and the succeeding enzyme of the diaminopimelate pathway DHDPR. A study of DHDPS and DHDPR requires a rigorous examination of the chemical nature of the substrates and products, as well as the enzymes themselves. Inhibitors of enzymes of the diaminopimelate pathway are also being investigated by other groups. For example inhibitors of diaminopimelate epimerase,[9,45,46,47,48] diaminopimelate decarboxylase,[9,45,49] succinyl-ε-keto-α-aminopimelate aminotransferase,[50] and diaminopimelate dehydrogenase[45,47] are being studied.

Ongoing research on DHDPS

Genetics and enzymology

The *dap A* locus, which encodes for DHDPS, has been mapped to 53 minutes on the *E. coli* chromosome[11] and subsequently cloned[51] and sequenced.[39] It encodes a 292 amino acid polypeptide of M_r 31 372. The *dap A* gene has also been cloned from other bacteria and plants, for example *Corynebacterium glutamicum,*[52,53] *Bacillus subtilis,*[54] *Brevibacterium lactofermentum,*[55] poplar[56] maize,[57] soybean,[58] wheat,[59] and *Nicotiana sylvestris* (tobacco).[60] Unlike some of the subsequent enzymes in the pathway the expression of *E. coli* DHDPS is constitutive,[40] rather than inducible. This means the expression of *E. coli* DHDPS is not regulated by the total *(S)*-lysine (12) pool.

DHDPS has been isolated and partially purified from a variety of bacterial[16,17,18,19,20,21,22,23] and plant sources.[24,25,26,27,28] During the course of these studies *E. coli* DHDPS was crystallised,[61] as well as being studied by electrospray mass spectrometry.[18] The *E. coli* enzyme is a homotetramer with a M_r of 134 000 as determined by gel filtration.[62] The published *E. coli dap A* sequence predicts a polypeptide of 292 amino acids with a M_r of 31 372.[63] The electrospray mass spectrometry gives a M_r of 31 346;[18] this was used to identify an error in the amino acid sequence predicted from the gene sequence. Cloned wheat and maize DHDPS also exist as homotetramers with the M_r of the monomers being 35 776[26] and 35 854[64] respectively, while pea DHDPS is a trimer.[28] A high level of homology at the amino acid level has been established between the DHDPS obtained from different sources,[65] for example 30% identity between wheat (*Triticum aestvum*) and *E. coli* enzymes,[59] 33% identity between *Brevibacterium lactofermentum* and *E. coli*,[55] and 87% identity between wheat and maize genes.[57,59]

The chemical nature of the substrate (S)-*aspartate β-semialdehyde*

Although the exact nature of *(S)*-aspartate β-semialdehyde (11) has not been determined in the literature it is always assumed to exist as the aldehyde, as suggested by the name.[65] Preliminary work in this area has suggested that *(S)*-aspartate β-semi-aldehyde (11) may not exist as the aldehyde (11a) but rather as a hydrate (11b) or even as a cyclic lactol (11c),[66] see figure I-5.

Figure I-5: (S)-*Aspartate β-semialdehyde (11), possible structures*

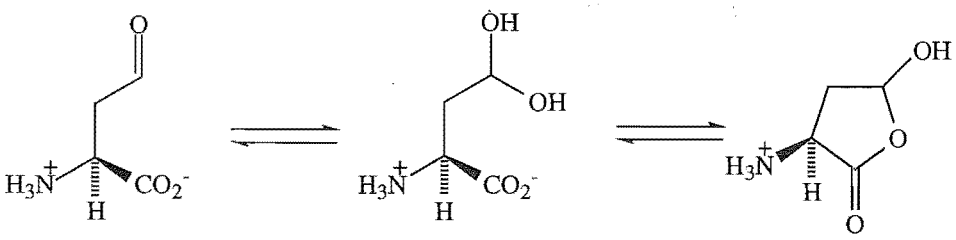

Aldehyde (11a) Hydrate (11b) Cyclic lactol (11c)

The chemical nature of the product dihydrodipicolinate

The literature usually reports the product of the DHDPS catalysed reaction as a 2,3-dihydropyridine.[65] However, as well as 2,3-dihydrodipicolinate (18) two other structures have been hypothesised for the product, namely 2,5-dihydrodipicolinate (27) and 4-hydroxy-2,3,4,5-tetrahydrodipicolinate (28).[62] In theory, there are five isomeric dihydropyridines (1,2-, 1,4-, 2,3-, 3,4-, 2,5-)[67] depending on the position of the double bonds in relation to the heteroatom nitrogen. Altogether this gives six different structures as possible products of the DHDPS catalysed reaction, see figure I-6.

Figure I-6: Possible products of the DHDPS catalysed reaction

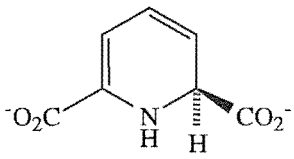

1,2-Dihydrodipicolinate (24)

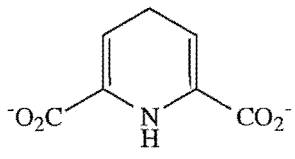

1,4-Dihydrodipicolinate (25)

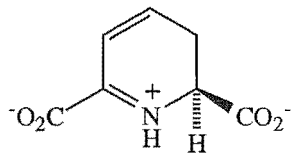

2,3-Dihydrodipicolinate (18)

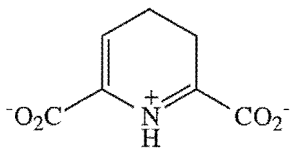

3,4-Dihydrodipicolinate (26)

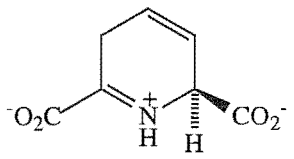

2,5-Dihydrodipicolinate (27)

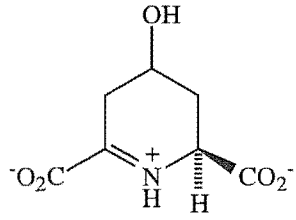

4-Hydroxy-2,3,4,5-tetrahydrodipicolinate (28)

Mechanism of the DHDPS catalysed reaction

The first step in the catalysis of *(S)*-aspartate β-semialdehyde (11) and pyruvate (17), to give dihydrodipicolinate (18), is the binding of pyruvate (17) with the loss of water, followed by the binding and reaction of *(S)*-aspartate β-semialdehyde (11). The pyruvate (17) binds to form a Schiff base with the ε-amino group of the active site lysine 161.[17] Lysine 161 is conserved in all known DHDPS sequences and the Schiff base can be trapped with sodium borohydride, see figure I-7.

Figure I-7: Sodium borohydride trapping of the Schiff base

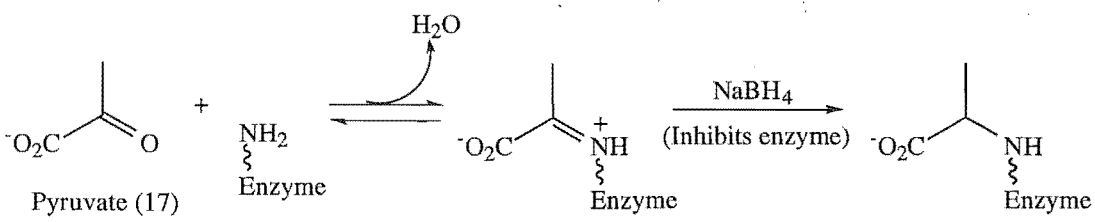

At the onset of this work little was known about the reaction mechanism of DHDPS, other than the initial binding of pyruvate (17) to form a Schiff base. How the molecule cyclises and generates the pyridine derivative was unknown, and this was also complicated by the lack of knowledge on the structure of the substrate *(S)*-aspartate β-semialdehyde (11), see figure I-8. Work since 1995, in parallel with the results reported in this thesis, using X-ray crystallography,[61] electrospray mass spectometry,[18] NMR spectroscopy,[68] and kinetic studies,[69] has greatly increased our knowledge of the mechanism of DHDPS.

Figure I-8: Reaction catalysed by DHDPS, as hypothesised at the onset of this work.

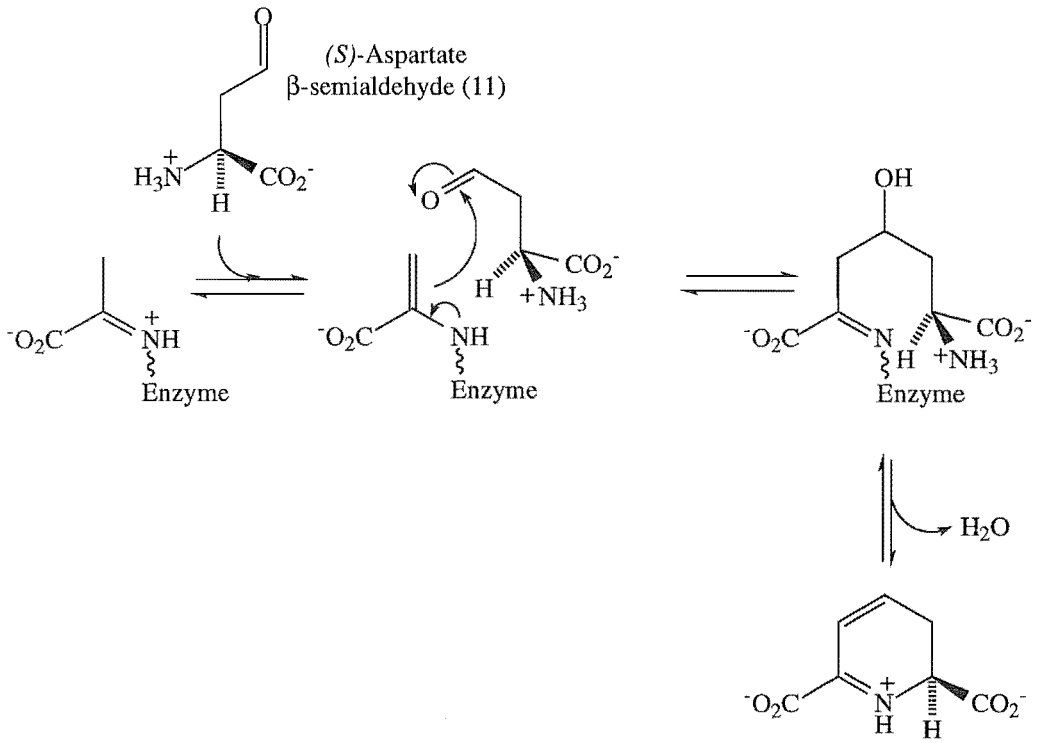

Dihydrodipicolinate (18)

Kinetic studies on DHDPS, including inhibition studies

A number of kinetic studies on DHDPS have been reported. The enzyme displays high specificity for both substrates with Michaelis-Menten constants (K_m values) ranging between 0.4 and 3.1 mM for *(S)*-aspartate β-semialdehyde (11), and between 0.5 and 11.8 mM for pyruvate (17).[65]

(i) Pyruvate analogues

Bromopyruvate (29)[18,21] and ethyl bromopyruvate (30)[28] irreversibly inactivate DHDPS, presumably by alkylation, and inhibition is competitive with respect to pyruvate (17), but noncompetitive with respect to *(S)*-aspartate β-semialdehyde (11), see figure I-9 and I-10. In a review on the diaminopimelate pathway by Cox, published in 1996,[65] it was stated that analogues of pyruvate such as phosphoenolpyruvate, phenylpyruvate, α-ketobutyrate, α-ketoglutarate, oxaloacetate, and fluoropyruvate were not recognised by DHDPS.

Figure I-9: Pyruvate analogues

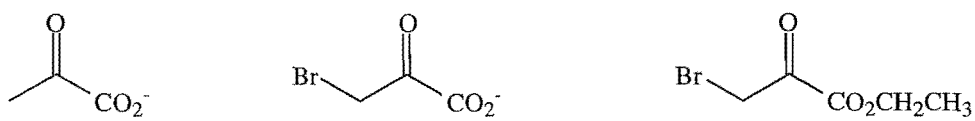

Pyruvate (17) Bromopyruvate (29) Ethyl bromopyruvate (30)

Figure I-10: Mode of inactivation by bromopyruvate (29)

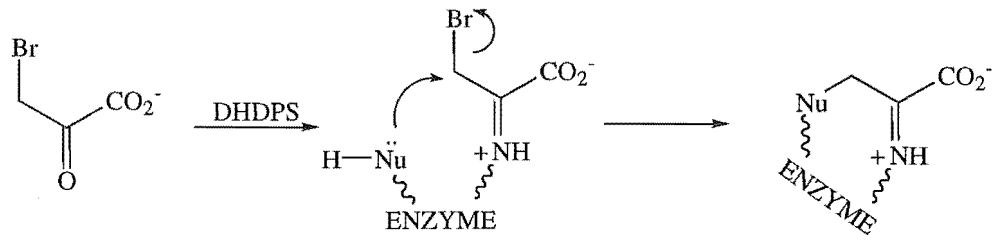

Bromopyruvate (29)

Adjacent nucleophile attacks the Schiff base releasing Br^-.

DHDPS is irreversibly inactivated.

(ii) *(S)*-aspartate β-semialdehyde analogues

Five membered ring heterocycles, based on a possible cyclic form of the substrate *(S)*-aspartate β-semialdehyde (11c), have been found to show some inhibition.[66] In preliminary studies, the best inhibitor of this type was found to be *(S)*-homoserine lactone (31) (*(S)*-2-amino-4-butyrolactone), see figure I-11. In the review on the diamino-pimelate pathway by Cox, published in 1996,[65] it was reported that some linear *(S)*-aspartate β-semialdehyde analogues were not recognised by DHDPS. Those tested included *(S)*-glutamate semialdehyde, *N*-acetyl *(S)*-aspartate β-semialdehyde, and succinic semialdehyde, as well as *(R)*-aspartate β-semialdehyde.

Figure I-11: (S)-*Aspartate β-semialdehyde analogues*

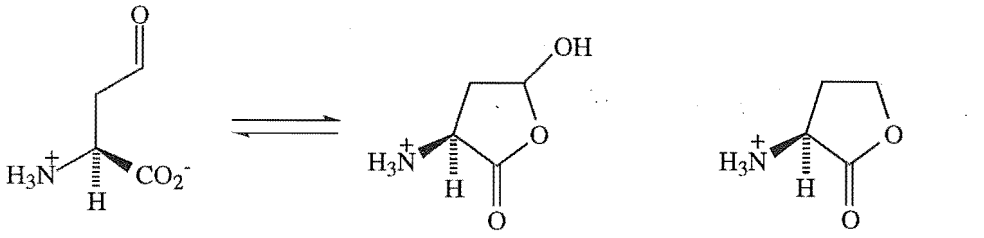

(S)-Aspartate β-semialdehyde (11a)

Cyclic lactol (11c)

(S)-Homoserine lactone (31)

(iii) *(S)*-Lysine (12) and *(S)*-lysine analogues

DHDPS enzymes can be classified into three categories: those from sporulating bacteria, these show no feedback inhibition by *(S)*-lysine (12); those from other bacteria, these show inhibition by *(S)*-lysine (12) only at high concentrations; and those from plants, these show potent inhibition by *(S)*-lysine (12). *E. coli* DHDPS is moderately inhibited by *(S)*-lysine (12), IC_{50} = 1 mM.[18] *(S)*-Lysine analogues, for example (2-aminoethyl)-*(R)*-cysteine (32) and *threo*-β-hydroxy-*(S)*-lysine (33) (see figure I-12), show similar inhibition but are less effective than *(S)*-lysine (12).[17]

Figure I-12: (S)-Lysine (12) and (S)-lysine (12) analogues

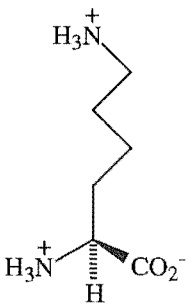

(S)-Lysine (12)

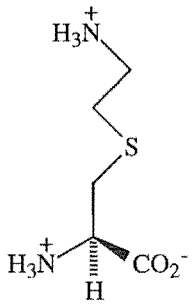

(2-Aminoethyl)-
(R)-cysteine (32)

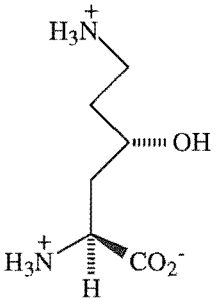

threo-4-Hydroxy-
(S)-lysine (33)

(iv) Combined substrate and/or reaction intermediate inhibitors

Diketopimelic acid (34) inhibits DHDPS and has been suggested to mimic both substrates, or an intermediate in the reaction, since it contains structural elements of both substrates, and shows competitive inhibition with respect to both substrates.[66] Recent work published by Karsten, in 1995,[70] shows acetopyruvate (35) is also a combined substrate inhibitor of DHDPS (where K_i is 5 μM). Both examples are shown in figure I-13.

Figure I-13: Combined substrate inhibitors

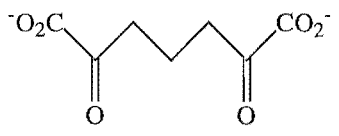

Diketopimelic acid (34)

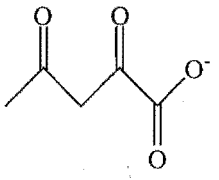

Acetopyruvate (35)

(v) Product inhibitors

Molecules designed to mimic the product dihydrodipicolinate (18), such as dipicolinic acid (36), have been found to inhibit the *E. coli* enzyme[17] (*E. coli* does not produce dipicolinate (36), unlike sporulating bacteria). A systematic investigation of heterocycles by Couper *et al.*[71] at the onset of this work found substituted pyridines (37) and piperidines (38) to be only moderate inhibitors of DHDPS, see figure I-14.

Figure I-14: Product inhibitors

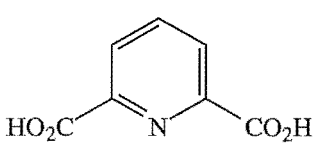

Dipicolinic Acid (36)

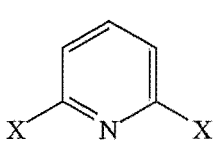

Pyridines (37)

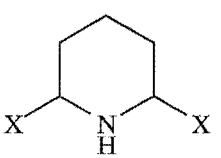

Piperidines (38)

Assay systems to measure the kinetics of DHDPS

Three assays have been reported for DHDPS.[62] Formation of a purple adduct with *o*-aminobenzaldehyde, which can give semi-quantitative measurements at 540 nm, has been noted. The product of the DHDPS catalysed reaction is reported to react with imidazole buffer and the product of this reaction can be detected at 270 nm. An extremely accurate quantitative assay, which couples the activity of DHDPS to DHDPR, has also been reported. This reaction is followed by monitoring the DHDPR utilisation of NADPH at 340 nm. While this third assay is extremely accurate it has been little used due to the difficulty in obtaining the enzymes required. Thus, the first two assays have been more widely used despite the lack of characterisation of the species being measured.

Ongoing research on DHDPR

Genetics and enzymology

The *dap B* gene, which has been mapped to 0.5 min on the *E. coli* chromosome, encodes for DHDPR.[11,72] It has been cloned and sequenced. Unlike the *dap A* gene, its expression is repressed by *(S)*-lysine (12).[72]

DHDPR has been isolated and purified from *E. coli,*[29,30] *Bacillus cereus,*[31] *B. megaterium,*[31] *B. subtilis,*[32] and maize.[33] Activity has also been detected in soybean, tobacco, and corn.[73] All of these enzymes cause the reduction of dihydrodipicolinate (18) to tetrahydrodipicolinate (19), utilising either NADPH or NADH. The *E. coli* enzyme is a homotetramer of M_r 110 000 as determined by gel filtration chromatography.[29] The *dap B* gene predicts the monomer to contain 273 amino acids, with a M_r of 28 798.[74] The M_r has also been determined, from an overexpressed *E. coli* gene, to be 28 758 ± 8 by electrospray mass spectrometry.[30] This matches the value of 28 757 calculated from the DNA sequence (from PCR).[74] The discrepancy between the predicted M_r from the *dap B* gene, and the M_r from the PCR prediction is due to a glycine residue, erroneously assigned as a valine residue, in the *dap B* sequence leading to a predicted M_r 42 greater than the actual value.[74]

The maize enzyme has a M_r of ~80 000 and is similar to the *E. coli* enzyme. However, DHDPR isolated from *Bacillus* sp. are very different. *Bacillus* sp. DHDPR[31] have a much higher M_r ~150 000 and are inhibited, noncompetitively, by dipicolinate. This indicates a role in the regulation of dipicolinate (36) biosynthesis used in spore formation. The *B. subtilis* form of DHDPR is a homotetramer, with a subunit of M_r ~18 500. While it may use NADPH or NADH it also requires FMN.[32]

The chemical nature of the product tetrahydrodipicolinate

The chemical synthesis of the potassium salt of 2,3,4,5-tetrahydrodipicolinate (19) was published in 1995 by Chrystal *et al.*[75] It exists in solution in equilibrium with the enamine (39) and an open chain form (40), see figure I-15.

Figure I-15: Tetrahydrodipicolinate (19)

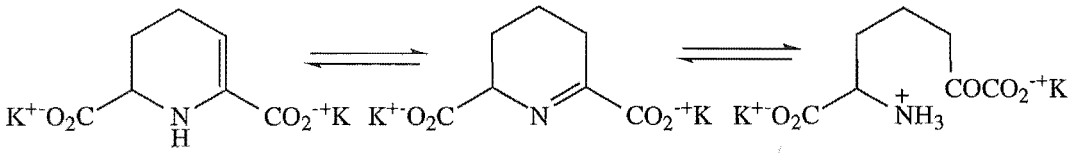

Enamine (39) 2,3,4,5-Tetrahydrodipicolinate (19) Open chain form (40)

The mechanism of the DHDPR catalysed reaction

Since the onset of this work, when there was very little published research on DHDPR, the X-ray structure of *E. coli* DHDPR has been resolved to 2.2 Å by Scapin *et al.*,[76] mechanistic studies have been performed by Reddy *et al.*,[30,77] and electrospray mass spectrometry has been performed by Wang *et al.*,[78] enhancing the knowledge of the mechanism of this enzyme. For the reaction of DHDPR see figure I-16.

Figure I-16: Reaction of DHDPR

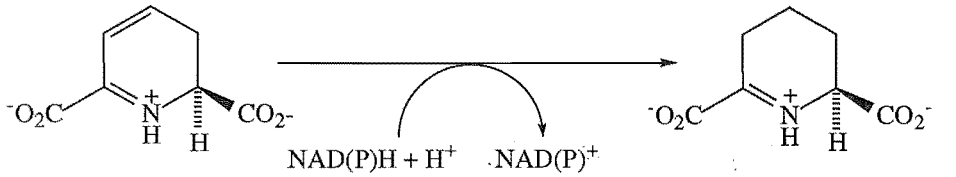

Dihydrodipicolinate (18) Tetrahydrodipicolinate (19)

Kinetic studies on DHDPR, including inhibition studies

Michaelis-Menten constants have been determined for *E. coli* DHDPR with respect to the substrate dihydrodipicolinate (18), K_m was found to be 50 ± 12 μM,[30] 9.0 μM,[29] and 190 μM.[74] The enzyme is unusual in that either NADPH or NADH are accepted as cofactors.[29,77] Often in metabolism NAD^+/NADH is concerned with oxidative breakdown of substrates to provide electrons for energy producing systems, whereas $NADP^+$/NADPH serve as donors of H^+/H^- for reductive biosynthesis. This allows the two pools to remain distinct.[79,80] It was noted that, with NADH as the cofactor, V_{max} was approximately half that for NADPH. However, values for *V/K* show that NADH is a more efficient substrate by a factor of two, because of its four fold lower value of K_m.[30]

In a review by Cox, published in 1996,[65] various substrate analogues had been shown to inhibit DHDPR. Dipicolinate (36) is a competitive inhibitor of *E. coli* DHDPR with respect to the substrate (K_i is 26 ± 6 μM), but inhibits uncompetitively against the

cofactor NADPH (K_i is 350 ± 5 μM).[30] Much weaker inhibition has been observed for other substrate analogues, for example isophthalic acid (41) (IC_{50} ~2 mM). Compounds with only one carboxylate group, such as picolinic acid (42) and pipecolic acid (43), are very poor inhibitors (IC_{50} >20 mm). Piperidine dicarboxylic acids (44) do not inhibit. Product inhibition by NADPH was also observed, being competitive with respect to NADPH (K_i is 190 ± 35 μM), and noncompetitive versus the substrate (K_i is 700 ± 200 μM). The structures of these inhibitors are shown in figure I-17.

Figure I-17: Inhibitors

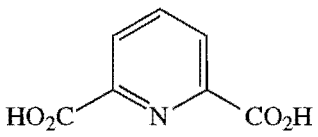

Dipicolinic acid (36)

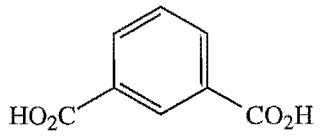

Isophthalic acid (41)

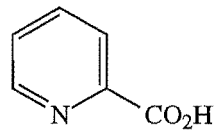

Picolinic acid (42)

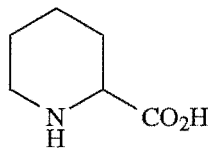

Pipecolic acid (43)

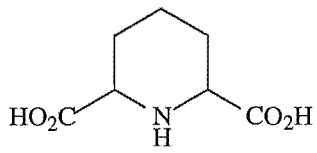

Piperidine dicarboxylic acids (44)

Assay systems to measure the kinetics of DHDPR

An assay measuring the activity of DHDPR has been described; this utilises reduction of dihydrodipicolinate (18), either from substrate produced enzymatically *in situ* from DHDPS, or from chemically synthesised substrate.[29] However, if the substrate is chemically synthesised a mixture of compounds and isomers result. This is problematic as the structure of the substrate is unknown, and the species produced in the chemical synthesis have been ill-characterised. The assay then quantifies activity by monitoring the oxidation of NADPH at 340 nm.

Conclusions; aims of this thesis

The primary aim of this research was to build up a more complete picture of the enzymology of *(S)*-lysine (12) biosynthesis using *E. coli* as a model. Preliminary work involved over-expressing the *E. coli dap A* gene to obtain supplies of DHDPS which were then purified. The *dap B* gene was also over-expressed to obtain supplies of DHDPR, which were then purified. An accurate time dependent assay was developed, using these purified enzymes. This enabled detailed kinetic studies of both DHDPS and DHDPR to be performed.

Detailed kinetic studies were carried out on DHDPS and K_m and V_{max} parameters will be reported. *(S)*-Aspartate β-semialdehyde (11), a substrate of DHDPS, was synthesised

optically pure from *(S)*-allylglycine. Kinetic studies were also carried out on DHDPR, and the K_m and V_{max} parameters will be reported for the substrate and both cofactors, NADPH and NADH.

Inhibition studies on DHDPS were carried out involving the inhibition by high substrate concentrations of *(S)*-aspartate β-semialdehyde (11) and the feedback inhibition by *(S)*-lysine (12). From inhibition studies using *(S)*-aspartate β-semialdehyde (11) analogues along with structural studies on *(S)*-aspartate β-semialdehyde (11) the solution structure of this substrate is reported. NMR studies on the DHDPS catalysed reaction, along with inhibition studies on product analogues of DHDPS and substrate analogues of DHDPR, have enabled the mechanisms of both enzymes to be more fully understood, and the product of the DHDPS catalysed reaction to be better characterised.

References

1. H.C. Neu *Science* **257**, 1064 (1992).
2. A.D. Dodge (Ed.) *'Herbicides and Plant Metabolism'* Cambridge University Press, Cambridge (1989).
3. R.A. La Rossa, S.C. Falco *Trends in Biotech.* **2**, 158 (1984).
4. W.O. Foye, T.L. Lenke, D.A. Williams *'Principles of Medicinal Chemistry'* 4th ed., Williams and Wilkins, Baltimore (1995).
5. C. Hansch (Ed.) *'Comprehensive Medicinal Chemistry. The Rational Design, Mechanistic Study and Therapeutic Application of Chemical Compounds, Volume 2 Enzymes and Other Molecular Targets'* Pergamon Press, Oxford (1992).
6. H.A. Guthrie *'Introductory Nutrition'* Ted Times Mirror/Mosby College Publishing, St. Louis (1989).
7. S.W.J. Bright, P.R. Shewry *CRC Critical Reviews in Plant Science* **1**, 49 (1983).
8. M. Mazelis, F.R. Whatley *FEBS Letts.* **84**, 236 (1977).
9. J.M. Girodeau, C. Agouridos, M. Masson, R. Pineau, F. Le Goffic *J. Med. Chem.* **29**, 1023 (1986).
10. G.M. Kishore, D.M. Shah *Ann. Rev. Biochem.* **57**, 627 (1988).
11. B.J. Bachmann *Microbiology Reviews* **54**, 130 (1990).
12. J-C. Patte *'Biosynthesis of Threonine and Lysine'* in F.C. Niedhardt (Ed.) 'Escherichia *and* Salmonella *Cellular and Molecular Biology'* 2nd edn., ASM Press, Washington D.C. (1996).
13. A.L. Leninger *Biochemistry* 2nd edn., Worth, N.Y., (1975).
14. P.L.R. Bonner, P.J. Lea *Meth. Plant Biochem.* **3**, 297 (1990).
15. J-C. Patte *'Diaminopimelic acid and lysine'* in K.M. Hermann, R. Somerville (Eds) *'Amino acids - biosynthesis and genetic regulation'* Addison-Wesley, Massachusetts, (1983).

16. Y. Yugari, C. Gilvarg *J. Biol. Chem.* **240**, 4710 (1965).
17. B. Laber, F-X. Gomis-Ruth, M.J. Romao, R. Huber *Biochem. J.* 288, 691 (1992).
18. E.B. Borthwick, S.J. Cornell, D.W. Tudor, A. Shneier, C. Abell, T.R. Coggins *Biochem. J.* **305**, 521 (1995).
19. L. Eggeling *Amino Acids* **6**, 261 (1994).
20. D.P. Stahly *Biochim. Biophys. Acta* **191**, 439 (1969).
21. F.H. Webster, R.V. Lechowich *J. Bacteriol.* **101**, 118 (1970).
22. F. Yamakura, Y. Ikeda, K. Kimura, T. Saskawa *J. Biochem.* **76**, 611 (1974).
23. D.A. Hoganson, D.P. Stahly *J. Bacteriol.* **124**, 1344 (1975).
24. R.M. Cheshire, B.J. Miflin *Phytochem.* **14**, 695 (1975).
25. R.M. Wallsgrove, M. Mazelis *Phytochem.* **20**, 2651 (1981).
26. R. Kumpaisal, T. Hashimoto, Y. Yamada *Plant Physiol.* **85**, 145 (1987).
27. M. Ghislain, V. Frankard, M. Jacobs *Planta* **180**, 480 (1990).
28. C. Dereppe, G. Bold, D. Ghisalba, E. Ebert, H-P. Shar *Plant Physiol.* **98**, 813 (1992).
29. H. Tamir, C. Gilvarg *J. Biol. Chem.* **249**, 3034 (1974).
30. S.G. Reddy, J.C. Sacchettini, J.S. Blanchard *Biochemistry* **34**, 3492 (1995).
31. K. Kimura, T. Goto *J. Biochem.* **81**, 1367 (1977).
32. K. Kimura J. Biochem. **77**, 405 (1975).
33. V.V.S. Tyagi, R.R. Henke, W.R. Farkas *Plant Physiol.* **73**, 687, (1983).
34. S.A. Simms, W.H. Voige, C. Gilvarg *J. Biol. Chem.* **259**, 2734 (1984).
35. B. Peterkofsky, C. Gilvarg *J. Biol. Chem.* **236**, 1432 (1961).
36. Y. Lin, R. Myhrman, M.L. Schray, M.H. Gelb *J. Biol. Chem.* **263**, 1622 (1988).
37. J.S. Wiseman, J.S. Nichols *J. Biol. Chem.* **259**, 8907 (1984).
38. P.J. White, B. Kelly *Biochem. J.* **96**, 75 (1965).
39. F. Richard, C. Richard, P. Ratet, J-C. Patte *J. Bacteriol.* **166**, 297 (1986).
40. U. Gallili *The Plant Cell* **7**, 899 (1995).
41. T.D.H. Bugg, C.T. Walsh *Nat. Prod. Reports* **9**, 199 (1992).
42. J.F. Powell *Biochem J.* **54**, 210 (1953).
43. M. Forman, A. Aronson *Biochem J.* **126**, 503 (1973).
44. M.G. Davis *'More about Enzymes: Structure and Catalytic Properties of Enzymes'* in S.M. Roberts, B.J. Price (Eds) *'Medicinal chemistry, The Role of Organic Chemistry in Drug Research'* Academic Press, London (1985).
45. Y. Song, D. Niederer, P.M. Lane-Bell, L.K.P. Larr, S. Crowley, M.M. Palcic, M.A. Pickard, D.L. Priess, J.C. Vederas *J. Org. Chem.* **59**, 5784 (1994).
46. W.S. Faraci *'Cytosolic Enzymes as Potential Antibacterial Targets'* in J. Sutcliffe, H. Georgopapadakou (Eds) *'Emerging targets in antibacterial and antifungal chemotherapy'* Chapman and Hall, New York (1992).

47. L.K. Lam, L.D. Arnold, T.H. Kalanton, J.G. Kellard, P.M. Lane-Bell, M.M. Palcic, M.A. Pickard, J.C. Vederas *J. Biol. Chem.* **263**, 11814 (1988).
48. R.J. Baumann, E.H. Bohme, J.S. Wiseman, M. Vaal, J.S. Nichols *Antimicrobial Agents Chemotherapy* **32**, 119 (1988).
49. J.G. Kellard, L.D. Arnold, M.M. Palcic, M.A. Pickard, J.C. Vederas *J. Biol. Chem.* **261**, 13216 (1986).
50. J.L. Roberts, J. Borgese, C. Chan, D.D. Keith, C-C. Wei *Heterocycles* **35**, 115 (1993).
51. F. Richard, C. Richard, C. Haziza, J-C. Patte *C. R. Acad. Sc. Paris, Series III,* **t 293**, 507 (1981).
52. J. Cremer, L. Eggeling, H. Sahm *Mol. Gen. Genet.* **220**, 478 (1990).
53. S. Bonnassie, J. Oreghia, A. M. Sicard *Nuc. Acids Res.* **18**, 6421 (1990).
54. N-Y. Chen, S-Q Jiang, D. A. Klein, H. Paulus *J. Biol. Chem.* **268**, 9448 (1993).
55. A. Pisabarro, M. Malumbres, L. M. Mateos, J. A. Oguiza, J. F. Morton *J. Bacteriol.* **175**, 2743 (1993).
56. M. Vauterin, M. Jacobs *Plant Mol. Biol.* **25**, 545 (1994).
57. D.C. Bittel, J.M. Shaver, D.A. Somers, B.G. Gengenbach *Theor. Appl. Genet.*, **92** 70 (1996).
58. G.W. Silk, B.F. Matthews, D.A. Somers, B.G. Gengenbach *Plant Mol. Biol* **26**, 298 (1994).
59. T. Kaneko, T. Hashimoto, R. Kumpaisal, Y. Yamada *J. Biol. Chem.* **265**, 17451 (1990).
60. M. Ghislain, V. Frankard, M. Jacobs *Plant J.* **8**, 733 (1995).
61. C. Mirwaldt, I. Korndorter, R. Huber *J. Microbiol.* **246**, 227 (1995).
62. J.G. Shedlarski *J. Biol. Chem.* **245**, 1362 (1970).
63. F. Richaud, C. Richaud, P. Ratet, J-C. Patte *J. Bacteriol.* **166**, 297 (1986).
64. D.A. Frisch, B.G. Gengenbach, A.M. Tommey, J.M. Selher, D.A. Somers, D.E. Myers *Plant Physiol.* **96**, 444 (1991).
65. R.J. Cox *Natural Product Reports* **13**, 29 (1996).
66. J.A. Gerrard *'Studies on Dihdyrodipicolinate Synthase'* D. Phil., Brasenose College, Oxford (1992).
67. U. Eisner, J. Kuthan *Chem. Rev.* **72**, 1 (1972).
68. S. Blicking, C. Renner, B. Laber, H-D. Pohlenz, T.A. Holak, R. Huber *Biochemistry* **36**, 24 (1997).
69. W.E. Karsten *Biochemistry* **36**, 1731 (1997).
70. W.E. Karsten *FASEB J.* **9**, A1298 (1995).
71. L. Couper, J.E. McKendrick, D.J. Robins, E.J.T. Chrystal *Bioorg. Med. Chem. Letts.* **4**, 2267 (1994).

72. J. Bouvier, C. Richard, F. Richard, J-C. Patte, P. Stragier *J. Biol. Chem.* **259**, 14829 (1984).
73. S.P. Chatterjee, B. K. Singh, C. Gilvarg *Plant. Mol. Biol.* **26**, 285 (1994).
74. J.A.E. Kraunsoe *'Studies in Lysine Biosynthesis'* Corpus Christi College, Oxford (1992).
75. E.J.T. Chrystal, L. Couper, D. J. Robins *Tetrahedron* **51**, 1041 (1995).
76. G. Scapin S.G. Reddy, J.S. Blanchard *Biochemistry* **34**, 3502 (1995).
77. S.G. Reddy, G. Scapin, J.S. Blanchard *Biochemistry* **35**, 13294 (1996).
78. F. Wang, J.S. Blanchard, X-J. Tang *Biochemistry* **36**, 3755 (1997).
79. B.T. Kaufman *TIBS* **18**, 278 (1993).
80. D. Dolphin, R. Poulsen, O. Avramonic (Eds) *'Pyridine Nucleotide Coenzymes, Parts A and B'* John Wiley & Sons, New York (1987).

Results and Discussion

Results and Discussion Chapter One

The Production of Required Enzymes and Substrates

Background work

To study the DHDPS and DHDPR enzyme-catalysed reactions, both the enzymes and substrates of these reactions were required. DHDPS catalyses the condensation of *(S)*-aspartate β-semialdehyde (11) and pyruvate (17) to form an unstable heterocyclic product. For detailed kinetic analysis pure *(S)*-aspartate β-semialdehyde (11) and pyruvate (17) were required. Pyruvate (17) is available commercially while there are several reported syntheses of *(S)*-aspartate β-semialdehyde (11) in the literature.[1,2,3,4] The gene encoding for *E. coli* DHDPS *(dap A)* was available on a multicopy plasmid.[2] This provided a ready source of this enzyme. In the second reaction DHDPR catalyses the reduction of the DHDPS product to tetrahydrodipicolinate (19). Because of the ease of synthesising the product of the DHDPS reaction enzymatically, as opposed to chemical synthesis where multiple compounds and isomers form (and it is unknown which compound is the substrate of DHDPR), this was the method of choice for synthesising this substrate. The gene encoding for *E. coli* DHDPR *(dap B)* was also available on a multicopy plasmid,[5] providing a source of this enzyme. The first part of this chapter deals with the synthesis of pure *(S)*-aspartate β-semialdehyde (11), as modified from literature procedures. While the second part of this chapter describes the production and purification of both DHDPS and DHDPR, again as modified from literature procedures.

Part A Synthesis of (S)-*Aspartate β-Semialdehyde*

Introduction

Previous syntheses of *(S)*-aspartate β-semialdehyde (11) in the literature[1,2] are based on the method of Black and Wright[3] which requires the ozonolysis of *(S)*-allylglycine (49). The four methods in the literature are: the original ozonolysis of *(S)*-allylglycine (49),[3] the oxidation of *(S)*-allylglycine (49) using catalytic osmium tetroxide with sodium periodate[2] (known as a Lemieux-Johnson reaction[6,7]), ozonolysis of diprotected *(S)*-allylglycine (49),[1] and hydrolysis of an enol ether derivative of *(S)*-aspartate β-semialdehyde (11).[4] It was decided to synthesise *(S)*-aspartate β-semialdehyde (11) by oxidation of diprotected *(S)*-allylglycine (49) as reported by Tudor *et al.*,[1] but instead of performing the oxidation by ozonolysis, the method using catalytic osmium tetroxide with sodium periodate[2,6,7] was employed.

Synthetic route to *(S)*-allylglycine

To synthesise *(S)*-aspartate β-semialdehyde (11) by oxidative cleavage of *(S)*-allylglycine (49) optically pure *(S)*-allylglycine (49) was required. The method of Gerrard[2] was followed with only minor changes to the first step (the formation of diethyl allylacetamidomalonate (46)). This synthesis used an enzymatic resolution to effect

stereo-control. Diethyl acetamidomalonate (45) underwent an allylation reaction using allyl bromide to yield diethyl allylacetamidomalonate (46).[8] This was then followed by a base catalysed hydrolysis, to yield *N*-acetyl allylglycine (48). The *(S)*-enantiomer was then selectively de-acetylated by the enzyme porcine kidney acylase (EC 3.5.1.14) to yield *(S)*-allylglycine (49), see figure 1-1.

Figure 1-1: Synthesis of optically pure (S)*-allylglycine (49)*

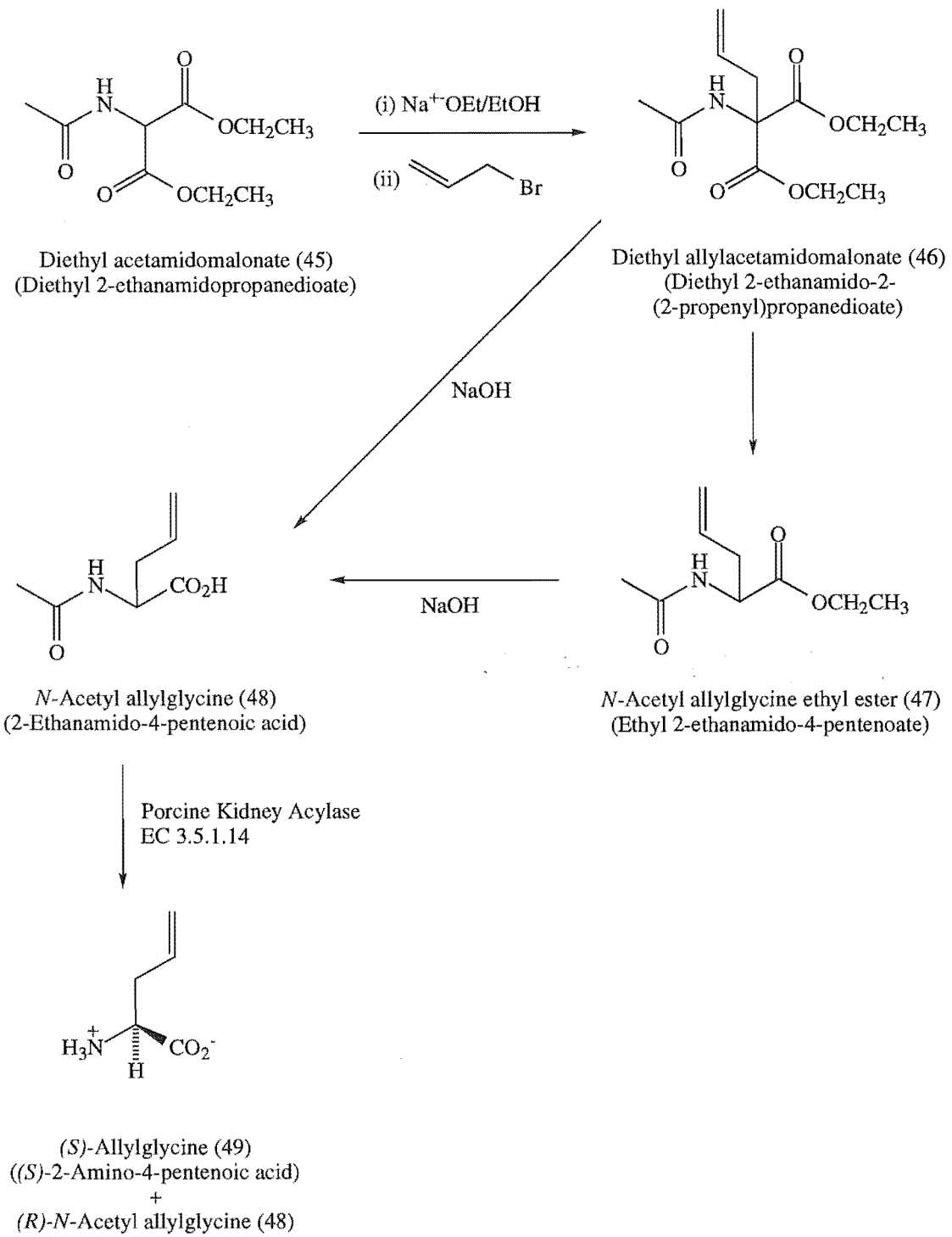

The allylation of diethyl acetamidomalonate (45) to give diethyl allylacetamidomalonate (46) was modified from the method of Gerrard.[2] It was shown that fewer side reactions occurred and a better yield was obtained if 1.5 equivalents of sodium ethoxide and allyl bromide were used. On prolonged heating under reflux, using less than 1.5 equivalents of both the sodium ethoxide and the allyl bromide, the reaction proceeded to give the product *N*-acetyl allylglycine ethyl ester (47). This compound is presumably formed by an S_N2 type dealkylation of diethyl allylacetamidomalonate (46) followed by decarboxylation *in situ*, see figure 1-2. This side reaction was not observed when the reaction time was decreased and the amount of sodium ethoxide and allyl bromide was increased to 1.5 equivalents. The diethyl allylacetamidomalonate (46) was obtained as a clear yellow oil, which crystallised on standing overnight, in a yield of 74%.

Figure 1-2: S_N2 type dealkylation followed by decarboxylation

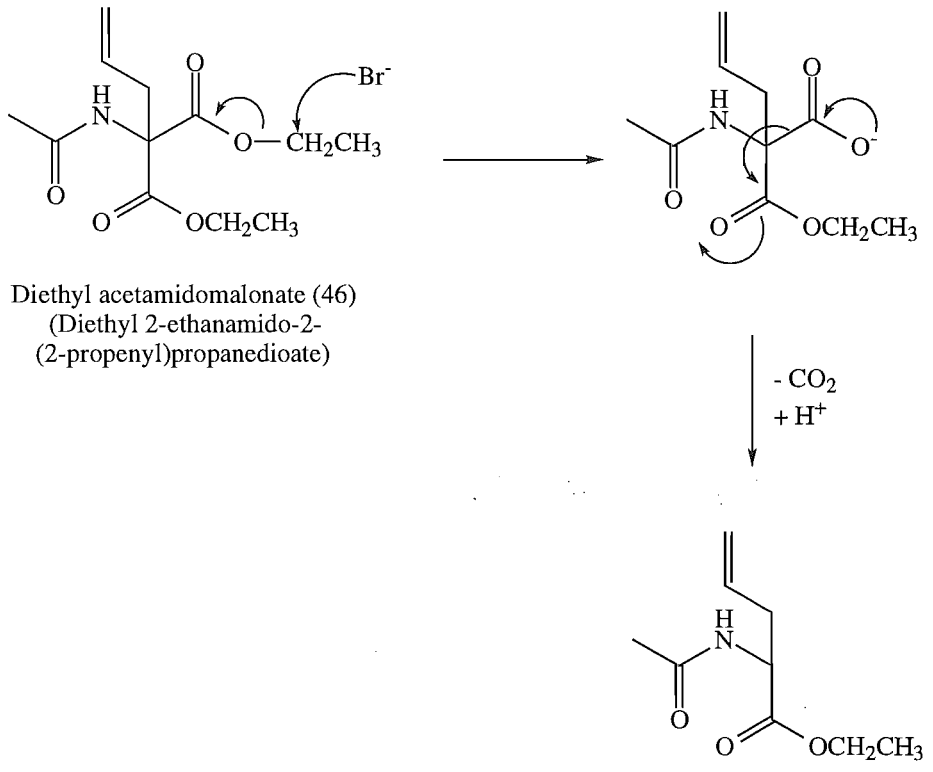

Diethyl acetamidomalonate (46)
(Diethyl 2-ethanamido-2-
(2-propenyl)propanedioate)

N-Acetyl allylglycine
ethyl ester (47)
(Ethyl 2-Ethanamido-
4-pentenoate)

N-Acetyl allylglycine (48) was formed by base hydrolysis and decarboxylation of diethyl allylacetamidomalonate (46), using sodium hydroxide in aqueous ethanol.[2] The reaction was heated under reflux until no starting material could be detected by ^{1}H NMR. The product (as recrystallised from hot propanone) gave *N*-acetyl allylglycine (48) as clear chunky crystals in 55% yield.

Acetolysis and optical resolution were carried out in aqueous solution by incubation of *N*-acetyl allylglycine (48) with porcine kidney acylase EC 3.5.1.14.[2] This enzyme selectively removes the acetyl group from the *(S)*-enantiomer, yielding *(S)*-allylglycine (49), but has negligible effect on the *(R)*-enantiomer.[9] Thus, the reaction was complete when half the *N*-acetyl allylglycine (48) remained (as monitored by ^{1}H NMR). *(S)*-Allylglycine (49) and *(R)-N*-acetyl allyl glycine (48) were then separated by ion exchange chromatography. The latter eluted at pH 7, whilst the required compound was eluted with aqueous ammonia. *(S)*-Allylglycine (49) was obtained as a white semi-crystalline solid of in 36% yield (the theoretical maximum yield was 50%).

Synthetic route to pure *(S)*-aspartate β-semialdehyde

(S)-Aspartate β-semialdehyde (11) was synthesised by oxidation of diprotected *(S)*-allylglycine (49) as reported by Tudor *et al.*,[1] but the oxidation was performed using a Lemieux-Johnson reaction[6,7] (which employs catalytic osmium tetroxide with sodium periodate) rather than using ozonolysis, see figure 1-3. The use of diprotected *(S)*-allylglycine (52) minimised the formation of unwanted side products. Thus, the *(S)*-aspartate β-semialdehyde (11) obtained was of higher purity and therefore greater stability.

(R,S)-Aspartate β-semialdehyde (11) was synthesised from *(R,S)*-allylglycine (49) also using this method.

Figure 1-3: Synthesis of (S)-*aspartate β-semialdehyde (11)*

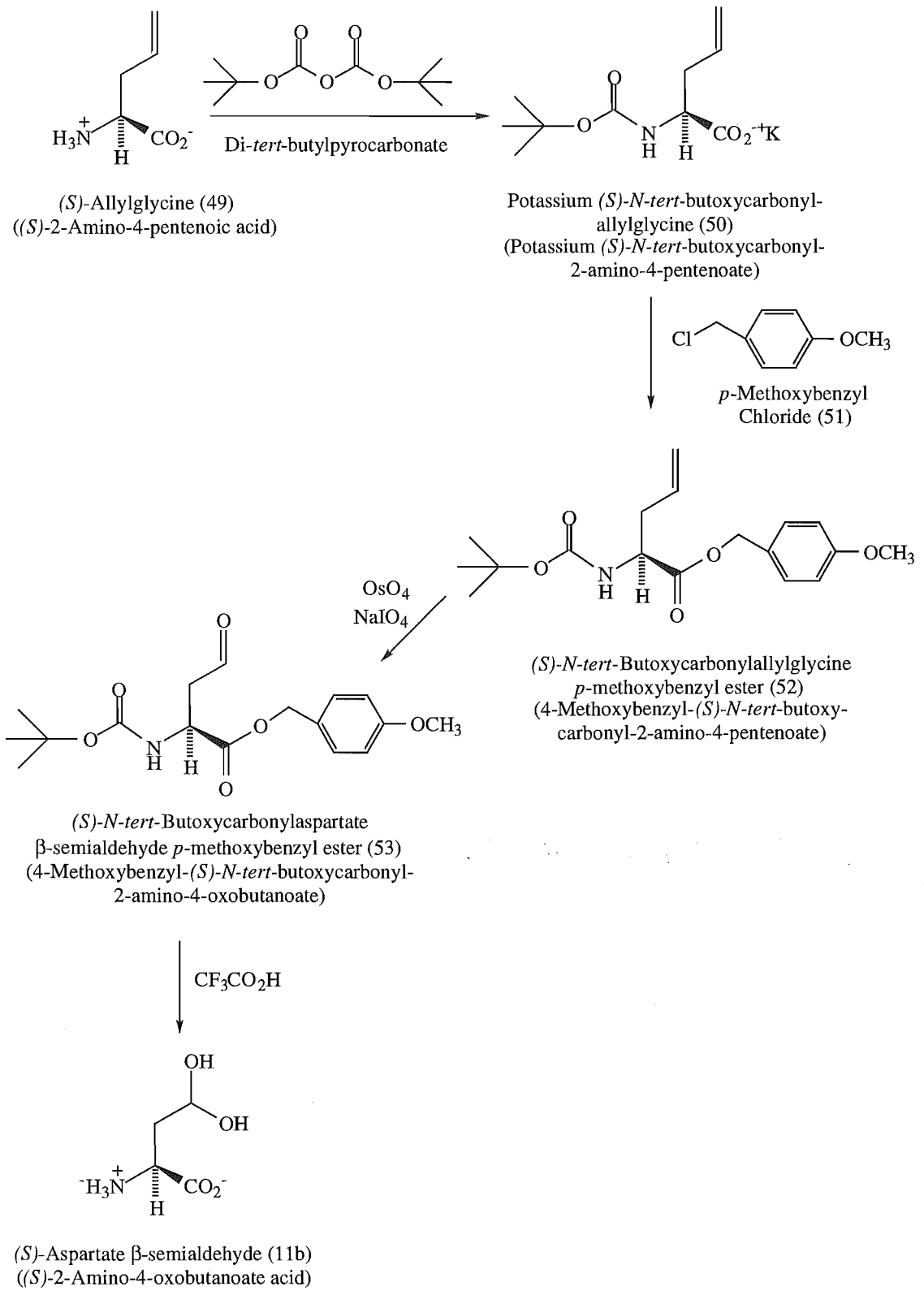

(S)-Allylglycine (49) was *N*-protected by a tertiary butyl group in quantitative yield using the reagent di-*tert*-butylpyrocarbonate.[1] This reaction was performed in base, with dioxane present, at room temperature. The product was obtained as a white oily solid which was purified to a white powder by washing with methanol.

C-Protection was as a *p*-methoxybenzyl ester.[1] *p*-Methoxybenzyl chloride (51), the protecting agent of choice, was synthesised from *p*-methoxybenzyl alcohol (anis alcohol) (54) by bubbling dry hydrochloride gas through the alcohol dissolved in ether,[10] see figure 1-4.

Figure 1-4: Synthesis of p-*methoxybenzyl chloride*[10]

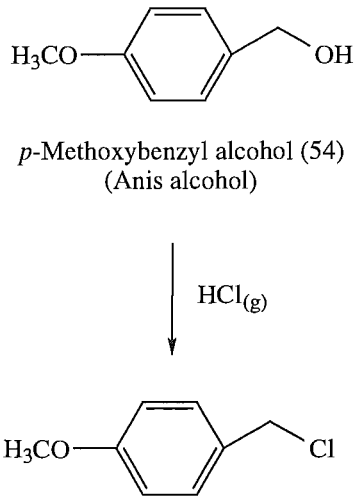

p-Methoxybenzyl alcohol (54)
(Anis alcohol)

p-Methoxybenzyl chloride (51)

A slight excess of *p*-methoxybenzyl chloride (54) was reacted with the *(S)-N-tert*-butoxycarbonylallylglycine (50) in DMF. The crude product contained a mixture of products due to the high reactivity of *p*-methoxybenzyl chloride (51) and its ability to polymerise. The desired product was obtained pure by chromatography as a clear yellow oil in a yield of 61%.

The alkene group of the diprotected *(S)*-allylglycine (52) was oxidised overnight at room temperature by a Lemieux-Johnson reaction using catalytic osmium tetroxide and three equivalents of sodium periodate, see figure 1-5,[2,6,7] rather than by ozonolysis,[1] to give the desired aldehyde. The major advantage of the Lemieux-Johnson reaction is the ease of reaction and the purity of the resulting product. In the synthesis of the diprotected *(S)*-aspartate β-semialdehyde (53) a relatively clean mixture of products was obtained, from this the desired product could be obtained pure as a clear oil by chromatography in 76% yield. The major impurity in this reaction was unreacted starting material, not the range of oxidised side products that commonly form in the ozonolysis of *(S)*-allylglycine (49).

Figure 1-5: Mechanism of the Lemieux-Johnson reaction

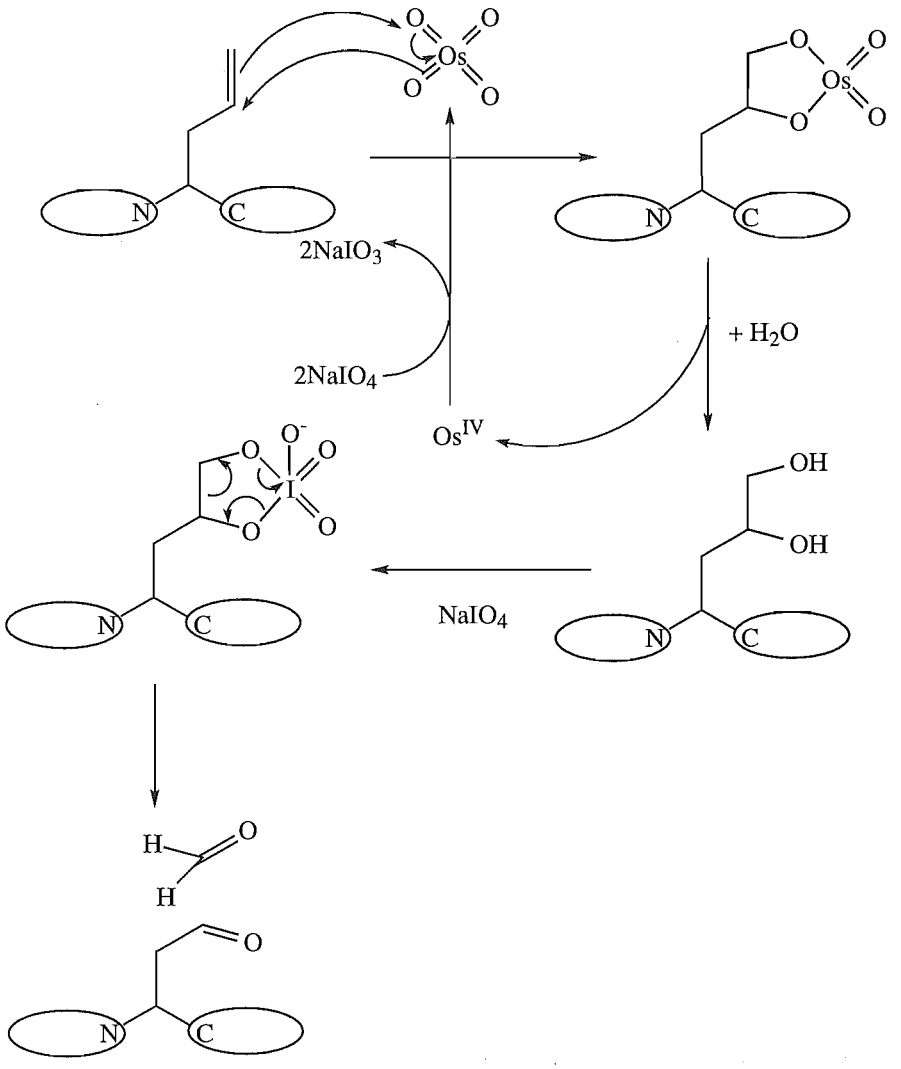

Deprotection of the diprotected *(S)*-aspartate β-semialdehyde (53) was performed in trifluoroacetic acid in dry dichloromethane, yielding the *(S)*-asparate β-semialdehyde (11) as the hydrate (11b) and the trifluoroacetate salt.[1] The product was obtained as a clear oil, in 90% yield. The optical rotation was measured confirming that the *(S)*-aspartate β-semialdehyde (11) synthesised was the *(S)* isomer and was of high optical purity. The rotation, as measured at the sodium D line, was + 3.17° when measured at a concentration of 1.5 g/100 ml in water, this agrees well with the literature.[1] Attempts to crystallise this oil proved fruitless (see Chapter Three).

Summary

Pure *(S)*-aspartate β-semialdehyde (11) was synthesised from diprotected *(S)*-allylglycine (52) as described by Tudor *et al.*,[1] except periodate-osmium tetroxide was used as the oxidising agent rather than ozone. The *(S)*-allylglycine (49) used in this synthesis was synthesised by the method of Gerrard,[2] with only minor changes to the reaction conditions in the first step where diethyl acetamidomalonate (45) undergoes an allylation to diethyl allylacetamidomalonate (46).

Part B Production of the DHDPS and DHDPR Enzymes

Introduction

Given the reported similarity in the properties and inhibition patterns of the *E. coli* and other bacterial enzymes it was decided to concentrate on the *E. coli* DHDPS and DHDPR enzymes. Ample supplies of the purified enzymes were required. Both the *dap A* gene (which encodes for DHDPS) and the *dap B* gene (which encodes for DHDPR) were available on multicopy plasmids,[2,5] thus, allowing their over-expression in *E. coli*. Crude enzyme extracts were then obtained which could be purified by standard biochemical procedures.

Over-expression of the *dap A* gene and purification of the DHDPS enzyme

The *E. coli dap A* gene had been cloned into pBluescript (a high copy number plasmid present at a level of 500 - 700 copies per cell) by Gerrard[2] to give pJG001, see figures 1-6 and 1-7. Since synthesis of DHDPS is constitutive,[11] incorporation of the *dap A* gene in a high copy number plasmid provided a simple and convenient means of over-expression.

Figure 1-6: pJG001

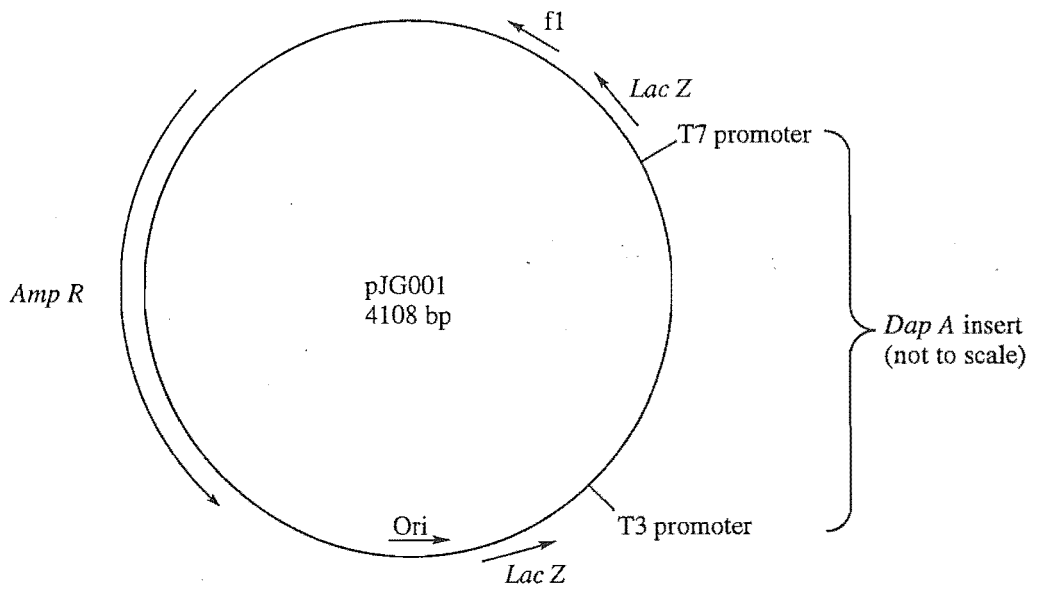

Figure 1-7: Dap A insert from pJG001 with surrounding restriction sites

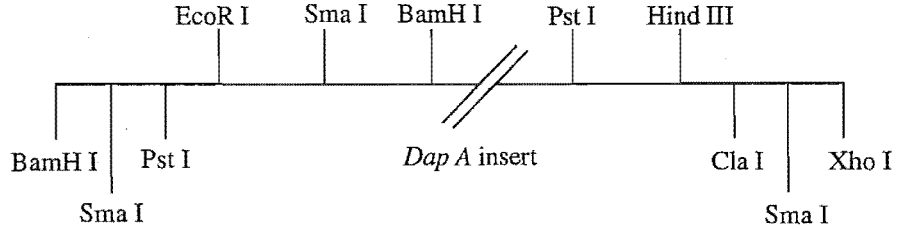

E. coli XL-Blue was transformed with pJG001 using the calcium chloride method[12] and successful transformants were identified by conferred ampicillin resistance. Verification that the plasmid pJG001 had been inserted in the *E. coli* was achieved by standard plasmid preparation via alkaline lysis[12] (derived from Birnboim and Doily) followed by restriction digests. DNA gel electrophoresis[13] was then performed to identify the plasmid DNA fragments. The plasmid was identified by a linear fragment of 4100 bp from a single restriction digest, and by two fragments of 3000 and 1100 bp from a double digest, see figure 1-8.

Figure 1-8: DNA agarose gels of the pJG001 plasmid digests

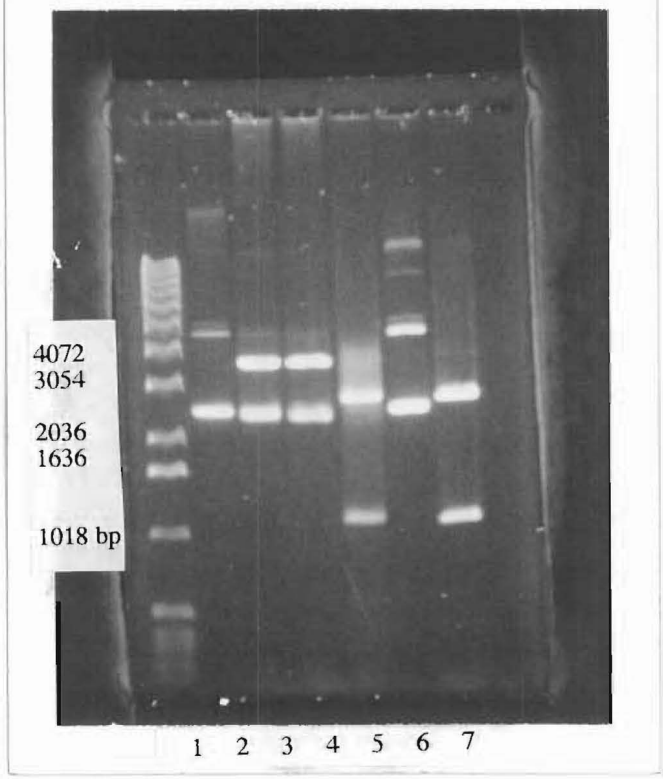

Lane 1: 1 kbp ladder: 1018, 1636, 2036, 3054, 4072 bp.
Lane 2: pJG001 uncut.
Lane 3: pJG001 Xho I digest, 4100 bp, and uncut pJG001.
Lane 4: pJG001 BamH I digest, 4100 bp, and uncut pJG001.
Lane 5: pJG001 Xho I and BamH I double digest, 3000 and 1100 bp.
Lane 6: pJG001 authentic sample uncut.
Lane 7: pJG001 authentic sample Xho I and BamH I double digest, 3000 and 1100 bp.

The *E. coli* transformed with pJG001 was then cultivated and purified. All purification procedures were monitored by the detection of DHDPS, with the *o*-amino-benzaldehyde assay (see Chapter Three) which, although does not provide quantitative analysis of enzyme activity, does detect very low levels of enzyme activity.

Purification of DHDPS

Purification of DHDPS was based on the method by Gerrard,[2] which was modified from Yugari and Gilvarg,[14] and Shedlarski.[15] Gerrard obtained a crude enzyme extract by freeze-thawing the *E. coli* cells which had over-expressed the *dap A* gene. The crude extract was then purified by DEAE fast flow Sepharose ion exchange chromatography followed by dialysis against dry Sephadex. The freeze-thaw cycles and ion exchange chromatography were slightly modified, see below, then dialysis and ion exchange chromatography on a high resolution column were performed.

After a standard overnight (~16 hrs) incubation *E. coli* cells were harvested by centrifugation and washed with buffer. All manipulations were performed at 0 to 4 °C to retain maximum activity. As the DHDPS enzyme resides in the periplasmic space (between the cell wall and the cell membrane) gentle disruption of the cell allows selective release of all the periplasmic proteins, including DHDPS, but few other proteins present in the cell. Previous work[2] had achieved this by freeze thaw cycles, which required cells that had been washed in Tris buffer to be harvested by centrifugation. The cell pellet was then flash frozen in liquid nitrogen and slowly thawed over 24 hours at 0 °C. Successive freeze thaw cycles produced more activity and it was found that between five and eight cycles was optimal; further cycles resulted in the release of significant amounts of other enzymes from the cell. A procedure involving seven freeze-thaw cycles was adopted as the general method. The crude extract was obtained by centrifugation, where it was either frozen for later work or purified. By SDS-PAGE it appeared a protein with M_r of ~31 kDa was the major component; this corresponds to DHDPS, see figure 1-9.

Other workers[16] had performed a heat shock on the crude DHDPS extract. However, it was found that a heat shock at 70 °C for 2 minutes destroyed DHDPS activity; when the precipitated proteins had been removed by centrifugation less specific activity (activity per miligram of protein) remained than was initially present. It was concluded that DHDPS was heat sensitive although it may be protected by pyruvate (this was not investigated). A Q-Sepharose anion exchange column was used for the charge-based purification rather than DEAE Sepharose. The proteins were eluted using a 0 to 1.0 M sodium chloride gradient, in buffer, and DHDPS was found to elute at between 0.4 and 0.6 M salt concentration. Active fractions were then pooled and dialysed against 20 mM Tris pH 8.0 at 4 °C containing 1 mM EDTA, 1 mM β-mercaptoethanol, and 1% ammonium sulfate.

Gel filtration, as an alternative to dialysis, was also investigated as a method of size-based purification. Gel filtration was performed on Sephacryl S-400 HR; however, it was found that the DHDPS, which exists as a native homotetramer (M_r ~125 600), dissociated into the trimer (M_r ~94 200), dimer (M_r ~62 800), and monomer (M_r ~31 400)

during chromatography. Thus, the DHDPS activity was spread over a large molecular weight range making isolation difficult with little increase in the purity of the enzyme, see figure 1-9.

The final step was a further charge-based purification performed on Q-Sepharose. This was used to purify and further concentrate the enzyme. Material to be used for DHDPS enzyme kinetic studies was purified, in batches, on a 1 ml Resource Q-Sepharose Column that gave high resolution. Whereas, material that was to be used for DHDPR enzyme kinetic studies was purified on the large Q-Sepharose column used for the initial purification. The use of the Resource Q-Sepharose column (which has a more uniform bead size than normal Q-Sepharose) greatly increased the purity of the DHDPS enzyme and was a crucial step in this fast purification procedure. Material purified on the Resource Q column had a specific activity of 4.7×10^{-1} $\mu mol \cdot s^{-1} mg^{-1}$, whereas material purified on the Q-Sepharose column had a lower specific activity, 2.0×10^{-1} $\mu mol \cdot s^{-1} mg^{-1}$, see figure 1-9.

During the course of the DHDPS enzyme studies an alternative purification of *E. coli* DHDPS was reported.[16] This purification gave crystalline material. In this case ultrasonication was used to obtain the crude extract, followed by a heat shock, this differed from the above procedure. However, multiple chromatography was performed (DEAE-Sepharose, Phenyl-Sepharose, Q-Sepharose) which was similar to the procedure developed here. The main advantage of the purification described in this thesis was that it gave a quick and simple method for obtaining a homogeneous solution of DHDPS appropriate for kinetic studies. The final DHDPS had been purified to a specific activity of 4.7×10^{-1} $\mu mol \cdot s^{-1} mg^{-1}$ of protein. This monomer was present as a single band on SDS-PAGE stained with Coomassie Brilliant Blue, its electrophoresis mobility corresponded to a monomer of molecular mass ~31 kDa, see figure 1-9.

Figure 1-9: SDS-PAGE of DHDPS protein purification

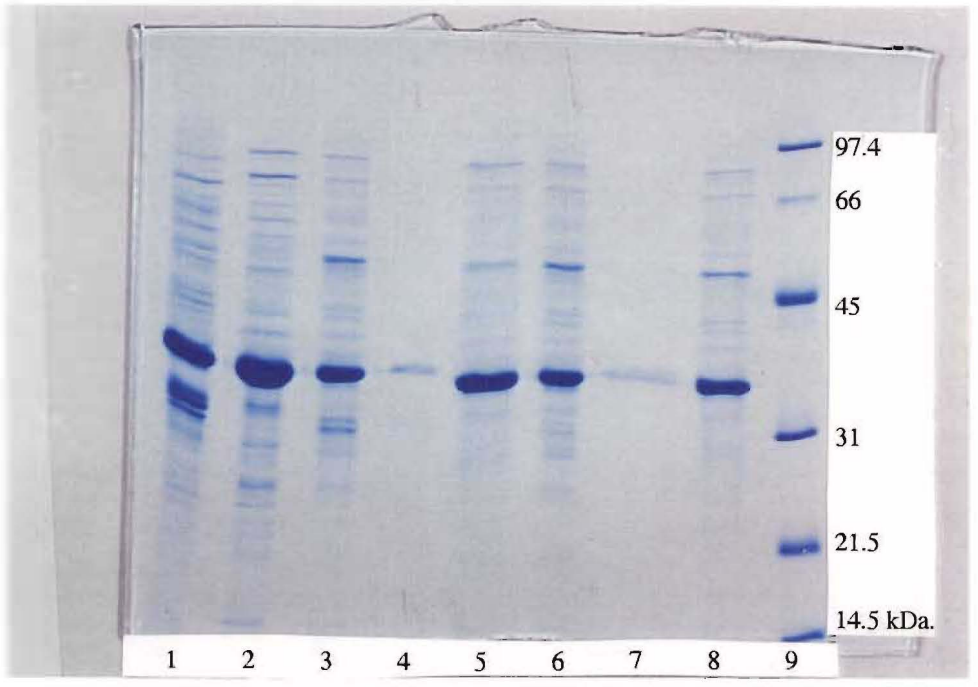

Lane 1 DHDPS crude supernatant.
Lane 2 DHDPS heat shock supernatant.
Lane 3 DHDPS ion exchange.
Lane 4 DHDPS gel filtration.
Lane 5 DHDPS second ion exchange.
Lane 6 DHDPS ion exchange.
Lane 7 DHDPS gel filtration.
Lane 8 DHDPS second ion exchange.
Lane 9 Molecular weight markers: 14.5, 21.5, 31, 45, 66, 97.4 kDa.

Over-expression of the *dap B* gene and purification of the DHDPR enzyme

The *dap B* gene had been cloned into pBluescript by Kraunsoe[5] to give the plasmid pJK001, see figures 1-10 and 1-11. *E. coli* XL-Blue was transformed with pJK001 using the calcium chloride method[11] and successful transformants were identified by conferred ampicillin resistance.

Figure 1-10: Restriction Map of pJK001

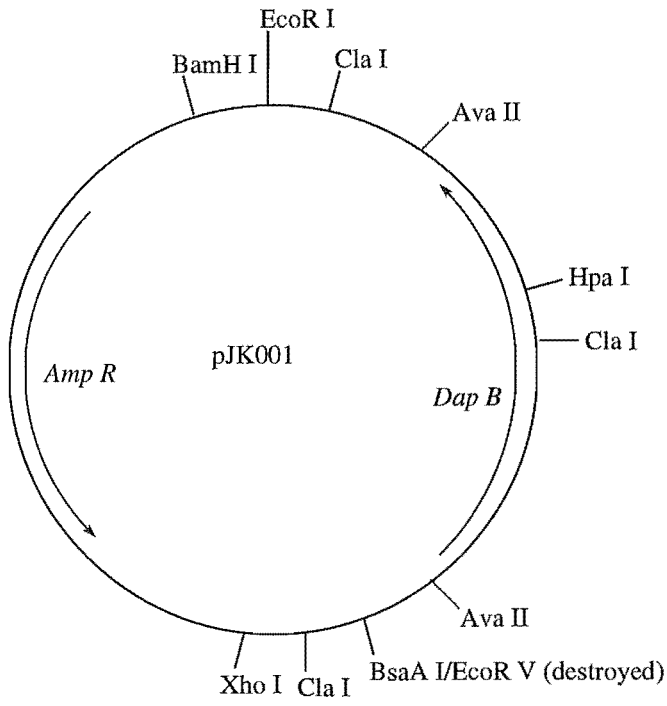

Figure 1-11: Dap B insert with surrounding restriction enzyme sites

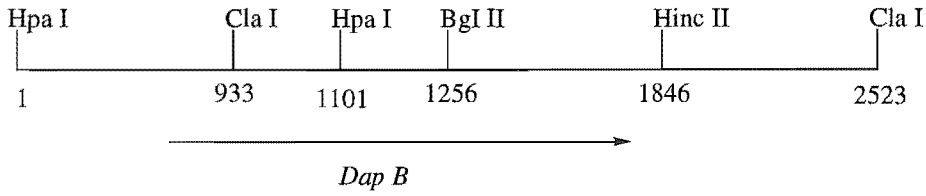

Standard plasmid preparation was performed by alkaline lysis[12] (derived from Birnboim and Doily) followed by restriction digests to verify that pJK001 was present in the transformants. DNA gel electrophoresis[13] was performed to identify the plasmid DNA fragments. XhoH I and BamH I double digest gave two fragments, 3000 bp and 2300 bp long, confirming the plasmid was pJK001, see figure 1-12.

Figure 1-12: DNA agarose gel of pJK001 plasmid digests

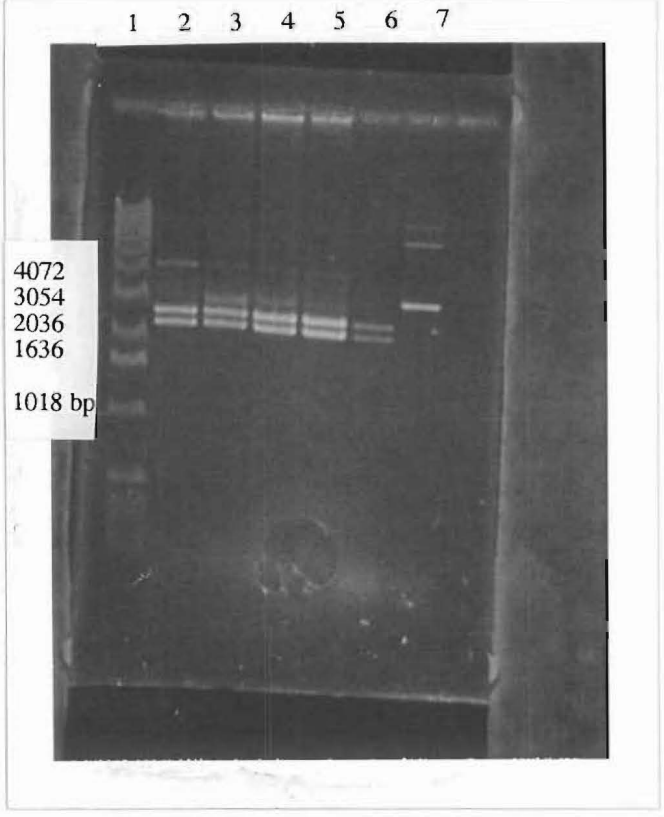

Lane 1: 1 kbp ladder: 1018, 1636, 2036, 3054, 4072 bp.
Lane 2: pJK001 Xho I and BamH I double digest, 3000 and 2300 bp.
Lane 3: pJK001 Xho I and BamH I double digest, 3000 and 2300 bp.
Lane 4: pJK001 Xho I and BamH I double digest, 3000 and 2300 bp.
Lane 5: pJK001 Xho I and BamH I double digest, 3000 and 2300 bp.
Lane 6: pJK001 authentic sample Xho I and BamH I double digest, 3000 and 2300 bp.
Lane 7: pJK001 authentic sample uncut.

Purification of DHDPR

The purification of DHDPR from *E. coli* XL-1 pJK001 was based on the method of Tamir and Gilvarg,[17] as modified by Kraunsoe.[5] This purification used ultrasonication to release the DHDPR enzyme, followed by an ammonium sulfate precipitation. Dialysis and ion exchange chromatography were then performed, and finally a heat shock to remove any contaminating NADPH utilising enzymes. Modifications to this reported procedure were made, as discussed below.

E. coli XL-1 Blue pJK001 was cultured overnight, after which the cells were harvested by centrifugation, washed with buffer, and then resuspended in buffer. DHDPR is present in the cell body, not in the periplasmic space as with DHDPS, so ultrasonication (ultrasound treatment is known to disrupt bacterial cell walls[18]) was used to disrupt the cell contents.

Crude preparations of DHDPR contain DHDPS and other enzymes which consume NADPH and interfere with the coupled assay,[19] this assay was used to follow the purification of DHDPR (see Chapter Three). However, DHDPR is unusually heat resistant[19] and can withstand treatment at 70 °C for 3 minutes without undue loss of activity; such treatment was employed to destroy contaminating enzyme activity of homoserine dehydrogenase and NADPH oxidase. Immediately after the ultrasonication the heat shock was performed, thus, removing the contaminating NADPH utilising enzymes as early as possible. This varies from the reported purification where the heat shock was performed as the final step.[5]

A 20 - 60% ammonium sulfate precipitation was then performed, this was found to contain more DHDPS enzyme than the 48 - 65% precipitation used by Kraunsoe.[5] The precipitated proteins were harvested by centrifugation. The pellet of cells was redissolved in buffer and dialysed to remove any excess ammonium sulfate so that ion exchange could be performed. A Q-Sepharose anion exchange column (rather than DE-52 cellulose as reported previously[5]) was then used to effect ion exchange chromatography and elution was performed using a buffered sodium chloride gradient, DHDPR eluted between 0.6 and 0.9 M sodium chloride concentration and the active fractions were pooled.

DHDPR was purified to a specific activity of 2.25 $\mu mol \cdot s^{-1} mg^{-1}$ of protein. The purified enzyme was homogeneous as judged by SDS-PAGE, stained with Coomassie Brilliant Blue. Its electrophoretic mobility corresponded to a monomer of molecular mass ~29 kDa (DHDPR exists as a homotetramer in its native form) see figure 1-13.

Figure 1-13: SDS-PAGE of DHDPR purified enzyme

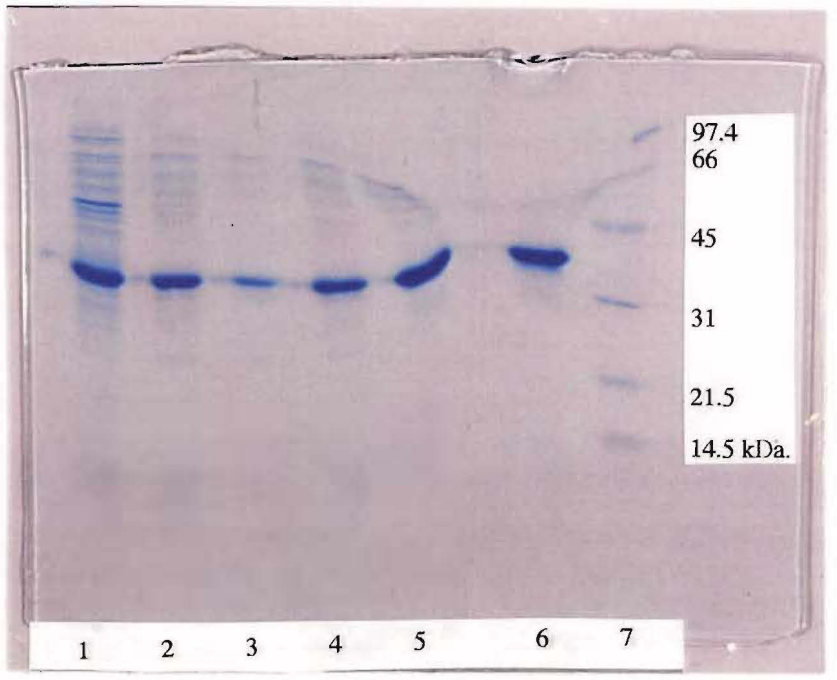

Lane 1 DHDPR crude extract.
Lane 2 DHDPR heat shock supernatant.
Lane 3 DHDPR 20 - 60% ammonium sulfate cut.
Lane 4 DHDPR dialysed sample.
Lane 5 DHDPR ion exchange.
Lane 6 DHDPR ion exchange.
Lane 7 Molecular weight markers: 14.5, 21.5, 31, 45, 66, 97.4 kDa.

During the course of these studies *E. coli* DHDPR was crystallised by Scapin *et al.*[20] Their purification[21] used a French press to obtain the crude extract of cells. This extract was treated with streptomycin sulfate, then dialysed, following which Q-Sepharose and gel filtration chromatography were performed. Ion exchange chromatography on a high performance anion exchange column was performed as the final step. This purification was more involved than the above procedure, although the fundamental steps of charge-based purification and sized-based purification are common to both procedures. Although their purification is complicated, it does yield very high quality enzyme that was able to be crystallised, whereas the purification developed above is fast and simple and yields protein that is suitable for enzyme kinetic studies.

Summary

Both the DHDPS and DHDPR enzymes were able to be over-expressed in *E. coli* and purified for use in enzyme kinetic studies. The purification of DHDPS was based on previous purifications,[2,14,15] however, it was optimised to give a fast and efficient purification. The purity of the DHDPS was greatly enhanced by the use of a Resource Q-Sepharose column; DHDPS was purified to an activity of 4.7 x 10^{-1} $\mu mol \cdot s^{-1} mg^{-1}$. The purification of DHDPR was also modified from existing procedures,[5,17] again providing a fast and efficient purification of the enzyme. Purified DHDPR had a specific activity of 2.25 $\mu mol \cdot s^{-1} mg^{-1}$. As both enzymes were obtained in high purity (~90%), they were appropriate for use in enzyme kinetic studies.

References

1. D.W. Tudor, T. Lewis, D.J. Robins *Synthesis* 1061, (1993).
2. J.A. Gerrard *'Studies on Dihydrodipicolinate Synthase'* D. Phil., Brasenose College, Oxford (1992).
3. S. Black, N. Wright *J. Biol. Chem.* **213**, 39 (1955).
4. C.V. Coulter, J.A. Gerrard, J.A.E. Kraunsoe, D.J. Moore, A.J. Pratt *Tetrahedron* **52**, 7127 (1996).
5. J.A.E. Kraunsoe *'Studies in Lysine Biosynthesis'* Part II, Corpus Christi College, Oxford (1992).
6. B.M. Trost (Ed.) *'Comprehensive Organic Synthesis'* Vol. 7 Oxidation, Pergamon Press, Oxford (1991).
7. R. Pappo, D.S. Allen (Jr), R.U. Lemieux, W.S. Johnson *J. Org. Chem.* **21**, 478 (1956).
8. N.F. Albertson *J. Am. Chem. Soc.* **68**, 450 (1946).
9. H.K. Chenault, J. Danmer, G.M. Whitesides *J. Am. Chem. Soc.* **111**, 6354 (1989).
10. R.L. Shriner, C.J. Hull *J. Org. Chem.* **10**, 228 (1945).
11. F. Richard, C. Richard, C. Haziza, J-C. Patte *C. R. Acad. Sc. Paris, Serie III,* **t 293**, 1362 (1981).
12. J.H. Miller *'A short course in bacterial genetics: a lab manual and handbook for* E. coli *and related bacteria'* Cold Spring Harbour Lab Press, N.Y. (1992).
13. E. Southern *Meth. Enz.* **68**, 152 (1979).
14. Y. Yugari, C. Gilvarg *J. Biol. Chem.* **240**, 4710 (1965).
15. J.G. Shedlarski *Meth. Enz.* **17b**, 129 (1971).
16. B. Laber, F-X. Gomis-Ruth, M.J. Romao, R. Huber *Biochem. J.* **288**, 691 (1992).
17. H. Tamir, C. Gilvarg *J. Biol. Chem.* **249**, 3034 (1974).
18. E.L. Harris, S. Angal (Eds) *'Protein Purification. A practical approach'* IRL Press, Oxford (1992).

19. W. Farkas, C. Gilvarg *J. Biol. Chem.* **240**, 4717 (1965).
20. G. Scapin, J.S. Blanchard, J.C. *Sacchettini Biochemistry* **34**, 3502 (1995).
21. S.G. Reddy, J.C. Sacchettini, J.S. Blanchard *Biochemistry* **34**, 3492 (1995).

Results and Discussion Chapter Two

DHDPS and DHDPR kinetics

Introduction

In order to study the kinetic properties of the two enzymes DHDPS and DHDPR a quantitative assay was required. This assay could then be used to undertake systematic kinetic studies on the two enzymes. The parameters of immediate interest were K_m and V_{max} values for both substrates of DHDPS, that is *(S)*-aspartate β-semialdehyde (11) and pyruvate (17), and for the substrate of DHDPR. In the case of DHDPR the parameters for the two possible cofactors, NADPH and NADH, were also required.

Assay methods

To obtain quantitative results the assay had to be capable of accurately measuring the initial rate of the enzyme catalysed reaction. The kinetics of both DHDPS and DHDPR were being studied, therefore, either two separate assays were required, or an assay that could be adapted to measure the activity of both of these enzymes. For DHDPS there are three assays in the literature: the imidazole buffer assay,[1] the *o*-aminobenzaldehyde assay,[1] and a coupled assay.[1,2] The *o*-aminobenzaldehyde assay yields qualitative results while both the imidazole buffer assay and the coupled assay have previously been used to obtain quantitative results. The coupled assay is also capable of measuring the kinetics of DHDPR.

The imidazole buffer assay for DHDPS activity

The imidazole buffer assay involves monitoring a rise in absorption at 270 nm on incubation of the DHDPS enzyme and its substrates (*(S)*-aspartate β-semialdehyde (11) and pyruvate (17)) in imidazole buffer.[1] Despite the fact that this assay seems relatively simple, some major problems are encountered; thus, making it unsuitable for generating detailed, readily interpretable, quantitative kinetic measurements. The exact nature of the chromophore formed from the imidazole buffer reacting with the enzymatic product is unknown. There is also a lag phase before the absorbance at 270 nm increases. While this assay assumes that the rate of the DHDPS enzyme catalysed reaction is rate determining this lag phase suggests that the formation of the chromophore detected at 270 nm may be the rate determining step. Thus, it is questionable whether the rate measured is actually the initial rate of the DHDPS catalysed reaction. However, since it is easy to perform, this assay continues to be used by other workers.[3]

The o-aminobenzaldehyde assay for DHDPS activity

The addition of *o*-aminobenzaldehyde (55) (as synthesised from *o*-nitrobenzaldehyde by the method of Smith and Opie[4]) to a solution containing the DHDPS catalysed reaction (the DHDPS enzyme and both substrates, *(S)*-aspartate β-semialdehyde (11) and pyruvate (17)) immediately results in a yellow solution which slowly develops a deep purple chromophore during the enzyme catalysed reaction; the latter colour fades over time. The formation of the purple chromophore can be enhanced, after the enzyme-catalysed reaction, by treatment with acid, such as 10% trichloroacetic acid. This assay is an extremely useful qualitative tool that was used to follow DHDPS protein purification; as it is both highly specific and extremely sensitive, detecting low levels of DHDPS present in crude extracts.

However, again there are several problems with this assay which limits its effectiveness for quantitative work. The nature of the purple chromophore has yet to be determined, although it has been estimated that the extinction coefficient (ε) is 1.224 x 10^{-3} $M^{-1}cm^{-1}$ at 540 nm at pH 8.5.[5] It is assumed that the rate of formation of the product, rather than the rate of complex formation, is the rate determining step. As with the imidazole buffer assay, a lag period, of at least 10 minutes, is associated with the generation of the measured chromophore. After the absorbance reaches its maximum it then slowly decreases over approximately two hours. To avoid the problem of a lag phase most workers leave the reaction for a specified period of time, generally 30 minutes, before recording the rate.[6] Thus, it is not clear which rate, that of the enzyme catalysed reaction or that of the purple complex formation, is being measured.

It has been hypothesised that the product of the enzymatic reaction is oxidised to dipicolinate (36),[3] which then reacts with *o*-aminobenzaldehyde (55) to form the purple chromophore, see figure 2-1. However, we found addition of *o*-aminobenzaldehyde (55) to dipicolinic acid (36) solutions does not result in the formation of a purple adduct, even under the exact conditions of the assay where acid is added.

Figure 2-1: Oxidation of dihydrodipicolinate (18) to dipicolinate (36)

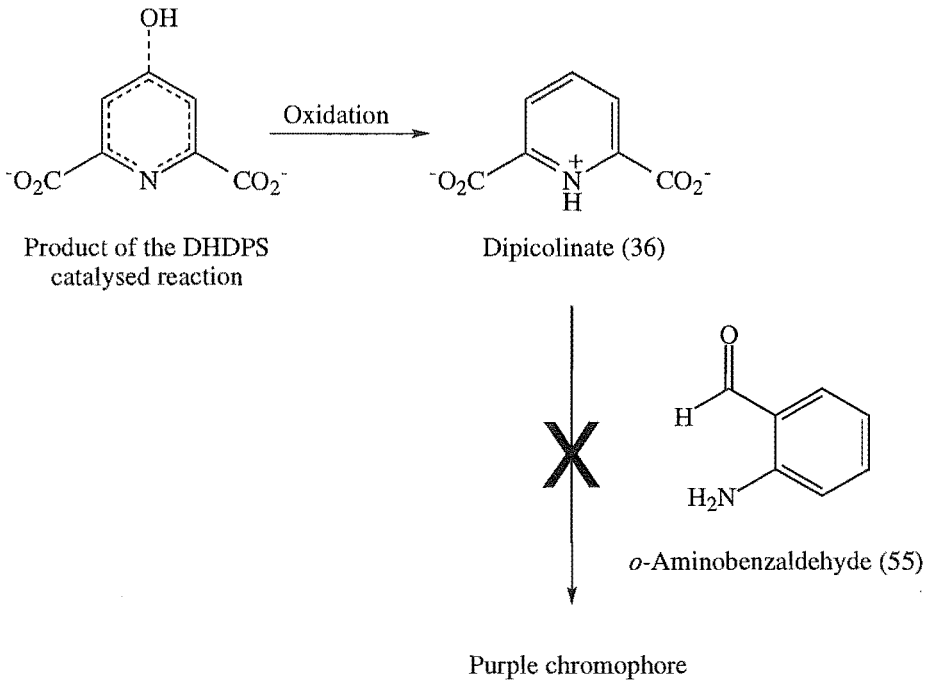

Product of the DHDPS catalysed reaction

Dipicolinate (36)

o-Aminobenzaldehyde (55)

Purple chromophore

Gerrard[7] hypothesised that the product of the DHDPS catalysed reaction initially forms a yellow dihydroquinazolium salt (56) (*o*-aminobenzaldehyde is known to form a yellow chromophore with imines[8]—this has been used to test for imines present in other biosynthetic pathways[9]). This dihydroquinazolium salt (56) may undergo further changes on standing which are enhanced by acid treatment, to generate the purple dihydroquinazolium salt (57)—detected at 540 nm, see figure 2-2. However, due to the instability of the purple complex, there is little evidence to support either of these hypothesised structural changes.

Figure 2-2: Possible reaction of dihydrodipicolinate with o*-aminobenzaldehyde to form the purple chromophore as suggested by Gerrard*[7]

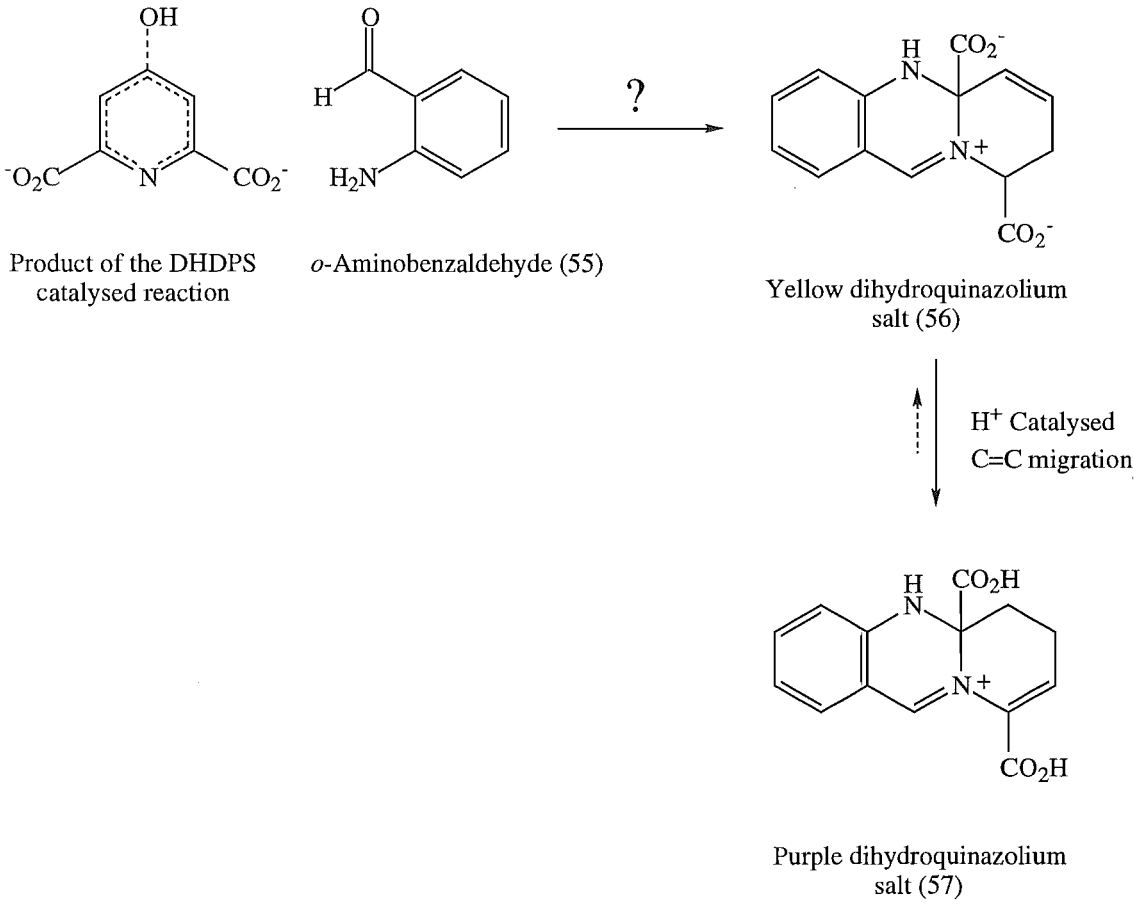

Product of the DHDPS catalysed reaction

o-Aminobenzaldehyde (55)

Yellow dihydroquinazolium salt (56)

Purple dihydroquinazolium salt (57)

It is obvious that, while the *o*-aminobenzaldehyde assay can be used for qualitative measurements, it is not suitable for quantitative work. Clearly, the product of the DHDPS catalysed reaction forms a purple complex in the presence of *o*-amino-benzaldehyde (55), the intensity of which is increased by acid treatment. The concentration of this adduct can be estimated by monitoring the absorbance at 540 nm. Anything further than this is conjecture. The *o*-aminobenzaldehyde assay was used during all stages of the purification of the DHDPS enzyme, but it was not used for kinetic studies.

The coupled assay for DHDPS and DHDPR activity

A coupled enzyme assay typically refers to following the activity of an enzyme by monitoring the activity of another enzyme that utilises the product of the first enzyme. If the second enzyme is present in excess, then the rate of reaction will depend entirely on the rate of the first reaction. This method is usually employed if the enzyme of interest is difficult to monitor but an enzyme catalysing a reaction of the product is relatively easy to monitor—say, by the reduction or oxidation of a nicotinamide cofactor. The DHDPS-DHDPR coupled assay involves following the activity of DHDPS by monitoring the activity of the following enzyme DHDPR, which is a NADPH dependent enzyme. Thus,

the activity can be measured by following the decrease in absorbance at 340 nm corresponding to the oxidation of NADPH to $NADP^+$,[1] see figure 2-3. This is easily quantifiable because, while NADPH has a strong absorbance at 340 nm (the extinction coefficient, ε_{340}, is 6.3 x 10^3 $M^{-1}cm^{-1}$) $NADP^+$ exhibits negligible absorbance at this wavelength,[10,11] see figure 2-4. This assay is able to measure DHDPS kinetics if DHDPR is present in excess, since under these conditions DHDPS becomes rate limiting. DHDPR kinetics can also be measured, if DHDPS is present in excess, as then DHDPR becomes rate limiting.

Figure 2-3: The coupled assay

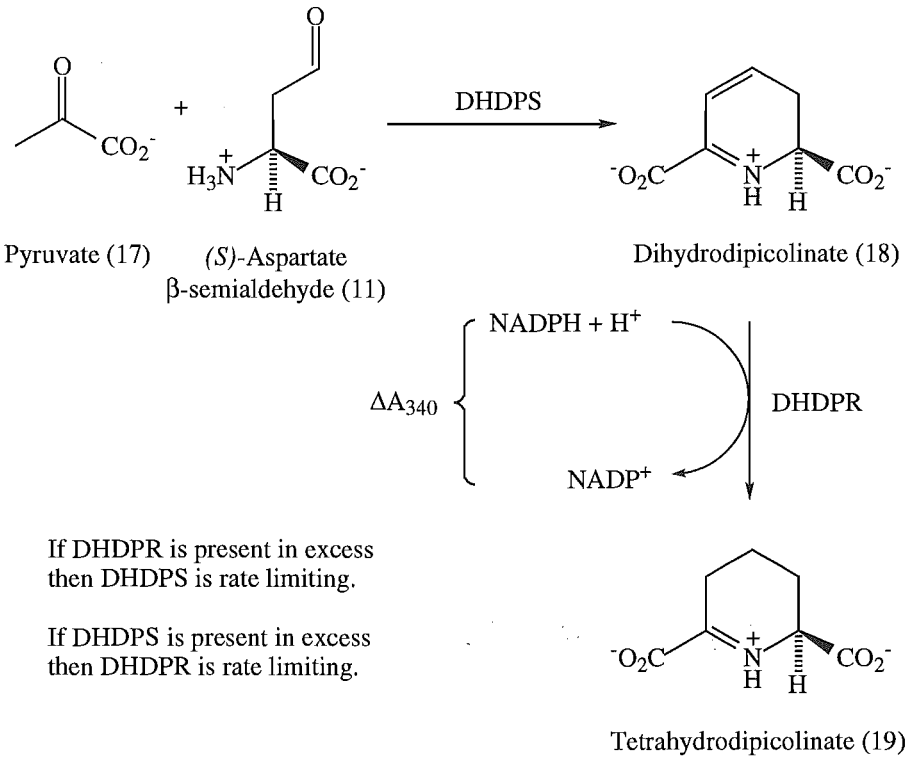

Figure 2-4: NADPH

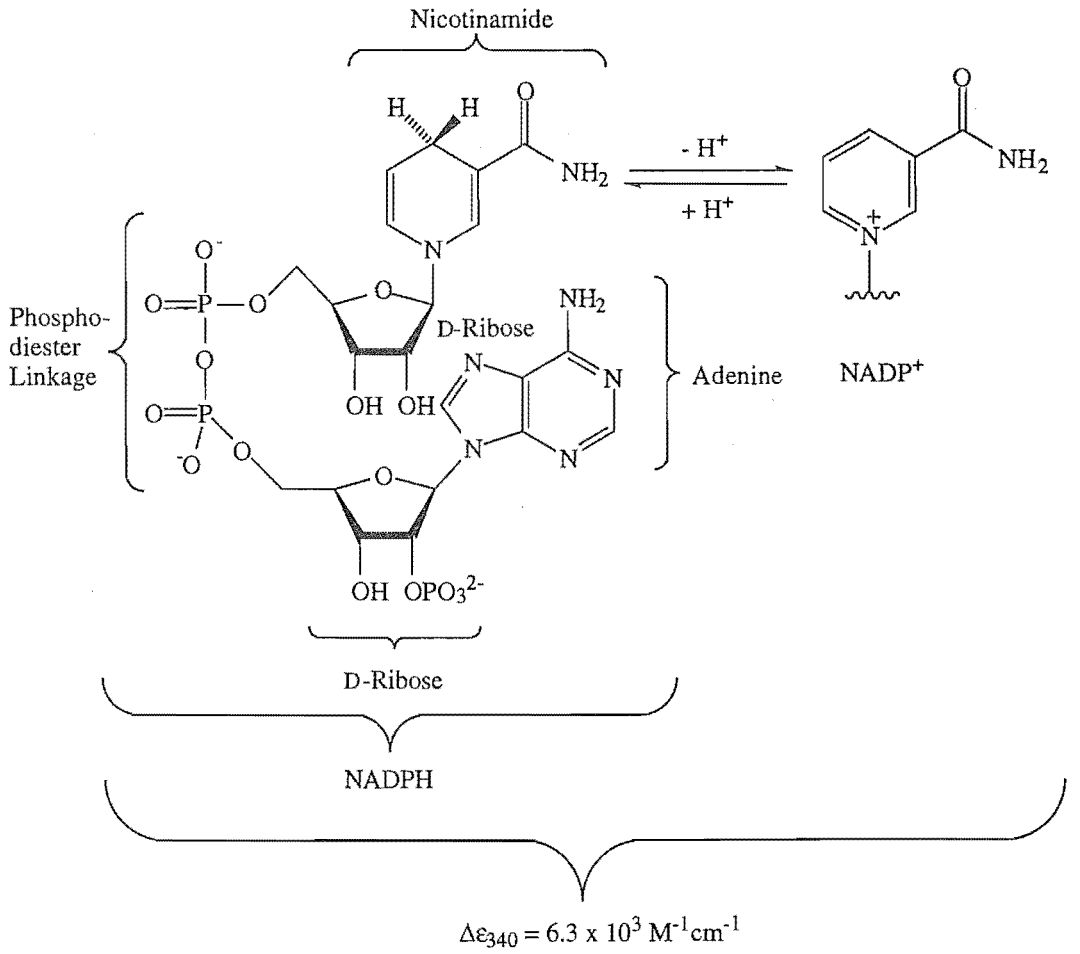

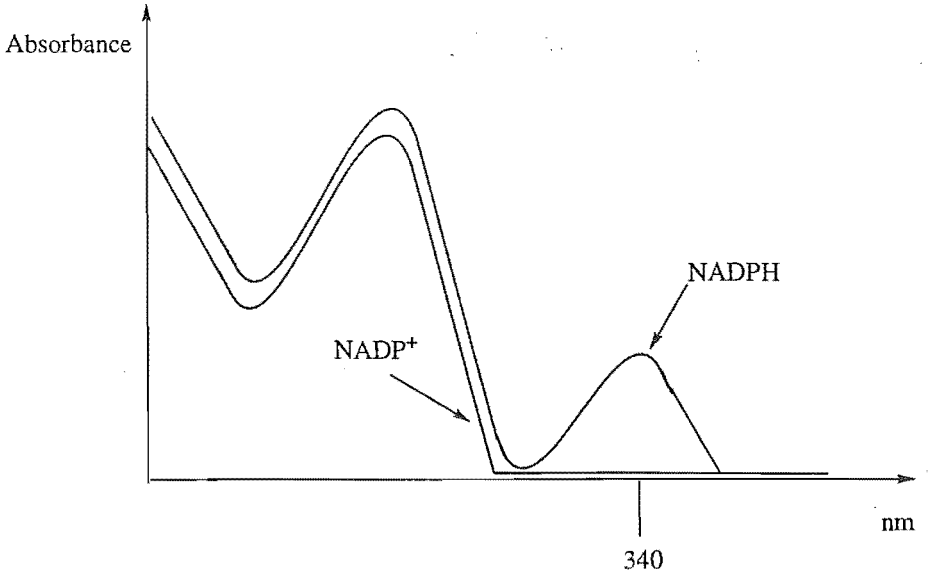

DHDPR activity can also be measured using this assay by following the decrease in absorbance at 340 nm, due to the conversion of NADPH to $NADP^+$. Since the use of chemically synthesised substrate is problematic (a mixture of compounds and isomers results and it is not known which is utilised by DHDPR)[12] DHDPS provided a convenient means of generating the substrate for DHDPR *in situ*.

Although the coupled assay was originally used by Yugari and Gilvarg in 1965,[1] it was little used until recently. With the ease of obtaining large (milligram) quantities of DHDPS and DHDPR, using molecular biological techniques, there has been a resurgence in the use of this assay.[13] This assay is ideal, giving sensitive and quantitative measurements of initial enzymatic rates of both the DHDPS and the DHDPR catalysed reactions.

Modifications to the coupled assay

The coupled assay was used to measure the kinetics of DHDPS and DHDPR since plentiful supplies of purified DHDPS and DHDPR, and *(S)*-aspartate β-semialdehyde (11) were available (see Chapter One). It was however optimised to make it most effective for the range of kinetic investigations under scrutiny.

The pH optimum of DHDPS is 8.4,[1] but it is advantageous to run the assay at near physiological pH, to best mimic the true biological situation. The original coupled assay measuring DHDPS activity used Tris buffer at pH 7.4.[1] However, due to the inadequate capacity of Tris to buffer near physiological pH (pH 7) an alternative buffer was sought. The buffering capacities of Hepes, Mops, Bis-Tris, and Mes are well known. Mops gives superior buffering capacity to Tris at pH 7.5 and below. At pH 7.5 Tris did not have significant buffering action to counteract the addition of *(S)*-aspartate β-semi-aldehyde as the trifluoroacetate salt, and consistent kinetics could not be obtained, as analysed by the Michaelis-Menten model and plotted on a Lineweaver-Burk (1/Rate versus 1/[Substrate]) plot (see the Appendix for the mathematical analysis of the Michaelis-Menten model and the Lineweaver-Burk plot, including a note on the units of activity used). Mops was found to buffer the assay adequately at pH 7.2, and consistent kinetics were obtained allowing K_m and V_{max} to be calculated. Using Mops buffer the pH of the assay mixture could be reduced to 6.8 and Michaelis-Menten kinetics were maintained, however, the K_m and V_{max} values did decrease significantly with the lowering of the pH. Since the substrate *(S)*-aspartate β-semialdehyde (11) is more stable at lower pH, as are some of the possible inhibitors that we wished to test we opted for Mops buffer at pH 7.2 as the best compromise for the coupled assay, this was close to physiological pH and still maintained reasonable enzyme activity. Table 2-1 shows the results of the kinetic studies while varying the buffer and pH, while figure 2-5 shows the Lineweaver-Burk plot of the DHDPS kinetics in Mops buffer at pH 7.2.

Table 2-1: DHDPS kinetic parameters while altering the buffer and pH, using (R,S)-*aspartate β-semialdehyde (11)*

Buffer and pH at 25 °C	K_m x 10^{-4} M	V_{max} x 10^{-1} µmol·$s^{-1}$$mg^{-1}$
Tris pH 7.5	-	-
Mops pH 7.5	5.11	11.4
Mops pH 7.4	2.63	7.46
Mops pH 7.3	2.73	6.98
Mops pH 7.2	2.67	3.67
Mops pH 7.1	1.66	4.91
Mops pH 7.0	1.78	3.87
Mops pH 6.9	1.30	2.98
Mops pH 6.8	1.12	2.24

Figure 2-5: Lineweaver-Burk plots of the results of the DHDPS assay utilising Mops buffer at pH 7.2

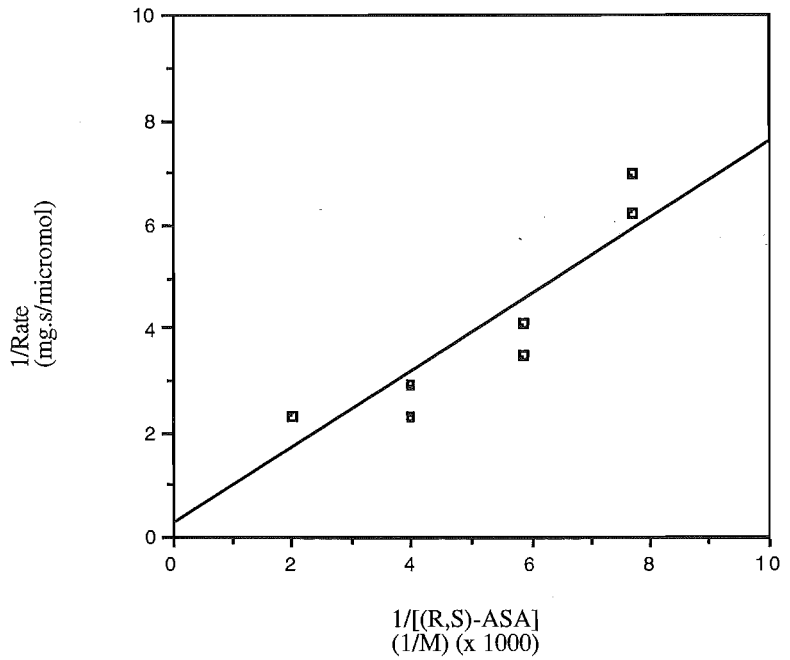

Enzyme kinetics of DHDPS

Enzyme kinetics of DHDPS, with respect to *(S)*-aspartate β-semialdehyde (11), were measured using the coupled assay with DHDPR present in an approximate 10-fold excess, and pyruvate (17) present in excess at 40 mM. The concentration of *(S)*-aspartate β-semialdehyde (11) was varied between 0.06 and 0.25 mM. Readings were taken in duplicate and the experiment was repeated until consistent kinetics were obtained. The results were interpreted in terms of the Michaelis-Menten model, analysing initial rates of reaction by Lineweaver-Burk (1/Rate versus 1/[Substrate]), Eadie Hofstee (Rate versus Rate/[Substrate]), and direct linear (Rate versus -[Substrate]) plots (detailed mathematical analysis of these three types of plots described are given in the Appendix).[14]

All three plots (Lineweaver-Burk, Eadie Hofstee, and direct linear) were used as each estimates the kinetic parameters K_m and V_{max} by slightly different mathematical approximations. The Lineweaver-Burk plot uses the reciprocal of both the rate and the concentration. This can lead to grouping of points distorting the appearance of any experimental error in the rate, making it difficult to judge which points are most accurate when plotting a straight line through the set of points. The Eadie-Hofstee plot does not have this same inherent problem, as the reciprocal of the concentration is modulated by being multiplied by the rate. With the direct linear plot a set of all possible K_m and V_{max} values are obtained for each rate measured at the various concentrations. This gives a range of values of which the median is taken to be the most accurate combination of K_m and V_{max}. The median is used as some pairs of lines may be nearly parallel and therefore some of the intersection points may be far from the correct values; such widely inaccurate estimates have a serious effect on the calculation of the mean, but hardly any effect on the median.

The three plots gave comparable values of K_m and V_{max}, see table 2-2 and figure 2-6. The Lineweaver-Burk plot does not suffer undue distortion as the values representing the inverse of the substrate concentration are evenly spaced. The data points are tightly grouped on either side of the line of best fit, thus, this plot gives an accurate estimate of K_m and V_{max}. The Eadie-Hofstee plot also has well spaced data points, again accurately estimating K_m and V_{max}. The direct linear plot has a small range of K_m and V_{max} values, this reflects the high accuracy of the data, and the median agrees well with the values from the two other plots.

Table 2-2: DHDPS kinetic parameters with respect to (S)-*aspartate β-semialdehyde (11)*

Type of plot	K_m x 10^{-4} M	V_{max} x 10^{-1} μmol·$s^{-1}$$mg^{-1}$
Lineweaver-Burk	1.24	7.08
Eadie-Hofstee	1.03	6.50
Direct linear	1.38	7.23

Figure 2-6: Kinetic plots of DHDPS activity with respect to (S)-*aspartate β-semi-aldehyde (11)*

(i) Lineweaver-Burk plot

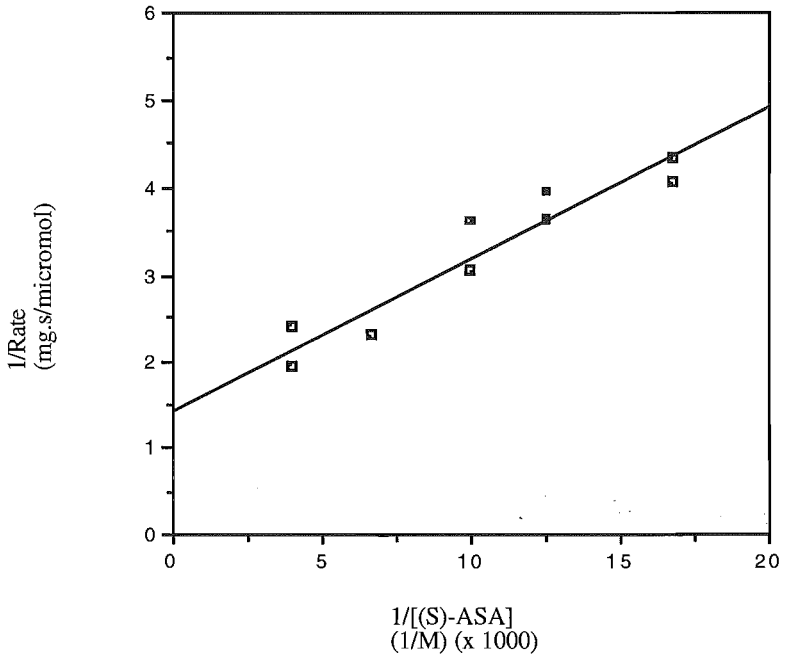

(ii) Eadie-Hofstee plot

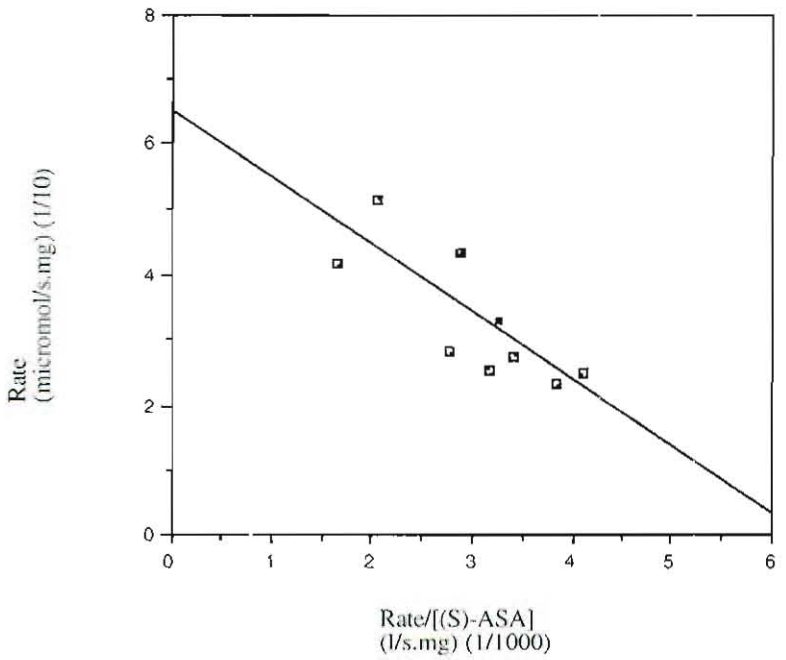

(iii) Direct linear plot

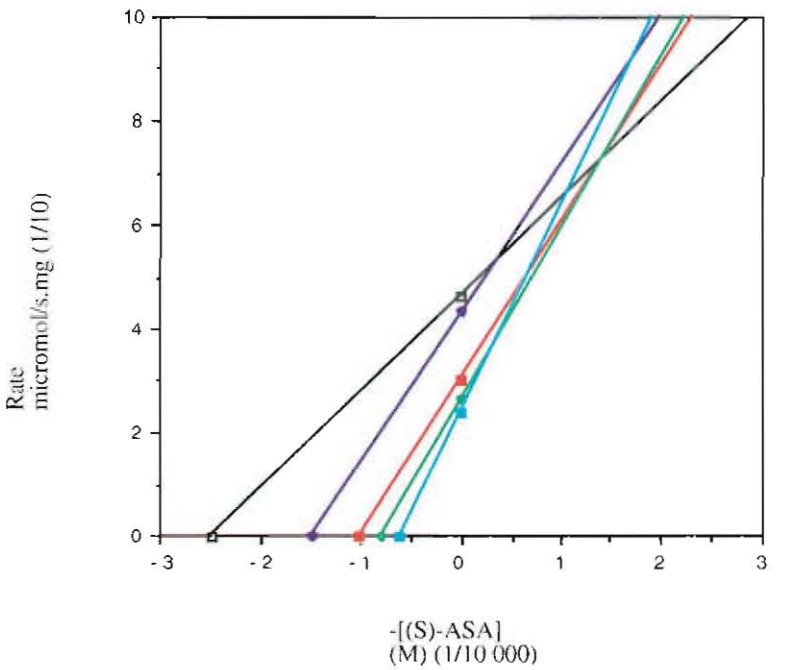

The range of the K_m for *(S)*-aspartate β-semialdehyde (11), from the plots above, was found to be (1.0 - 1.4) x 10^{-4} M and the range of V_{max} was found to be (6.5 - 7.2) x 10^{-1} $\mu mol \cdot s^{-1} mg^{-1}$. These values are similar to those obtained by Yugari and Gilvarg[1] who also used the coupled assay. At pH 7.4, at 25 °C, they found the K_m to be 1.3 x

10^{-4} M. Karsten[13] reports a K_m of (1.7 ± 0.1) x 10^{-4} M using the coupled assay. All these three values are considerably lower than those obtained using the imidazole buffer assay. For example, Couper *et al.*[3] report the K_m to be 2.3 x 10^{-4} M, while Laber *et al.*[15] report the K_m to be 5.5 x 10^{-4} M, although this last value is probably twice the true value as racemic aspartate β-semialdehyde (11) was used.

DHDPS from other bacterial sources are reported to have K_m values for *(S)*-aspartate β-semialdehyde (11) in the millimolar range, approximately 10 fold larger than that determined here for the *E. coli* enzyme. For example the *Bacillus subtilis* K_m was 3.13 x 10^{-3} M,[≠16] the *B. licheniformis* K_m was 2.6 x 10^{-3} M,[17] the *B. sphaericus* K_m was 5.1 x 10^{-3} M,[≠18] and the *Corynebacterium glutamicum* K_m was 6.2 x 10^{-3} M.[≠19] While sporulating *B. megaterium* had a K_m for aspartate β-semialdehyde (11) comparable to that calculated for *E. coli*, this K_m was 4.6 x 10^{-4} M.[≠20] (Where ≠ values were measured using racemic aspartate β-semialdehyde (11).)

DHDPS from various plant sources are reported to have K_m values for *(S)*-aspartate β-semialdehyde (11) in the millimolar and 10 fold lower range, for example the pea K_m is 4.0 x 10^{-4} M,[≠21] the maize K_m is 6.0 x 10^{-4} M,[≠22] the wheat K_m is 1.6 x 10^{-3} M,[≠23] and the spinach leaf K_m is 1.4 x 10^{-3} M.[≠24]

The kinetic parameters of DHDPS with respect to pyruvate (17) were also determined. In this case *(S)*-aspartate β-semialdehyde (11) was present in excess at 2.5 mM, while pyruvate (17) was varied between 0.05 and 0.5 mM. Again all three plots (Lineweaver-Burk, Eadie-Hofstee, and direct linear plots) were used and gave comparable K_m and V_{max} values, see table 2-3. In this case the Lineweaver-Burk plot reflects the high quality of the data where the data points are well spaced and close to the line of best fit, see figure 2-7.

Table 2-3: DHDPS kinetic parameters with respect to pyruvate (17)

Type of plot	K_m x 10^{-4} M	V_{max} x 10^{-1} μmol·s^{-1}mg^{-1}
Lineweaver-Burk	1.14	4.76
Eadie-Hofstee	1.12	4.85
Direct linear	1.34	5.49

Figure 2-7: Kinetics plot of DHDPR activity with respect to pyruvate (17)
(i) Lineweaver-Burk plot

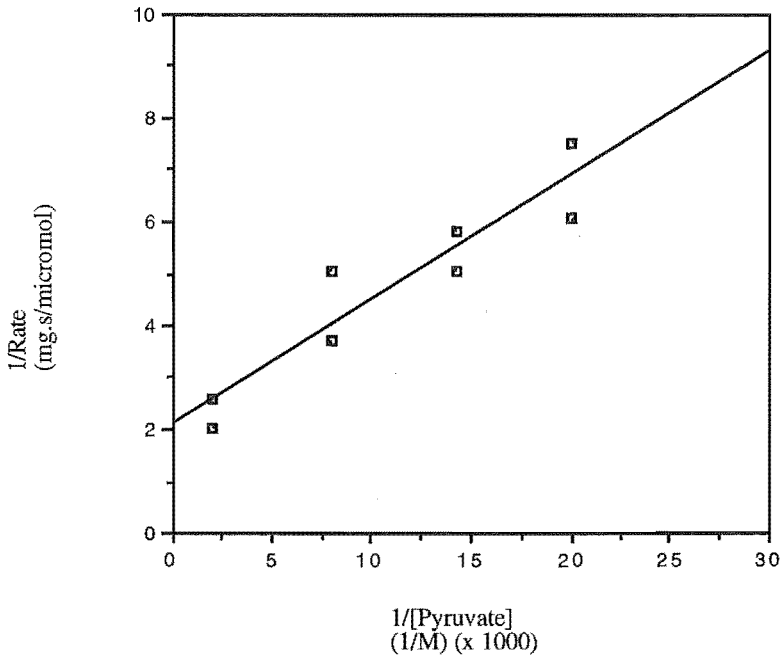

The range of K_m (for pyruvate), from the above plots, was found to be (1.1 - 1.3) x 10^{-4} M and the range of V_{max} was found to be (4.8 - 5.5) x 10^{-1} $\mu mol \cdot s^{-1} mg^{-1}$. Again, these values are much closer to those obtained using the coupled assay by Yugari and Gilvarg,[1] who report a K_m of 2.5 x 10^{-4} M, and by Karsten,[13] where K_m was reported as (1.7 $\pm$ 0.3) x 10^{-4} M (at pH 8), than those obtained using the imidazole buffer, for example Laber *et al.*,[15] report a K_m of 5.7 x 10^{-4} M.

DHDPS K_m values for pyruvate (17) can be compared with those from a range of different sources, for example the *Bacillus subtilis* K_m is 1.07 x 10^{-3} M,[16] the *B. licheniformis* K_m is 5.3 x 10^{-3} M,[17] the *B. sphaericus* K_m is 9.0 x 10^{-3} M,[18] and the *B. megaterium* K_m is 5.0 x 10^{-3} M.[20] DHDPS from plant sources had similar K_m values, for example the pea K_m is 1.7 x 10^{-3} M,[21] the maize K_m is 2.1 x 10^{-3} M,[22] and the wheat K_m is 1.18 x 10^{-2} M.[23] Again the K_m values were 10 fold larger, in the millimolar range.

Possible inhibition of DHDPS by high substrate concentrations of* (S)-*aspartate β-semialdehyde

Previous literature has reported that substrate inhibition occurs at *(S)*-aspartate β-semialdehyde (11) concentrations greater than 2 mM for wheat DHDPS;[24] spinach DHDPS,[25] maize DHDPS,[22] and the *B. licheniformis* enzyme[26] also showed inhibition, although it was uncertain if this was true inhibition or an artefact of the assay.[24] No substrate inhibition by *(S)*-aspartate β-semialdehyde (11) has been reported for *E. coli*[15] or pea DHDPS.[21] No inhibition was observed on increasing the *(S)*-aspartate β-semialdehyde (11) concentration up to 2.5 mM, with pyruvate (17) at 10.0 mM or 5.0 mM. However, as pyruvate (17) is present at a reasonably high concentration this may protect against inhibition by *(S)*-aspartate β-semialdehyde (11). At pyruvate (17) concentrations of 1.0 mM and 5.0 mM, increasing the *(S)*-aspartate β-semialdehyde (11) concentration from 1.0 mM to 10 mM increased rather than decreased the rate, even though again pyruvate (17) should have been rate limiting. Thus, no evidence of inhibition by high concentrations of *(S)*-aspartate β-semialdehyde (11) was observed.

Feedback inhibition of* (S)-*lysine on DHDPS

DHDPS is a branch point enzyme in the synthesis of the aspartate family of amino acids. It is the first enzyme in the diaminopimelate pathway, thus, it is the first enzyme committed to *(S)*-lysine (12) biosynthesis. It is important that cells produce amino acids as required, otherwise costly metabolic products and energy are wasted. Thus, the synthesis of *(S)*-lysine (12) is regulated by the enzyme DHDPS in some organisms. In these organisms, DHDPS is feedback inhibited by *(S)*-lysine (12). As such, if high levels of *(S)*-lysine (12) are present in the cell, the DHDPS enzyme is inhibited and no further *(S)*-lysine (12) is synthesised.

Inhibition kinetics were run at a range of inhibitor and substrate concentrations, and kinetics were plotted on Lineweaver-Burk plots to estimate K_m and V_{max}, see table 2-4. Kinetics were also plotted as Dixon (1/Rate versus [Inhibitor]) and modified Dixon ([Substrate]/Rate versus [Inhibitor]) plots to determine the type of inhibition (competitive, noncompetitive, uncompetitive, or mixed) and to estimate the inhibition constant K_i (see the Appendix for detailed analysis of these plots). Inhibition of *(S)*-lysine (12) on DHDPS, with respect to *(S)*-aspartate β-semialdehyde (11), was shown to be uncompetitive as the Dixon plot comprises of a series of nearly parallel lines while the modified Dixon plot has a series of lines with a common intercept at a positive substrate concentration upon rate value. The K_i' was found to be in the range of (3.4 - 3.9) x 10^{-4} M, as determined from the modified Dixon plot, see figure 2-8.

Table 2-4: Kinetic parameters of the feedback inhibition of (S)*-lysine (12) on DHDPS activity with respect to* (S)*-aspartate β-semialdehyde (11)*

[*(S)*-Lysine] mM	K_m x 10^{-4} M	V_{max} x 10^{-1} µmol·$s^{-1}$$mg^{-1}$
0	1.19	6.03
0.25	1.34	4.59
0.50	1.13	3.70
0.75	0.916	3.16

Figure 2-8: Kinetic plots of the feedback inhibition of (S)*-lysine (12) on DHDPS activity with respect to* (S)*-aspartate β-semialdehyde (11)*

(i) Dixon plot

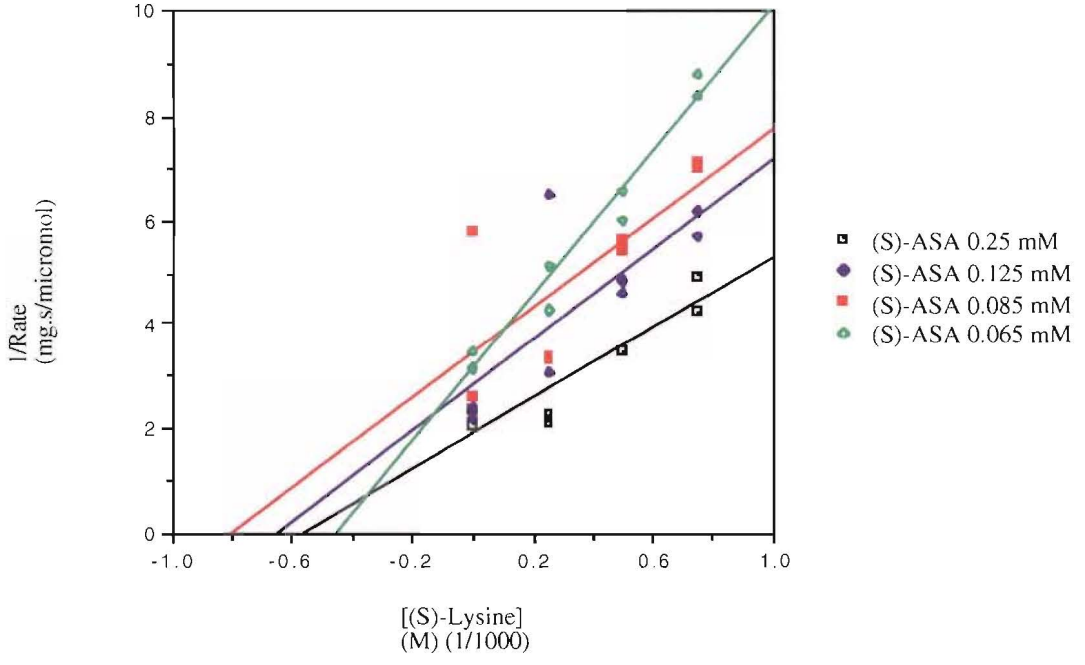

(ii) Modified Dixon plot

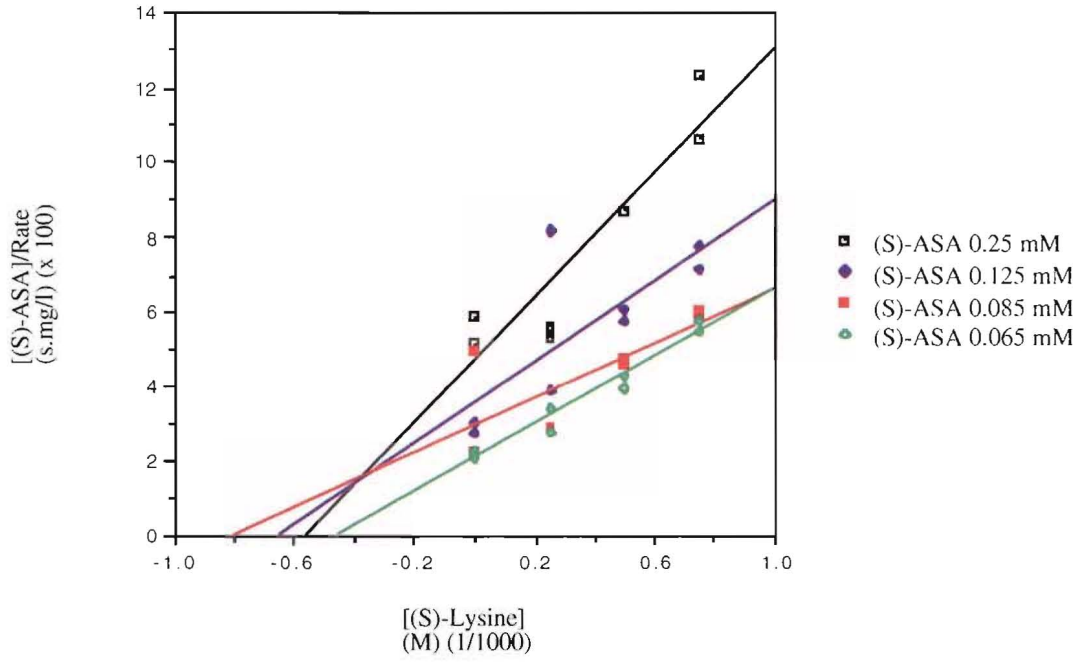

The inhibition of *(S)*-lysine (12) on DHDPS with respect to pyruvate (17) was also uncompetitive with a K_i' in the range of (3.1 - 3.8) x 10^{-4} M, again this value was determined from the modified Dixon plot, see table 2-5 and figure 2-9. These results suggest that the *(S)*-lysine (12) binding site is allosteric, that is at a site remote to the active site. However, because early results suggested there may be mixed inhibition, it is possible that the *(S)*-lysine (12) binding site may slightly overlap with the *(S)*-aspartate β-semialdehyde (11) binding site.

Recently[27,28] the allosteric binding site for *(S)*-lysine (12) has been localised by X-ray crystallography, where it was found to be at the dimer interface (DHDPS is a homotetramer made up of a dimer of dimers). It should also be noted that the word 'allosteric' implies a cooperativity effect, however, often the terms allosteric inhibitor and allosteric binding site are used when cooperativity has not been proven. Thus, they are often used to simply describe binding at a remote site as opposed to at the active site.

Table 2-5: Kinetic parameters of the feedback inhibition of (S)*-lysine (12) on DHDPS activity with respect to pyruvate (17)*

[*(S)*-Lysine] mM	K_m x 10^{-4} M	V_{max} x 10^{-1} µmol·s^{-1}mg^{-1}
0	1.22	6.58
0.25	1.34	6.19
0.50	0.615	3.89
0.75	0.531	3.02

Figure 2-9: Kinetic plots of the feedback inhibition of (S)*-lysine (12) on DHDPS activity with respect to pyruvate (17)*

(i) Dixon plot

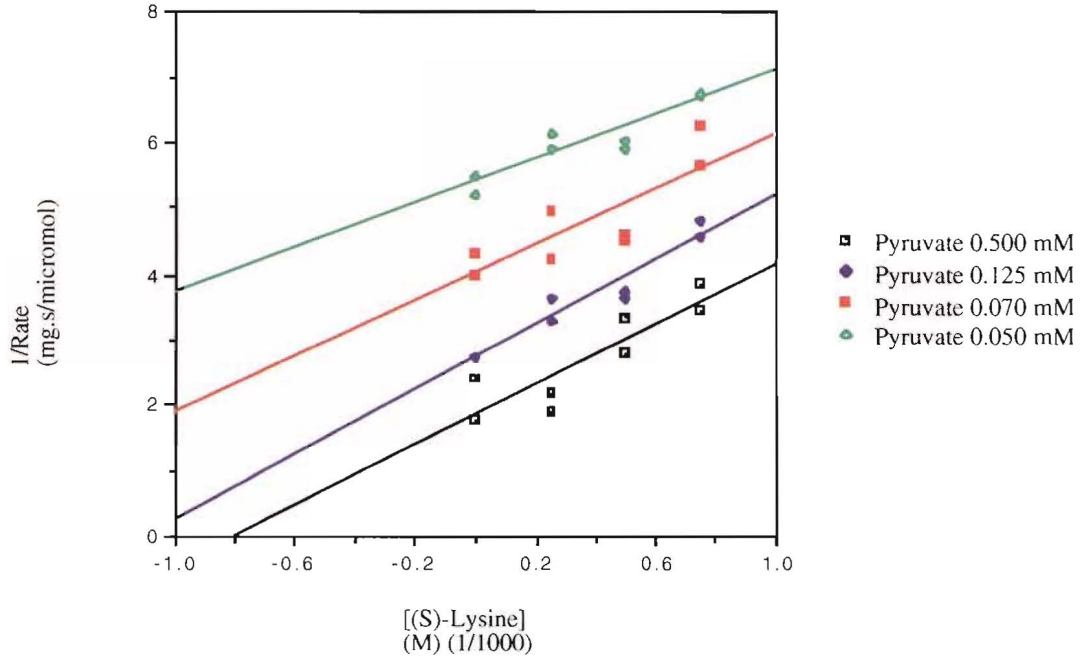

(ii) Modified Dixon plot

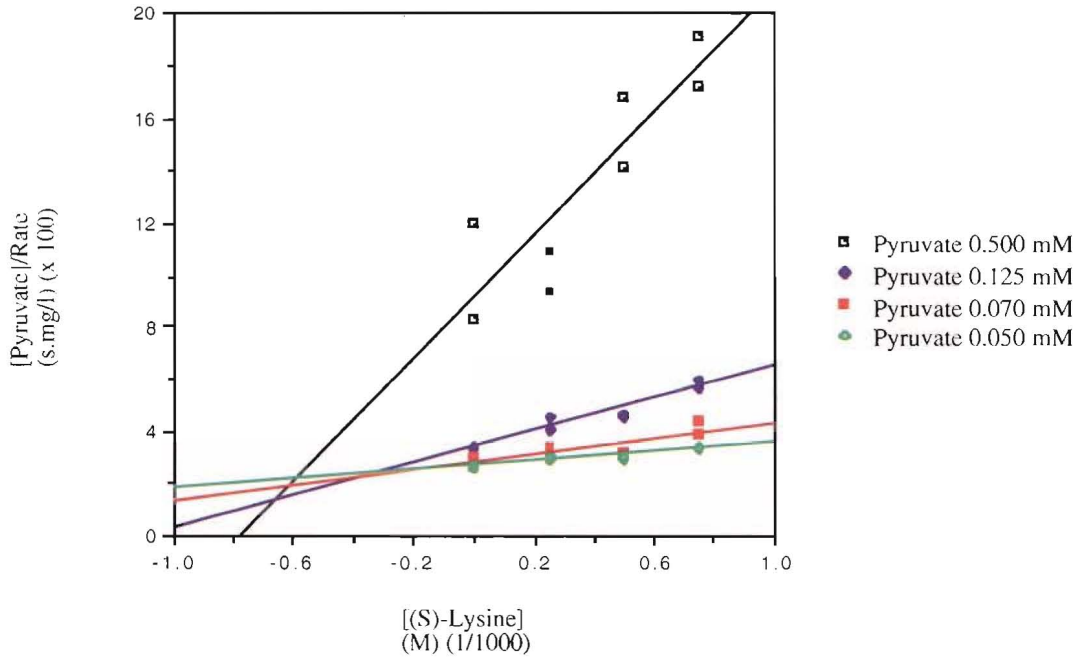

It has been reported[29] that feedback inhibition by *(S)*-lysine (12) on bacterial enzymes is not as significant as on plant enzymes. These results support this assertion. Typically the IC_{50} value for *(S)*-lysine (12) is 0.01 to 0.05 mM for DHDPS from plants,[21,22,23,24,25] but the IC_{50} value of bacterial DHDPS is around 1.0 mM.[15] Because of the weaker inhibition of *(S)*-lysine (12) on bacterial DHDPS than plant DHDPS, it is possible that introduction of bacterial DHDPS into plants might result in more nutritious crops. Transgenic crops such as wheat supplement with *E. coli* DHDPS are being studied with this in mind. Other crops under scrutiny include potato plants expressing *E. coli* DHDPS in their chloroplasts,[30] and tobacco plants expressing *E. coli* DHDPS.[31]

Enzyme kinetics of DHDPR

The kinetic studies of DHDPR were measured using the coupled assay following the oxidation of NADPH at 340 nm. The substrate of the DHDPR catalysed reaction was synthesised *in situ* from *(S)*-aspartate β-semialdehyde (11) by DHDPS. Since this product may be unstable (dihydropyridines are prone to oxidation in the air[32]) the *(S)*-aspartate β-semialdehyde (11) was added to the reaction cuvette as the penultimate ingredient of the assay, DHDPR being added last to initiate the enzymatic reaction. However, the *(S)*-aspartate β-semialdehyde (11) did have to be added at least five minutes before the assay was started, or the formation of the DHDPS product (rather than its utilisation) was rate-limiting and bi-phasic kinetics were observed over the five minutes of the assay, see figure 2-10.

Figure 2-10: DHDPR kinetics

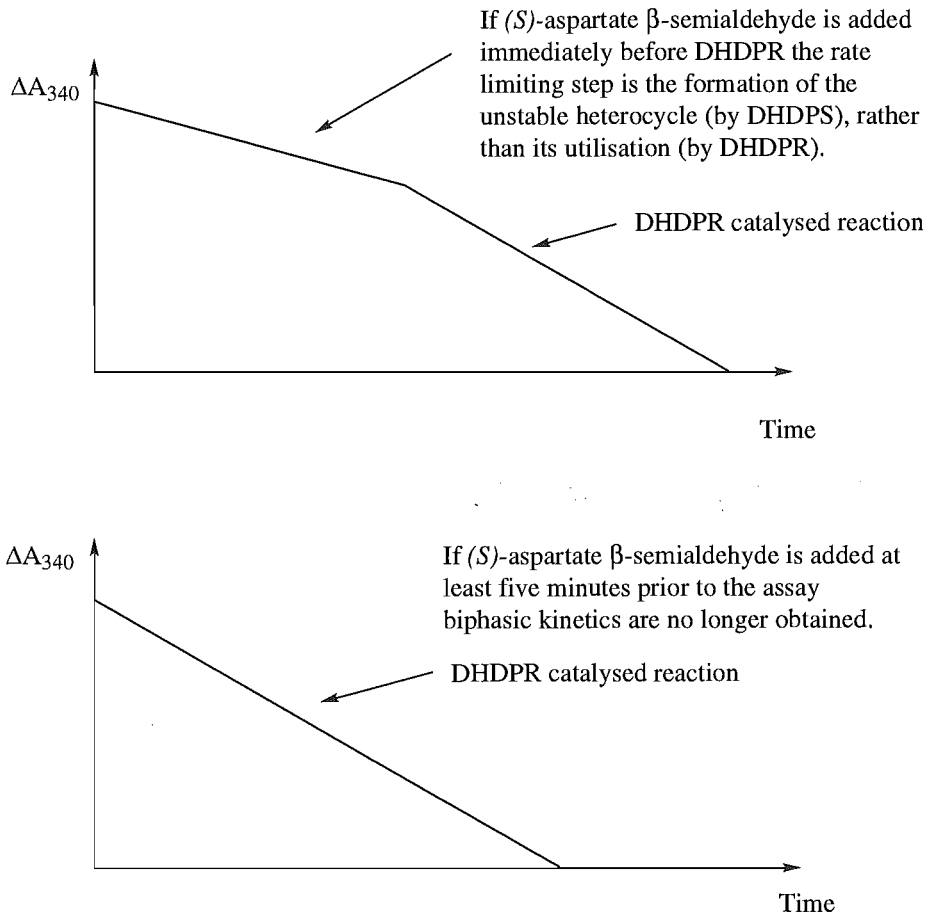

The K_m and V_{max} values of DHDPR with respect to the substrate were measured. DHDPS was present in approximately 10 fold excess of DHDPR, and pyruvate (17) was present in excess at 40 mM in the cuvette. A range of substrate concentrations from 0.05 to 0.30 mM were used, and NADPH was present at 0.162 mM. Readings were taken in duplicate and the experiment was repeated until consistent kinetics were obtained. The results were subject to Michaelis-Menten analysis using Lineweaver-Burk, Eadie-Hofstee, and direct linear plots to determine the kinetic parameters. All three methods

gave consistent estimates of the enzyme parameters K_m and V_{max}, see table 2-6. The Lineweaver-Burk plot (where the data points hardly deviate from the line of best fit) and the direct linear plot show that the data is highly consistent and accurate, see figure 2-11.

Table 2-6: DHDPR kinetic parameters with respect to the substrate

Type of plot	K_m x 10^{-4} M	V_{max} $\mu mol \cdot s^{-1} mg^{-1}$
Lineweaver-Burk	4.93	5.27
Eadie-Hofstee	5.04	5.39
Direct linear	5.29	5.71

Figure 2-11: Kinetic plots of DHDPR activity with respect to the substrate
(i) Lineweaver-Burk plot

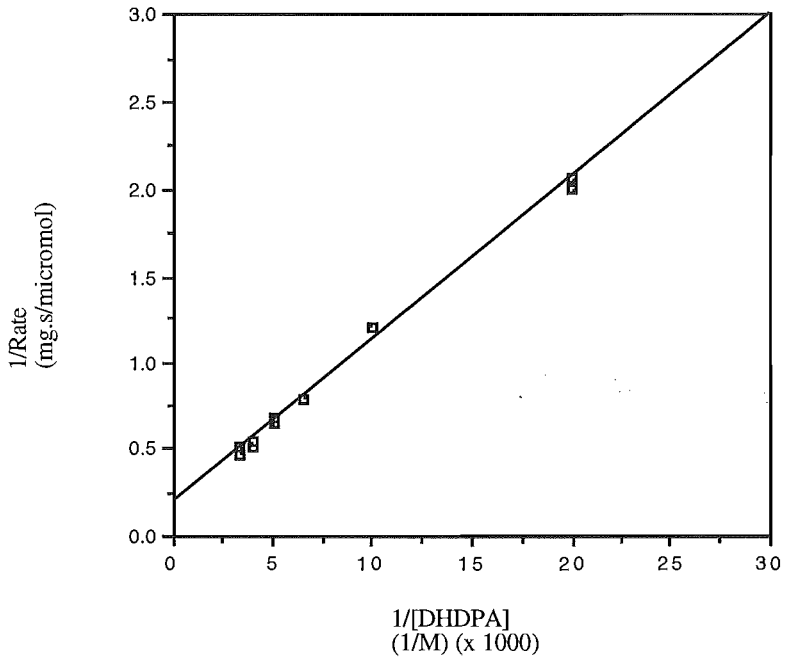

(ii) Direct linear plot

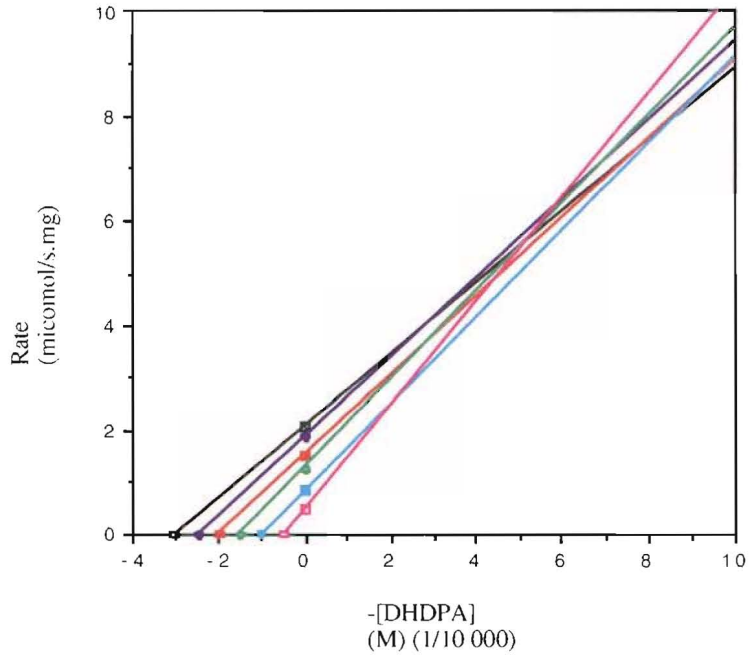

For DHDPR, with respect to the substrate, K_m was found to be in the range of (4.9 - 5.3) x 10^{-4} M, while V_{max} was found to be in the range of 5.3 - 5.7 $\mu mol \cdot s^{-1} mg^{-1}$. A variety of K_m values have been reported, for example previous studies on *E. coli* DHDPR by Kraunsoe[33] generated a K_m value of 1.90 x 10^{-4} M; which is comparable to the value given above. However, Tamir and Gilvarg[12] reported a much lower K_m of 9.0 x 10^{-6} M (at pH 7.5 in Tris buffer) for *E. coli* DHDPR. More recent studies on *E. coli* DHDPR by Reddy *et al.*[34] generated a K_m value of (5.0 $\pm$ 1.2) x 10^{-5} M.

In sporulating bacteria, for example *Bacillus* sp., the K_m of DHDPR with respect to substrate appears to vary very little. For *B. subtilis* K_m is 7.7 x 10^{-4} M,[35] for *B. cereus* K_m is 6.2 x 10^{-6} M,[36] and for *B. megaterium* K_m is 5.9 x 10^{-6} M.[36] In plants only maize DHDPR has been studied and this has a K_m similar to that obtained for *E. coli*, 4.3 x 10^{-4} M,[37] however this value was obtained using chemically synthesised dihydrodipicolinate (18) which exists as a mixture of compounds and isomers, not all of which can be utilised by DHDPR. Thus, this value may be artifically inflated. We expect DHDPR from the same source to have the same K_m, however DHDPR from different sources is likely to have different kinetic parameters even if there is a high degree of homology.

The K_m and V_{max} parameters of the cofactor, NADPH, of DHDPR were also determined. DHDPR is an unusual enzyme in that it can utilise NADPH or NADH; most nicotinamide dependent enzymes show a marked preference for one of these two cofactors.[34,38,39] However, due to the greater stability towards acid hydrolysis of

NADPH (conferred by the phosphate group) this is normally the cofactor of choice in the assay.[11] The kinetics were more complicated for this system because NADPH utilisation is the method of monitoring the reaction, so when the NADPH is rate limiting there is only a very short period of enzyme reaction before all the NADPH has been used. The NADPH concentration was varied between 0.01 and 0.04 mM, while the substrate was present in excess due to the very high levels of *(S)*-aspartate β-semialdehyde (11) (35 mM) and pyruvate (17) (40 mM) employed. Again the kinetics were analysed by the Michaelis-Menten model and plotted by the three different methods previously discussed, see table 2-7. Here the data showed slightly more deviation from the line of best fit in both the Lineweaver-Burk and Eadie-Hofstee plots. The direct linear plot gave the median values of the K_m and V_{max} parameters, see figure 2-12.

Table 2-7: DHDPR kinetic parameters with respect to NADPH

Type of plot	K_m x 10^{-5} M	V_{max} $\mu mol \cdot s^{-1} mg^{-1}$
Lineweaver-Burk	1.96	4.14
Eadie-Hofstee	1.45	3.58
Direct linear	1.65	3.63

Figure 2-12: Kinetic plot of DHDPR activity with respect to NADPH
(i) Direct linear plot

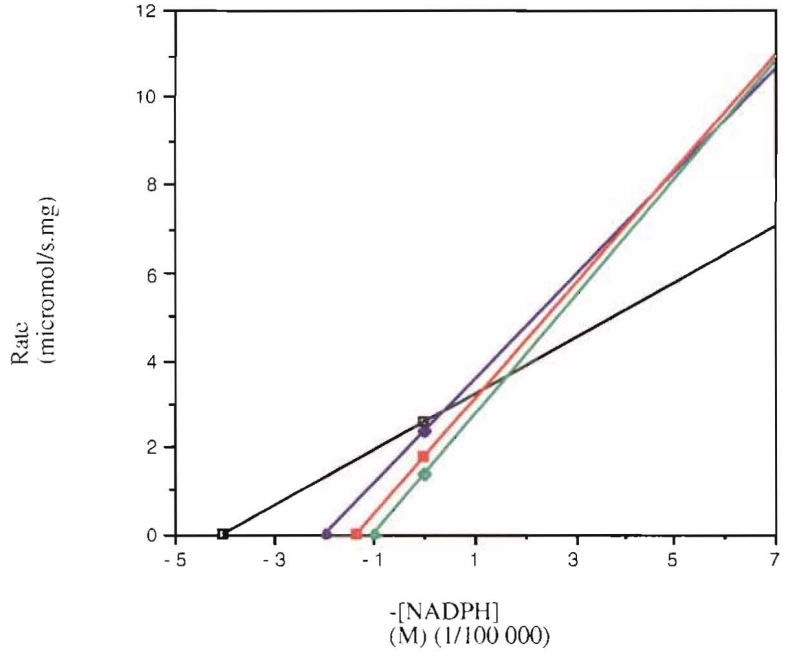

For DHDPR the K_m, with respect to NADPH, was found to be in the range of (1.5 - 2.0) x 10^{-5} M, while V_{max} was found to be in the range of 3.6 - 4.1 $\mu mol \cdot s^{-1} mg^{-1}$. The K_m value is comparable to other reports for *E. coli* DHDPR. Tamir and Gilvarg[12] found the K_m to be less than 1.0 x 10^{-5} M in Tris buffer at pH 7.5, and Reddy *et al.*[34] found the K_m to be (8 $\pm$ 2.5) x 10^{-6} M. These low K_m values reflect the high affinity of the DHDPR enzyme for the cofactor NADPH.

The K_m of DHDPR with respect to NADPH in *Bacillus* sp. is also very low, for *B. subtilis* K_m is 7.2 x 10^{-5} M,[35] while for *B. cereus* K_m is 8 x 10^{-6} M,[36] and for *B. megaterium* K_m is 1.3 x 10^{-5} M.[36] This high affinity for the cofactor is also shown in plant sources of DHDPR, for example maize where the K_m is 4.6 x 10^{-5} M.[37] Inhibition of DHDPR by the cofactor product $NADP^+$ has been observed in *B. cereus* and *B. megaterium*, with K_i being 5.5 x 10^{-5} M and 1.2 x 10^{-4} M, respectively.[36]

DHDPR can also utilise NADH, however, the nicotinamide is quickly hydrolysed in acidic conditions and must be made up immediately prior to use. Some DHDPR kinetics were determined using NADH as the cofactor, these were plotted on Lineweaver-Burk, Eadie-Hofstee, and direct linear plots, see table 2-8. Here the Lineweaver-Burk plot gave the median value for K_m; the V_{max} being nearly identical to that obtained from the Eadie-Hofstee plot, see figure 2-13.

Table 2-8: DHDPR kinetics with respect to NADH

Type of plot	K_m x 10^{-6} M	V_{max} $\mu mol \cdot s^{-1} mg^{-1}$
Lineweaver-Burk	5.36	1.95
Eadie-Hofstee	4.95	1.96
Direct linear	6.56	2.36

Figure 2-13: Kinetic plot of DHDPR activity with respect to NADH
(i) Lineweaver-Burk plot

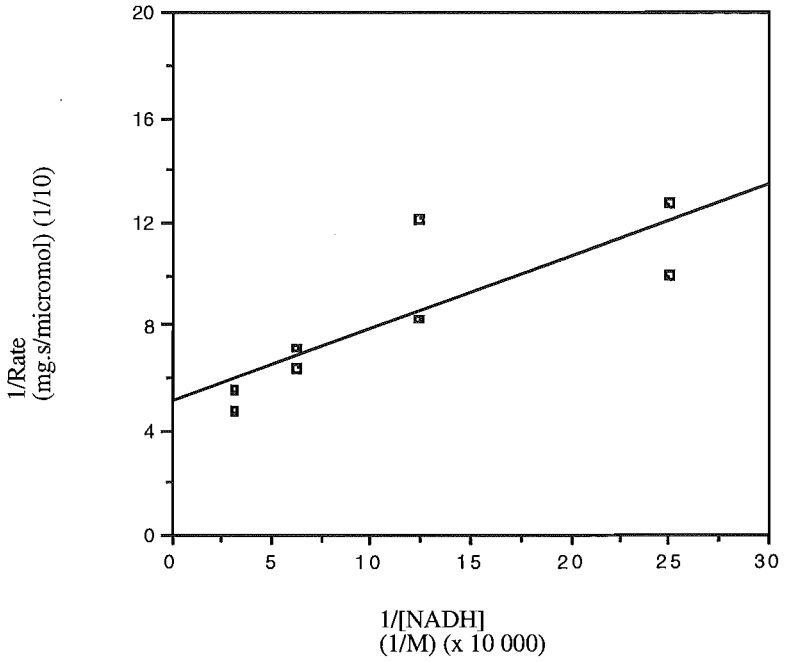

The K_m was found to be in the range of (5.0 - 6.6) x 10^{-6} M and V_{max} was found to be in the range of 2.0 - 2.4 $\mu mol \cdot s^{-1} mg^{-1}$. This K_m is lower than that of NADPH, as is the V_{max}. Studies by Reddy *et al.*[34] have found NADH to be a better cofactor than NADPH, as NADH exhibits a K_m value of approximately four times lower than that for NADPH (showing NADH has a greater affinity for DHDPR than NADPH). Initial studies performed by Farkas and Gilvarg[40] also reported that the rate of the DHDPR catalysed reaction mediated by NADPH is approximately half that found when NADH is used. However, as NADPH has greater chemical stability it is the cofactor of choice in the coupled assay.

Summary

In this chapter the kinetics of both DHDPS and DHDPR have been thoroughly investigated using the coupled assay. DHDPS, at a pH 7.2, had a K_m for *(S)*-aspartate β-semialdehyde (11) in the range of (1.0 - 1.4) x 10^{-4} M and a V_{max} in the range of (6.5 - 7.2) x 10^{-1} $\mu mol \cdot s^{-1} mg^{-1}$, while for pyruvate K_m was in the range of (1.1 - 1.3) x 10^{-4} M and V_{max} was in the range of (4.8 - 5.5) x $10^{-1} \mu mol \cdot s^{-1} mg^{-1}$. High concentrations of the substrate *(S)*-aspartate β-semialdehyde (11) did not cause inhibition of *E. coli* DHDPS, but *E .coli* DHDPS was found to be feedback inhibited by *(S)*-lysine (12). Inhibition of DHDPS by *(S)*-lysine (12) was shown to be uncompetitive with respect to *(S)*-aspartate β-semialdehyde (11) with a K_i' in the range of (3.4 - 3.9) x 10^{-4} M. Inhibition with

respect to pyruvate (17) was also uncompetitive with a K_i' in the range of (3.1 - 3.8) x 10^{-4} M.

The kinetic parameters of DHDPR with respect to its substrate and the two possible cofactors, NADPH and NADH, were also measured. For DHDPR, at pH 7.2, with respect to the substrate, K_m was found to be in the range of (4.9 - 5.3) x 10^{-4} M, while V_{max} was in the range of 5.3 - 5.7 $\mu mol \cdot s^{-1} mg^{-1}$. The K_m, with respect to NADPH, was found to be in the range of (1.5 - 2.0) x 10^{-5} M, while V_{max} was found to be in the range of 3.6 - 4.1 $\mu mol \cdot s^{-1} mg^{-1}$. The K_m, with respect to NADH, was found to be in the range of (5.0 - 6.6) x 10^{-6} M and V_{max} was found to be in the range of 2.0 - 2.4 $\mu mol \cdot s^{-1} mg^{-1}$. As the K_m for NADH is considerably lower than that for NADPH, NADH is a more efficient cofactor.

References

1. Y. Yugari, C. Gilvarg *J. Biol. Chem.* **240**, 4710 (1965).
2. J.G. Shedlarski *Meth. Enz.* **17b**, 129 (1971).
3. L. Couper, J.E. McKendrick, D.J. Robins, E.J.T. Chrystal *Bioorg. and Med. Chem. Letts* **4**, 2267 (1994).
4. L.I. Smith, J.W. Opie *Org. Synth.* Coll. Vol. **III** 56 (1955).
5. F. Yamakura, Y. Ikeda, K. Kimura, T. Sasakawa *J. Biochem.* **76**, 611 (1974).
6. D.A. Frisch, B.G. Gengenbach, A.M. Tommey, J.M. Sellner, D.A. Somers, D.E. Myers *Plant Physiol.* **96**, 444 (1991).
7. J.A. Gerrard *'Studies on Dihydrodipicolinate Synthase'* D. Phil., Brasenose College, Oxford (1992).
8. C. Schopf, F. Oechler *Justus Liebigs Ann. der Chim.* **523**, 1 (1936).
9. H.J. Vogel, B.D. Davis, *J. Am. Chem. Soc.* **74**, 109 (1952).
10. A. L. Lehninger, D.L. Nelson, M.M. Cox *'Principles of Bochemistry'* 2nd ed., Worth, N.Y. (1993).
11. D. Dolphin, R. Poulsen, O. Avramonic (Eds) *'Pyridine Nucleotide Coenzymes, Parts A and B'* John Wiley & Sons, New York (1987).
12. H. Tamir, C. Gilvarg *J. Biol. Chem.* **249**, 3034 (1974).
13. W.E. Karsten *Biochemistry* **36**, 1731 (1997).
14. A. Cornish-Bowden, C.W. Wharton *'Enzyme Kinetics'* IRL Press, Oxford (1988).
15. B. Laber, F-X. Gomis-Ruth, M.J. Romao, R. Huber *Biochem. J.* **288**, 691 (1992).
16. F. Yamakura, Y. Ikeda, K. Kimura, T. Saskawa *J. Biochem.* **76**, 611 (1974).
17. S.M. Halling, D.P. Stahly *Biochim. Biophys. Acta* **452**, 580 (1976).
18. A.T.M. Bartlett, P.J. White *J. Gen. Microbiol.* **132**, 3169 (1986).

19. L. Eggeling *Amino Acids* **6**, 261 (1994).
20. F.H. Webster, R.V. Lechowich *J. Bacteriol.* **101**, 118 (1970).
21. C. Dereppe, G. Bold, O. Ghisalba, E. Ebert, H-P. Schar *Plant Physiol.* **98**, 813 (1992).
22. D.A. Frisch, B.G. Gengenbach, A.M. Tommey, J.M. Sellner, D.A. Somers, D.E. Myers *Plant Physiol.* **96**, 444 (1991).
23. R. Kumpaisal, T. Hashimoto, Y. Yamada *Agric. Biol. Chem.* **53**, 355 (1989).
24. R. Kumpaisal, T. Hashimoto, Y. Yamamada *Plant Physiol.* **85**, 145 (1987).
25. R.M. Wallsgrove, M. Mazelis *Phytochem.* **20**, 2651 (1981).
26. D.P. Stahly *Biochim. Biophys. Acta* **191**, 439 (1969).
27. S. Blickling, C. Renner, B. Laber, H-D. Pohlenz, T.A. Holak, R. Huber *Biochemistry* **36**, 24 (1997).
28. S. Blickling, J. Knablein *Biol. Chem.* **378**, 207 (1997).
29. G. Galili *The Plant Cell* **7**, 899 (1995).
30. A. Pearl, O. Shaul, G. Galili *Plant Mol. Biol.* **19**, 815 (1992).
31. T. Kwon, T. Sashara, T. Abe *J. Plant Physiology* **146**, 615 (1995).
32. U. Eisner, J. Kuthan *Chem. Rev.* **72**, 1 (1972).
33. J.A.E. Kraunsoe *'Studies in Lysine Biosynthesis'* Part II, Corpus Christi College, Oxford (1992).
34. S.G. Reddy, J.C. Sacchettini, J.S. Blanchard *Biochemistry* **34,** 3492 (1995).
35. K. Kimura, T. Goto *J. Biochem* **77**, 415, (1975).
36. K. Kimura, T. Goto *J. Biochem* **81**, 1367, (1977).
37. V.V.S. Tyagi, R.R. Henke, W.R. Farkas *Plant Physiol.* **73**, 687, (1983).
38. S.G. Reddy, G. Scapin, J.S. Blanchard *Biochemistry* **35,** 13294 (1996).
39. G. Scapin, J.S. Blanchard, J.C. Sacchettini *Biochemistry* **34**, 3502 (1995).
40. W. Farkas, C. Gilvarg *J. Biol. Chem.* **240**, 4717 (1965).

Results and Discussion Chapter Three

The Structure of (S)-*Aspartate β-Semialdehyde*

Introduction

Although *(S)*-aspartate β-semialdehyde (11) had been prepared in previous studies, the biologically relevant structure was unknown. It could possibly exist in solution as an aldehyde (11a), a hydrate (11b), or a cyclic lactol (11c), see figure 3-1. While the literature had always assumed *(S)*-aspartate β-semialdehyde (11) existed as the aldehyde (11a) there was no evidence for this. The question of whether cyclic or acyclic forms of *(S)*-aspartate β-semialdehyde (11) predominate in aqueous solution, and what form of *(S)*-aspartate β-semialdehyde (11) the enzyme DHDPS recognises, were key issues addressed in this research.

Figure 3-1: Possible structures of (S)-*aspartate β–semialdehyde (11)*

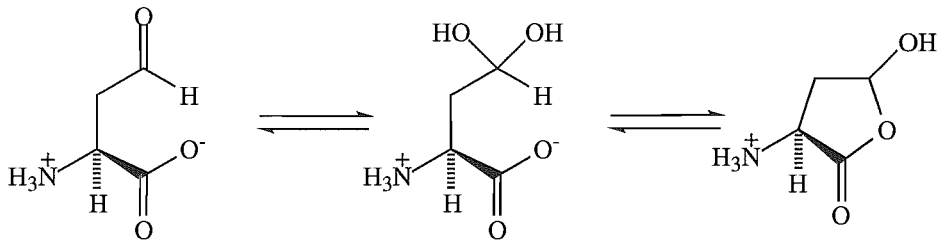

Linear aldehyde (11a) Linear hydrate (11b) Cyclic lactol (11c)

In previous literature reports, *(S)*-aspartate β-semialdehyde (11) has always been assumed to exist as an aldehyde.[1] However, this seemed unlikely on examination of the chemical properties of *(S)*-aspartate β-semialdehyde (11). In the original report of the synthesis of *(S)*-aspartate β-semialdehyde (11) by Black and Wright it was noted that: 'the usual aldehyde derivatives did not readily form with this substance'.[2] Recent work by Tudor *et al.*[3] concluded, from spectral data, that the molecule exists predominantly as the hydrate (11b). While a study on succinic semialdehyde derivatives, which are structurally similar to *(S)*-aspartate β-semialdehyde (11), by Salmon-Legagneur,[4] concluded that the acyclic form (58) is a minor component of an equilibrium which favours a five-membered cyclic lactol (59), see figure 3-2.

Figure 3-2: Equilibrium of the aldehyde with the cyclic lactol

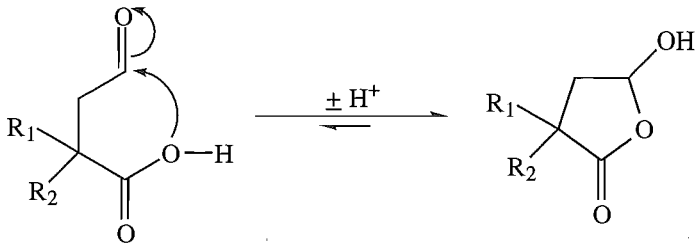

Acyclic form (58) Cyclic lactol (59)

In the literature[5,6] it was further noted that some aspartate β-semialdehyde derivatives were reported in the lactol form (for example 60 and 61 in figure 3-3), although little data is available on these compounds.

Figure 3-3: Derivatives of aspartate β-semialdehyde (11) reported as lactols

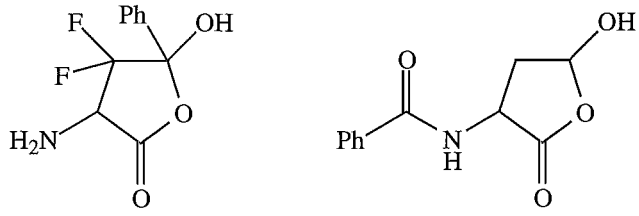

(60) (61)

Previous work by Gerrard[7] had shown that *(S)*-homoserine lactone (31) (*(S)*-2-amino-4-butyrolactone), a five membered cyclic molecule, inhibited the enzyme DHDPS, see figure 3-4. This result suggested that the substrate *(S)*-aspartate β-semialdehyde (11) of the DHDPS catalysed reaction, may exist as the cyclic lactol (11c).

Figure 3-4: (S)*-Homoserine lactone (31)*

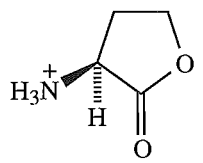

(S)-Homoserine lactone (31)
(*(S)*-2-Amino-4-butyrolactone)

Studies were undertaken to determine the exact structure of *(S)*-aspartate β-semialdehyde (11) as recognised by the DHDPS enzyme. This work involved DHDPS inhibition studies, using a variety of compounds that mimicked the different hypothesised structures of *(S)*-aspartate β-semialdehyde (11). Structural studies on *(S)*-aspartate β-semialdehyde (11) were also performed, these utilised NMR (including two-dimensional NMR) and infra-red spectroscopy.

Analogues of a possible cyclic lactol form of *(S)*-aspartate β-semialdehyde

(S)-Homoserine lactone (31) had been shown to inhibit DHDPS. It is possible that it acts as a substrate analogue if *(S)*-aspartate β-semialdehyde (11) binds to DHDPS as a cyclic lactol (11c).[7] Alternatively, it may act as an inhibitor while binding at a remote site (that is, not at the active site). For example homoserine lactone (31) derivatives have been hypothesised to act as global starvation signals in cells.[8] Thus, the type of inhibition that homoserine lactone (31) has on DHDPS needed to be determined. This would then clarify the structure of *(S)*-aspartate β-semialdehyde (11) as recognised by the enzyme. If homoserine lactone (31) is acting as a substrate analogue then inhibition of DHDPS should be competitive with respect to *(S)*-aspartate β-semialdehyde (11). However, if homoserine lactone (31) inhibits DHDPS by binding at a remote site either uncompetitive or noncompetitive inhibition should result. In either case, homoserine lactone (31) may be an important drug lead, as potent inhibitors of DHDPS are potentially of interest as antibacterial and/or herbicidal agents. Modification of homoserine lactone (31) is one way to develop such inhibitors.

Samples of both racemic homoserine lactone (31) and *(S)*-homoserine lactone (31) were tested for inhibition of DHDPS. Two other cyclic analogues were investigated, *(S)*-3-aminopyrrolid-2-one (62) and 2-aminocyclopentanone (63), see figure 3-5. *(S)*-3-Aminopyrrolid-2-one (62), which is a lactam (cyclic amide), is more stable towards hydrolysis than homoserine lactone (31), which is a lactol (cyclic ester), while 2-amino-cyclopentanone (63) is stable to hydrolysis. *(S)*-3-Aminopyrrolid-2-one (62) was synthesised from the enantiomerically pure *(S)*-α,γ-diaminobutyrate (65).[9] The other analogue, 2-aminocyclopentanone (67), was synthesised, as the racemate, from cyclopentanone (67).[10]

Figure 3-5: Homoserine lactone (31) and analogues

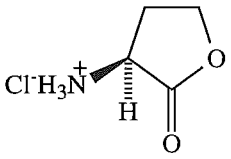

(S)-Homoserine lactone (31)

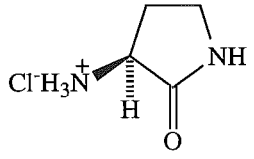

(S)-3-Aminopyrrolid-2-one (62)

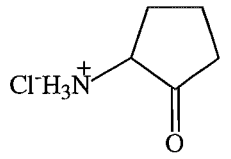

2-Aminocyclopentanone (63)

Stability studies on homoserine lactone

Homoserine lactone (31) (2-amino-4-butyrolactone) is known to hydrolyse to homoserine (64) (2-amino-4-hydroxybutanoic acid) see figures 3-6 and 3-7.

Figure 3-6: Hydrolysis homoserine lactone (31)

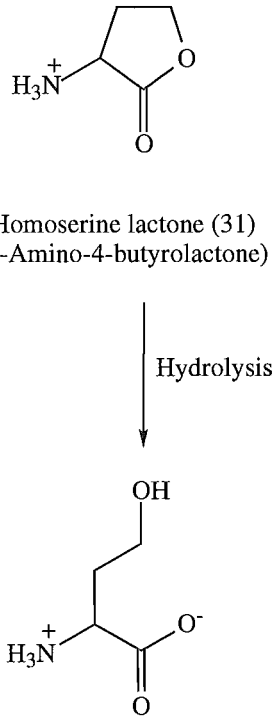

Homoserine lactone (31)
(2-Amino-4-butyrolactone)

Homoserine (64)
(2-Amino-4-hydroxybutanoic acid)

Figure 3-7: NMR of homoserine lactone (31) hydrolysis to homoserine (64)

(i) ^{1}H NMR

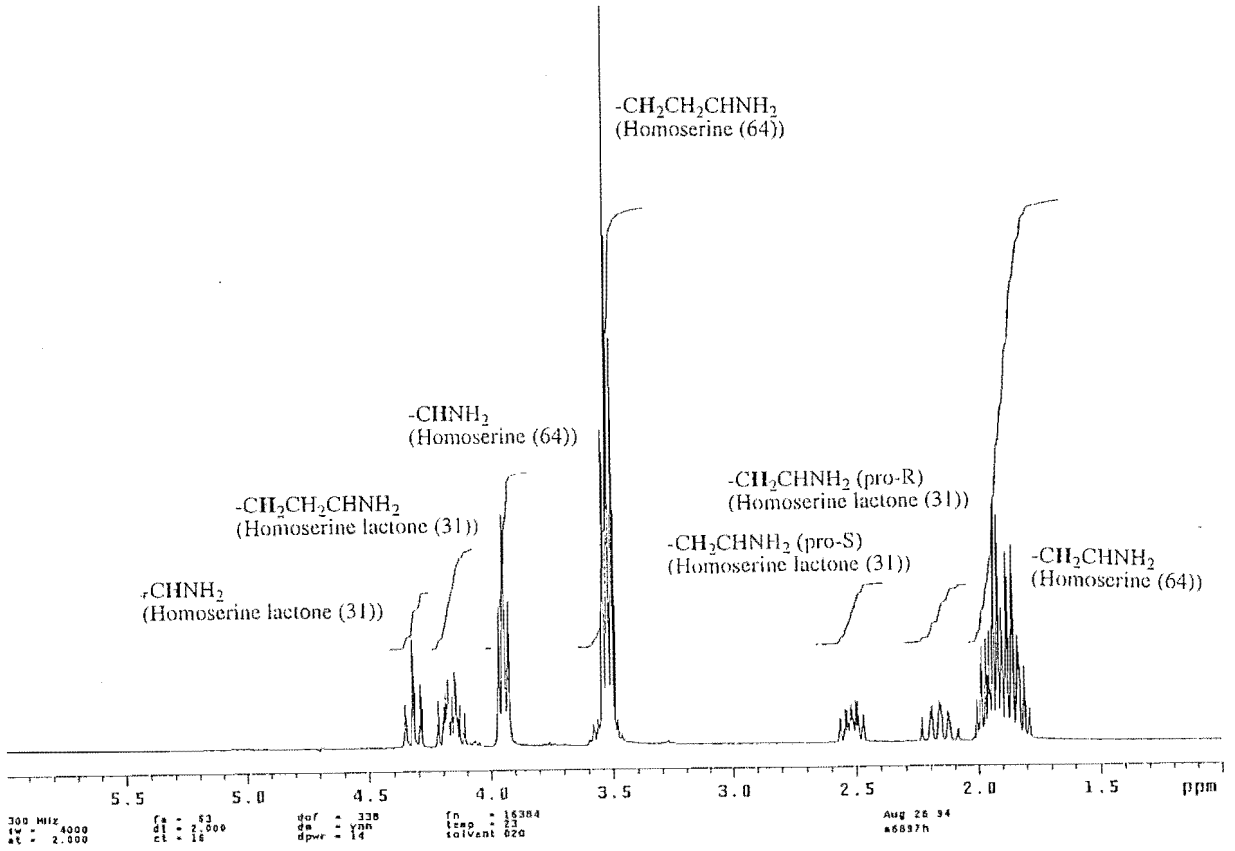

(ii) ^{13}C NMR

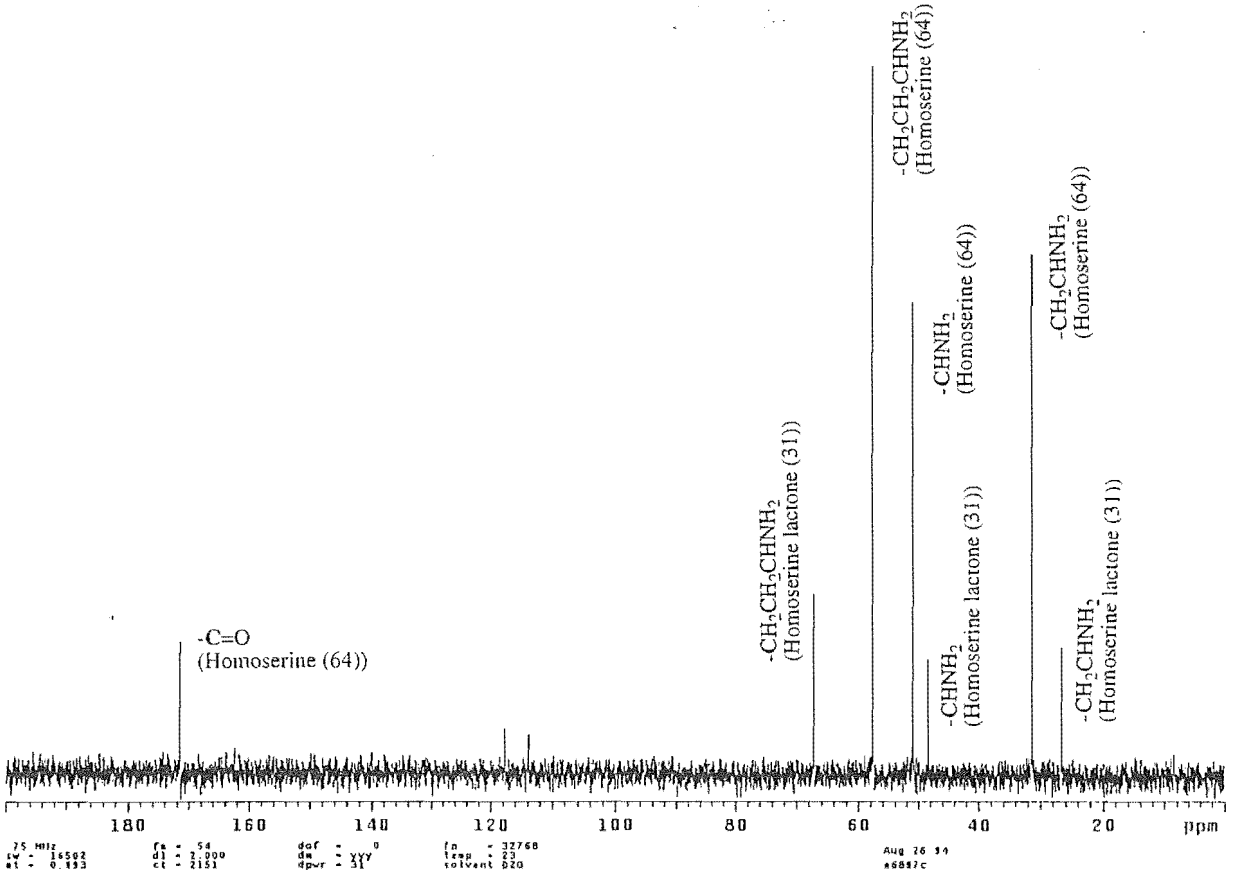

The hydrolytic stability of homoserine lactone (31) under the enzyme assay conditions is important in interpreting inhibition data. A study of the stability of homoserine lactone (31) with respect to pH was undertaken. Initial stability studies on homoserine lactone (31) were performed by following the ^{1}H NMR in phosphate buffer (KH_2PO_4/K_2HPO_4—which is NMR silent). Homoserine lactone (31) had a half-life of approximately 120 minutes, at pH 8.0, showing ~10% decomposition in 30 minutes. At pH 7.0 slightly less decomposition occurred, whereas at pH 1 less then 10% decomposed over 24 hours. Thus, it was found that homoserine lactone (31) was quickly hydrolysed in basic conditions, but was relatively stable in acid. As the coupled assay had been modified to run at pH 7.2 over five minutes (see Chapter Two) it was feasible to run kinetics measuring the effect of homoserine lactone (31) on DHDPS using this assay with minimal decomposition of the lactone. To minimise the hydrolysis of homoserine lactone (31) it was freshly prepared in Mops buffer at pH 3.5, before addition to the assay.

Effect of homoserine lactone on DHDPS kinetics

DHDPS activity was inhibited by homoserine lactone (31) at a range of concentrations. Dixon and modified Dixon plots were used to determine the exact nature of inhibition (competitive, noncompetitive, uncompetitive, or mixed) and to the calculate K_i values. The inhibition was found to be reversible and noncompetitive with respect to both substrates, as both the Dixon and modified Dixon plots show a series of straight lines that have a common intercept on the x-axis (which in both cases represents inhibitor concentration), see tables 3-1 and 3-2, and figures 3-8 and 3-9. K_i, from the Dixon and modified Dixon plots, was found to be in the range of (1.2 - 2.2) x 10^{-2} M with respect to *(S)*-aspartate β-semialdehyde (11), and in the range of (0.8 - 1.5) x 10^{-2} M with respect to pyruvate (17). This reversible noncompetitive inhibition is consistent with the inhibition occurring at an allosteric site, and is compatible with the hypothesis that the molecule is acting in its capacity as a global starvation signal in *E. coli*.[8]

Table 3-1: Kinetic parameters of the inhibition of homoserine lactone (31) on DHDPS activity with respect to (S)*-aspartate β-semialdehyde (11)*

[Homoserine lactone] mM	K_m x 10^{-4} M	V_{max} x 10^{-1} μmol·s^{-1}mg^{-1}
0	1.24	7.08
40	1.08	2.94
60	0.803	1.63
80	0.853	1.22

Figure 3-8: Kinetic plots of the inhibition of homoserine lactone (31) on DHDPS activity with respect to (S)*-aspartate β-semialdehyde (11)*

(i) Dixon plot

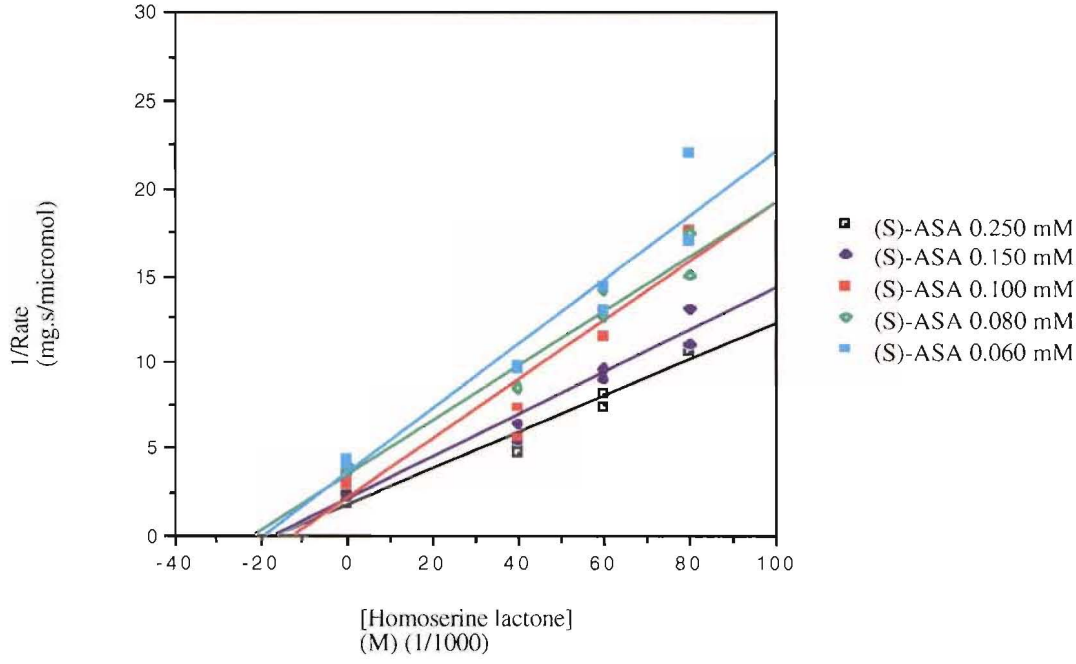

(ii) Modified Dixon plot

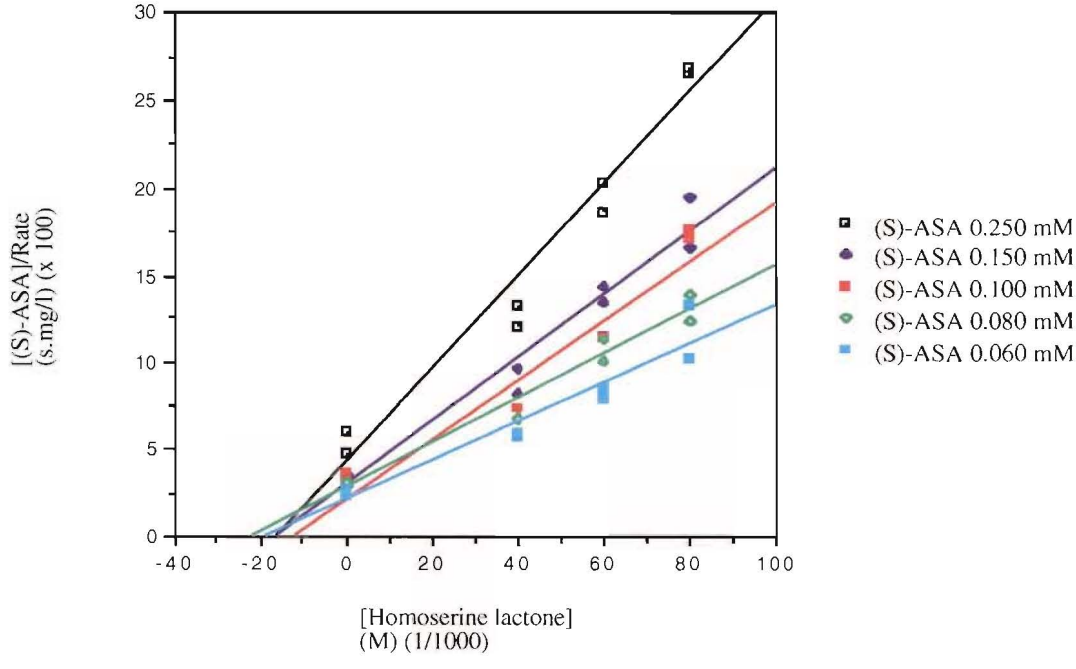

Table 3-2: Kinetic parameters of the inhibition of homoserine lactone (31) on DHDPS activity with respect to pyruvate (17)

[Homoserine lactone] mM	K_m x 10^{-4} M	V_{max} x 10^{-1} µmol·s^{-1}mg^{-1}
0	1.14	4.76
40	0.973	1.80
60	0.624	1.17
80	0.796	1.22

Figure 3-9: Kinetic plots of the inhibition of homoserine lactone (31) on DHDPS activity with respect to pyruvate (17)

(i) Dixon plot

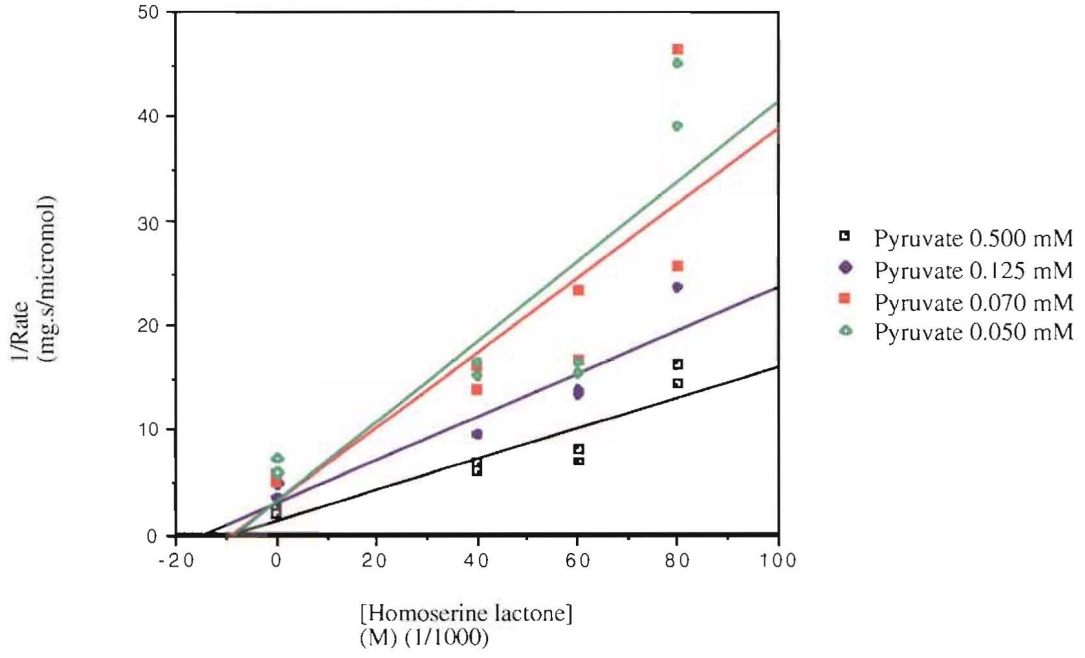

(ii) Modified Dixon plot

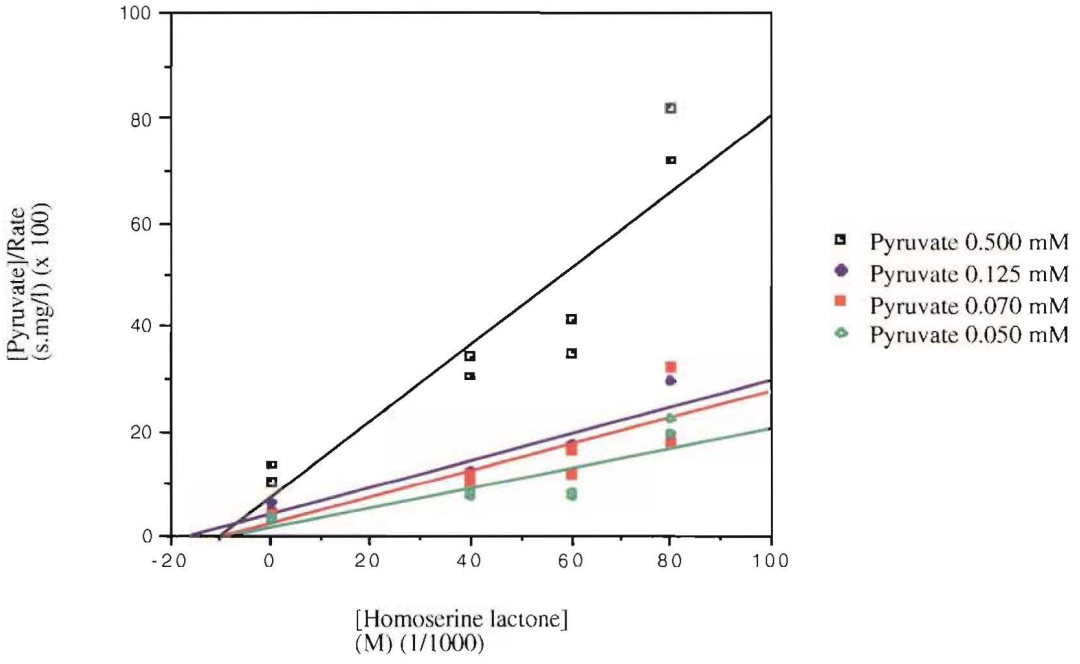

Inhibition by homoserine lactone (31) with respect to *(S)*-aspartate β-semialdehyde (11) was repeated using optically pure *(S)*-homoserine lactone (31), to determine if the enzyme was specifically inhibited by the *(S)*-isomer. The results, however, were inconclusive. Inhibition was still noncompetitive and K_i, as determined from the Dixon and modified Dixon plots, was found to be in the range of (3.2 - 3.7) x 10^{-2} M. This increase in K_i probably reflects the decrease in the quality of data, rather than a decrease in the affinity of the inhibitor for DHDPS when only the *(S)*-isomer is present, see table 3-3 and figure 3-10.

Table 3-3: Kinetic parameters of the inhibition of (S)*-homoserine lactone (31) on DHDPS activity with respect to* (S)*-aspartate β-semialdehyde (11)*

[*(S)*-Homoserine lactone] mM	K_m x 10^{-4} M	V_{max} x 10^{-1} µmol·s^{-1}mg^{-1}
0	1.13	7.57
40	0.425	2.48
60	1.65	3.79
70	0.674	1.92

Figure 3-10: Kinetic plots of the inhibition of (S)-*homoserine lactone (31) on DHDPS activity with respect to* (S)-*aspartate β-semialdehyde (11)*

(i) Dixon plot

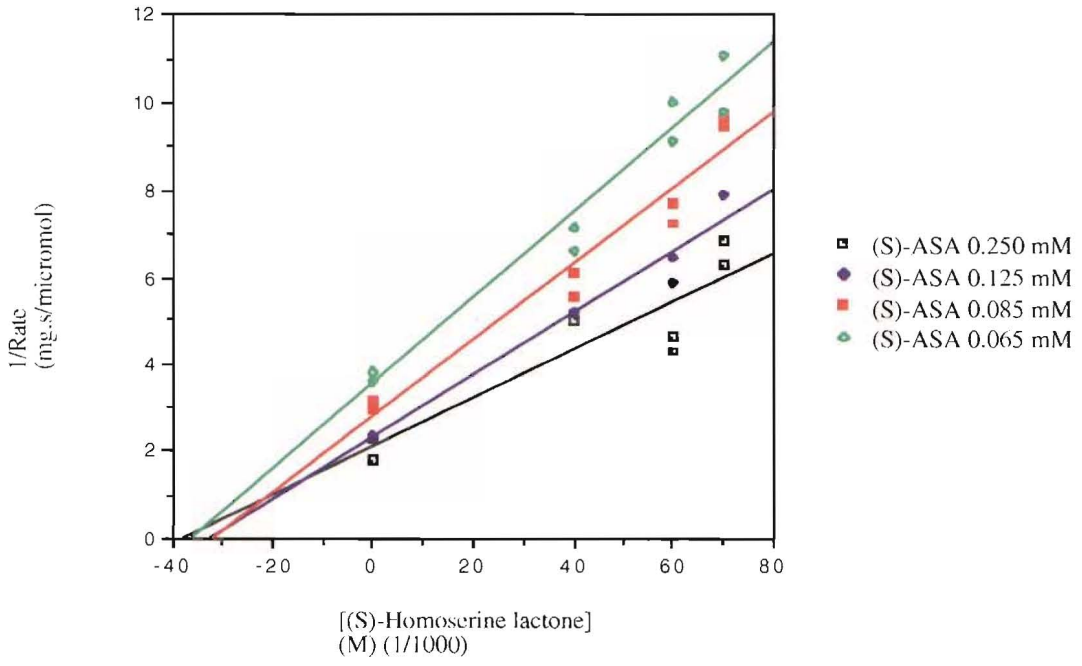

(ii) Modified Dixon plot

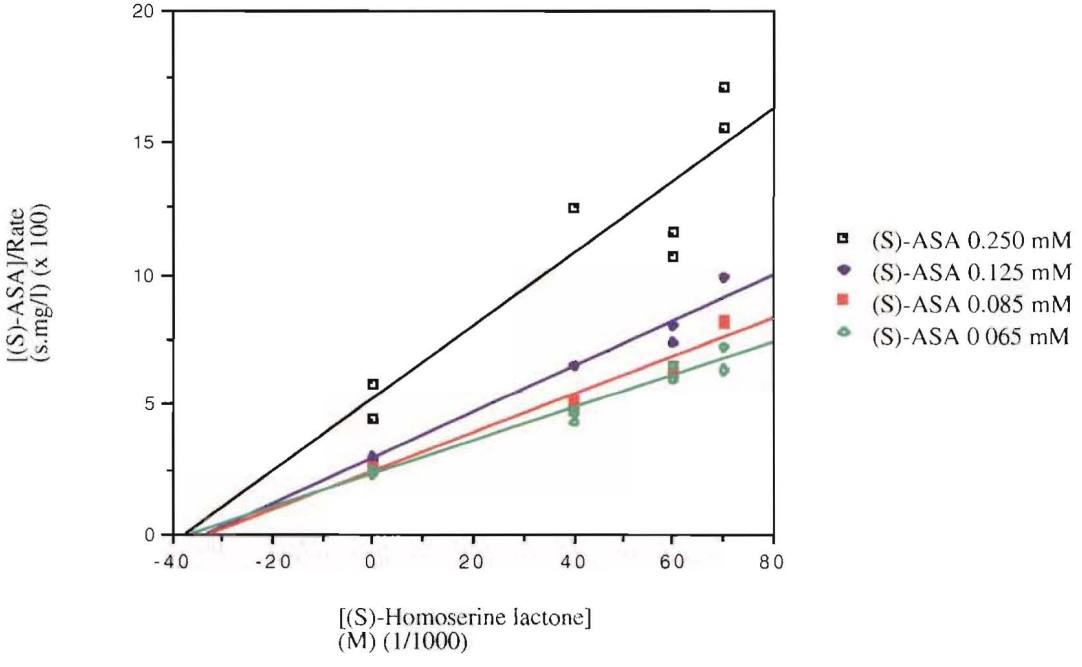

(S)-*3-Aminopyrrolid-2-one*

(S)-3-Amino-pyrrolid-2-one (66),[9] which is more stable towards hydrolysis than homoserine lactone (31), was synthesised as an analogue of *(S)*-homoserine lactone (31) from the enantiomerically pure *(S)*-α,γ-diaminobutyrate (65), see figure 3-11.

Figure 3-11: Synthesis of (S)-*3-aminopyrrolid-2-one*

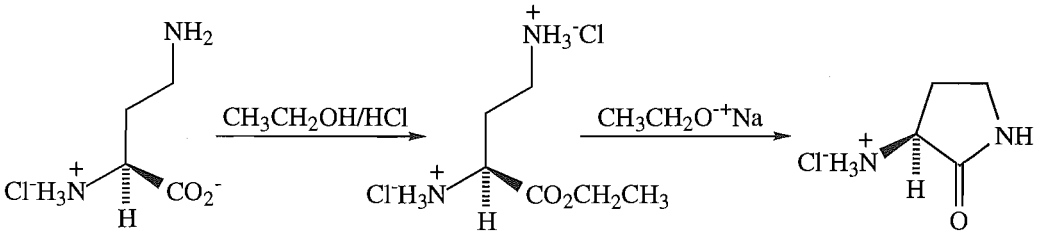

(S)-α,β-Diaminobutyrate hydrochloride (65)

Ethyl *(S)*-α,β-diaminobutyrate dihydrochloride (66)

(S)-3-Aminopyrrolid-2-one (62)

(S)-α,γ-Diaminobutyrate hydrochloride (65) was converted to the ethyl ester dihydrochloride (66) by Akabori and Nimano's method[11] (a Fischer esterification). The free ester, on liberation at 0 °C, cyclised to give *(S)*-3-aminopyrrolid-2-one (62).[9] Although this esterification did not go to completion, re-reacting the reaction mixture increased the ratio of product to starting material. Care had to be taken on purification of the product that hydrolysis to the starting material did not occur. The ethyl *(S)*-α,γ-diaminobutyrate dihydrochloride (66) was obtained as a white sticky solid in a yield of 86%. Attempts to crystallise the resinous mass with ethanol-toluene failed. However, as the material was pure by ^{1}H NMR the second cyclisation step was performed on the unpurified product. The cyclisation of ethyl *(S)*-α,γ-diaminobutyrate dihydrochloride (66), to yield *(S)*-3-aminopyrrolid-2-one (62), was performed in sodium ethoxide at -5 °C. The product was obtained as a yellow-brown solid in 32% yield, compared to a literature value of 97%.[9] There was difficulty in getting the ester to cyclise, and in removing the sodium chloride by-product. Cyclisation was acheived in low yield after initial attempts resulted in the conversion of the starting material (ethyl *(S)*-α,γ-diamino-butyrate dihydrochloride (66)) to the diamine.

The effect of 3-aminopyrrolid-2-one (62) on the activity of DHDPS was then tested; no inhibition of DHDPS activity was observed with this molecule, showing that replacement of the ring oxygen with nitrogen decreased binding to the enzyme.

2-Aminocyclopentanone

2-Aminocyclopentanone (63), which is related to homoserine lactone (31) by exchange of the ring oxygen with a carbon, is unable to undergo hydrolytic ring opening. It was synthesised and tested for inhibition of DHDPS. For the synthetic scheme see figure 3-12.

Figure 3-12: Synthetic scheme

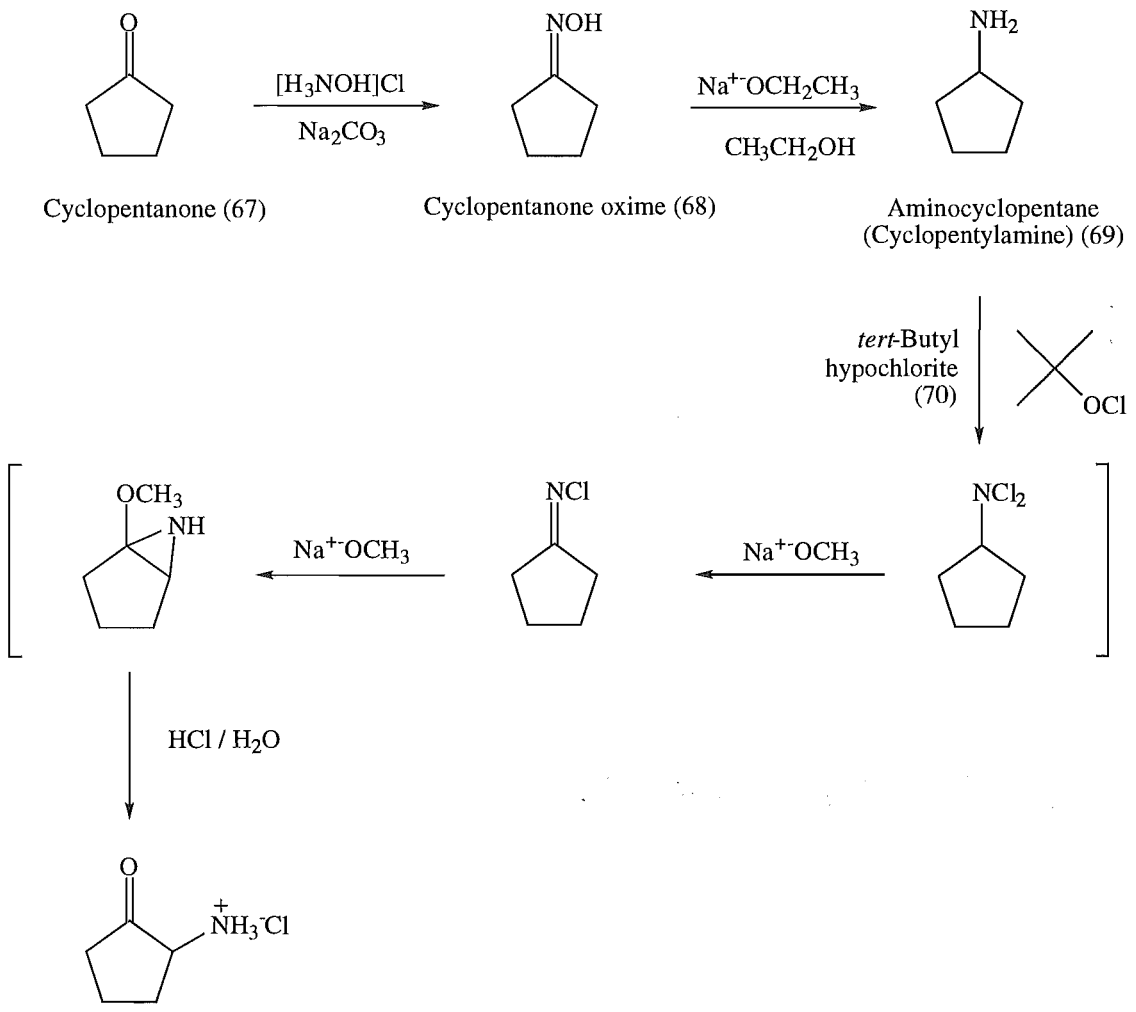

2-Aminocyclopentanone (63)

Cyclopentanone oxime (68) was prepared, as pure white micro-crystals, from cyclopentanone (67)[12,13] in a yield of 66%. When the material was left to slowly crystallise, large white needle crystals formed (~2mm x ~2mm thick by up to 40 mm long). The oxime was converted to aminocyclopentane (69)[14] by treatment with sodium ethoxide in ethanol.[15] The amine was purified by fractionally distillation under reduced pressure, and obtained as a clear, faintly yellow, oil in a yield of 39%.

2-Aminocyclopentanone (63) was then synthesised from the aminocyclopentane (69) via an elaborate one pot cyclisation procedure.[10] The first step involved adding *tert*-butyl

hypochlorite (70) in dry toluene, dropwise, to a solution of the aminocyclopentane (69) in dry toluene, while maintaining the temperature below 10 °C. The *tert*-butyl hypochlorite (70) was synthesised from *tert*-butyl alcohol (71) in acidic conditions with sodium hypochlorite (6.75%),[16] see figure 3-13.

Figure 3-13: Production of tert-*butyl hypochlorite (74)*

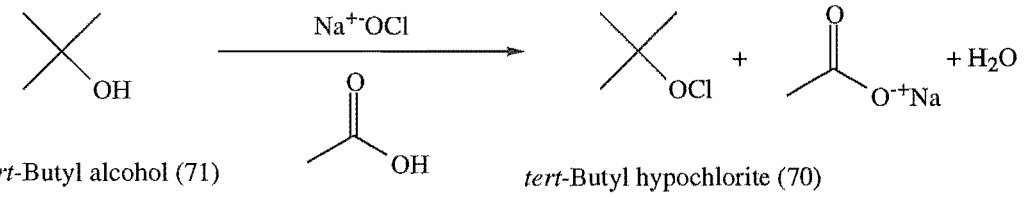

tert-Butyl alcohol (71) *tert*-Butyl hypochlorite (70)

The aminocyclopentane (69) and *tert*-butyl hypochlorite (70) were reacted with sodium methoxide until all the imine species (=NCl) had been converted to the amine (-NH-). The 2-aminocyclopentanone (63)) was readily purified by recrystallisation from hot isopropyl alcohol yielding of 11% of the product.

2-Aminocyclopentanone (63) was tested for inhibition of DHDPS, and it was found to be a reversible noncompetitive inhibitor as the Dixon and modified Dixon plots, which showed a series of lines that had a common intercept with the x-axis (on which inhibitor concentration was plotted), were almost identical. The inhibition constant, K_i (again calculated from the Dixon and modified Dixon plots), with respect to *(S)*-aspartate β-semialdehyde (11), was in the range of (1.2 - 2.4) x 10^{-1} M, see table 3-4 and figure 3-14. This K_i value is greatly increased relative to that of homoserine lactone (31), thus, showing a greatly decreased affinity for the remote site with the removal of the ring oxygen.

Table 3-4: Kinetic parameters of the inhibition of 2-aminocyclopentanone (63) on DHDPS activity with respect to (S)-*aspartate β-semialdehyde (11)*

[2-aminocyclo-pentanone] mM	K_m x 10^{-4} M	V_{max} x 10^{-1} μmol·s^{-1}mg^{-1}
0	0.706	5.16
60	1.02	4.81
80	1.21	3.86

Figure 3-14: Kinetic plots of the inhibition of 2-aminocyclopentanone (63) on DHDPS activity with respect to (S)*-aspartate β-semialdehyde (11)*

(i) Dixon plot

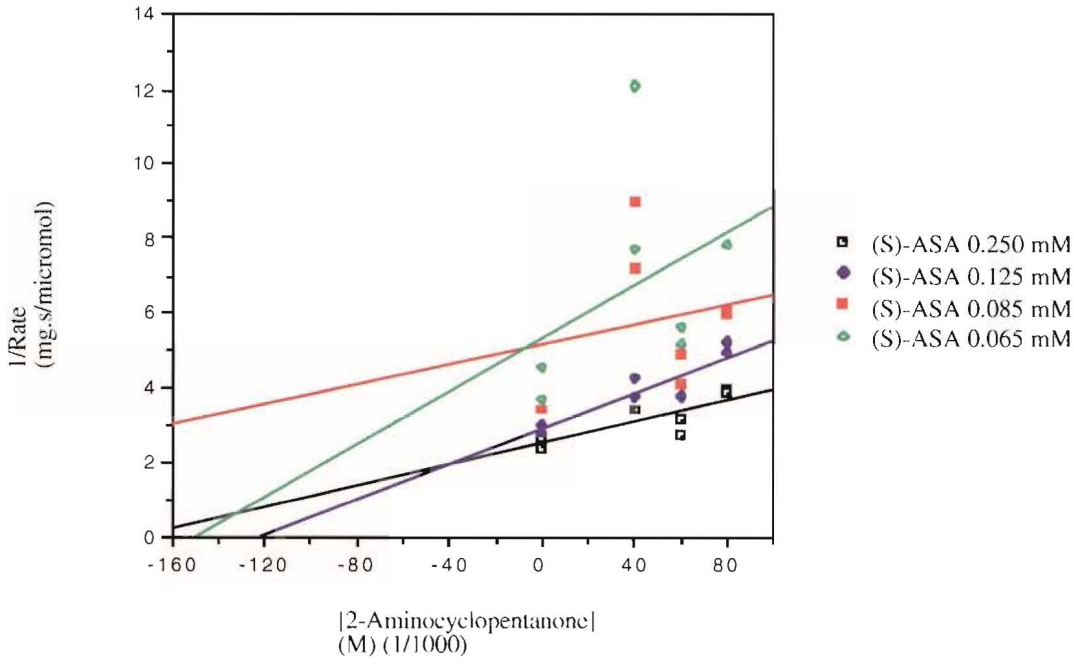

(ii) Modified Dixon plot

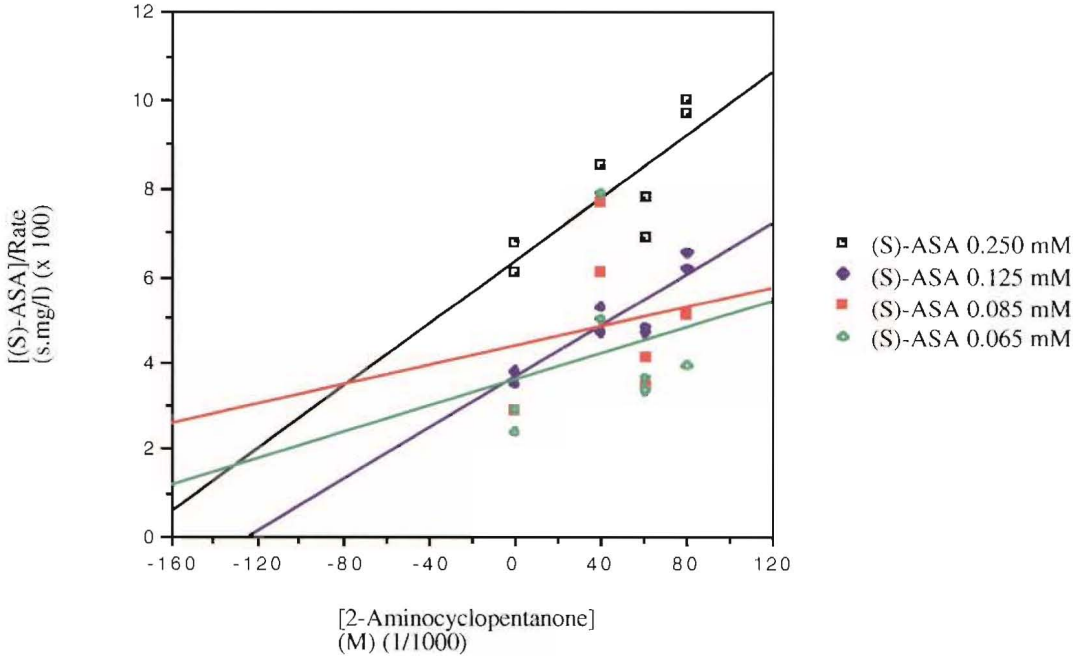

As neither homoserine lactone (31) nor 2-aminocyclopentanone inhibit DHDPS competitively it can be assumed that they do not bind at the active site, thus, they do not mimic the biologically significant structure of *(S)*-aspartate β-semialdehyde (11). This provides evidence that *(S)*-aspartate β-semialdehyde (11) does not bind to DHDPS as the cyclic lactol (11c).

Structural studies on *(S)*-aspartate β-semialdehyde

Structural studies were then performed on *(S)*-aspartate β-semialdehyde (11). These initially involved attempts to crystallise *(S)*-aspartate β-semialdehyde (11), using different counter ions. Later the work involved spectroscopic studies, using mainly NMR spectroscopy (including two-dimensional NMR), and infra-red spectroscopy.

Attempts to prepare crystalline derivatives of (S)*-aspartate β-semialdehyde*

Attempts were made to crystallise salts of *(S)*-aspartate β-semialdehyde (11) with a variety of counter ions. The trifluoroacetate salt originally prepared did not yield any crystals. Picrylsulfonic acid (75), then, was investigated as it forms highly crystalline salts. Picrylsulfonic acid (75)[17,18] was synthesised by the aromatic nitration of 1-chloro-2,4-dinitrobenzene (72) followed by nucleophilic substitution of the chloro substitutent by a sulfonic group, see figure 3-15.

Figure 3-15: Synthesis of picrylsulfonic acid (75)[17,18]

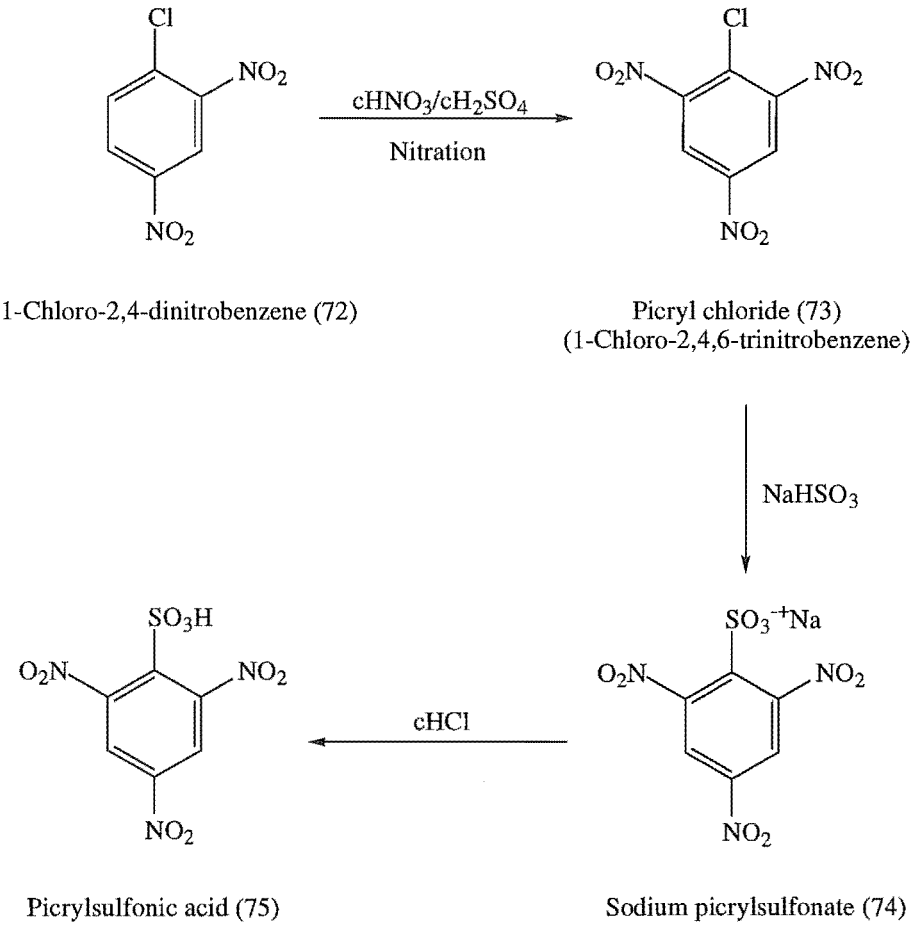

The aromatic nitration of 1-chloro-2,4-dinitrobenzene (72), to give picryl chloride (73), was performed using concentrated sulfuric acid and fuming concentrated nitric acid. The product formed as a yellow solid in 93% yield. The picryl chloride (73) was then converted to sodium picrylsulfonate (74) by the addition of sodium bisulfite in ethanol and heating under reflux. Recrystallisation gave the sodium picrylsulfonate (74) as fine yellow crystals in 8.8% yield. The sodium picrylsulfonate (74) was converted to the acid with concentrated hydrochloric acid, this was then crystallised from acidic aqueous ethanol as pale yellow needle crystals in 38% yield.

Diprotected *(S)*-aspartate β-semialdehyde (53) was deprotected by picrylsulfonic acid (75). The reaction was performed in water, with anisole present as a scavenger, and monitored by ^{1}H NMR. The solvent was removed *in vacuo*, resulting in a white fluffy solid. The product was confirmed by ^{1}H NMR as being the picrylsulfonate salt of *(S)*-aspartate β-semialdehyde (11). Attempts to crystallise this solid in water, water/dioxane, water/acetonitrite, ethanol, and diethyl ether all failed.

Spectroscopic work

Spectroscopic and structural studies were performed on *(S)*-aspartate β-semialdehyde (11), at pH 7. By ^{1}H NMR a slight trace of aldehyde was present, as indicated by the presence of a low intensity resonance at δ_H 9.61 ppm, see figure 3-16. Attempts to derivatise the aldehyde were unsuccessful; standard aldehyde tests with semi-carbazide, 2,4-dinitrophenylhydrazine, hydroxylamine, benzaldehyde, and dimedone all proved negative.

Figure 3-16: NMR of (S)*-aspartate β-semialdehyde (11)*

(i) ^{1}H NMR of (S)*-aspartate β-semialdehyde (11) at pH 1*

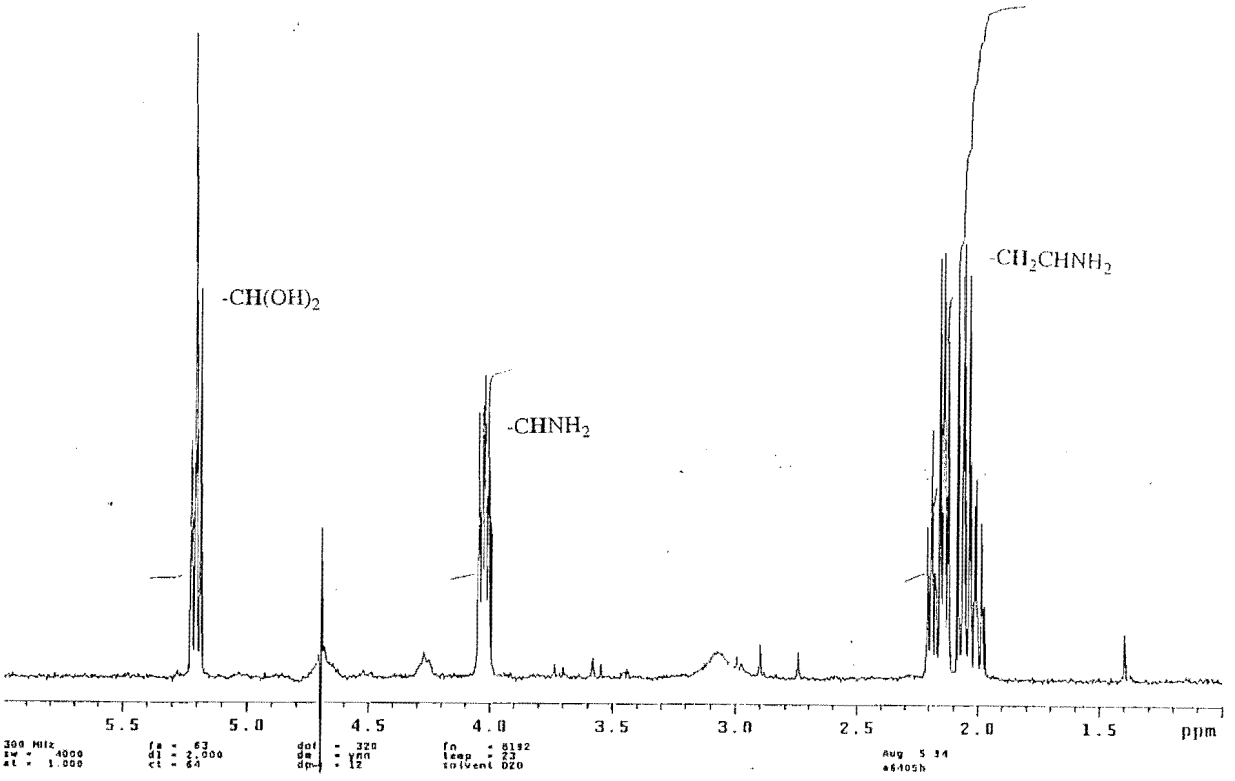

(ii) ^{13}C NMR of (S)-*aspartate β-semialdehyde (11) at pH 1*

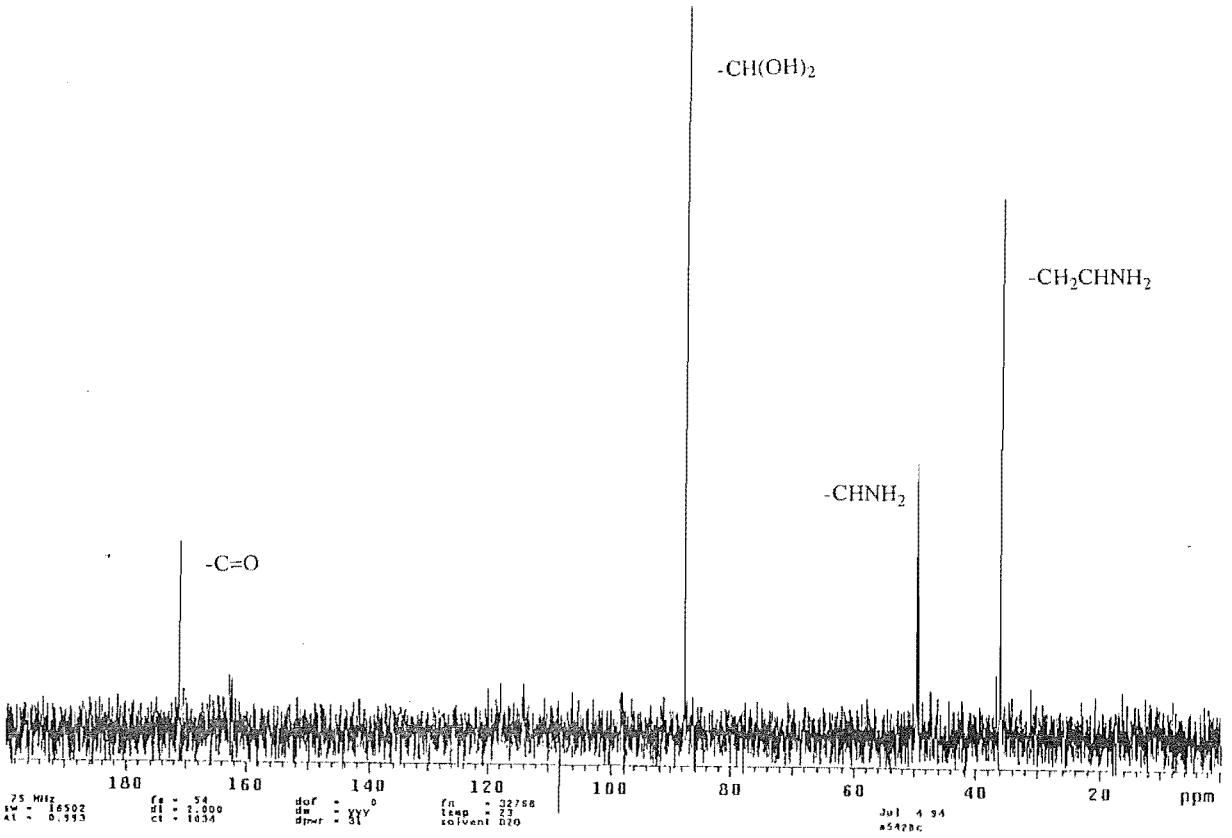

(iii) ^{1}H NMR of (S)-*aspartate β-semialdehyde (11) at pH 7, showing the aldehyde peak present at δ_H 9.61 ppm*

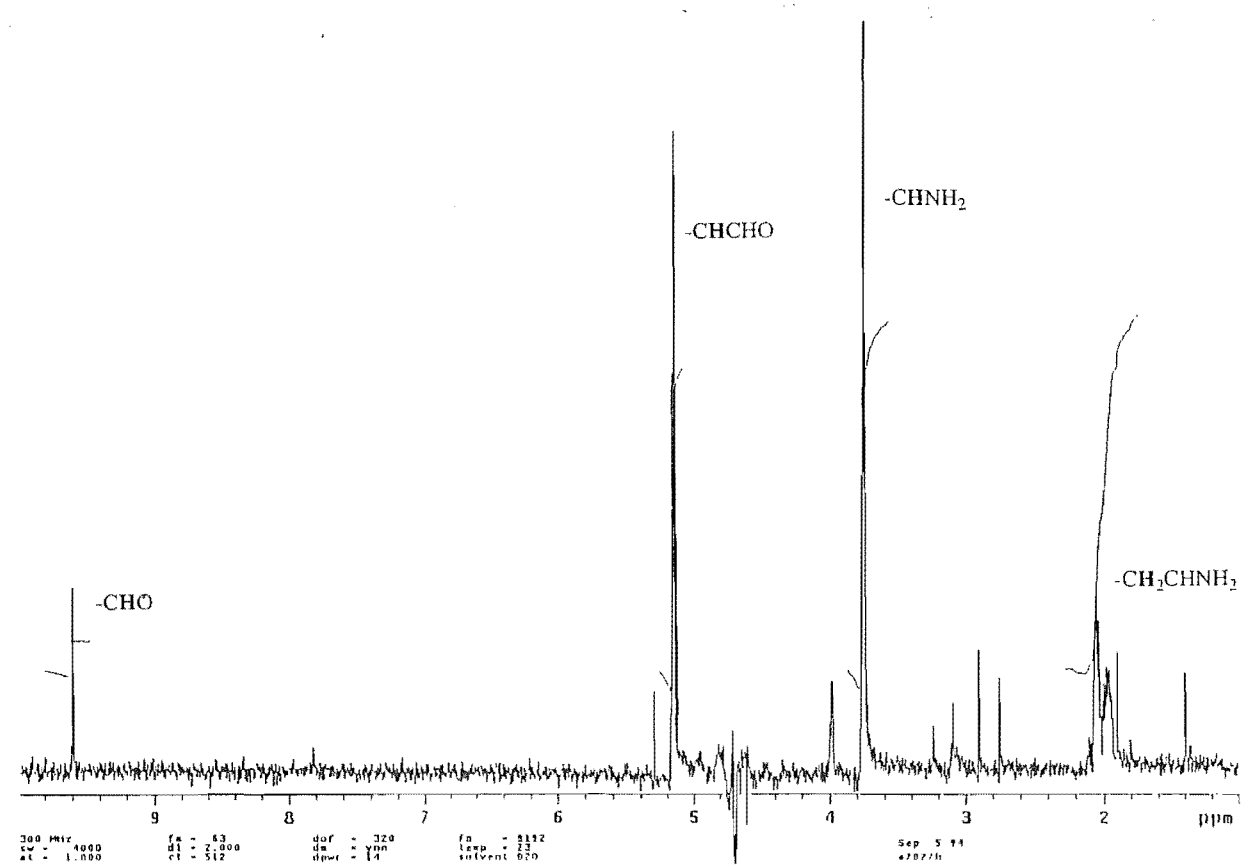

Heteronuclear multibond coupling (HMBC) NMR experiments were performed to distinguish between the cyclic form of *(S)*-aspartate β-semialdehyde (11) and acyclic species (specifically to distinguish between the cyclic lactol form (11c) and the linear hydrate form (11b)). Experiments performed on homoserine lactone (31) (analogous to the proposed cyclic *(S)*-aspartate β-semialdehyde (11) structure) showed clear coupling between the carbonyl carbon and the α-proton, the pro-*S* β-proton (the stereochemistry was assigned on the basis of nOe measurements), and both the γ-protons. Comparison experiments performed on *(S)*-aspartate β-semialdehyde (11), showed coupling between the carbonyl carbon and the α and β protons, but no evidence of coupling between the carbonyl carbon and the γ-proton. Coupling between the carbonyl carbon and the γ-proton would be expected if *(S)*-aspartate β-semialdehyde (11) was predominantly cyclic, see figures 3-17 and 3-18.

This evidence suggested that a cyclic form of *(S)*-aspartate β-semialdehyde (11) was not present at detectable levels. Infra-red spectra of both *(S)*-aspartate β-semialdehyde (11) and homoserine lactone (31) were also performed. While infra-red spectra of aqueous solutions of *(S)*-aspartate β-semialdehyde (11) and homoserine lactone (31) were not well resolved, some structural information could be obtained. Homoserine lactone (31), in a potassium bromide disc, absorbs strongly at 1774 cm^{-1} and in aqueous solution at 1784 cm^{-1}, corresponding to the γ-lactone absorbance. For *(S)*-aspartate β-semialdehyde (11), however, no γ-lactone absorbance was observed. These results further support the notion that *(S)*-aspartate β-semialdehyde (11), in solution, at physiological pH, does not exist significantly in a cyclic form, but rather exists predominantly as the linear hydrate (11b).

Figure 3-17: Coupling in HMBC NMR experiments

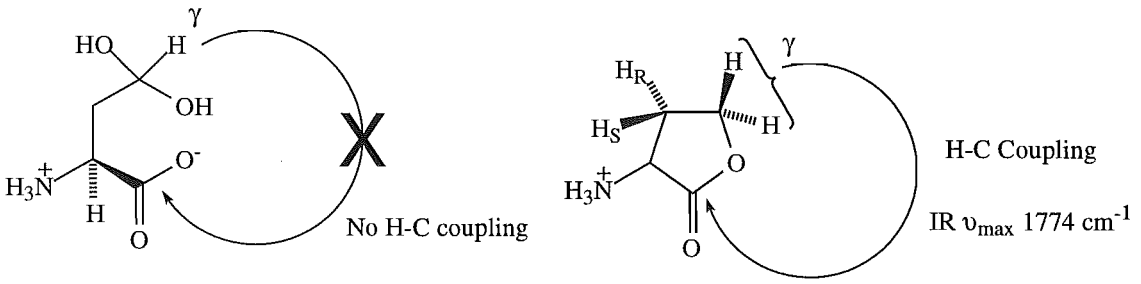

(S)-Aspartate β-semialdehyde (11)

Homoserine lactone (31)

Figure 3-18: HMBC NMR experiments

(i) HMBC NMR of homoserine lactone (31)

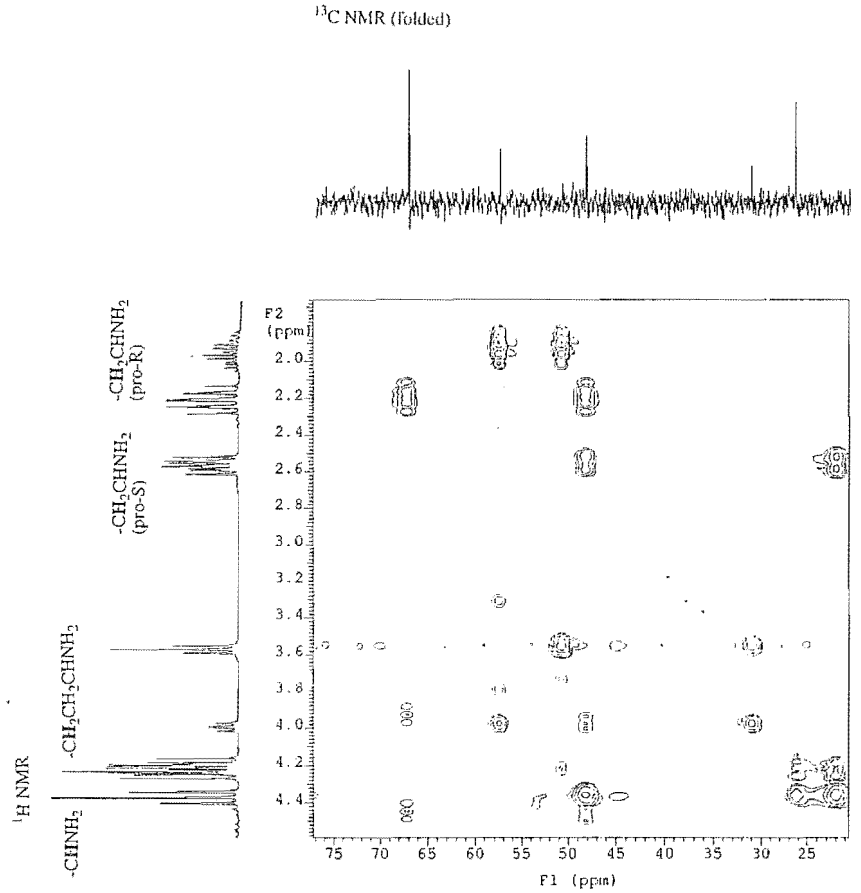

(ii) HMBC NMR of (S)*-aspartate β-semialdehyde (11)*

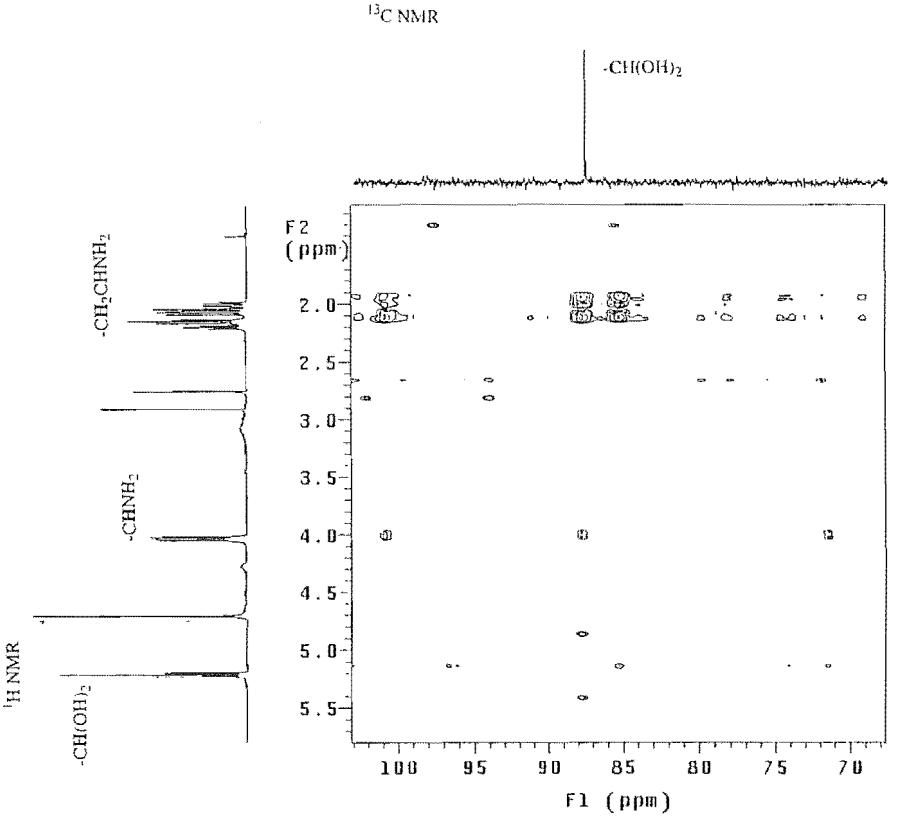

Solution properties of* (S)*-aspartate β-semialdehyde as a function of time and pH

The ^{1}H NMR properties of *(S)*-aspartate β-semialdehyde (11) were studied as a function of time and pH to provide information about the structure equilibria in solution. It was found that *(S)*-aspartate β-semialdehyde (11) was stable in deuterium oxide (D_2O) for greater than 96 hours (~4 days). It was observed that the resonances due to the β protons decreased in intensity over this time due to exchange with deuterium oxide, see figure 3-19.

Figure 3-19: Exchange of β protons in deuterium oxide

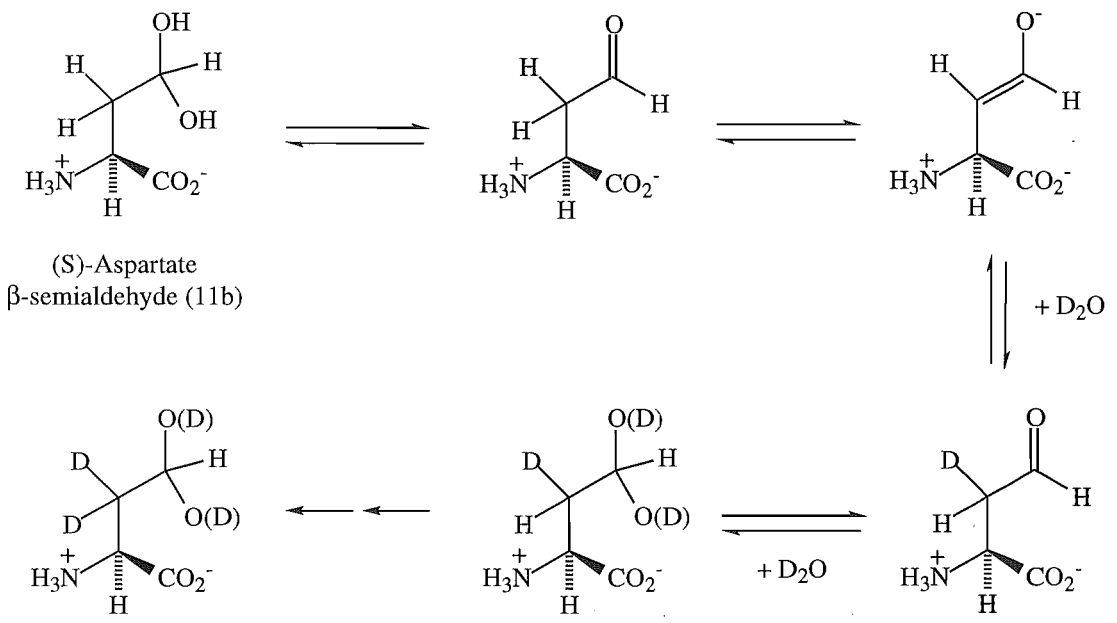

At pH 1 and 4 no aldehyde peak was present; at pH 7 a peak appeared at δ_H 9.61 ppm, corresponding to an aldehyde moiety, started to appear (this had been observed in the initial ^{1}H NMR studies performed), see figures 3-20 and 3-16 (iii). This was slightly more pronounced at pH 9. This showed that, while a small amount of the free aldehyde was present above pH 7, it was not a significant species in aqueous solutions of *(S)*-aspartate β-semialdehyde (11).

Figure 3-20: Aldehyde formation in (S)*-asparate β-semialdehyde (11)*

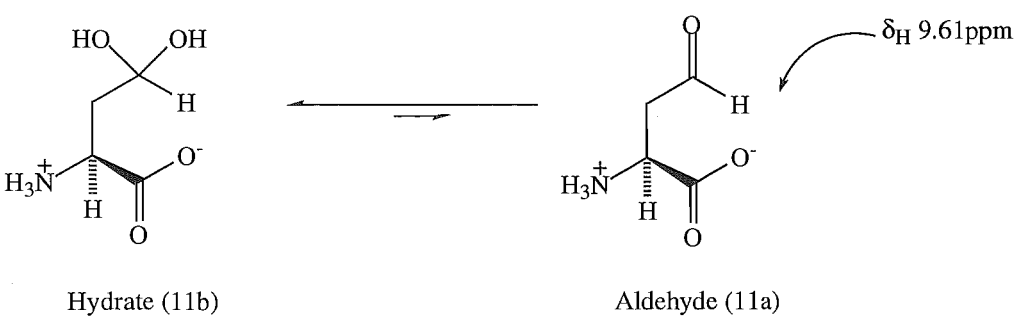

The structural studies on *(S)*-aspartate β-semialdehyde (11) strongly suggest that, in aqueous solution, *(S)*-aspartate β-semialdehyde (11) exists predominantly as the linear hydrate (11b). This correlates with the enzymological studies which suggest that DHDPS recognises a linear form of *(S)*-aspartate β-semialdehyde (11).

Analogues of the hydrate form of *(S)*-aspartate β-semialdehyde

Since *(S)*-aspartate β-semialdehyde (11) appears to exist predominantly as a linear hydrate (11b) in aqueous solutions, analogues of this structure were tested as possible inhibitors of DHDPS. *S*-Methyl-*(R)*-cysteine (76) and the corresponding sulfoxide (77) and sulfone (78), together with *(R)*-cysteine sulfinic acid (79) were tested for inhibition of DHDPS. Finally other amino acids, namely *(S)*-aspartic acid (9), *(S)*-asparagine (80), and *(S)*-glutamic acid (81), were tested. The chemical structures of these analogues are shown in figure 3-21.

Figure 3-21: Structure of (S)*-aspartate β-semialdehyde hydrate (11b) and analogues*

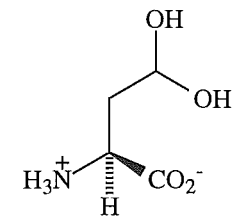

(S)-Aspartate β-semialdehyde (11b)

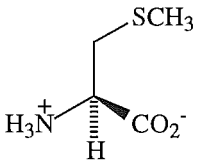

S-Methyl-*(R)*-cysteine (76)

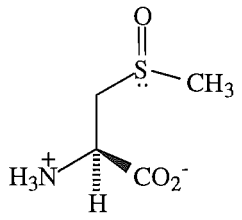

S-Methyl-*(R)*-cysteine sulfoxide (77) (2 Diastereoisomers)

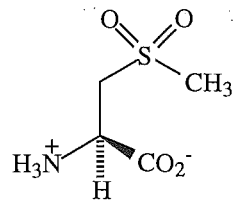

S-Methyl-*(R)*-cysteine sulfone (78)

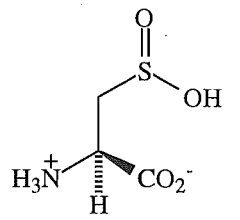

(R)-Cysteine sulfinic acid (79)

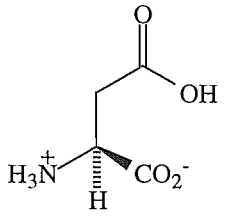

(S)-Aspartic acid (9)

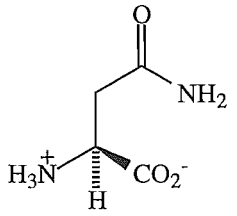

(S)-Asparagine (80)

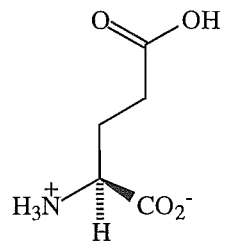

(S)-Glutamic acid (81)

S-*Methyl*-(R)-*cysteine*

Inhibition studies on DHDPS showed *S*-methyl-*(R)*-cysteine (76) did not inhibit at concentrations up to 50 mM.

S-*Methyl*-(R)-*cysteine sulfoxide*

Hydrogen peroxide was used to oxidise *S*-methyl-*(R)*-cysteine (76) to the corresponding sulfoxide (77),[19] see figure 3-22. This sulfoxide precipitated out of solution on addition of methanol and acetone. The reaction proceeded in an unoptimised yield of 23%. The sulfoxide was produced as a mixture of two diastereoisomers. Identification of the product was by ^{1}H NMR and ^{13}C NMR comparing the spectra from the product with that of the starting material and then comparing both of these to methionine and methionine sulfoxide.[20] The $-SCH_3$ resonance moved from δ_H 2.08 in the sulfide, to δ_H 2.75 in the sulfoxide (compared to methionine δ_H 2.15 and methionine sulfoxide δ_H 2.80). The $-CH_2-$ peaks also moved down field as did the α proton, δ_H 3.86 (in the sulfide) to δ_H 4.11 - 4.21 (in the sulfoxide). Mass spectra confirmed the sulfoxide was present as the corresponding protonated molecular ion was observed, and infra-red spectra indicated a distinctive sulfoxide stretch at 1022 cm^{-1}.

Figure 3-22: Synthetic scheme[19]

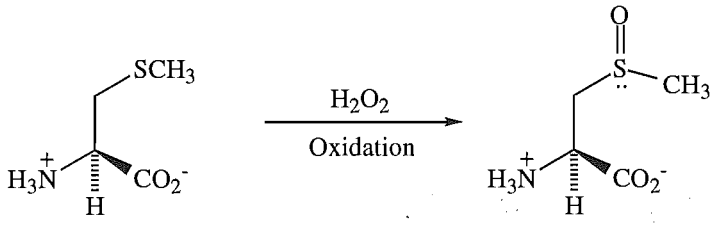

S-Methyl-*(R)*-cysteine (76)

S-Methyl-*(R)*-cysteine sulfoxide (77)
(Two diastereoisomers)

Inhibition studies on DHDPS showed *S*-methyl-*(R)*-cysteine sulfoxide (77), like *S*-methyl-*(R)*-cysteine (76), did not inhibit at concentrations up to 50 mM.

S-*Methyl*-(R)-*cysteine sulfone*

The two step oxidation was performed with ammonium molybdate and perchloric acid, followed by hydrogen peroxide,[21] see figure 3-23. Mass spectra was consistent with sulfone generation. Sulfone absorbances were identified in the infra-red spectra at 1410 and 1387 cm^{-1}. NMR spectra were also obtained and showed that no starting material or sulfoxide was present.

Figure 3-23: Synthetic scheme[21]

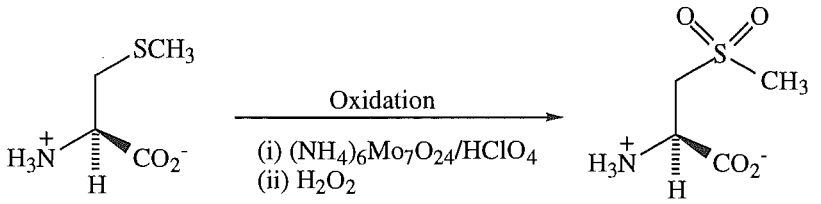

S-Methyl-*(R)*-cysteine (76) *S*-Methyl-*(R)*-cysteine sulfone (78)

Inhibition studies on *S*-methyl-*(R)*-cysteine sulfone (78), again like *S*-methyl-*(R)*-cysteine (76) and the sulfoxide (77), did not show any inhibition at concentrations up to 50 mM.

(R)-*Cysteine sulfinic acid*

(R)-Cysteine sulfinic acid (79) was tested as a possible inhibitor of DHDPS. It was found to be a moderate inhibitor; at 10 mM there was 37% inhibition, while at 50 mM there was 89% inhibition. Detailed kinetics were, therefore, run and it was found that this compound was a moderately strong reversible uncompetitive inhibitor, with respect to *(S)*-aspartate β-semialdehyde (11), as the Dixon plot consists of a series of nearly parallel lines, while the modified Dixon plot has a series of lines that have a common intercept at a positive substrate concentration upon rate value. K_i' (calculated from the modified Dixon plot) was in the range of (6.1 - 8.6) x 10^{-3} M, see table 3-5 and figure 3-24.

Table 3-5: Kinetic parameters of the inhibition of (R)*-cysteine sulfinic acid (79) on DHDPS activity with respect to* (S)*-aspartate β-semialdehyde (11)*

[*(R)*-cysteine sulfinic acid] mM	K_m x 10^{-4} M	V_{max} x 10^{-1} μmol·$s^{-1}$$mg^{-1}$
0	1.92	7.37
10	0.547	3.30
20	0.679	2.66
30	0.543	1.49

Figure 3-24: Kinetic plots of the inhibition of (R)*-cysteine sulfinic acid (79) on DHDPS activity with respect to* (S)*-aspartate β-semialdehyde (11)*

(i) Dixon plot

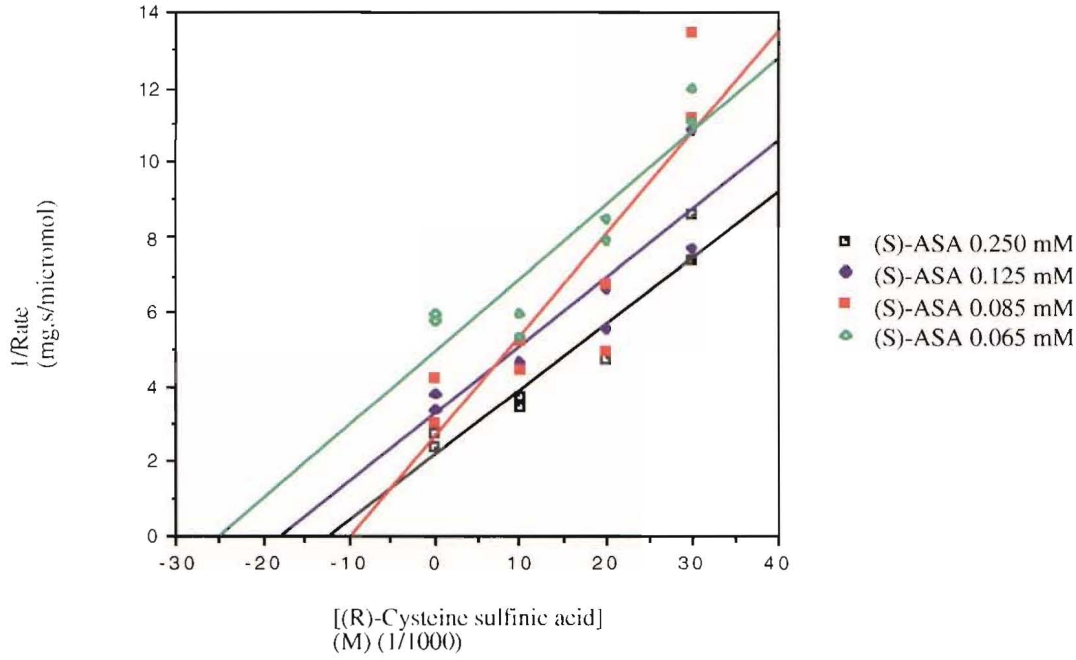

(ii) Modified Dixon plot

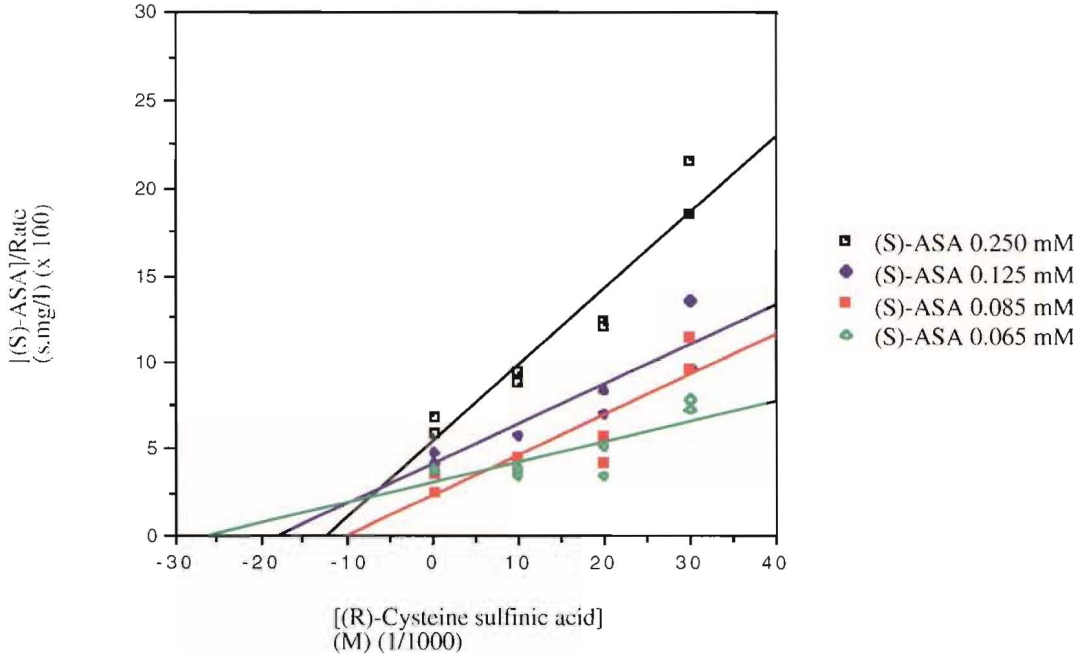

Effect of* (S)*-aspartic acid on DHDPS kinetics

As *(R)*-cysteine sulfinic acid (79) inhibits DHDPS it was hypothesised that related amino acids may also inhibit DHDPS. *(S)*-Aspartic acid (9) was also tested as an inhibitor of DHDPS. This amino acid is similar to *(R)*-cysteine sulfinic acid (79), it has the same length carbon backbone but a carboxylic acid moiety as opposed to the sulfinic acid group. *(S)*-Aspartic acid (9) was found to be a mixed inhibitor of DHDPS, with respect to *(S)*-aspartate β-semialdehyde (11), as the Dixon plot shows a series of lines that have common intercept at a positive inverse rate value, while the modified Dixon plot comprises of a series of straight lines with a common intercept at a negative value of substrate concentration upon rate. K_i (calculated from the Dixon plot) was in the range of (0.9 - 1.4) x 10^{-2} M and K_i' (calculated from the modified Dixon plot) was in the range of (2.1 - 3.9) x 10^{-2} M, see table 3-6 and figure 3-25. One interpretation of the observation that *(S)*-aspartic acid is a mixed inhibitor (it has properties of both uncompetitive and competitive inhibition) is that the *(S)*-lysine (12) feedback inhibition allosteric site and the *(S)*-aspartate β-semialdehyde hydrate (11b) active site, of DHDPS, may overlap and that *(S)*-aspartic acid (9) binds there.

Table 3-6: Kinetic parameters of the inhibition of (S)*-aspartic acid (9) on DHDPS activity with respect to* (S)*-aspartate β-semialdehyde (11)*

[*(S)*-aspartic acid] mM	K_m x 10^{-4} M	V_{max} x 10^{-1} μmol·s^{-1}mg^{-1}
0	1.48	6.40
10	1.37	5.38
20	0.586	2.46
30	2.50	3.67

Figure 3-25: Kinetic plots of the inhibition of (S)*-aspartic acid (9) on DHDPS activity with respect to* (S)*-aspartate β-semialdehyde (11)*

(i) Dixon plot

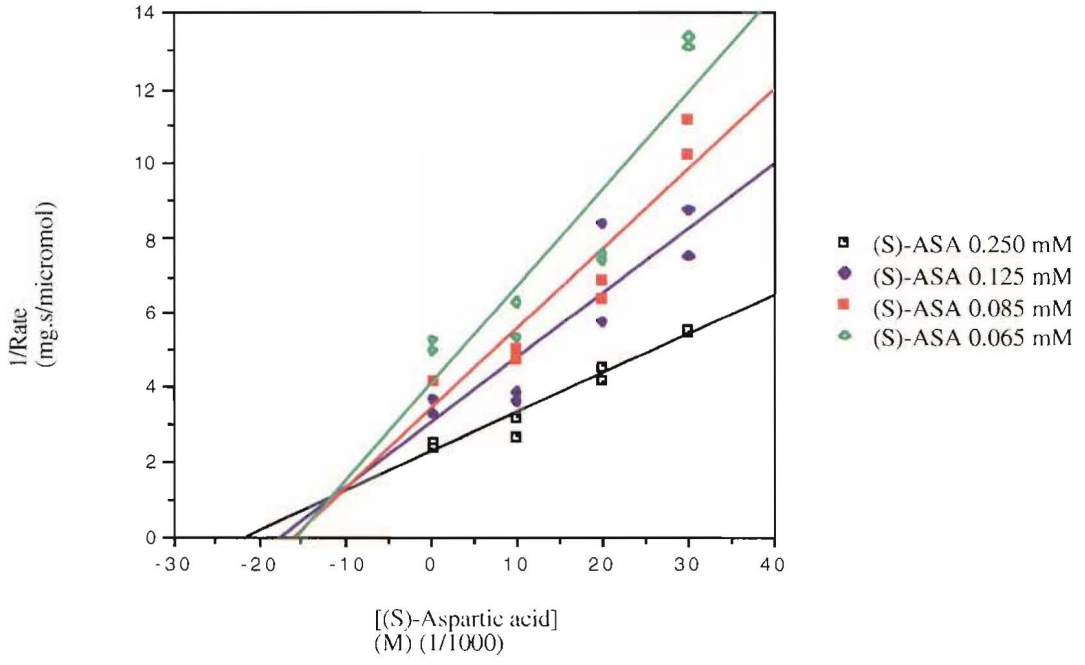

(ii) Modified Dixon plot

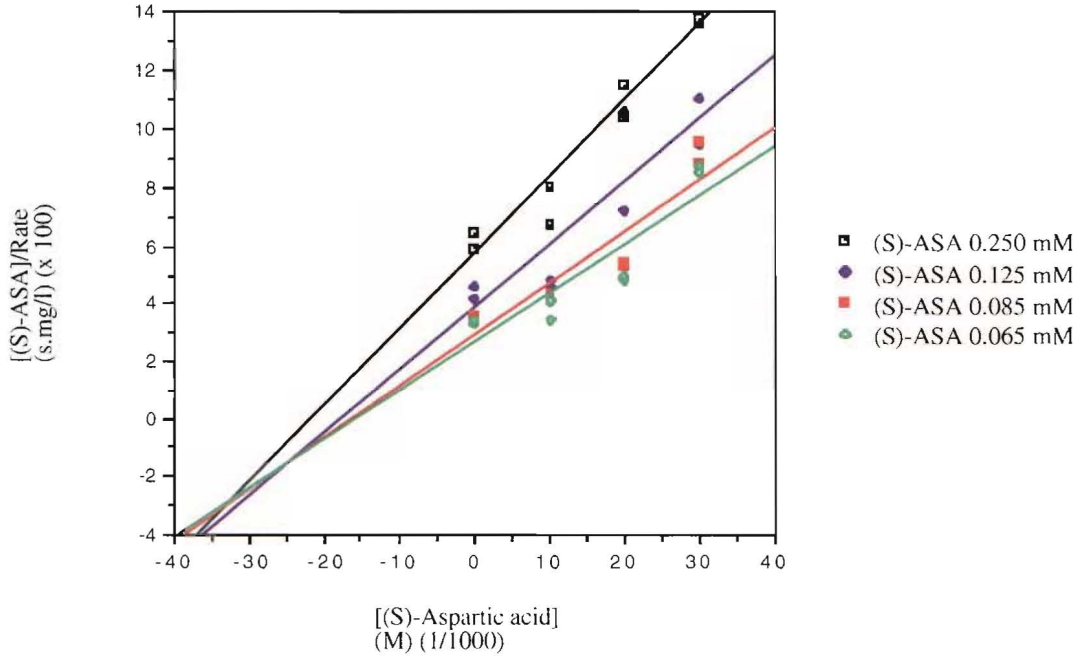

(S)-Asparagine (80), which is analogous to *(S)*-aspartic acid (9) with an amide group rather than a carboxylic acid group, was tested for inhibition of DHDPS. However, it did not show inhibition at concentrations up to 50 mM.

Effect of* (S)-*glutamic acid on DHDPS kinetics

(S)-Glutamic acid (81), which contains a carbon backbone one unit larger than *(S)*-aspartic acid (9), was tested as an inhibitor of DHDPS. *(S)*-Glutamic acid (81) was found to be an uncompetitive inhibitor of DHDPS, with respect to *(S)*-aspartate β-semi-aldehyde (11), like *(R)*-cysteine sulfinic acid (79), the Dixon plot gave a series of almost parallel lines, where the modified Dixon plot gave a series of lines with a common intercept at a positive substrate concentration upon rate value. K_i' (calculated from the modified Dixon plot) was in the range of (0.9 - 1.6) x 10^{-2} M, see table 3-7 and figure 3-26.

Table 3-7: Kinetic parameters of the inhibition of (S)-*glutamic acid (81) on DHDPS activity with respect to* (S)-*aspartate β-semialdehyde (11)*

[*(S)*-glutamic acid] mM	K_m x 10^{-4} M	V_{max} x 10^{-1} μmol·$s^{-1}$$mg^{-1}$
0	1.91	6.43
10	6.09	4.93
20	1.05	3.05
30	2.20	0.997

Figure 3-26: Kinetic plots of the inhibition of (S)-*glutamic acid (81) on DHDPS activity with respect to* (S)-*aspartate β-semialdehyde (11)*

(i) Dixon plot

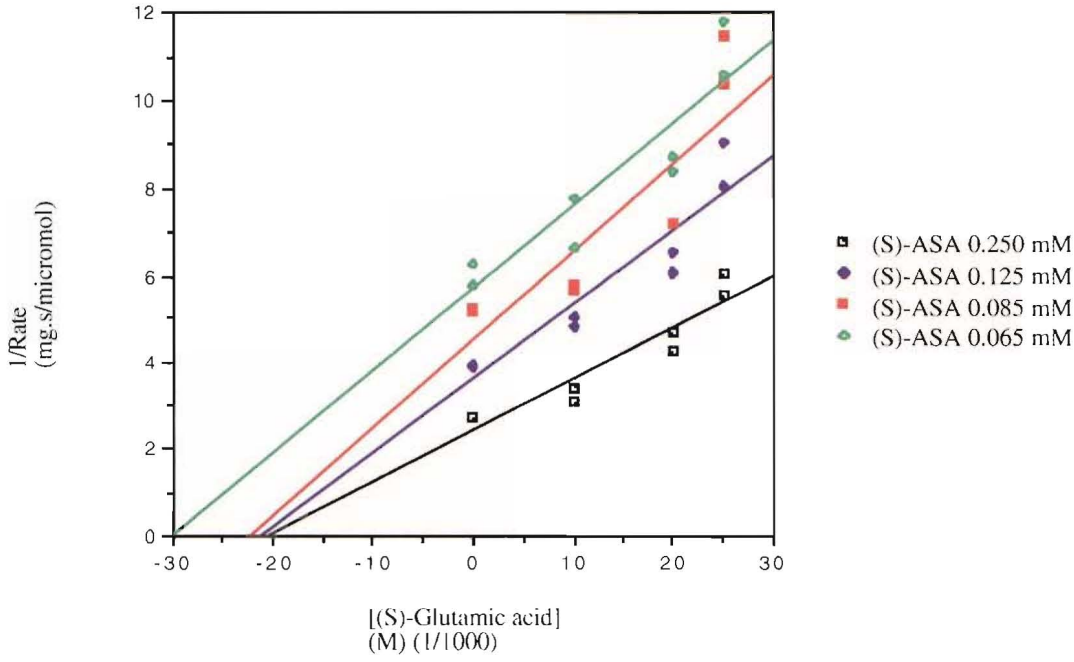

(ii) Modified Dixon plot

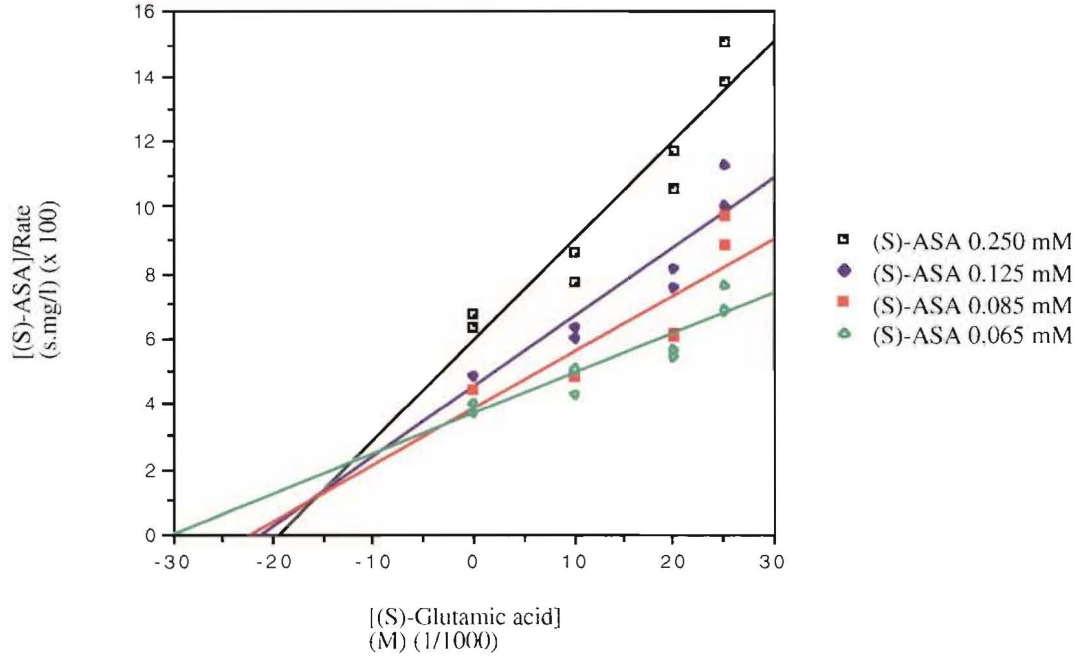

Summary

Analogues of the hypothesised cyclic lactol structure of *(S)*-aspartate β-semialdehyde (11) were tested for inhibition against DHDPS. These analogues included homoserine lactone (31), *(S)*-3-aminopyrrolid-2-one (62), and 2-aminocyclopentanone (63). Homoserine lactone (31) was found to be a reversible noncompetitive inhibitor of DHDPS with respect to both substrates, K_i with respect to *(S)*-aspartate β-semialdehyde (11) was in the range of (1.2 - 2.2) x 10^{-2} M, and K_i with respect to pyruvate (17) was in the range of (0.8 - 1.5) x 10^{-2} M. 2-Aminocyclopentanone (63) also showed reversible noncompetitive inhibition with respect to *(S)*-aspartate β-semialdehyde (11), but K_i was greatly increased, and found to be in the range of (1.2 - 2.4) x 10^{-1} M. *(S)*-3-Aminopyrrolid-2-one (62) did not inhibit DHDPS. Since these cyclic molecules do not competitively inhibit DHDPS it is unlikely that the substrate *(S)*-aspartate β-semialdehyde (11) binds to the enzyme in a cyclic form.

The solution structure of *(S)*-aspartate β-semialdehyde (11) was determined by spectroscopic means, including NMR and infra-red spectroscopy, to be the linear hydrate (11b). No cyclic lactol (11c) was observed at physiological pH and only traces of free aldehyde (11a) were present.

Analogues of the hydrate form of *(S)*-aspartate β-semialdehyde (11b) were then tested as inhibitors of DHDPS. These included *S*-methyl-*(R)*-cysteine (76) and the corresponding sulfoxide (77) and sulfone (78), *(R)*-cysteine sulfinic acid (79), *(S)*-aspartic acid (9), *(S)*-asparagine (80), and *(S)*-glutamic acid (81). *(R)*-Cysteine sulfinic acid (76), and *(S)*-glutamic acid (81) were uncompetitive inhibitors of DHDPS, with respect to *(S)*-aspartate β-semialdehyde (11), *(R)*-cysteine sulfinic acid (79) had a K_i' in the range of (6.1 - 8.6) x 10^{-3} M, while *(S)*-glutamic acid (81) had a K_i' in the range of (0.9 - 1.6) x 10^{-2} M. *(S)*-Aspartic acid (9) was a mixed type inhibitor of DHDPS, with respect to *(S)*-aspartate β-semialdehyde (11), where K_i was in the range of (0.9 - 1.4) x 10^{-2} M, and K_i' was in the range of (2.1 - 3.9) x 10^{-2} M. It is suggested that these inhibitors bind to the *(S)*-lysine (12) feedback inhibition site, as they do not compete with the substrate for the active site.

References

1. R.J. Cox *Natural Product Reports* **13**, 29 (1996).
2. S. Black, N. Wright *J. Biol. Chem.* **213**, 39 (1955).
3. D.W. Tudor, T. Lewis, D.J. Robins *Synthesis* 1061, (1993).
4. F. Salmon-Legagneur *Bull. Soc. Sci. Bret.* **50**, 106 (1975).
5. J.P. Whitten, C.L. Barney, E.W. Huber, P. Bey, J.R. McCarthy *Tet. Lett.* **30**, 3649 (1989).
6. D. Ben-Ishai, R. Moshenberg, J. Altman *Tetrahedron* **33**, 1533 (1977).

7. J.A. Gerrard *'Studies on Dihydropicolinate Synthase'* D. Phil, Brasenose College, Oxford (1992).
8. G.W. Huisman, P. Kolter *Science* **265**, 537 (1994).
9. S. Wilkinson *J. Chem. Soc.* **154**, 104 (1951).
10. H.E. Baumgarten, J.M. Patersen *Org. Synth* Coll. Vol. **V**, 909 (1973).
11. V.S. Akabori, S. Numano *Bull. Chem. Soc. Japan* **11**, 214 (1936).
12. *'Dictionary of Organic Compounds'* 5th ed. C-03623 (1982).
13. A.J. Vogel *'A Textbook of Practical Organic Chemistry'* 3rd ed. Longman, London (1956) p 348 (III, 76).
14. *'Dictionary of Organic Compounds'* 5th ed. C-03681 (1982).
15. A.J. Vogel *'A Textbook of Practical Organic Chemistry'* 3rd ed. Longman, London (1956) p 418 (III, 121).
16. M.J. Mintz, C. Walling *Org. Synth* Coll. Vol. **V**, 184 (1973).
17. P.F. Frankland, F.H. Garner *J. Soc. Chem. Ind.* **89**, 257 (1920).
18. C. Golumbic, J.S. Fruton, M. Bergmann *J. Org. Chem.* **11**, 518 (1946).
19. C.R. Johnson, M.P. Westrick *Meth. Enz.* **143**, 281 (1987).
20. C.I. Poucher, J. Behnke *'The Aldrich Library of ^{13}C and ^{1}H FTNMR Spectra'* Aldrich, USA (1993).
21. D.W. Griffith *Meth. Enz.* **143**, 274 (1987).

Results and Discussion Chapter Four

Analogues of Dipicolinate Species

Introduction

The enzyme DHDPS catalyses the condensation of *(S)*-aspartate β-semialdehyde (11) and pyruvate (17), the product (normally formulated as dihydrodipicolinate (18)) is then reduced by DHDPR, to yield tetrahydrodipicolinate (19), see figure 4-1. The condensation reaction presumably generates a reduced pyridine derivative, but, at the onset of this work, there was uncertainty about the exact nature of this heterocycle. It was not known whether the product was a dihydropyridine or a hydroxytetrahydropyridine which could be subsequently dehydrated to give a dihydropyridine. The literature usually reports the product of the DHDPS catalysed reaction as 2,3-dihydrodipicolinate (18), although both 2,5-dihydrodipicolinate (27) and 4-hydroxy-2,3,4,5,-tetrahydrodipicolinate (28) have also been hypothesised,[1] see figure 4-2. Work on isolating or synthesising these compounds is difficult due to the ring instability, so stable analogues of these three possible intermediates, hydroxytetrahydrodipicolinate (28), dihydrodipicolinate (18), and tetrahydrodipicolinate (19), were investigated in an effort to obtain further information about the DHDPS and DHDPR catalysed reactions and the substrates and products concerned.

Figure 4-1: Possible scheme for the DHDPS catalysed condensation of (S)*-aspartate β-semialdehyde (11) and pyruvate (17), followed by the DHDPR catalysed reaction*

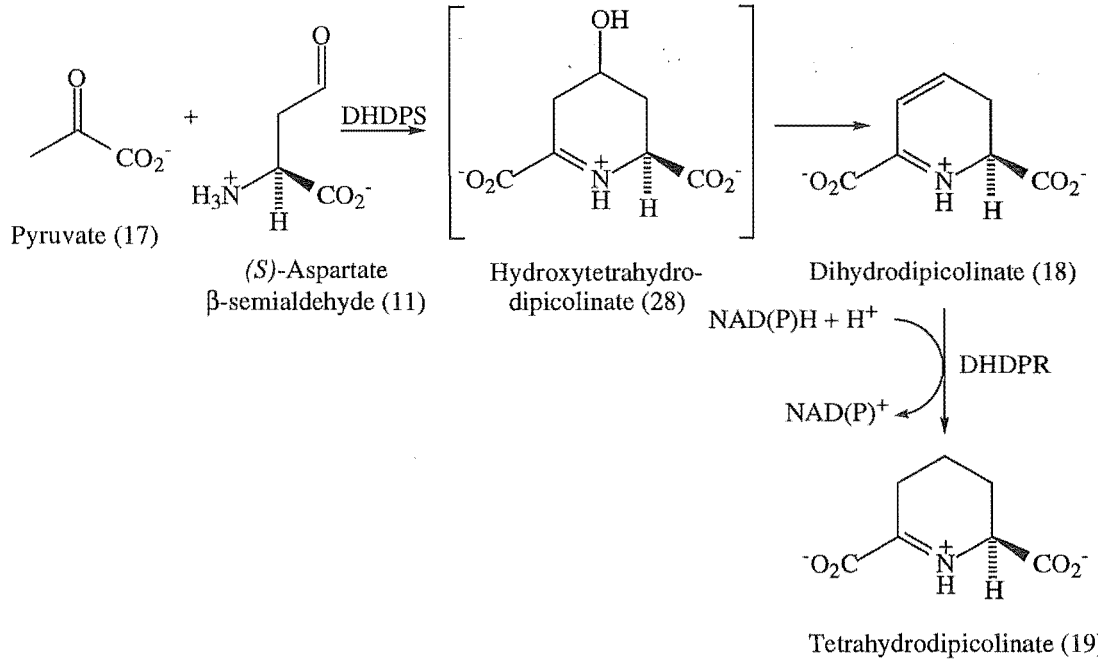

Figure 4-2: Hypothesised structures of the product of the DHDPS catalysed reaction

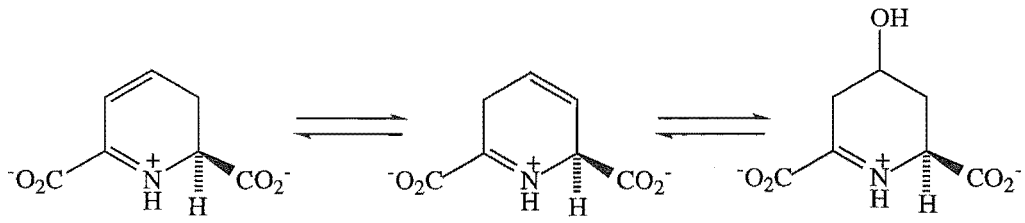

2,3-Dihydrodipicolinate (18) 2,5-Dihydrodipicolinate (27) 4-Hydroxy-2,3,4,5-tetrahydrodipicolinate (28)

If the initially formed product is a hydroxytetrahydropyridine it is most likely to be 4-hydroxy-2,3,4,5-tetrahydrodipicolinate (28); this retains the chirality of *(S)*-aspartate β-semialdehyde (11). If a dihydropyridine is formed, either from the DHDPS catalysed reaction or from a subsequent dehydration, there are theoretically five possible isomers—depending on the position of the double bonds in relation to the ring nitrogen,[2] see figure 4-3.

Figure 4-3: The five isomeric dihydropyridines

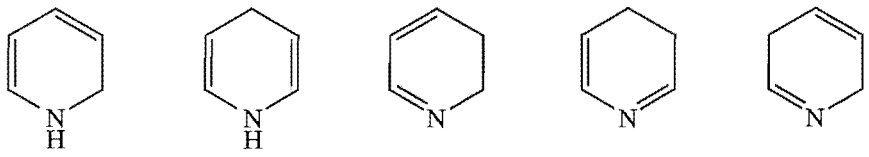

1,2- (82) 1,4- (83) 2,3- (84) 3,4- (85) 2,5- (86)

A 2,5-dihydropyridine (86) seems unlikely as the π electrons are not conjugated. Both 2,3- and 3,4-dihydropyridines (84 and 85 respectively) allow conjugation of electrons over three carbons and the nitrogen. However, 2,3-dihydropyridines (84) are extremely unstable[3] so this structure is also unlikely. 1,2- and 1,4-dihydropyridines (82 and 83 respectively) are more stable as they allow conjugation of electrons over four carbon atoms and the nitrogen. It may be noted that in the reduction of dihydrodipicolinate (18) to tetrahydrodipicolinate (19), by DHDPR, NAD(P)H is employed, an example of a stable 1,4-dihydropyridine (83). Since the stereochemistry of the chiral centre is unchanged during the biosynthesis of *(S)*-lysine (12) the 1,2-dihydropyridine (82) structure seems intrinsically most likely. Thus, if the product initially formed by the DHDPS catalysed reaction is a dihydropyridine it is most probably 1,2-dihydrodipicolinate (24). An alternative intermediacy of a dihydropyridine might involve generation of 2,3-dihydrodipicolinate (18), as a reactive intermediate, by dehydration of 4-hydroxy-2,3,4,5-tetrahydrodipicolinate (28) at the active site of DHDPR. The alternative structures for the product of the DHDPS catalysed reaction are shown in figure 4-4.

Figure 4-4: Alternative structures of dihydrodipicolinate or hydroxytetrahydrodipicolinate

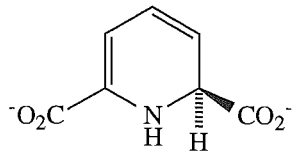

1,2-Dihydrodipicolinate (24)
Retains stereochemistry, and allows conjugation of electrons over four carbons and the nitrogen.

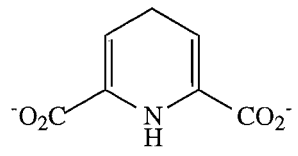

1,4-Dihydrodipicolinate (25)
Allows conjugation of electrons over four carbons and the nitrogen.

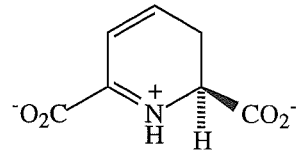

2,3-Dihydrodipicolinate (18)
Retains stereochemistry, and allows conjugation of electrons over three carbons and the nitrogen.

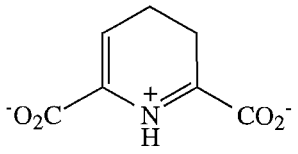

3,4-Dihydrodipicolinate (26)
Allows conjugation of electrons over three carbons and the nitrogen.

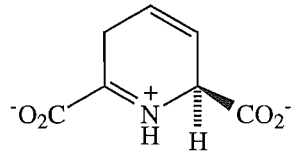

2,5-Dihydrodipicolinate (27)
Retains stereochemistry.

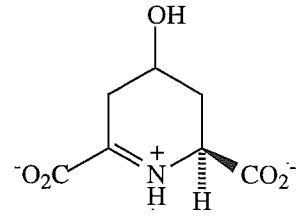

4-Hydroxy-2,3,4,5-tetrahydro-*(2S)*-dipicolinate (28)
Retains stereochemistry.

Work on dihydropyridines reported in the literature focusses on 1,4-dihydropyridines (83),[4] and 1,2-dihydropyridines (82).[5] Dihydropyridines are useful intermediates in organic synthesis, and have been successfully used in alkaloid synthesis.[6] They undertake stereospecific hydride transfers,[7] and have also been used in the pharmaceutical industry for the treatment of angina[8] and as anti-hypertension drugs.[9]

Studies aimed at providing information about the structure of the product of the DHDPS enzyme catalysed reaction have been of two types: NMR studies of the DHDPS enzymatic reaction, and DHDPS and DHDPR inhibition studies using mimics of the possible cyclic intermediates.

NMR studies on the DHDPS catalysed reaction to determine the structure of the product

Work on determining the structure of the product of the DHDPS enzymatic reaction involved following the reaction by NMR, in conjunction with a literature search on dihydropyridines and their NMR data. Figure 4-5 shows the chemical shifts of various dihydropyridines.[10,11]

Figure 4-5: NMR resonances of various dihydropyridines[10,11]

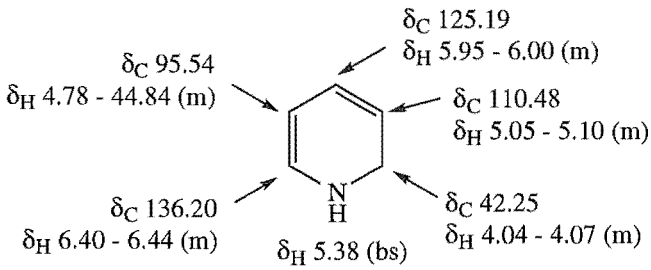

1,2-
(82)

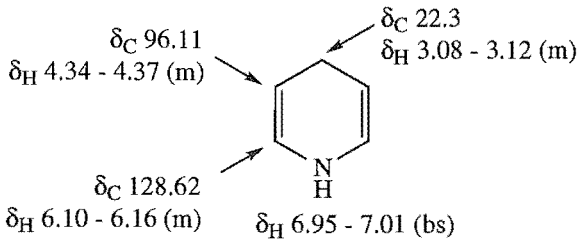

1,4-
(83)

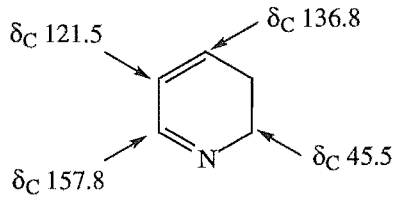

2,3-
(84)

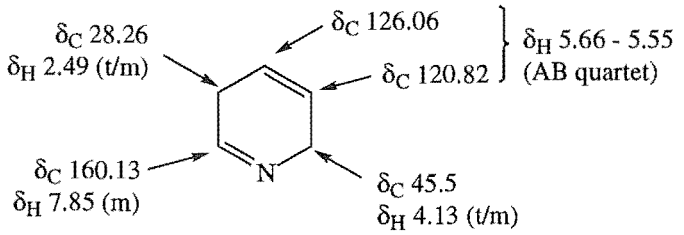

2,5-
(86)

In the ^{1}H NMR studies resonances due to the substrates, *(S)*-aspartate β-semi-aldehyde (11) and pyruvate (17), were well resolved in deuterium oxide (buffered at pH 7.2) with ~15% aqueous present (the enzyme was introduced in this aqueous solution). As many dihydropyridines are relatively unstable the experiments were performed on a short time scale in an inert environment. *(S)*-Aspartate β-semialdehyde (11) and pyruvate (17) were relatively stable in these conditions, and did not form detectable amounts of the corresponding Schiff base. High buffer concentrations (1 M) were required as *(S)*-

aspartate β-semialdehyde (11), present in high concentration, was introduced as the trifluoroacetate salt. Phosphate buffer (K_2HPO_4/KH_2PO_4), at pH 7.2, was used rather than Mops buffer as this is ^1H NMR silent. Kinetics performed on the two buffers showed they gave comparable K_m and V_{max} values for *(S)*-aspartate β-semialdehyde, thus, phosphate does not significantly affect catalysis by DHDPS. The K_m and V_{max} values were calculated from Lineweaver Burk plots, see table 4-1 and figure 4-6.

Table 4-1: DHDPS kinetic parameters comparing the buffering ability of Mops to phosphate in the DHDPS coupled assay

Buffer and pH at 25 °C	K_m x 10^{-4} M	V_{max} x 10^{-1} μmol·s^{-1}mg^{-1}
Mops pH 7.2	1.24	7.08
Phosphate pH 7.2	1.41	8.11

Figure 4-6: Lineweaver Burk plots comparing the buffering ability of Mops to phosphate in the DHDPS coupled assay

(i) 200 mM Mops buffer at pH 7.2

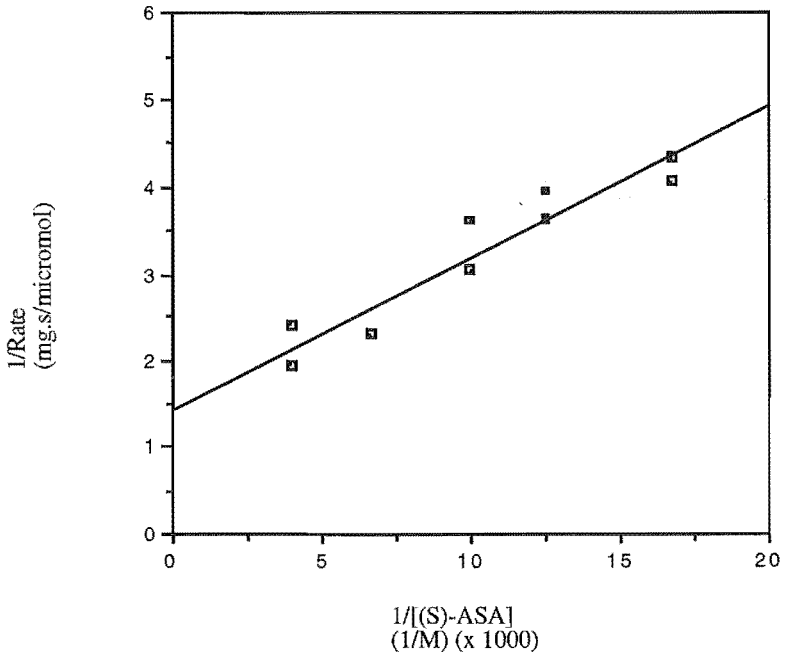

(ii) 200 mM Phosphate buffer at pH 7.2

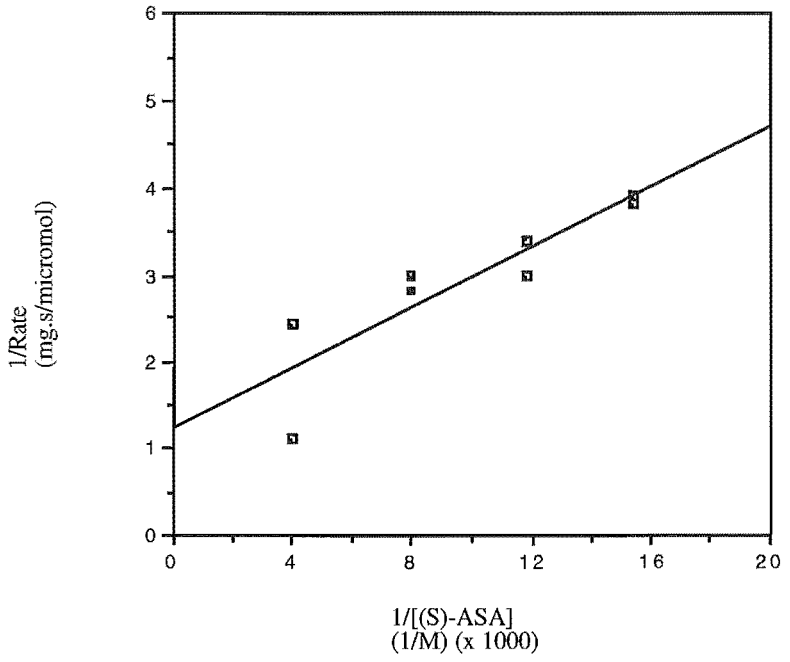

A chemical change, assumed to be due to enzyme catalysis, was observed as the substrates diminished over time (~2 hours). Peaks in the regions of δ_H 1.6 - 2.6, 3.4 - 4.4, 7.5 - 8.6 ppm appeared but the product could not be resolved, see figure 4-7. These peaks were absent from the control (*(S)*-aspartate β-semialdehyde (11) and pyruvate (17) without the DHDPS enzyme). However, it did appear that no vinylic proton was present, this suggested the structure could be the 4-hydroxy-2,3,4,5-tetrahydrodipicolinate (28). Comparison with the ^{1}H NMR data of synthesised 2,3,4,5-tetrahydrodipicolinate (19),[12,13] which exists in equilibrium with an enamine form (39) and an open chain form (40), supports this, see figure 4-8. 2,3,4,5-Tetrahydrodipicolinate (19) (with no vinylic proton) has all of its ^{1}H NMR resonances in the regions of δ_H 1.55 - 1.72, 2.25, and 4.30 ppm. However, the enamine (39) contains a vinylic proton as a doublet of doublets at δ_H 5.20 ppm. The literature also notes that, in samples of 2,3,4,5-tetrahydro-dipicolinate (19) that had been left for some time trace formation of dipicolinic acid was detected by the appearance of a ^{1}H NMR resonance at δ_H 8.34 ppm.[12,13]

Figure 4-7: ^1H NMR resonance of (S)-aspartate β-semialdehyde (11) and pyruvate (17)

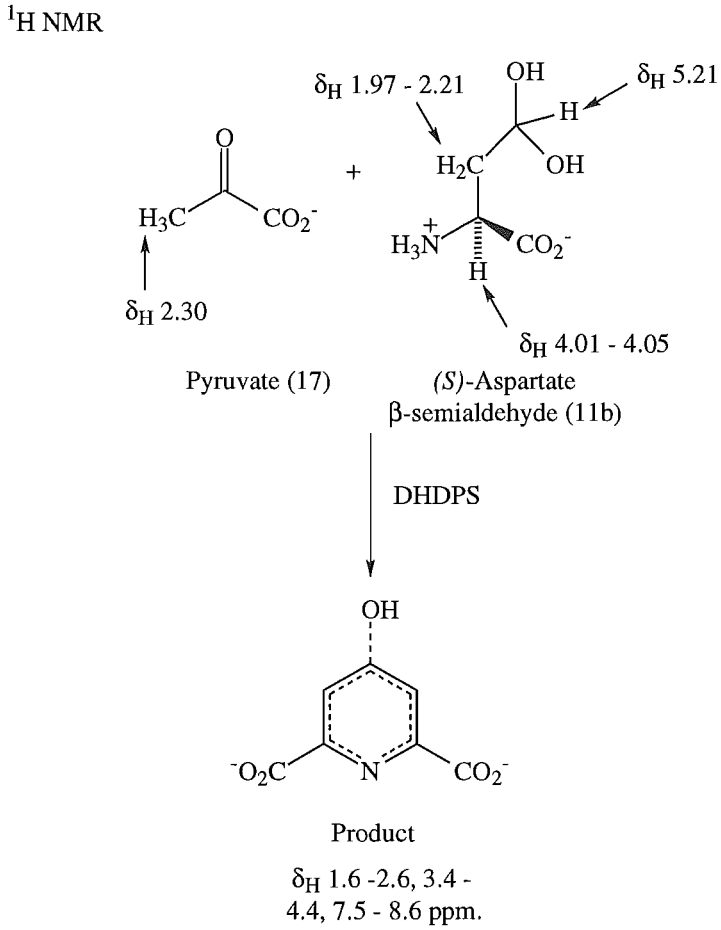

Figure 4-8: ^1H NMR of tetrahydrodipicolinate (19) [12,13]

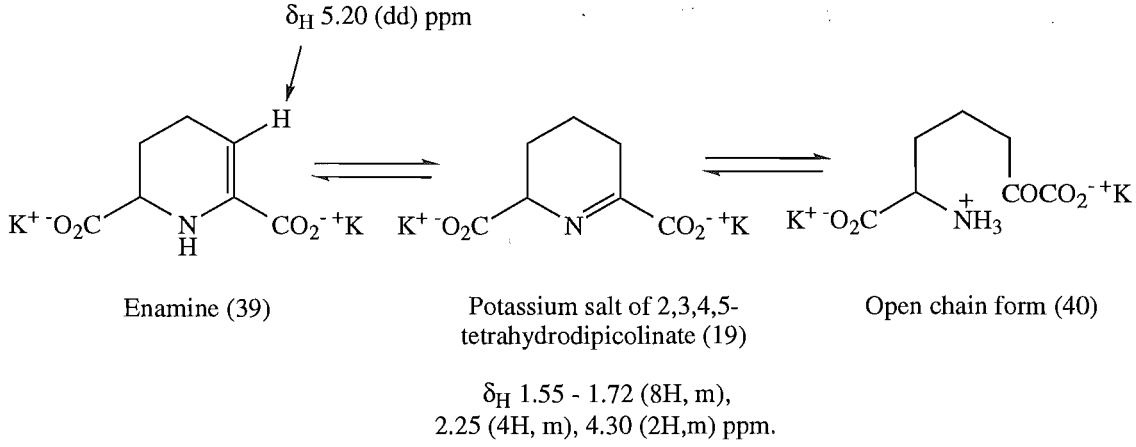

Work published this year,[14] using isotopically labelled metabolites and two dimensional NMR, has demonstrated that *(4S)*-4-hydroxy-2,3,4,5-tetrahydro-*(2S)*-dipicolinate (28) is, in fact, produced by DHDPS catalysis (at pH 8). It is not clear whether the *(4S)*-4-hydroxy-2,3,4,5-tetrahydro-*(2S)*-dipicolinate (28) undergoes DHDPR induced reduction directly or if, prior to reduction, the material undergoes a dehydration to a species such as 2,3-dihydrodipicolinate (18). Since 2,3-dihydro-

pyridines are unstable[3] the presence of such a species would be difficult to detect. A mechanism for the biosynthesis of *(4S)*-4-hydroxy-2,3,4,5-tetrahydro-*(2S)*-dipicolinate (28), based on this NMR work and X-ray crystallography, has been hypothesised.[14] The NMR results obtained above are consistent with those published, see figures 4-9 and 4-10.

Figure 4-9: Reported NMR of (4S)*-4-hydroxy-2,3,4,5-tetrahydro-*(2S)*-dipicolinate (28)* [14]

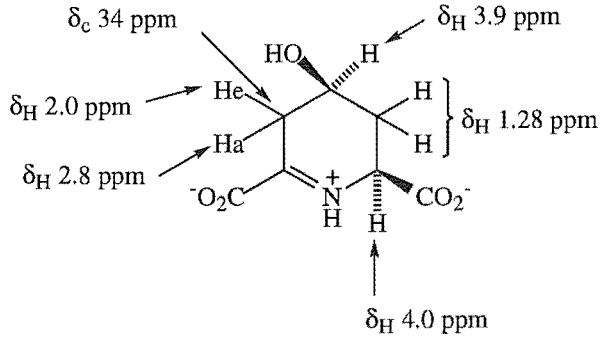

(4S)-4-Hydroxy-2,3,4,5-tetrahydro-*(2S)*-dipicolinate (28)

Figure 4-10: ^{1}H NMR results obtained in this study

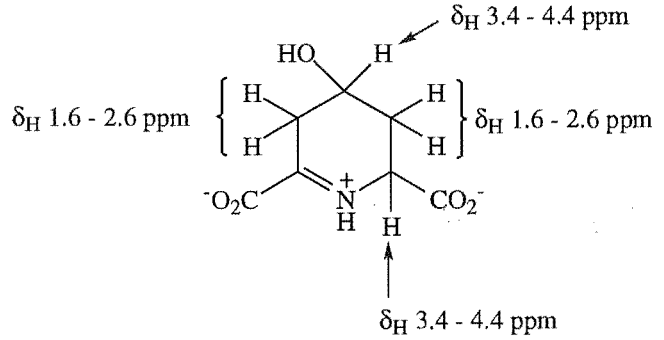

4-Hydroxy-2,3,4,5-tetrahydrodipicolinate (28)

It was also noted that a red coloured complex formed in both the experiment and the control (*(S)*-aspartate β-semialdehyde (11) and pyruvate (17) without the DHDPS enzyme) suggesting that a non-enzymatic process was also occurring. It has been documented that dipicolinate (36) forms non-enzymatically from *(S)*-aspartate β-semialdehyde (11) and pyruvate (17) under very vigorous conditions: an equimolar ratio of sodium pyruvate (17) (in 11 M potassium hydroxide) and aspartate β-semialdehyde (11) (in 2 M hydrochloric acid),[15] see figure 4-11.

Figure 4-11: Non-enzymatic synthesis of dipicolinate (36)[15]

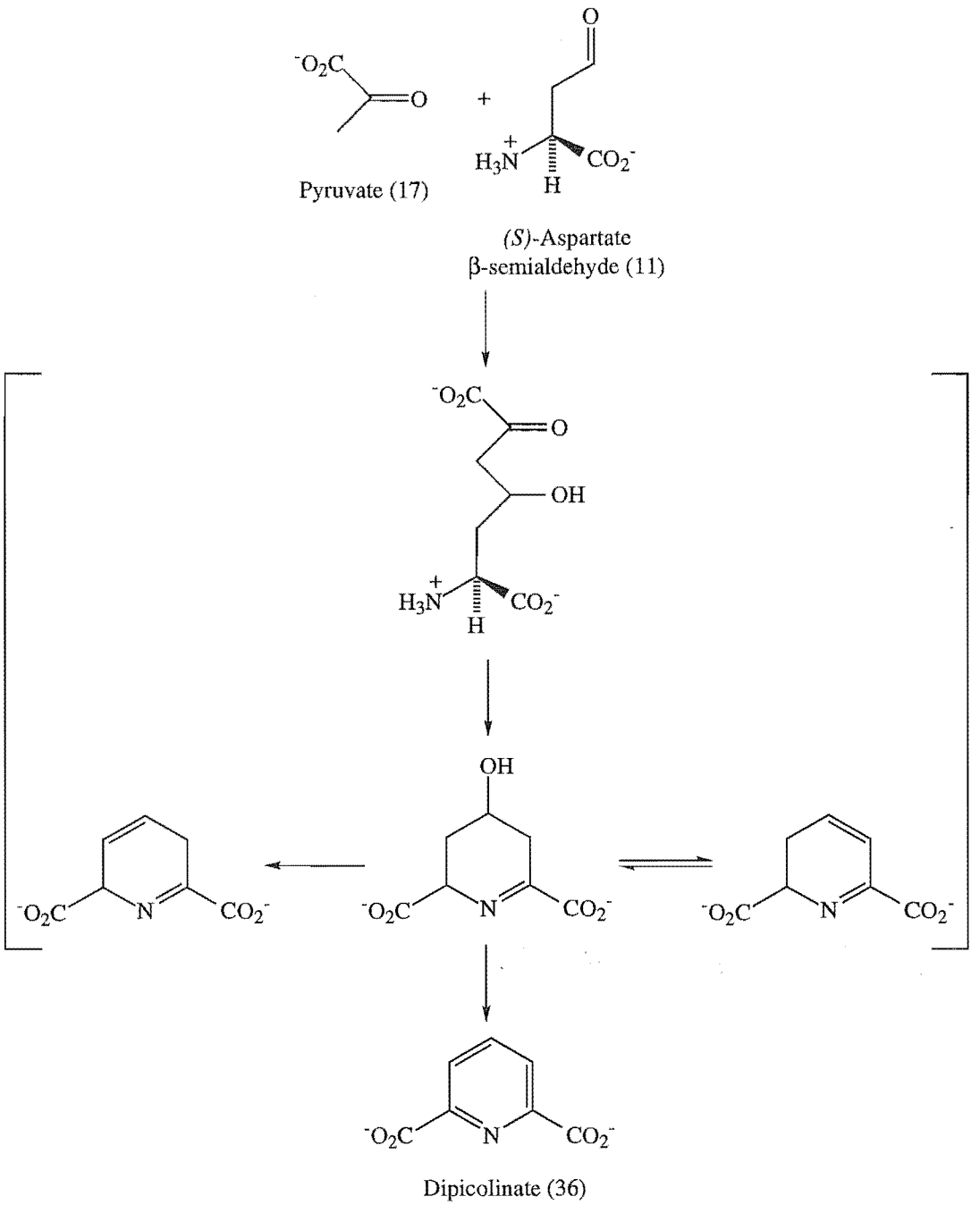

Mechanism of DHDPS

From these results and those published in the literature the information on the DHDPS catalysed reaction can be summarised. The first step in the condensation of *(S)*-aspartate β-semialdehyde (11) and pyruvate (17) to give dihydrodipicolinate (18) is the binding of pyruvate (17). A "ping-pong" mechanism has been postulated[16] where one equivalent of pyruvate (17) binds per subunit (DHDPS is a homotetramer), with the loss of water, followed by binding and reaction of *(S)*-aspartate β-semialdehyde (11). The pyruvate (17) binds to form a Schiff base with the ε-amino group in the active site lysine 161.[17] An imine is formed and this has been observed by electrospray mass spectroscopy.[18,19] Lysine 161 has been found to be the only conserved lysine in all known DHDPS sequences, and the imine formed with this residue is easily trapped by sodium borohydride, see figure 4-12.

Figure 4-12: Sodium borohydride trapping of the Schiff base

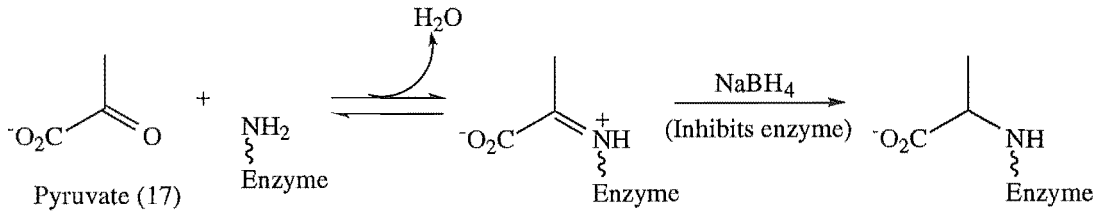

In 1995, the crystal structure of *E. coli* DHDPS at 2.5 Å resolution was published.[17] DHDPS is a homotetramer where each monomer is active. Each monomer is composed of two domains: an eight-fold α/β barrel and a *C*-terminal α-helical domain (residues 224 to 292). The active site lysine 161 is located in the α/β barrel and has access via two entrances from the *C*-terminal side of the barrel. There are adjacent aspartate residues, aspartate 187 and aspartate 188, which form an entrance for the substrates and may have a mechanistic role. As well as Schiff base formation an aldol type condensation and a cyclisation have to occur.

The product of the DHDPS enzyme catalysed reaction is *(4S)*-hydroxy-2,3,4,5-tetrahydro-*(2S)*-dipicolinate (28),[14] rather than a dihydrodipicolinate isomer as previously assumed.[17,18,20,21] The proposed mechanism resulting in the formation of *(4S)*-hydroxy-2,3,4,5-tetrahydro-*(2S)*-dipicolinate[14] is shown in figure 4-13.

Figure 4-13: Mechanism of DHDPS resulting in (4S)-hydroxy-2,3,4,5-tetrahydro-dipicolinate (28) formation[14]

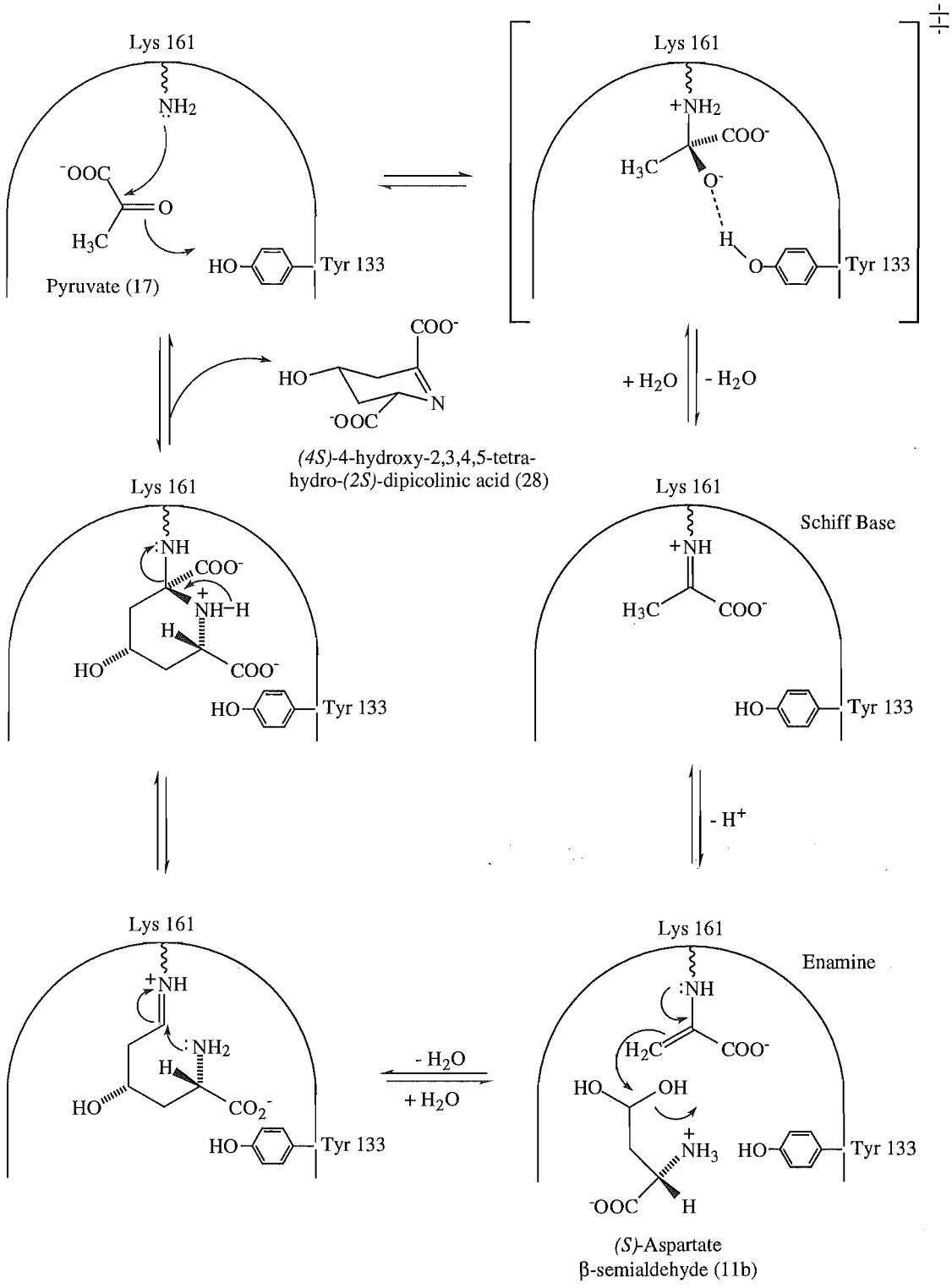

DHDPS has been classified as a type I aldolase, that is its reversible reaction is catalysed through a Schiff base intermediate between the active site lysine and a carbonyl carbon of the substrate. Unlike type II aldolases, a metal ion is not required for catalysis. DHDPS is similar to the type I aldolase fructose-1,6-bisphosphate[22] which cleaves fructose 1,6-bisphosphate into dihydroxyacetone phosphate and glyceraldehyde 3-

phosphate (this enzyme catalysis is a key step in glycolysis). DHDPS also shows considerable homology with the type I aldolase *N*-acetylneuraminate lyase which converts *N*-acetylneuraminic acid (sialic acid) (87) to pyruvate (17) and *N*-acetyl-D-mannosamine (88) via Schiff base formation with an active site lysine residue followed by a retro-aldol reaction, see figure 4-14.[23,24]

Figure 4-14: N-*Acetyl neuraminate lyase from* E. coli[23,24]

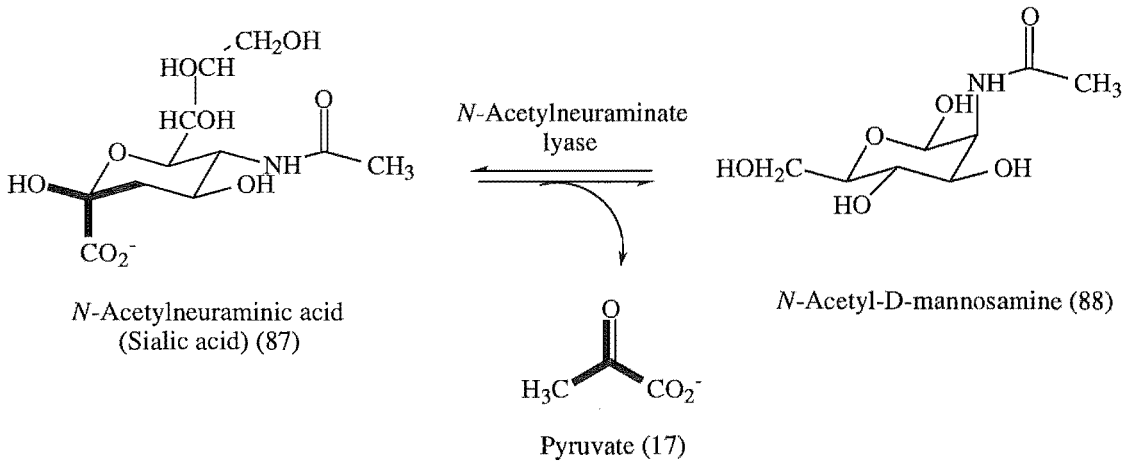

Mechanism of DHDPR

Mechanistic studies have also been published on DHDPR,[25] and *E. coli* DHDPR has recently been crystallised,[26] enhancing the knowledge of the mechanism of this enzyme. X-Ray crystallography shows the enzyme has two domains. A dinucleotide binding domain is present, this has a central seven stranded parallel β-sheet surrounded by four α-helices, and the NAD(P)H cofactor binds to the *C*-terminal end of the β-sheet. There is also a substrate binding domain consisting of a β-sandwich of four β-strands and two α-helices. By X-ray crystallography it has been determined that the cofactor donates its 4-pro-R hydride in the formation of tetrahydrodipicolinate (19). From these X-ray crystallography results and the results above on the mechanism of DHDPS it is hypothesised that 4-hydroxy-2,3,4,5-tetrahydrodipicolinate (28) undergoes a dehydration, *in situ*, to form 2,3-dihyrodipicolinate (18) prior to the reduction forming tetrahydrodipicolinate (19), see figure 4-15.

Figure 4-15: Modification of the mechanism proposed by Reddy et al. in 1995[25]

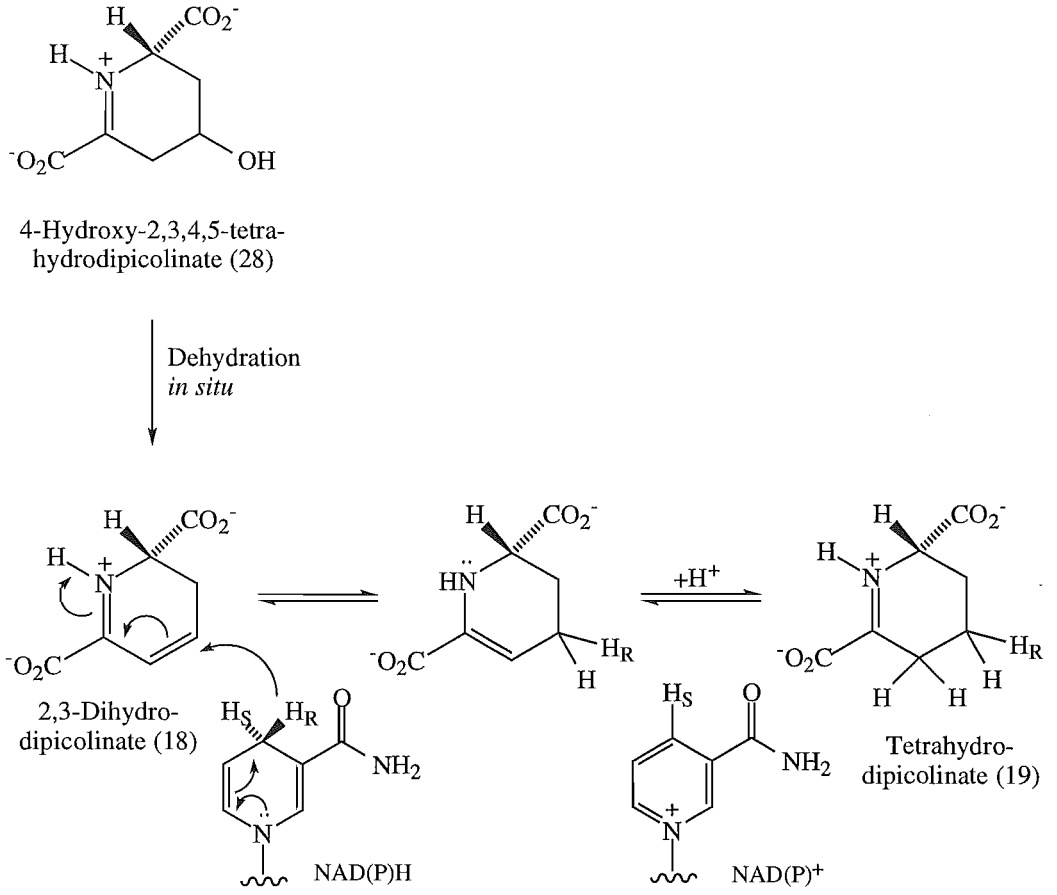

Inhibition studies on DHDPS and DHDPR

Stable analogues of the proposed intermediates in the biosynthetic reactions were investigated in an effort to obtain further structural information about the DHDPS and DHDPR catalysed reactions and provide new types of inhibitors. Initially a range of commercially available cyclic compounds were tested as inhibitors of both DHDPS and DHDPR. Most of these compounds were aromatic and were derivatives of either pyridine or benzene, however, the nonaromatic cyclic compounds piperidine and morpholine were also tested. Further inhibition studies were then performed using partially reduced aromatic compounds, tetrahydrodipicolinic acid mimics, in an effort to gain more information.

The cyclic compounds were tested for inhibition of DHDPS and DHDPR. Previously results obtained in this area used the imidazole buffer assay to measure DHDPS enzyme activity, however, due to the uncertainties in this assay it is difficult to quantify the inhibition accurately. An extensive study of the inhibition of *E. coli* DHDPS by pyridine and piperidine derivatives has been completed by Couper *et al.*[21] These results are based on the imidazole buffer assay and so the data is not definitive. They report that the most potent inhibitors in their study are the *N*-oxide of dipicolinic acid and the di-imidate of dimethyl pyridine-2,6-dicarboxylate (both have IC_{50} values of ~0.2

mM). Dipicolinate (36) was found to be a competitive inhibitor of DHDPS, IC_{50} = 4 x 10^{-4} M. However, this data is in conflict with the IC_{50} value of 1.2 x 10^{-3} M reported by Laber *et al.*,[27] again using the imidazole buffer assay. Tamir and Gilvarg[28] found *E. coli* DHDPR was inhibited by dipicolinate (36), with a K_i of 1 x 10^{-3} M, and isophthalic acid (41), with a K_i of 1.5 x 10^{-2} M.[28] Reddy and Blanchard[25] found dipicolinic acid (36) inhibited DHDPR competitively with respect to dihydrodipicolinate (18), K_i was 2.6 $\pm$ 0.6 x 10^{-5} M, and uncompetitively with respect to NADPH, K_i was 3.3 $\pm$ 0.5 x 10^{-4} M. While picolinic acid (42) and pipecolic acid (43) had shown inhibition of maize DHDPR.[29]

The cyclic compounds were tested for inhibition of DHDPS and DHDPR, where the concentration of *(S)*-aspartate β-semialdehyde (11) was 0.25 mM, and pyruvate (17) was present in vast excess at 40 mM. Most compounds were tested in aqueous solutions at concentrations up to 100 mM or to the limit of their solubility. Some compounds had considerably greater solubility in methanol: in these cases the assay was run in 10% methanol. (10% Methanol decreased the enzyme rate by approximately 20%, but inhibition could still be clearly quantified.) Initially an introductory survey of the cyclic compounds was performed to determine which compounds were strong inhibitors. Detailed kinetic studies were then performed on these inhibitors.

Initially pyridine (89) and pyridine (89) derivatives were tested for inhibition of DHDPS and DHDPR, these compounds contained the heteroatom nitrogen, see figure 4-16 and table 4-2.

Figure 4-16: Pyridine and pyridine derivatives

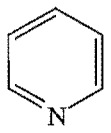

Pyridine (89)

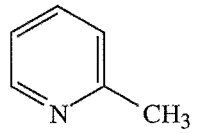

2-Methyl pyridine (90)

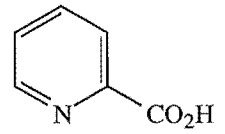

Picolinic acid (42)

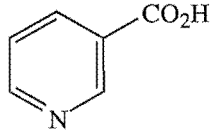

Nicotinic acid (91)

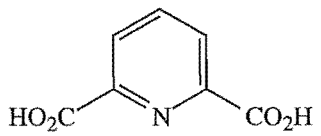

Dipicolinic acid (36)

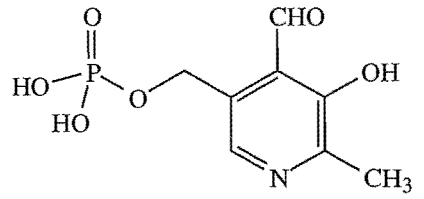

Pyridoxal 5-phosphate (92)

Table 4-2: Inhibition by pyridine (89) derivatives

(i) DHDPS

Compound	Concentration mM	Inhibition %
Pyridine (89)	100	0
2-Methyl pyridine (90)	100	0
Picolinic acid (42)	1.0	0
	10	5
	50	80
	100	91
Nicotinic acid (91)	10	0
	50	86
Dipicolinic acid (36)	1.0	2
	2.5	16
Pyridoxal 5-phosphate (92)	0.1	0

(ii) DHDPR

Compound	Concentration mM	Inhibition %
Pyridine (89)	100	0
2-Methyl pyridine (90)	100	0
Picolinic acid (42)	10	0
	50	22
	100	60
Nicotinic acid (91)	1.0	0
	10	22
	50	55
Dipicolinic acid (36)	0.01	0
	0.1	10
	1.0	75
	2.5	80
Pyridoxal 5-phosphate (92)	0.1	0

Pyridine (89) itself did not inhibit either enzyme, nor did 2-methyl pyridine (90). Pyridine carboxylic acids, for example picolinic acid (42), nicotinic acid (91), and dipicolinic acid (36) were found to be inhibitors of both enzymes. Picolinic acid (42), which has the carboxylic acid group in the two position on the ring was a weak inhibitor of DHDPS and DHDPR. Nicotinic acid (91), where the carboxylic acid group is in the three position on the ring, also gave weak inhibition of DHDPS. However, for DHDPR

the inhibition of nicotinic acid (91) was stronger than that for picolinic acid (42). This result for DHDPR is unexpected as groups in the 2- position on the ring more closely resemble the reaction intermediates than when they are in the 3- position. Dipicolinic acid (36), which contains two carboxylic acid groups, in the 2- and 6- positions on the ring, appeared to be a moderate inhibitor of DHDPS, it was not a potent inhibitor as suggested by Couper *et al.*[21] and Laber *et al.*[27] For DHDPR dipicolinic acid (36) appeared to be a strong inhibitor, IC_{50} of ~5 x 10^{-4} M.

Pyridoxal 5-phosphate (92), which is a coenzyme in many biological systems, contains an acidic group at the three position like nicotinic acid (91), and was tested for inhibition. However, it has a strong absorbance at 340 nm which interfered with the absorbance change monitored in the assay. Thus, only low concentrations gave interpretable data. No inhibition of either DHDPS or DHDPR was observed at 0.1 mM, thus, pyridoxal 5-phosphate (92) is not a potent inhibitor of these enzymes.

Benzene derivatives were also tested as inhibitors of DHDPS and DHDPR, see figure 4-17 and table 4-3.

Figure 4-17: Benzene derivatives

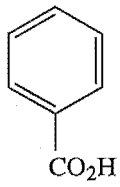

Benzoic acid (93)

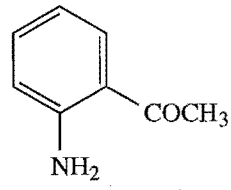

2-Aminoacetophenone (94)

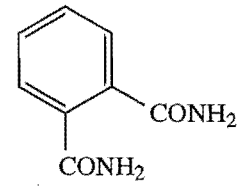

Phthalimide (95)

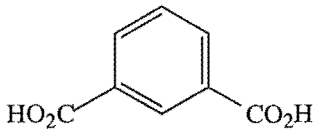

Isophthalic acid (41)

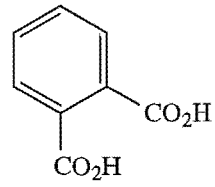

Phthalic acid (96)

Table 4-3: Inhibition by benzene derivatives

(i) DHDPS

Compound	Concentration mM	Inhibition %
Benzoic acid (93)	1.0	5
	10	39
	50	85
2-Aminoacetophenone (94)	0.1	7
Phthalimide (95)	0.1	12
	1.0	33
Isophthalic acid (41)	5.0	5
	10	17
Phthalic acid (96)	1.0	0
	10	70
	12.5	95

(ii) DHDPR

Compound	Concentration mM	Inhibition %
Benzoic acid (93)	10	0
	50	100
2-Aminoacetophenone (94)	0.1	0
Phthalimide (95)	1.0	0
Isophthalic acid (41)	1.0	0
	2.5	21
Phthalic acid (96)	0.1	0
	1.0	30
	10	71

Benzoic acid (93), analogous to picolinic acid (42) but lacking nitrogen, showed weak inhibition of DHDPS and DHDPR. This inhibition may be in part due to a pH effect even though the assay is buffered at pH 7.2. 2-Aminoacetophenone (94), like pyridoxal 5-phosphate (92), has a strong absorbance at 340 nm limiting the range of concentrations which could be evaluated accurately. Kinetic data was inaccurate at 1 mM, and no significant inhibition of either enzyme was observed at 0.1 mM. Phthalimide (95) was a moderate inhibitor of DHDPS, but it did not inhibit DHDPR. Isophthalic acid (41) which is analogous in structure to dipicolinic acid (36), but without the nitrogen, was a moderate inhibitor of DHDPS and a strong inhibitor of DHDPR. Phthalic acid (96),

where the two carboxylic acid groups are side by side, gave moderate inhibition for DHDPS and DHDPR.

Piperidine (97) and morpholine (98) were also tested as inhibitors of DHDPS and DHDPR, see figure 4-18 and Table 4-4. Piperidine (97) inhibited DHDPS and DHDPR at high concentrations. Whereas, morpholine (98) did not show any inhibition of DHDPS at concentrations up to 100 mM, but showed weak inhibition of DHDPR.

Figure 4-18: Piperidine and morpholine

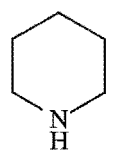

Piperidine (97)

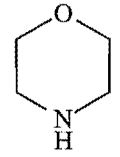

Morpholine (98)

Table 4-4: Inhibition by piperidine (97) and morpholine (98)

(i) DHDPS

Compound	Concentration mM	Inhibition %
Piperidine (97)	10	0
	100	100
Morpholine (98)	100	0

(ii) DHDPR

Compound	Concentration mM	Inhibition %
Piperidine (97)	1.0	0
	10	46
	50	88
	100	100
Morpholine (98)	1.0	0
	25	23
	50	45
	100	84

From these results it can be concluded that for DHDPS dipicolinic acid (36), phthalimide (95), isophthalic acid (41), and phthalic acid (96) are moderate inhibitors, while picolinic acid (42), nicotinic acid (91), benzoic acid (93), and piperidine (97) are weak inhibitors. No potent product inhibitors of DHDPS were discovered. While the most potent inhibitors of DHDPR, were dipicolinic acid (36) and isophthalic acid (41).

Phthalic acid (96) was a moderate inhibitor of DHDPR, but picolinic acid (42), nicotinic acid (91), benzoic acid (93), piperidine (97), and morpholine (98) were all only weak inhibitors. Thus, it was decided to undertake detailed kinetic studies on the inhibition of DHDPR by dipicolinic acid (36) and isophthalic acid (41). It was noted that all the cyclic compounds tested showed greater inhibition of DHDPR than of DHDPS. This possibly reflects a stronger binding of the substrate than the product, and highlights the increased difficulty in finding product inhibitors rather than substrate inhibitors. The cyclic diacids mimic both the substrate and product of the DHDPR catalysed reaction, whereas they only mimic the product (not the substrate) of the DHDPS catalysed reaction.

Inhibition of DHDPR by dipicolinic acid

In the literature dipicolinic acid (36) is reported to be an inhibitor of *E. coli* DHDPR. Reddy and Blanchard[25] found dipicolinic acid (36) inhibited DHDPR competitively with respect to the substrate, K_i was (2.6 $\pm$ 0.6) x 10^{-5} M, and uncompetitively with respect to NADPH, K_i was (3.3 $\pm$ 0.5) x 10^{-4} M. Tamir and Gilvarg[28] found that dipicolinic acid (36) competitively inhibited DHDPR with respect to the substrate where K_i was 1 x10^{-3} M. The preliminary studies suggested an IC_{50} value of ~5 x 10^{-4} M.

Some studies had also been performed on DHDPR from other sources. In maize dipicolinic acid (36) also competitively inhibited DHDPR with respect to the substrate dipicolinate (18), K_i was reported to be 9 x 10^{-4} M.[29] For sporulating bacteria the pattern of inhibition changes to noncompetitive indicating the dipicolinic acid (36) binds at an allosteric site, this is most likely to be a feedback inhibtion site as these organisms use dipicolinic acid (36) in spore formation. The literature[30] cites *Bacillus cereus*, and *B. megaterium* as being inhibited noncompetitively by dipicolinate (36) with respect to the substrate, with K_i being 8.5 x 10^{-5} M,and 1.4 x 10^{-4} M respectively. *B. subtilis* is also inhibited by dipicolinic acid (36), here inhibition is noncompetitive at 0.1 mM, then uncompetitive at 1.0 mM.[31,32]

Dixon and modified Dixon plots were used to determine K_i and the nature of the inhibition of DHDPR by dipicolinic acid (36). The inhibition was found to be reversible and competitive with respect to the substrate as the Dixon plots shows a series of lines with a common intercept at a positive inverse rate value and the modified Dixon plot shows a series of nearly parallel lines, see table 4-5 and figure 4-19. K_i (from the Dixon plot) was found to be in the range of (4.3 - 4.4) x 10^{-4} M. Thus, dipicolinic acid is a strong inhibitor of DHDPR and as it inhibits competitively (binding at the active site) it closely resembles the substrate. It was found that the quality of the data obtained in the detailed inhibition studies on DHDPR was poorer than that obtained in the DHDPS inhibition studies reported in Chapter Three. One factor which compromised these studies is the absorbance of the inhibitor at 340nm interfering with the assay. There was

also the problem that the cyclic molecules inhibit both of the enzymes of the assay. However, DHDPR was still found to be rate limiting in these DHDPR inhibition studies. The Dixon and modified Dixon plots were used as an indicator of the type of inhibition obtained, rather than the trend in the K_m and V_{max} values obtained from the Lineweaver-Burk plot, as the latter method is more prone to individual inacurracies. The K_i value of (4.3 - 4.4) x 10^{-4} M falls between the two reported values for *E. coli* DHDPR.

Table 4-5: Kinetic parameters of the inhibition of dipicolinic acid (36) on DHDPR activity with respect to the substrate

[Dipicolinate] mM	K_m x 10^{-4} M	V_{max} µmol·s^{-1}mg^{-1}
0	0.837	2.26
0.10	6.14	6.54
0.50	28.3	41.7
1.0	6.13	3.85

Figure 4-19: Kinetic plots of the inhibition of dipicolinic acid (36) on DHDPR activity with respect to the substrate

(i) Dixon plot

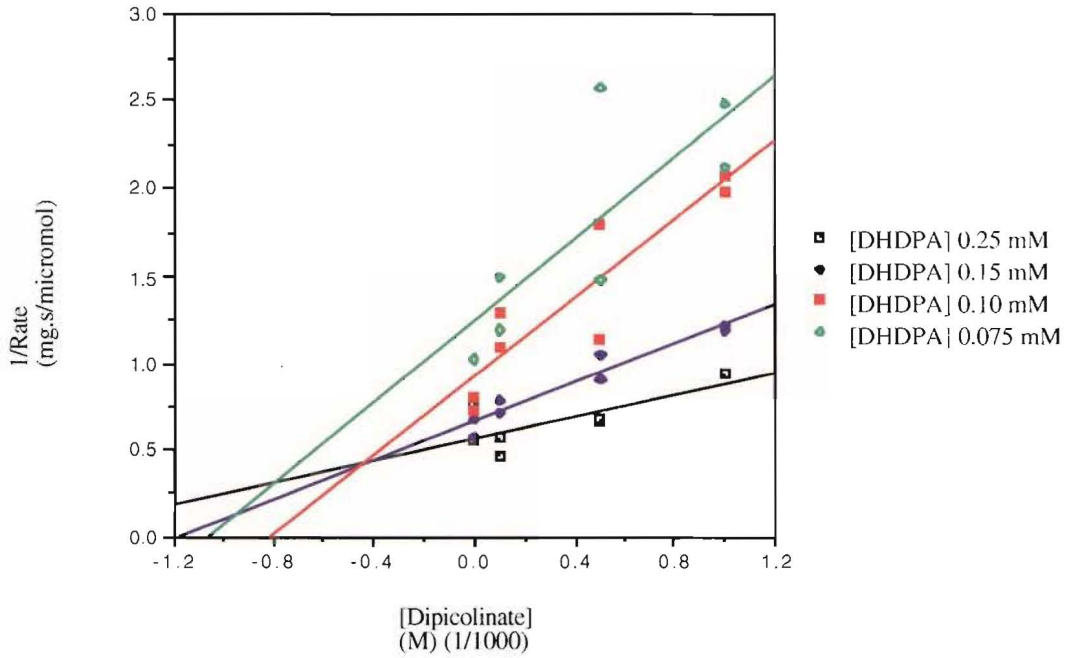

(ii) Modified Dixon plot

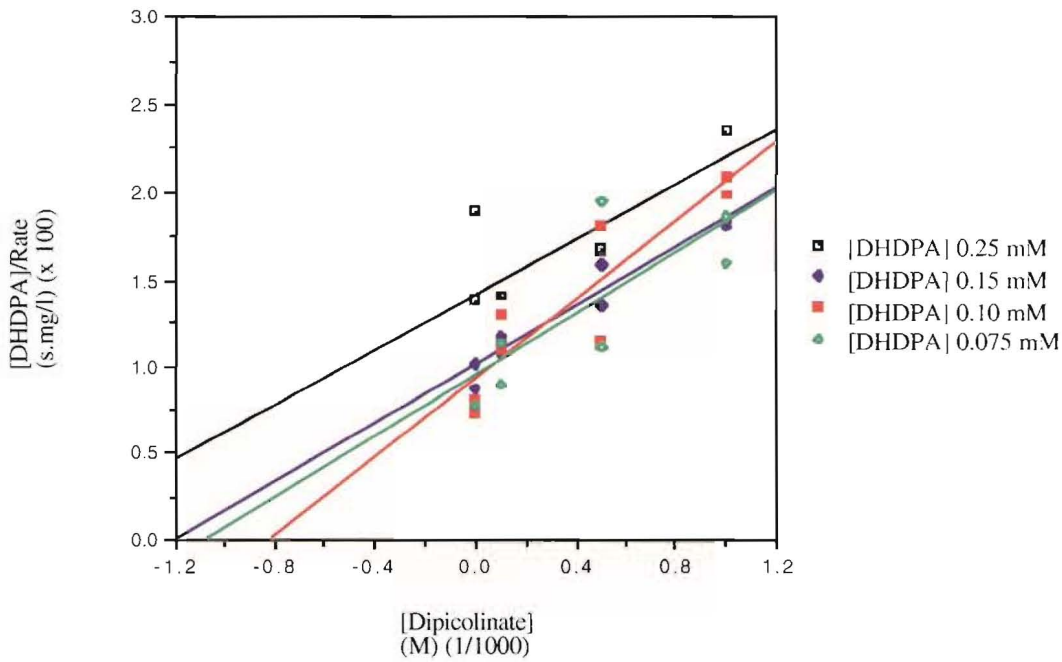

Inhibition of DHDPR by isophthalic acid

The inhibition of DHDPR by isophthalic acid (41) was also found to be reversible and competitive with respect to the substrate, again the Dixon plots shows a series of lines with a common intercept at a positive inverse rate value and the modified Dixon plot shows a series of nearly parallel lines (althogh the data is not as consistent as in the above case with dipicolinc acid (36)), see table 4-6 and figure 4-20. K_i (again calculated from the Dixon plot) was found to be in the range of (5.4 - 5.6) x 10^{-3} M. Thus, while isophthalic acid (41) binds at the active site like dipicolinic acid (36), it is a weaker inhibitor, by about a factor of ten. The only structural difference between isophthalic acid (41) and dipicolinic acid (36) is the removal of the heterocycle nitrogen, thus, this nitrogen appears to be important to binding.

Table 4-6: Kinetic parameters of the inhibition of isophthalic acid (41) on DHDPR activity with respect to the substrate

[Isophthalate] mM	K_m x 10^{-4} M	V_{max} µmol·s^{-1}mg^{-1}
0	11.0	15.6
2.5	8.86	9.23
5.0	3.71	5.08
7.5	8.36	7.49

Figure 4-20: Kinetic plots of the inhibition of isophthalic acid (41) on DHDPR activity with respect to the substrate

(i) Dixon plot

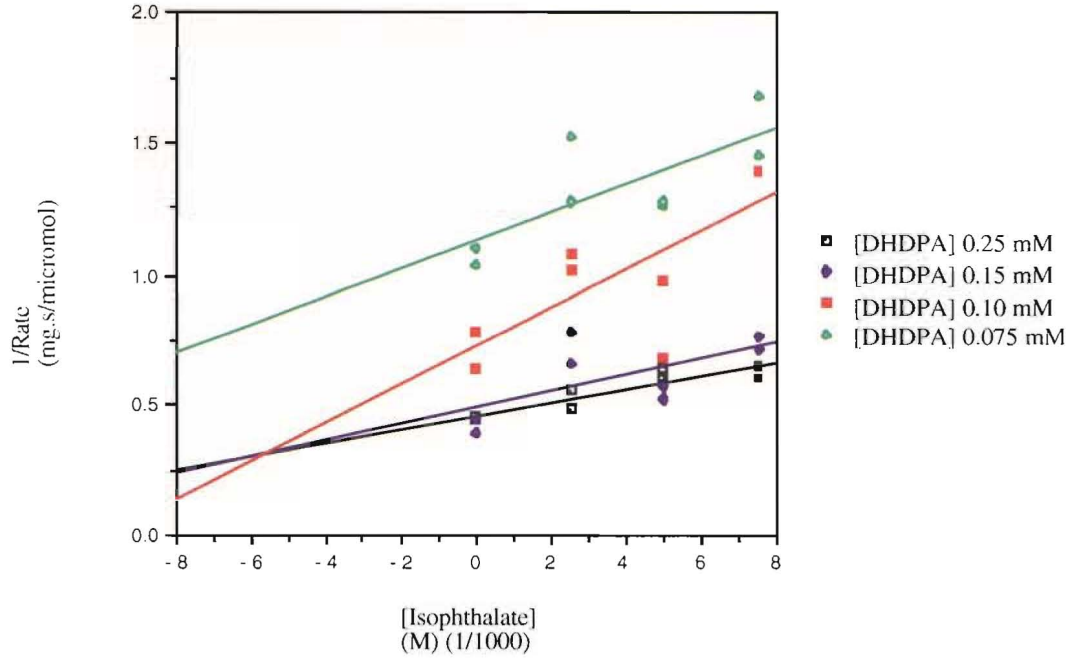

(ii) Modified Dixon plot

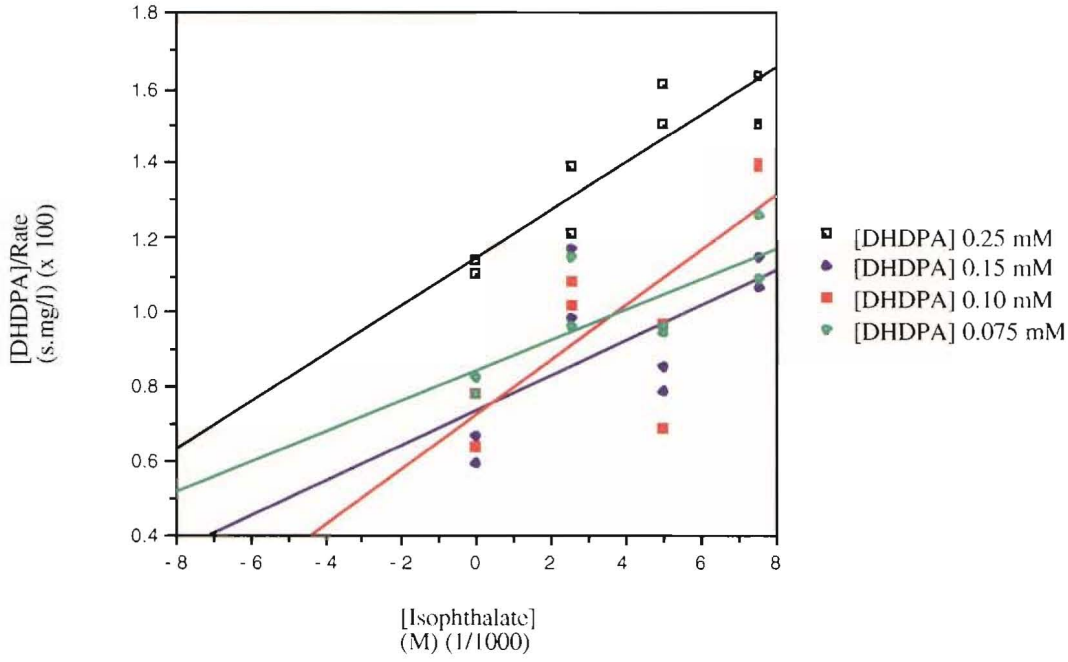

In the literature[28] *E. coli* DHDPR is reported to be competitively inhibited by isophthalic acid (41) with respect to the substrate, K_i was found to be 1.5 x10^{-2} M, this value is higher than that found above. This report also found the inhibition by dipicolinic acid (36) to have a higher K_i value than that obtained in this research.

Inhibition of DHDPS and DHDPR by tetrahydrodipicolinate mimics

Mimics of the 4-hydroxy-2,3,4,5-tetrahydrodipicolinate were synthesised as possible inhibitors of DHDPS and DHDPR. As noted previously 2,3,4,5-tetrahydrodipicolinate (19) (Δ^2- species) is in equilibrium with the enamine (39) (Δ^3- species) and an open chain form (40) generated by hydrolysis,[12,13] see figure 4-21. This complex chemistry will affect any tetrahydropyridine of this type. It was decided to concentrate inhibition studies on reduced isophthalic acids which are more stable than the corresponding reduced dipicolinic acids. Δ^3-Tetrahydroisophthalic acid (99) and Δ^2-tetrahydroisophthalic acid (100) were synthesised and tested for inhibition of both DHDPS and DHDPR.

Figure 4-21: 2,3,4,5-Tetrahydrodipicolinate (19)

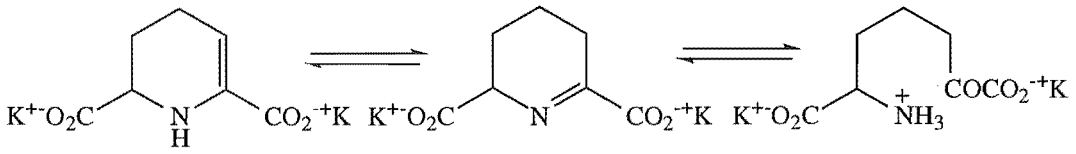

Enamine (39) 2,3,4,5-Tetrahydrodipicolinate (19) Open chain form (40)

It was hypothesised that Δ^2-tetrahydroisophthalic acid (100) may be a stronger inhibitor of DHDPS and DHDPR than the Δ^3-tetrahydroisophthalic acid (99) as this mimics the imine (19). As Δ^3-tetrahydroisophthalic acid (99) mimics the enamine (39) inhibition may depend on the extent of the tautomerism to this form.

Reduction of isophthalic acid to Δ^3-tetrahydroisophthalic acid

The method of Perkin and Pickles[33] was used to synthesise Δ^3-tetrahydroisophthalic acid (99). Isophthalic acid (41) was reduced in aqueous solution, at 70 °C, by sodium amalgam, see figure 4-22. The reaction did not go to completion and some starting material was recovered. However, some Δ^3-tetrahydroisophthalic acid (99) was obtained. The yield of the reaction was low (4.7%), as the reaction gave a mixture of different products; the extraction of Δ^3-tetrahydroisophthalic acid (99) was tedious due to this mixture of products formed, but was successfully achieved by repeated fractional crystallisation.

Figure 4-22: Reduction of isophthalic acid at 70 °C[33]

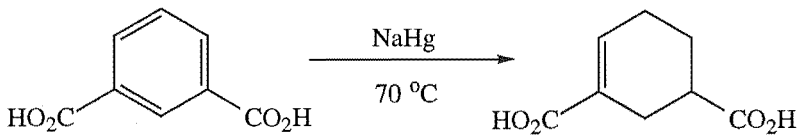

Isophthalic acid (41) Δ^3-Tetrahydroisophthalic acid (99)

Reduction of isophthalic acid to Δ^2-, Δ^3-, Δ^4-tetrahydroisophthalic acids

The reaction conditions used to synthesise Δ^3-tetrahydroisophthalic acid (99) can be modified to make a mixture of Δ^2-, Δ^3-, and Δ^4-tetrahydroisophthalic acids (100, 99, and 101 respectively). Since it has been reported[33] that these can be separated it was decided to try these as a route to Δ^2- and Δ^4-tetrahydroisophthalic acids (100 and 101 respectively). The reaction above was performed at 45 °C under a constant stream of carbon dioxide,[33] see figure 4-23. In the report by Perkin and Pickles[33] it was stated that this method synthesised all three isomers, and that these could be separated by fractional crystallisation. A reasonable amount of material was obtained at the end of the reaction, however this material could not be separated into unreacted starting material, and the various reaction products—not only are there the three possible tetrahydroisophthalic acids (100, 99, and 101) but also possible dihydroisophthalic acids. Repeated attempts at fractional crystallisation in both water and methanol/diethyl ether were fruitless, probably due to the very low solubilites of this material in these solvents. The material could not be purified effectively by chromatography.

Figure 4-23: Reduction of isophthalic acid at 45 °C under carbon dioxide[33]

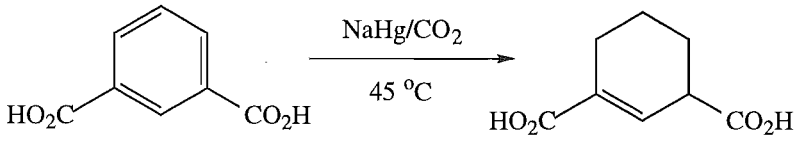

Isophthalic acid (41)

Δ^2-Tetrahydroisophthalic acid (100)

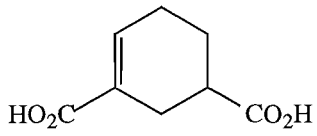

Δ^3-Tetrahydroisophthalic acid (99)

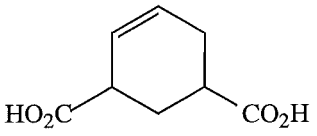

Δ^4-Tetrahydroisophthalic acid (101)
(*cis*- and *trans*-)

Synthesis of Δ^2-tetrahydroisophthalic acid from cyclohexanone

In view of the difficulty in separating a mixture of Δ^2-, Δ^3-, and Δ^4-tetrahydroisophthalic acids (100, 99, and 101 respectively) a synthesis that produced only Δ^2-tetrahydroisophthalic acid (100) was required. There were two such syntheses in the literature, both reported in the same paper.[34] Kon and Nandi[34] reported that Δ^2-tetrahydroisophthalic acid (100) could be synthesised from cyclohexanone (102) or from 1,3-dibromopropane (108) and diethyl malonate (109). The synthesis of Δ^2-tetrahydroisophthalic acid (100) was first attempted from cyclohexanone (102), see figure 4-24.

Figure 4-24: Synthetic scheme[34]

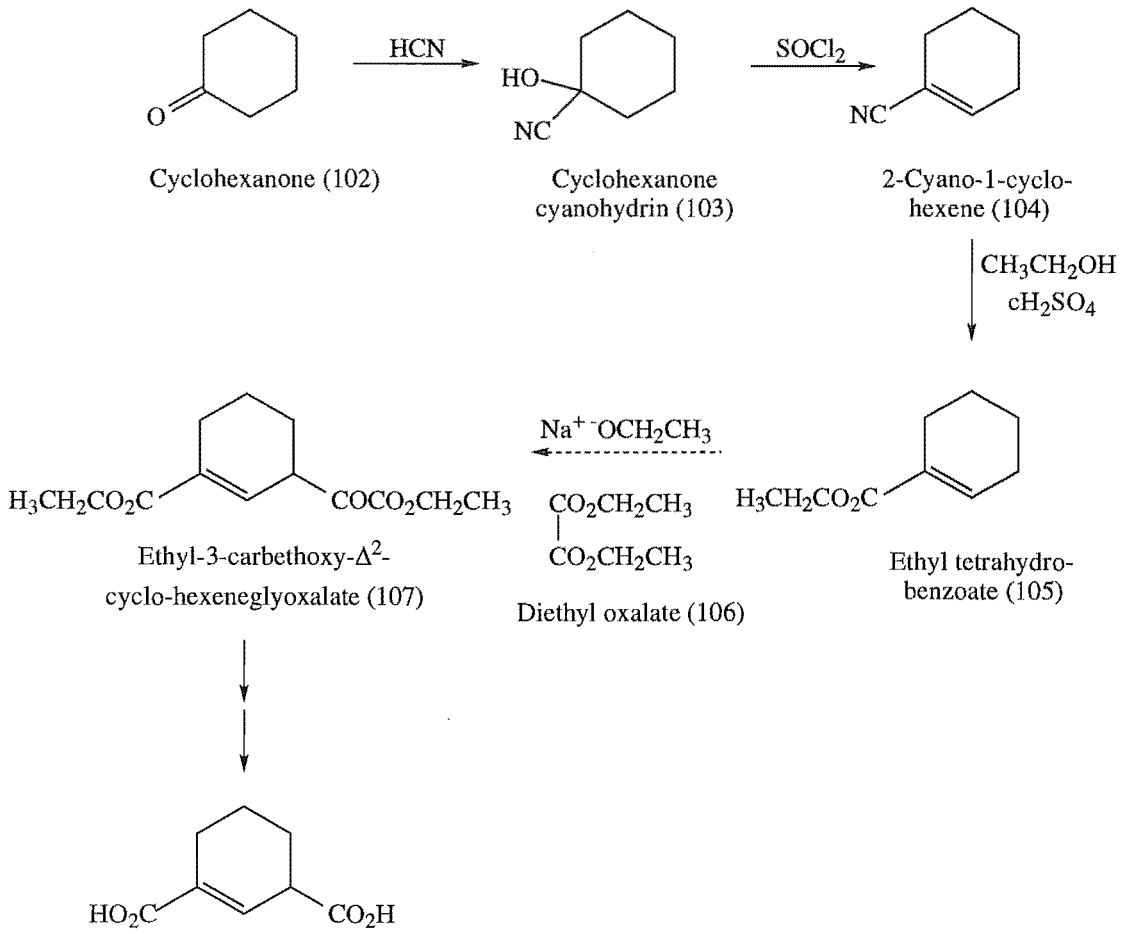

Initially cyclohexanone cyanohydrin (103) was synthesised from cyclohexanone (102) by the method of Ruzika and Brugger.[35] This involved producing hydrogen cyanide *in situ* to add a cyano group to the carbonyl carbon. The reaction gave a reasonable yield of the cyanohydrin (103), 66.3%. The next step involved a dehydration, using thionyl chloride, to form the ring double bond. While the reaction itself proved to be straightforward, difficulties were encounted in removing the thionyl chloride, and extracting the product from the reaction mixture—this was achieved by repeated fractional distillation yielding pure 2-cyano-1-cyclohexene (104) in 19% yield.

The synthesis of ethyl tetrahydrobenzoate (105)[36] was performed in acidic ethanol at 120 °C. The esterification occured in reasonable yield (56.7 %), and no further purification was required, however, the compound was unstable and hydrolysis to the acid was observed to occur relatively rapidly even at -20 °C. Unfortunately, condensation of ethyl tetrahydrobenzoate (105) with diethyl oxalate (106) as reported by Kon and Nandi[34] was problematic. This route was not pursued further due to success with the alternative route from 1,3-dibromopropane (108) and diethyl malonate (109).

Synthesis of Δ^2-tetrahydroisophthalic acid from 1,3-dibromopropane and diethyl malonate

Δ^2-Tetrahydroisophthalic acid (100) was synthesised from 1,3-dibromopropane (108) and diethyl malonate (109), as reported by Kon and Nandi[34] with minor modifications, see figure 4-25.

Figure 4-25: Synthetic scheme[34]

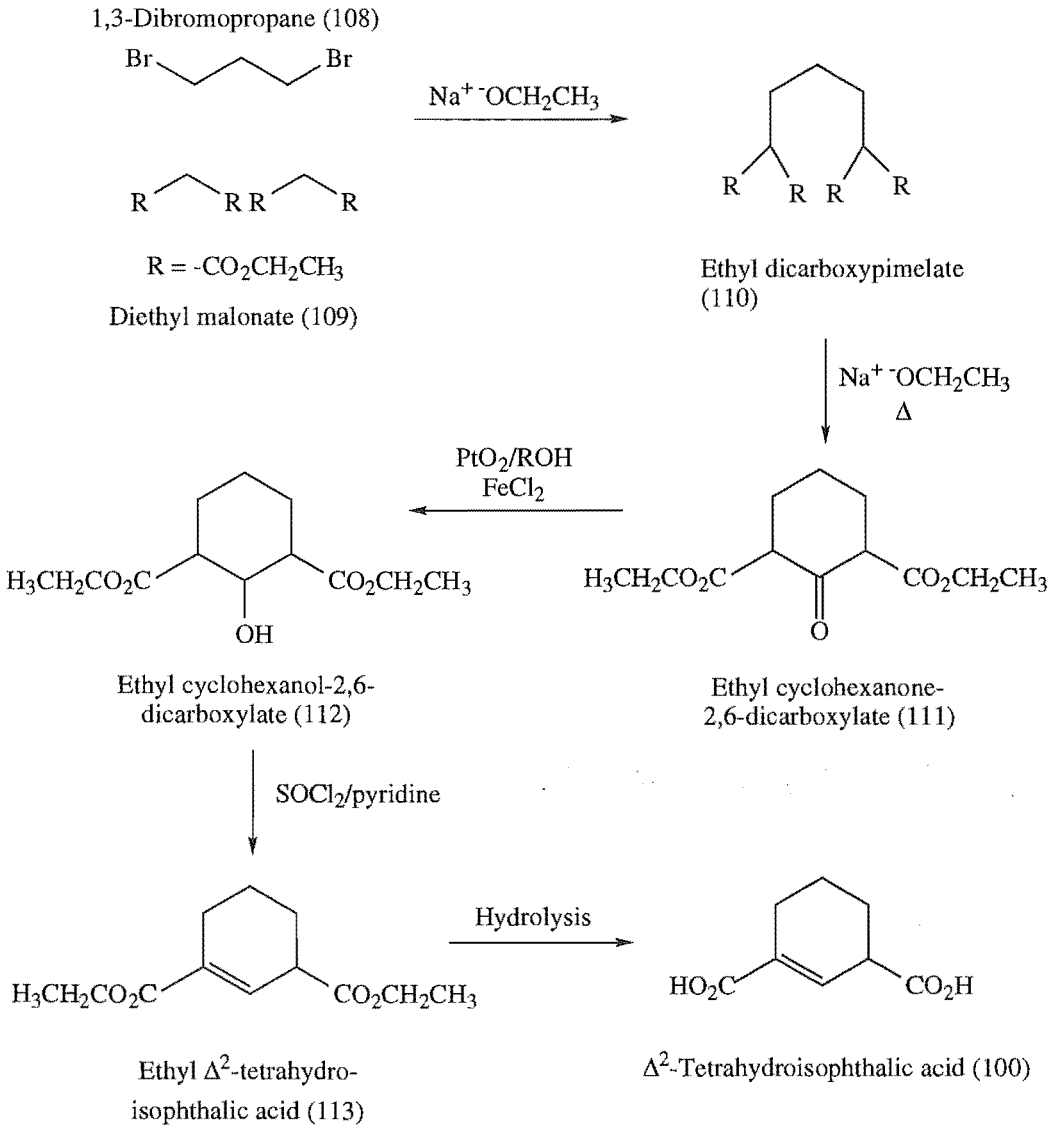

Ethyl dicarboxypimelate (110) was synthesised from 1,3-dibromopropane (108) and diethyl malonate (109) via Uschakov's method as reported by Kon and Nandi[34] and modified according to the method of Adams and Kamm.[37] The product was purified by fractional distillation, and unreacted diethyl malonate was also recovered in the distillation. Ethyl dicarboxypimelate (110) was then cyclised to give the ketonic ester, ethyl cyclohexanone-2,6-dicarboxylate (111).[34] Two portions of sodium ethoxide (each 1.9 equivalents) were required to drive this reaction to completion. A yield of 37.5% was obtained after purification by chromatography, this was a slight increase over literature

reports (31.0%[34]). The NMR of this compound was complex due to enol formation, however, with the use of two dimensional NMR (COSY—proton proton coupling, and HSQC—proton carbon coupling) the two tautomers could be assigned; for these reasons two dimensional NMR was used throughout this synthesis of Δ^2-tetrahydroisophthalic acid (100) to assign NMR spectra. Mass spectra confirmed the ketone (111) had been obtained, and a distinct carbonyl stretch, corresponding to the ketone, was also seen in the infra-red spectrum at 1657 cm^{-1} (the carboxylic acid carbonyl peak occurred at 1730 cm^{-1}).

Ethyl cyclohexanol-2,6-dicarboxylic acid (112) was synthesised by the reduction of the ketone moiety to a hydroxy group using Adam's catalyst (platinum oxide) and ferrous chloride under a hydrogen atmosphere.[34] The product was obtained in high yield (92.4%) by chromatography (literature yield of 67.4%[33]). A broad singlet at δ_H 4.63 ppm was observed in the ^1H NMR from the proton next to the hydroxy group. Two molecular ions of m/z 244 were also observed by GCMS, which was able to separate the two stereoisomers. The dehydration of this compound to give ethyl Δ^2-tetrahydro-isophthalic acid (113) was performed using thionyl chloride in pyridine. Initial attempts using the conditions as quoted by Kon and Nandi,[34] thionyl chloride (1.3 equivalents) in pyridine (2.4 equivalents) for 20 hours, gave only a small amount of product and a large proportion of side products. To counteract the side product formation and to increase the amount of product the conditions were altered to increased amounts of thionyl chloride (44 equivalents) and pyridine (98 equivalents) but with a shorter time of reaction (90 minutes).[38] The product was purified by chromatography and obtained in a yield of 35.7%. The vinylic proton was observed as a broad singlet at δ_H 7.00 ppm in the ^1H NMR, in the ^{13}C NMR the two vinylic carbons were observed at δ_c 132.4 and 135.2 ppm. Again a molecular ion of m/z 226 was observed by GCMS, verifying the identify of the compound.

Hydrolysis of ethyl Δ^2-tetrahydroisophthalic acid (113) to Δ^2-tetrahydroisophthalic acid (100) was carried out by the methodology of Abell *et al.*[39] This involved heating under reflux the ethyl Δ^2-tetrahydroisophthalic acid (113) with potassium carbonate (2.0 equivalents) in 10% aqueous methanol for 20 hours. The product was obtained as a white solid of reasonable purity after multiple extractions.

Inhibition of DHDPS and DHDPR by Δ^2-tetrahydroisophthalic acid and Δ^3-tetrahydroisophthalic acid

Δ^2-Tetrahydroisophthalic acid (100) did not show potent inhibtion of DHDPS, there was 15% inhibition at 5 mM, yet this did not greatly increase with increasing inhibitor concentration, there was 13% inhibition at 10 mM, 17% at 20 mM, and 23% at 40 mM. Δ^2-Tetrahydroisophthalic acid (100) did not show potent inhibition of DHDPR, there was 9% inhibition at 10 mM, and again this did not greatly increase with increasing concentration of the analogue, at 20 mM there was 16% inhibition, and at 40 mM there was 21% inhibition.

Δ^3-Tetrahydroisophthalic acid (99) showed significant inhibition of DHDPS with 22% inhibition at 5 mM, 38% at 10 mM, and 91% at 30 mM, giving an IC_{50} value of ~1.5 x 10^{-2} M. Δ^3-Tetrahydroisophthalic acid (99) showed stronger inhibition of DHDPR with 58% inhibition at 5 mM, 66% at 10 mM, and 84% at 30 mM, giving an IC_{50} value of ~4 x 10^{-3} M. Thus, Δ^3-tetrahydroisophthalic acid (99) shows similar inhibition to isophthalic acid, whereas, Δ^2-tetrahydroisophthalic acid (100) shows only slight inhibition.

These results are contrary to what we had originally expected. It was hypothesised that Δ^2-tetrahydroisophthalic acid (100) would be a stronger inhibitor of DHDPS and DHDPR than the Δ^3-tetrahydroisophthalic acid (99) as the double bond in the Δ^2 position more closely resembles 4-hydroxy-2,3,4,5-tetrahydrodipicolinate (28) (the imine). The results obtained, where Δ^3-tetrahydroisophthalic acid (99) is a stronger inhibitor than Δ^2-tetrahydroisophthalic acid (100), suggest that significant tautomerism of the imine (28) to the enamine (39) (where the double bond is in the Δ^3 position) may occur. Other rearrangements, such as dehydration, may also occur, giving rise to a new species Alternatively, the alteration of the mimic to exclude a nitrogen atom in the ring sufficiently alters binding so as to remove any relationship between the site of the double bond and inhibition.

Summary

NMR studies performed on the DHDPS enzymatic reaction gave results that were consistent with the product being 4-hydroxy-2,3,4,5-tetrahydrodipicolinate (28), rather than 2,3-dihydrodipicolinate (18). A variety of cyclic compounds (mainly aromatic) were tested as product inhibitors of DHDPS, and substrate inhibitors of DHDPR. Of these the best inhibitors of DHDPR were dipicolinic acid (36) and isophthalic acid (41). Dipicolinic acid (36) was determined to be a competitive inhibitor of DHDPS with respect to the substrate, K_i was in the range of (4.3 - 4.4) x 10^{-4} M. Similarly isophthalic acid (41) was also a competitive inhibitor of DHDPS with respect to the substrate, K_i was in the range of (5.4 - 5.6) x 10^{-3} M.

Isomers of tetrahydroisophthalic acid were then synthesised and tested for inhibition of DHDPS and DHDPR. Δ^2-Tetrahydroisophthalic acid (100) did not show potent inhibition of DHDPS or DHDPR. However, Δ^3-tetrahydroisophthalic acid (99) was a moderate inhibitor of DHDPS, IC_{50} was ~1.5 x 10^{-2} M, and a stronger inhibitor of DHDPR, IC_{50} was ~4 x 10^{-3} M. Thus, it is hypothesised that the 4-hydroxy-2,3,4,5-tetrahydrodipicolinate (28) tautomerises to give the enamine (39).

References

1. J.G. Shedlarski, C. Gilvarg *J. Biol. Chem.* **245**, 1362 (1970).
2. U. Eisner, J. Kuthan *Chem. Rev.* **72**, 1 (1972).
3. J-L. Bettiol, R.J. Sundberg *J. Org. Chem.* **58**, 814 (1993).
4. A. Sausins, G. Duburs *Heterocycles* **27**, 291 (1988).
5. D.F. Maynard, W.H. Okamura *J. Org. Chem.* **60**, 1763 (1995).
6. P. Mangeny, R. Gosmini, S. Raussou, M. Comercon, A. Alexakis *J. Org. Chem.* **59**, 1877 (1994).
7. R.D., La Reau, W. Wan, V.E. Anderson *Biochemistry* **28**, 3619 (1989).
8. D. Lednicer, L.A. Mitscher, G.I. Georg *'The Organic Chemistry of Drug Synthesis'* John Wiley & Sons, New York (1990).
9. S. Goldmann, L. Born, S. Kazda, B. Pittel, M. Schramm *J. Med. Chem.* **33**, 1413 (1990).
10. M-C. Lasne, J.L. Ripoll *Tet. Lett.* **25**, 3847 (1984).
11. D.D. Tanner, C-M. Yang *J. Org. Chem.* **58**, 1840 (1993).
12. L. Couper, D.J. Robins *Tet. Lett.* **33**, 2717 (1992).
13. E.J.T. Chrystal, L. Couper, D.J. Robins *Tetrahedron* **51**, 1041 (1995).
14. S. Blickling, C. Renner, B. Laber, H-D. Pohlenz, T.A. Holak, R. Huber *Biochemistry* **36**, 24 (1997).
15. K. Kimura *J. Biochem.* **75**, 961 (1974).
16. R.J. Cox *Natural Product Reports* **13**, 29 (1996).
17. C. Mirwaldt, I. Korndorter, R. Huber *J. Microbiol.* **246**, 227 (1995).
18. B. Laber, F-X. Gomis-Ruth, M.J. Romao, R. Huber *Biochem. J.* **288**, 691 (1992).
19. E.B. Borthwick, S.J. Cornell, D.W. Tudor, A. Shneier, C. Abell, T.R. Coggins *Biochem. J.* **305**, 521 (1995).
20. W.E. Karsten *Biochemistry* **36**, 1730 (1997).
21. L. Couper, J.E. McKendrick, D.J. Robins, E.J.T. Chrystal *Bioorg. Med. Chem. Letts.* **4**, 2267 (1994).
22. J.A. Littlechild, H.C. Warton *TIBS* **18**, 36 (1993).
23. T. Izard, M.C. Lawrence, R.L. Malby, G.C. Lilley, P.M. Colman *Structure* **2**, 361 (1994).

24. M.C. Lawrence, J.A.R.G. Barbosa, B.J. Smith, N.E. Hall, P.A. Pilling, H.C. Ooi, S.M. Marcuccio *J. Mol. Biol.* **266**, 381 (1997).
25. S.G. Reddy, J.C. Sacchettini, J.S. Blanchard *Biochem.* **34,** 3492 (1995).
26. G. Scapin, J.S. Blanchard, J.C. Sacchettini *Biochem.* **34**, 3502 (1995).
27. B. Laber, F-X. Gomis-Ruth, M.J. Romao, R. Huber *Biochem. J.* **288**, 691 (1992).
28. H. Tamir, C. Gilvarg *J. Biol. Chem.* **249**, 3034 (1974).
29. V.V.S. Tyagi, R.R. Henke, W.R. Farkas *Plant Physiol.* **73**, 687, (1983).
30. K. Kimura, T. Goto *J. Biochem* **81**, 1367, (1977).
31. K. Kimura *J. Biochem.* **77**, 405 (1975).
32. K. Kimura *J. Biochem.* **77**, 415 (1975).
33. W.H. Perkin, S.S. Pickles *J. Chem. Soc.* **87**, 293 (1905).
34. G.A.R. Kon, B.L. Nandi *J. Chem. Soc.* **136**, 1628 (1933).
35. von L. Ruzika, W. Brugger *Helv. Chem. Acta* **9**, 399 (1926).
36. R. Adams, A.F. Thal *Org. Synth* Coll. Vol. **I**, 270 (1941).
37. R. Adams, R.M. Kamm *Org. Synth* Coll. Vol. **I**, 250 (1941).
38. A. Schwartz, P. Madan *J. Org. Chem.* **51**, 5463 (1996).
39. A.D. Abell, M. Brandt, M.A. Levy, D.A. Holt *J.Chem. Soc. Perkin Trans. I* 1663 (1997).

Results and Discussion Conclusion

Chemically and optically pure *(S)*-aspartate β-semialdehyde (11) was synthesised from diprotected *(S)*-allylglycine (52), where the oxidation was performed using a Lemieux-Johnson reaction. Both the *dap A* and *dap B* genes were over-expressed in *E. coli.* to produce milligram quantities of the corresponding enzymes, DHDPS and DHDPR via large growth cultures. These enzymes were purified to high levels for use in kinetic studies.

A coupled assay, using both DHDPS and DHDPR, and following the utilisation of NADPH (at 340 nm) by DHDPR, was optimised to run in Mops buffer at pH 7.2, and was used for kinetic studies on the two enzymes. Quantitative kinetics of DHDPS were obtained when DHDPR was present in excess, and quantitative kinetics of DHDPR were obtained when DHDPS was present in excess. DHDPS was found to have a K_m for *(S)*-aspartate β-semialdehyde (11) in the range of (1.0 - 1.1) x 10^{-4} M with a V_{max} in the range of (6.5 - 7.2) x 10^{-1} $\mu mol \cdot s^{-1} mg^{-1}$, while K_m for pyruvate (17) was in the range of (1.1 - 1.3) x 10^{-4} M and V_{max} was in the range of (4.8 - 5.5) x 10^{-1} $\mu mol \cdot s^{-1} mg^{-1}$. Feedback inhibition on DHDPS occurred in the presence of moderate to high levels of *(S)*-lysine (12), as expected for bacterial DHDPS enzymes. Inhibition was reversible and uncompetitive with respect to *(S)*-aspartate β-semialdehyde (11), where K_i' was in the range of (3.4 - 3.9) x 10^{-4} M. Inhibition was also reversible and uncompetitive with respect to pyruvate (17), with a K_i' in the range of (3.1 - 3.8) x 10^{-4} M.

DHDPR was determined to have a K_m for its substrate in the range of (4.9 - 5.3) x 10^{-4} M with a V_{max} in the range of 5.3 - 5.7 $\mu mol \cdot s^{-1} mg^{-1}$. The Michaelis-Menten constant, K_m, for NADPH was in the range of (1.5 - 2.0) x 10^{-5} M and V_{max} was in the range of 3.6 - 4.1 $\mu mol \cdot s^{-1} mg^{-1}$. NADH also acts as a cofactor for DHDPR, with a K_m in the range of (5.0 - 6.6) x 10^{-6} M and V_{max} in the range of 2.0 - 2.4 $\mu mol \cdot s^{-1} mg^{-1}$. NADH is a better cofactor than NADPH as it has a considerably lower K_m.

Analogues of a possible cyclic lactol structure of *(S)*-aspartate β-semialdehyde (11c) were tested as potential inhibitors of DHDPS. These mimics included homoserine lactone (31), *(S)*-3-aminopyrrolid-2-one (62), and 2-aminocyclopentanone (63). Homoserine lactone (31) was found to be a reversible noncompetitive inhibitor of DHDPS with respect to both substrates, K_i with respect to *(S)*-aspartate β-semialdehyde (11) was in the range of (1.2 - 2.2) x 10^{-2} M, and K_i with respect to pyruvate (17) was in the range of (0.8 - 1.5) x 10^{-2} M. 2-Aminocyclopentanone (63) also showed reversible non-competitive inhibition with respect to *(S)*-aspartate β-semialdehyde (11), but K_i was greatly increased to be in the range of (1.2 - 2.4) x 10^{-1} M. However, *(S)*-3-amino-pyrrolid-2-one (62) did not inhibit DHDPS. Since these cyclic molecules do not inhibit

DHDPS competitively it is unlikely that the substrate *(S)*-aspartate β-semialdehyde (11) binds to the enzyme in a cyclic form.

The solution structure of *(S)*-aspartate β-semialdehyde (11) was determined by spectroscopic means, including NMR, and infra-red spectroscopy, to be predominately the linear hydrate (11b). No cyclic lactol (11c) was observed at physiological pH and only traces of free aldehyde were present, and these could not be derivatised efficiently.

Analogues of the hydrate form of *(S)*-aspartate β-semialdehyde (11b) were tested as inhibitors of DHDPS. These included *S*-methyl-*(R)*-cysteine (76) and the corresponding sulfoxide (77) and sulfone (78), *(R)*-cysteine sulfinic acid (79), *(S)*-aspartic acid (9), *(S)*-asparagine (80), and *(S)*-glutamic acid (81). *(R)*-Cysteine sulfinic acid (79), and *(S)*-glutamic acid (81) were reversible uncompetitive inhibitors of DHDPS, where K_i' for *(R)*-cysteine sulfinic acid (79) was in the range of (6.1 - 8.6) x 10^{-3} M, while K_i' for *(S)*-glutamic acid (81) was in the range of (0.9 - 1.6) x 10^{-2} M. *(S)*-Aspartic acid (9) was a reversible mixed type inhibitor with a K_i in the range of (0.9 - 1.4) x 10^{-2} M, and a K_i' in the range of (2.1 - 3.9) x 10^{-2} M. It was suggested that these inhibitors may bind to the *(S)*-lysine (12) allosteric site.

NMR studies were consistent with the hypothesis that the structure of the DHDPS enzymatic reaction product is 4-hydroxy-2,3,4,5-tetrahydrodipicolinate (28), rather than 2,3-dihydrodipicolinate (18).

A range of cyclic compounds were tested as product inhibitors of DHDPS, and substrate inhibitors of DHDPR. The most potent inhibitors of DHDPR were dipicolinic acid (36) and isophthalic acid. Dipicolinic acid (36) was found to be a reversible competitive inhibitor of DHDPR with respect to the substrate, with a K_i in the range of (4.3 - 4.4) x 10^{-4} M. Isophthalic acid (41) was a slightly weaker inhibitor of DHDPR. Inhibition was again reversible and competitive with respect to the substrate, with a K_i in the range of (5.4 - 5.6) x 10^{-3} M. Δ^2-Tetrahydroisophthalic acid (100) was found to give only slight inhibition of DHDPS and DHDPR. Whereas, Δ^3-tetrahydroisophthalic acid (99) was a moderate inhibitor of the two enzymes, IC_{50} (DHDPS) ~ 1.5 x 10^{-2} M, and IC_{50} (DHDPR) ~4 x 10^{-3} M. These different inhibition properties of Δ^2- and Δ^3-tetrahydroisophthalic acid might be indicative of the tautomerism equilibria of enzyme-bound tetrahydrodipicolinate (19).

Experimental

Experimental

Equipment and Suppliers

Chemicals were generally purchased from Aldrich Chemicals, Sigma Chemical Company Ltd., or BDH Laboratory Supplies; media for bacterial cultures was purchased from Life Technologies Ltd.

pH measurements were made using a standard meter fitted with a Russell Combination (Tris compatible) Electrode type no. TR/CMAW 711/TB.

Centrifugation was performed in an Eppendorf Centrifuge 5403, on a small scale ($\leq$1.5 ml) at up to 15 000 rpm using a 16 F24-11 rotor, and on a large scale ($\leq$50 ml) at up to 5000 rpm using a 16A4-44 rotor, at 4 °C.

Agarose gels were routinely run on a Hoefer Horizontal Submarine Unit using a Bio-Rad 300 power pack.

Q-Sepharose and Sephacryl media were purchased from Pharmacia, and Pharmacia XK-26 columns were run using Gilson Minipuls M312 peristaltic pumps and a Gilson FC-203B fraction collector.

Polyacrylamide gel electrophoresis (PAGE) were routinely run on a Hoefer Sturdier Slab Gel Electrophoresis Unit SE 400, using a Bio-Rad 300 Power Pack.

Ultra-violet (UV) spectroscopy was performed on a Hewlett Packard 8452A Diode Array Spectrophotometer.

Thin layer chromatography (TLC) was performed on Merck DC-Plastikfolien Kiesegel 60 F254 20 x 20 cm plastic backed plates, and visualisation was afforded by ultra-violet light and/or iodine staining.

Radial chromatography was performed on a chromatotron (a centrifugally accelerated radial thin layer chromatograph) (Harrison Research Inc.) using a 1 mm, 2 mm, or 4 mm silica plate, and an elution gradient of 100% petroleum ether (50/70) to 100% diethyl ether. The plate was washed and reactivated with methanol. Visualisation of non-coloured compounds was achieved using an ultra-violet lamp.

Melting points (mp) less than 200 °C were recorded on a Reichert Hotstage microscope and are uncorrected. Melting points greater than 200 °C were measured using an Electrothermal melting point apparatus and are uncorrected.

Nuclear magnetic resonances (NMR) (^{1}H: 300 MHz and ^{13}C: 75 MHz) were performed on a Varian Unity 300 instrument, or on a Varian XL 300 instument, and peaks are quoted in ppm. Multiplicities are denoted as singlet (s), broad singlet (bs), doublet (d), broad doublet (bd), triplet (t), quartet (q), quintet (qu), doublet of doublets (dd), doublet of triplets (dt), or multiplet (m). For ^{1}H NMR the spectra were referenced to tetramethylsilane (TMS), if run in deuterated chloroform ($CDCl_3$). For samples run in deuterium oxide (D_2O) the spectra was referenced to the residual protonated solvent at 4.70 ppm, and for samples run in deuterated methanol (CD_3OD) the spectra was referenced to the residual protonated solvent at 3.30 ppm. For ^{13}C NMR run in deuterated chloroform ($CDCl_3$) the spectra was referenced to the residual protonated solvent at 77.0 ppm, and for samples run in deuterated methanol (CD_3OD) the spectra was referenced to the residual protonated solvent at 49.3 ppm.

Infra-red (IR) spectroscopy was performed on a Perkin Elmer 1600 FTIR Spectrophotometer or on a Shimadzu FTIR-8201 PC Spectrophotometer. Maxima are recorded in wave numbers (cm^{-1}) and denoted weak (w), medium (m), or strong (s).

Mass spectroscopy (MS), electron ionisation (EI), chemical ionisation (CI), and fast atom bombardment (FAB)—using glycerol (gly), nitrobenzyl alcohol (NOBA), or thioglycerol (thio), were recorded on a Kratos MS80RFA magnetic sector double focussing mass spectrometer operating a 4 kV accelerating voltage. Where possible the high resolution mass of the parent ion is compared with the expected calculated value. The relative intensities of the fragment ions are quoted as a percentage.

Optical rotation dispersion (ORD) spectroscopy were recorded using a Jasco J-20C Recording Spectropolarimeter. $[\alpha]_D^t$ is the specific rotation at t °C as measured at the sodium D line (589.3 nm), and the concentration is given in g/100 ml.

Solvents were purified by routine means:
Dichloromethane was dried over calcium chloride.
Diethyl ether was distilled from concentrated sulfuric acid (50 $ml \cdot l^{-1}$), and stored over sodium wire. For dry diethyl ether, the solvent was distilled from sodium in the presence of benzophenone, immediately prior to use.
Ethanol (dry) was distilled from magnesium ethoxide immediately prior to use.
Methanol (dry) was distilled from magnesium methoxide immediately prior to use.
Petroleum ether (50/70) was distilled from phosphorous pentoxide.
Tetrahydrofuran was distilled from sodium in the presence of benzophenone.
Toluene was dried over calcium chloride, and stored over sodium wire.

Moisture sensitive reactions were performed under dry nitrogen.

Experimental Part I

The Production of Required Enzymes and Enzyme Substrates

Part A Synthesis of (S)-*Aspartate β-Semialdehyde*

Diethyl allylacetamidomalonate (**46**) (diethyl 2-ethanamido-2-(2-propenyl)-propanedioate)[1,2]

Sodium ethoxide was prepared by adding sodium wire (0.66g, 28.7 mmol) to freshly distilled dry ethanol (20 ml), and allowing it to react under a calcium chloride drying tube. Diethyl acetamidomalonate (45) (4.126 g, 18.9 mmol) was added to the solution of sodium ethoxide, followed by freshly distilled allyl bromide (1-bromo-2-propene) (2.46 ml, 3.43 g, 28.4 mmol). The solution was then heated under reflux on an oil bath (bath temperature 122 °C) for 18 hours after which time no starting material remained (TLC (diethyl ether) R_f 0.35 (starting material), 0.51 (product), visualised by iodine). The reaction mixture was cooled to room temperature, and the solvent removed *in vacuo*. The resulting residue was resuspended in distilled water (10 ml), forming a heterogeneous mixture. The mixture was extracted with chloroform (3 x 10 ml), the combined organic layers were dried over magnesium sulfate, and the solvent removed *in vacuo* to yield the diethyl allylacetamidomalonate (46) as a yellow oil which crystallised on standing overnight. A small sample was recrystallised from benzene to yield a white solid.

The yield of diethyl allylacetamidomalonate (46) was 3.60g (14.0 mmol, 74.1%).
Mp 44 - 46 °C, literature 46 °C.[2]
^{1}H NMR (300 MHz, $CDCl_3$) δ_H 1.26 (6H, t, J = 7.4 Hz, 2 x -CH_2**C**H_3), 2.04 (3H, s, -NHCOC**H**$_3$), 3.08 (2H, d, J = 7.4 Hz, -**C**H_2CH=CH_2), 4.25 (4H, q, J = 7.4 Hz, 2 x -**C**$H_2$$CH_3$), 5.09 - 5.16 (2H, m, -CH=**C**H_2), 5.51 - 5.65 (1H, m, -**C**H=CH_2), 6.77 (1H, bs, -N**H**-) ppm.
IR (KBr disc) υ_{max} 3417 (N-H (m)), 2985 (C-H (w)), 1738 (C=O (s)), 1680 (C=O (s)), 1500 (s), 1308 (m), 1232 (m) cm^{-1}.
MS m/z (EI) 257 (M^+, 48%), 198 (MH-2(CH_2CH_3)$^+$, 55%), 184 (M-$CO_2CH_2CH_3^+$, 69%), 174 (92%), 142 (100%), 68 (53%), 43 (CH_3CO^+, 98%).

***N*-Acetyl allylglycine ethyl ester** (**47**) (ethyl 2-ethanamido-4-pentenoate)

Sodium ethoxide was prepared by adding sodium wire (1.34 g, 58.3 mmol) to freshly distilled dry ethanol (30 ml), and allowing it to react under a calcium chloride drying tube. Diethyl acetamidomalonate (45) (12.7 g, 58.3 mmol) was added to the solution of sodium ethoxide, followed by freshly distilled allyl bromide (1-bromo-2-propene) (6.3 ml, 61 mmol). The solution was heated under reflux for 19 hours on an oil bath (bath temperature 120 °C). The solvent was removed *in vacuo* after the reaction was cooled to room temperature, and the resulting mixture was resuspended in distilled water

(25 ml). The mixture was extracted with chloroform (3 x 25 ml) and dried over magnesium sulfate. The solvent was removed *in vacuo* to yield a yellow oil which was analysed by ^{1}H NMR and shown to contain starting material. The material was redissolved in ethanol (30 ml), and sodium (0.35 g, 15.2 mmol) was added followed by allyl bromide (1.6 ml, 15.5 mmol). The reaction mixture was heated under reflux for a further 18 hours whereupon a deep red colour formed. The solvent was removed *in vacuo* to give a red oil, this was resuspended in distilled water (30 ml), acidified (pH <4) with glacial acetic acid (0.5 ml), and extracted with chloroform (3 x 30 ml). The combined organic layers were dried over magnesium sulfate, and the solvent again removed *in vacuo* to yield *N*-acetyl allylglycine ethyl ester (47) as a red oil.

The yield of *N*-acetyl allylglycine ethyl ester (47) was 7.30 g (39 mmol, 66.9%).
TLC (diethyl ether) R_f 0.26, visualised by iodine.
^{1}H NMR (300 MHz, $CDCl_3$) δ_H 1.22 (3H, t, J = 7.3 Hz, -CH_2C**H**$_3$), 1.96 (3H, s, -NHCOC**H**$_3$), 2.41 - 2.53 (2H, m, -C**H**$_2$CH=CH_2), 4.10 - 4.18 (2H, m, -OC**H**$_2$$CH_3$), 4.60 - 4.64 (1H, m, -NHC**H**COOCH_2CH_3), 5.02 - 5.08 (2H, m, -CH=C**H**$_2$), 5.54 - 5.66 (1H, m, -C**H**=CH_2), 6.13 (1H, bs, -N**H**-) ppm.
IR ($CHCl_3$ solution) υ_{max} 3433 (N-H (w)), 3034 (C-H (m)), 1734 (C=O (s)), 1676 (C=O (s)), 1509(s), 1377 (w), 1236 (m), 1196 (w) cm^{-1}.
MS m/z (E.I.) 185 (M^+, 40%), 144 (M-$CH_2CH=CH_2^+$, 75%), 112 (M-$CO_2CH_2CH_3^+$, 75%), 102 ($H_2NCHCO_2CH_2CH_3^+$, 85%), 70 ($H_3CCONHC^+$, 85%), 43 (CH_3CO, 100%).

***N*-Acetyl allylglycine (48)** (2-ethanamido-4-pentenoic acid)[1,3]

Diethyl allylacetamidomalonate (46) (31.2g, 122 mmol), was dissolved water and ethanol (1:1) (210 ml). Sodium hydroxide (4.90 g, 122 mmol) was added and the reaction was heated under reflux for 72 hours. The disappearance of starting material was monitored by TLC. The reaction had not gone to completion. A 1.0 ml aliquot was removed, the solvent was removed *in vacuo*, the residue was washed with ethyl acetate, and the aqueous layer acidified with concentrated hydrochloric acid to pH 1 before being extracted into ethyl acetate. The organic layer was dried over magnesium sulfate and the solvent removed *in vacuo*. The residue was analysed by ^{1}H NMR (300 MHz, D_2O) showing the reaction had gone to 90% conversion. Sodium hydroxide (2.45 g, 61.2 mmol) was added and the reaction was heated under reflux for a further 18 hours. The reaction was cooled and concentrated *in vacuo* to 105 ml, then washed with ethyl acetate (2 x 140 ml) to remove any remaining starting material. The aqueous layer was acidified to pH 1 with concentrated hydrochloric acid. The product was extracted into ethyl acetate (3 x 140 ml), dried with magnesium sulfate, and the solvent removed *in vacuo*. Recrystallisation in hot propanone yielded the *N*-acetyl allylglycine (48) as pure clear chunky crystals.

The yield of *N*-acetyl allylglycine (48) was 10.8 g (67.8 mmol, 55.4%).
Mp 116 - 118 °C (literature 118 °C[1]).
^{1}H NMR (300 MHz, D_2O) δ_H 1.90 (3H, s, -NHCOC**H**$_3$), 2.32 - 2.54 (2H, m, -C**H**$_2$CH=CH$_2$), 4.28 - 4.32 (1H, m, -NHC**H**COOH), 5.01 -5.10 (2H, m, -CH=C**H**$_2$), 5.60 - 5.74 (1H, m, -C**H**=CH$_2$) ppm.
IR (KBr disc) υ_{max} 3341 (N-H (s)), 2934 (C-H (w)), 2454 (b), 1928 (b), 1722 (HOC=O (s)), 1541 (HNC=O (s)), 1231 (m) cm^{-1}.
MS m/z (EI) 139 (55%), 116 (M-$CH_2CH=CH_2^+$, 62%), 74 ($H_2NCHCO_2H^+$, 77%), 70 ($H_3CCONHC^+$, 72%), 43 (CH_3CO^+, 100%).

***(S)*-Allylglycine (49)** (*(S)*-2-amino-4-pentenoic acid)[1,4]

N-Acetyl allylglycine (48) (10.21 g, 62.12 mmol) was placed in a conical flask and dissolved in water (300 ml), the solution was then brought to pH 7.5 by the addition of 1 M NH_3 (aq). Porcine kidney acylase EC 3.5.1.14 (~16 mg, ~2.3 x 10^4 units) was then added, and the reaction incubated at 37 °C, with shaking at 180 rpm, for 20 hours. The reaction was monitored by removing 1.0 ml aliquots from the reaction, removing the solvent *in vacuo* and then analysing the residue by ^{1}H NMR (300 MHz, D_2O). When 50% of the starting material remained, the enzyme was denatured by heating the solution under reflux, and then removed by filtration. The filtrate was acidified with concentrated hydrochloric acid and then washed with ethyl acetate (3 x 150 ml). The aqueous layer was evaporated *in vacuo* to yield a yellow-white solid which was purified by ion exchange chromatography (Dowex 50W-X8(H) 16 - 40 mesh cation exchanger). The Dowex column was acidified with 2 M hydrochloric acid and then washed with distilled water until the elutant was neutral, before loading the material on to the column. *(R)-N*-Acetyl allylglycine (48) was eluted first with water. *(S)*-Allylglycine (49) was eluted with 1 M NH_3(aq), the solvent was then removed *in vacuo* to yield the titled product as a white semi-crystalline solid.

The yield of *(S)*-allylglycine (49) was 2.66 g (23.1 mmol, 36.0%).
Mp (decomposition) 210 °C (literature 180 °C,[1] 251 - 253 °C[5]).
^{1}H NMR (300 MHz, D_2O) δ_H 2.44-2.59 (2H, m, -C**H**$_2$CH=CH$_2$), 3.68-3.72 (1H, m, -C**H**CH$_2$CH= CH$_2$), 5.14-5.20 (2H, m, -CH=C**H**$_2$), 5.60-5.74 (1H, m, -C**H**=CH$_2$) ppm.
IR (KBr disc) υ_{max} 3433 (N-H (w)), 2934 (C-H (s)), 1587 (C=O, (s)), 1513 (s), 1405 (s) cm^{-1}.
MS m/z (CI (C_4H_{10})) 116 (MH^+, 100%), 74 (M-$CH_2CH=CH_2^+$, 80%), 70 (M-CO_2H^+, 67%).

Potassium *(S)-N-tert*-butoxycarbonylallylglycine (50) (potassium *(S)-N-tert*-butoxycarbonyl-2-amino-4-pentenoate)[6]

To a solution of *(S)*-allylglycine (49) (602 mg, 5.23 mmol) in water (15.0 ml) was added dioxane (7.2 ml), $KHCO_3$ (575 mg, 5.75 mmol) and di-*tert*-butyl pyrocarbonate (1.14 g, 5.23 mmol) with continuous stirring at room temperature for 20 hours. The solvents were removed by azeotroping with ethanol (~50 ml) *in vacuo*, yielding a white oily solid. The solid was washed with methanol (~10 ml) which was then removed *in vacuo* to yield the product as a white powdery solid.

The yield of the potassium *(S)-N-tert*-butoxycarbonylallylglycine (50) was 1.36 g (5.38 mmol, quantitative).
Mp >230 °C.
^{1}H NMR (300 MHz, D_2O) δ_H 1.35 (9H, s, 3 x -C**H**$_3$), 2.31-2.41 (2H, m, -C**H**$_2$CH=CH$_2$), 3.91 (1H, m, -C**H**CH$_2$CH=CH$_2$), 5.04 - 5.23 (2H, m, =C**H**), 5.66 - 5.75 (1H, m, -C**H**=CH$_2$) ppm.
IR (KBr disc) υ_{max} 3416 (C-H (s)), 1686 (w), 1618 (C=O (s)), 1384 (C-O (s)), 1173 (m) cm^{-1}.
MS m/z (FAB(thio)) 292 (MK_2^+, 5%), 255 (MHK^+, 10%), 185 (12%), 147 (100%).

***p*-Methoxybenzyl chloride (51)**[7]

p-Methoxybenzyl alcohol (54) (55.0 ml, 60.9 g, 0.441 mol) in dry diethyl ether (250 ml) was saturated with dry hydrogen chloride gas at 0 °C for 5.5 hours. The reaction vessel was then stoppered and stored at -20 °C for 40 hours. Removal of the excess hydrogen chloride was afforded by distillation over a water bath at 32 - 38 °C at atmospheric pressure. The residual *p*-methoxybenzyl chloride was distilled under reduced pressure, bp 94 - 98 °C (~1.5 mm Hg), to give a clear liquid. The product was then stored at -20 °C, stabilised with potassium carbonate.

The yield of *p*-methoxybenzyl chloride (51) was 45.0 ml (51.9 g, 0.332 mol, 75.3%).
Bp 94 - 98 °C (~1.5 mm Hg).
^{1}H NMR δ_H (300 MHz, $CDCl_3$) 3.76 (3H, s, -OC**H**$_3$), 4.53 (2H, s, -C**H**$_2$Cl), 6.85 (2H, d, J = 8.8 Hz, aryl), 7.28 (2H, d, J = 8.8 Hz, aryl) ppm.
IR (thin film) υ_{max} 2959 (C-H (w)), 2836 (w), 1611 (C=C aryl, (s)), 1514 (C=C aryl, (s)), 1304 (m), 1249 (C-O (s)), 1176 (m), 1033 (m) cm^{-1}.
MS m/z (EI) 156 (M^+, 28%), 121 ($M\text{-}Cl^+$, 100%), 77 (Ph^+, 10%).

(*S*)-*N*-*tert*-Butoxycarbonylallylglycine *p*-methoxybenzyl ester (52) (4-methoxybenzyl *(S)-N-tert*-butoxycarbonyl-2-amino-4-pentenoate)[6]

To a solution of potassium *(S)-N-tert*-butoxycarbonylallylglycine (50) (0.504 g, 1.99 mmol) in DMF (3.5 ml) was added *p*-methoxybenzyl chloride (51) (0.331 ml, 2.44 mmol). The mixture was stirred continuously for 48 hours. The solvent was then removed by azeotroping with xylene *in vacuo*. The crude product was analysed by TLC ((diethyl ether and pet ether (1:1)) R_f 0.15, 0.34 (product), 0.68). The crude product was purified by radial chromatography (4 mm silica plate). The *(S)-N-tert*-butoxycarbonyl-allylglycine *p*-methoxybenzyl ester (52) was obtained as a brown oil.

The yield of *(S)-N-tert*-butoxycarbonylallylglycine *p*-methoxybenzyl ester (52) was 408 mg (1.22 mmol, 61.3%).
^{1}H NMR (300MHz, $CDCl_3$) δ_H 1.44 (9H, s, 3 x -C**H**$_3$), 2.46 - 2.50 (2H, m, -C**H**$_2$CH=CH$_2$), 3.82 (3H, s, -OC**H**$_3$), 4.38 - 4.42 (1H, m, -C**H**CH$_2$CH=CH$_2$), 5.05 - 5.17 (5H, m, =C**H**$_2$, -C**H**$_2$ aryl, -N**H**-), 5.60 - 5.69 (1H, m, -C**H**=CH$_2$), 6.87 - 6.91 and 7.26 - 7.31 (4H, m, aryl) ppm.
IR ($CDCl_3$) υ_{max} 3439 (N-H (s)), 2982 (C-H (m)), 1710 (C=O (s)), 1614 (m), 1515 (s), 1249 (m), 1174 (m) cm^{-1}.
MS m/z (EI) 335 (M^+, 10%), 279 (M-tBu$^+$, 54%), 121 ($CH_3OC_6H_4CH_2^+$, 100%), 70 (82%).

(*S*)-*N*-*tert*-Butoxycarbonylaspartate β-semialdehyde *p*-methoxybenzyl ester (53) (4-methoxybenzyl *(S)-N-tert*-butoxycarbonyl-2-amino-4-oxobutanoate)[1]

(S)-N-tert-Butoxycarbonylallylglycine *p*-methoxybenzyl ester (52) (105 mg, 0.313 mmol) was dissolved in water and dioxan (3:1) (9.0 ml). A catalytic amount of osmium tetroxide (OsO_4) (< 1 mg) was added to this mixture. The mixture was stirred at room temperature for 30 minutes during which time a blue-black colour appeared. Sodium periodate ($NaIO_4$) (0.250 g, 1.17 mmol) was then added slowly over 30 minutes. The reaction was then stirred for 16 hours. The mixture was partitioned between ethyl acetate (7 ml) and water (7 ml). The organic layer was washed with water (2 x 7 ml), then evaporated *in vacuo* to yield a yellow black oil (TLC (diethyl ether and pet ether (3:1)) R_f 0.76 (starting material), 0.53, 0.40 (product)). The yellow-black product was dissolved in diethyl ether and passed through a silica plug to remove any last traces of osmium tetroxide The product was purified by radial chromatography (4 mm silica plate). The solvent was removed *in vacuo* to yield the *(S)-N-tert*-butoxycarbonylaspartate β-semialdehyde *p*-methoxybenzyl ester (53) as a clear oil.

The yield of *(S)-N-tert*-butoxycarbonylaspartate β-semialdehyde *p*-methoxybenzyl ester (53) was 79.8 mg (0.237 mmol, 75.7%).
^{1}H NMR (300 MHz, $CDCl_3$) δ_H 1.42 (9H, s, 3 x -C**H**$_3$), 3.02 - 3.06 (2H, m,

-C**H**$_2$-CHO), 3.81 (3H, s, -OC**H**$_3$), 4.57 - 4.63 (1H, m, -C**H**CH$_2$CHO), 5.11 (2H, s, -C**H**$_2$ aryl), 5.42 (1H, bd, -N**H**-), 6.89 and 7.26 (4H, m, almost A_2B_2, aryl), 9.71 (1H, s, -C**H**O) ppm.

IR ($CDCl_3$) υ_{max} 3436 (N-H (w)), 2981 (C-H (w)), 1715 (C=O (s)), 1516 (s), 1501 (m), 1250 (s), 1174 (s) cm^{-1}.

MS m/z (EI) 337 (M^+, 10%), 281 (27%), 202 (32%), 137 ($CH_3OPhCH_2O^+$, 65%), 121 ($CH_3OPhCH_2^+$, 100%), 72 (70%).

***(S)*-Aspartate β-semialdehyde hydrate trifluoroacetate (11b)** (*(S)*-2-amino-4-oxobutanoate)[6]

(S)-N-tert-butoxycarbonylaspartate β-semialdehyde *p*-methoxybenzyl ester (53) (72.0 mg, 0.214 mmol) was dissolved in dry dichloromethane (1.5 ml). The reaction was stirred under nitrogen and trifluoroacetic acid (1.5 ml) was added via a syringe. The reaction was stirred for two hours, going a deep red colour. The solvent was then removed *in vacuo* to give a brown oily residue, which was partitioned between water (7.0 ml) and ethyl acetate (3 x 7.0 ml). The aqueous layer was then concentrated to yield the *(S)*-aspartate β-semialdehyde hydrate trifluoroacetate (11b) as a pale yellow oil.

The yield of *(S)*-aspartate β-semialdehyde hydrate trifluoroacetate (11b) was 47.2 mg (0.190 mmol, 89.6%).

^{1}H NMR (300 MHz D_2O) δ_H 1.97 - 2.21 (2H, m, -C**H**$_2$CHNH$_2$), 4.01 -4.05 (1H, m, -C**H**NH$_2$), 5.21 (1H, t, J = 5.9 Hz, -C**H**(OH)$_2$) ppm.

^{13}C NMR (75 MHz D_2O) δ_C 36.2 (-**C**H$_2$CHNH$_2$), 49.7 (-**C**HNH$_2$), 87.7 (-**C**H(OH)$_2$), 118.0 (-**C**CF$_3$), 162 (-**C**CF$_3$), 171.2 (-**C**=O).

HMBC[8] δ_H *ca.* 2.1 coupling to δ_C 49.7, 87.7, and 171.2; δ_H *ca.* 4.0 coupling to δ_C 36.2, 87.7, and 171.2; δ_H *ca.* 5.2 coupling to δ_C 36.2, and 49.7.

$[\alpha]_D^{23}$ = + 3.17° (*c* = 1.5, H_2O).

IR (KBr disc) υ_{max} 3414 (O-H (s)), 1678 (C=O (s)), 1522 (w), 1437 (m), 1201 (s), 1143 (s) cm^{-1}.

MS m/z (FAB (gly)) 136 (M^+, 15%), 118 (28%), 93 (100%), 77 (Ph^+,75%).

Part B Production of the DHDPS and DHDPR enzymes

A. Standard Microbiology and Molecular Biology Methods

Main sources

J.H. Miller *'A short course in bacterial genetics: a lab manual and handbook for* E. coli *and related bacteria'* Cold Spring Harbor, New York (1992).

F.M. Ausubel (Ed.) *'Short Protocols in Molecular Biology'* Wiley Interscience, New York (1989).

T. Maniatis, E.F. Fritsch., J. Sambrook *'Molecular Cloning: A Laboratory Manual'* 2nd ed., Cold Spring Harbor, N. Y. (1990).

G.D. Fasman *'CRC Practical Handbook of Biochemistry and Molecular Biology'* CRC Press, Florida (1989).

Bacterial cultures

All *E. coli* cultures were grown under sterile conditions. All media and equipment were either autoclaved at 121 °C for 20 minutes, filtered through a 0.2 micron acrodisc (Gellman Sciences), or purchased sterile. Solutions were made up in sterile deionised water. During the transfer of cultures all equipment was flamed, and manipulations were carried out in a laminar flow hood. Each experiment was accompanied by an appropriate control to monitor for contamination.

Media

(Plus 15g select agar for plates, pH 7.0.)

Luria-Bertani medium (LB broth)

Per litre of medium:

Bactotryptone (casein hydrolysate)	10 g
Yeast extract	5 g
Sodium chloride (NaCl)	10 g

adjusted to pH 7.0 with 5 M NaOH (optional), autoclaved 20 minutes at 121 °C.

Antibiotics

Stock solutions (1000 x) of antibiotics were stored at -20 °C. The following concentrations were used for selection:

Ampicillin	60 $\mu g ml^{-1}$
Tetracycline	25 $\mu g ml^{-1}$

Added through an acrodisc to sterile media at <48 °C.

E. coli XL1-Blue

E. coli XL1-Blue can be obtained from Stratgene; it was a kind gift from Jane Lancaster (Crop and Food Research Ltd, Christchurch, New Zealand), and was selected and maintained on tetracycline plates.

Preparation of glycerol freezes

1.0 ml of an overnight culture was added to 0.25 ml of sterile 80% glycerol (propan-1,2,3,-triol) in deionised water in a screw top eppendorf. The tube was gently vortexed before being frozen in liquid nitrogen (-196 °C) for long term storage.

Plate preparation

Plates were poured, in a laminar flow hood and/or in close proximity to a flame, at ~50 °C, directly into sterile petri dishes. 30 - 35 ml of media per plate was adequate for overnight growth on LB media. Any bubbles were removed by quickly flaming the surface before the agar had hardened. The plates were allowed to set overnight before use. The plates could be stored for several weeks if sealed with parafilm and kept at 4 °C.

Incubation of colonies

Agar plates were streaked with *E. coli* XL-1 Blue (from a glycerol freeze, an overnight culture, or a single colony on an agar plate) using a flamed sterilised nichrome wire; the concentration was successively decreased across the plate to allow for selection of single colonies. The plates were incubated, inverted, overnight at 37 °C. Individual colonies were selected out with a wire loop, or wire stab, and used to innoculate 5ml of liquid medium. These starter cultures were grown overnight in a shaker incubator (37 °C, 180 rpm) and subsequently used to innoculate larger quantities of media.

Single colonies remained viable on an agar plate for approximately three to four weeks if stored at 4 °C, with the plate sealed with parafilm. The bacteria were restreaked if the plate had been stored for more than two days.

Transformation by the calcium chloride method

Day one:

0.2 ml of overnight culture was grown in 10 ml of LB broth (37 °C, 310 rpm) for two hours.

The cells were chilled on ice, then centrifuged (8000 rpm, 5 minutes), and the supernatant was decanted off.

The pellet was resuspended in 5 ml of 10 mM NaCl and chilled on ice for 20 minutes before recentrifuging (8000 rpm, 5 minutes).

The pellet was resuspended in 2.5 ml of 100 mM $CaCl_2$ and chilled on ice for 20 minutes before recentrifuging (8000 rpm, 5 minutes).

The pellet was finally resuspended in 0.6 ml of 100 mM $CaCl_2$ and chilled on ice for 30 minutes to give competent cells.

Day two:
2 µl of plasmid DNA and 0.1 ml of competent cells, prepared earlier, were added to an eppendorf and incubated on ice for 30 minutes then heat shocked for 2 minutes at 42 °C, and chilled on ice for a further 2 minutes.

The cells were then transferred to a flask containing 5 ml of LB broth and incubated (37 °C, 250 rpm) for 2 hours.

0.2 ml of the cells was plated out on the appropriate antibiotic plate, while 3 ml was centrifuged (8000 rpm, 5 minutes) and the pellet spread on an appropriate antibiotic plate.

Standard plasmid preparation by alkaline lysis
(Derived from Birnboim and Doily)

Solution I (4 °C)	50 mM Glucose
	10 mM EDTA pH 8.0
	25 mM Tris.HCl pH 8.0
Solution II (R.T.)	0.2 mM NaOH
	1% SDS
Solution III (4 °C)	3 M Sodium acetate pH 4.8
TE buffer	10 mM Tris.HCl pH 8.0
	1 mM EDTA

A single bacterial colony was used to innoculate 5 ml of LB broth containing appropriate antibiotics and incubated overnight (37 °C, 180 rpm).

1.5 ml of culture was then transferred to an eppendorf and centrifuged (760 rpm, 2 minutes).

The supernatant was removed by aspiration and the pellet resuspended in 100µl of ice cold solution I and chilled on ice for 10 minutes.

200 µl of freshly prepared solution II was added slowly and mixed by gentle rotation, and chilled on ice for 5 minutes.

150 µl of ice-cold solution III was added and gently mixed until the viscosity decreased and a white precipitate formed; this mixture was chilled on ice for 20 minutes.

The tube was centrifuged (12 000 rpm, 5 minutes), the supernatant was decanted off and strained into a fresh tube.

250 µl of isopropyl alcohol was added to the supernatant, mixed and stored on ice for 20 minutes.

The tube was centrifuged (12 000 rpm, 5 minutes) and then the supernatant was carefully removed.

The pellet was rinsed with 1 ml of ethanol at 4 °C, centrifuged (12 000 rpm, 1 minute), and the supernatant aspirated out.

The pellet was dissolved in 200 µl of 0.3 M sodium acetate and vortexed briefly.

400 µl of 100% ethanol (ice-cold) was added and mixed, and the solution stored on ice for 10 minutes.

The tube was then centrifuged (12 000 rpm, 5 minutes), and supernatant was aspirated out.

The pellet was dried in a vacuum dessicator for 5 minutes, and then dissolved in 20 µl of TE buffer by vortexing briefly.

Restriction digests

1% Agarose gel	0.3 g Agarose
	30 ml TAE buffer
TAE buffer	0.80 mM Tris.HCl pH 8.0
	0.40 mM Glacial acetic acid
	0.02 mM EDTA
Loading dye	30% Glycerol
	0.25% Bromophenol blue
	0.25% Xylene cyanol
	RNAse was added to a final concentration of 10 $mgml^{-1}$.

Restriction digests were typically performed in 15 µl volumes. 1.5 µl of the manufacturer's 10 x restriction enzyme buffer was used and digests were incubated at the appropriate temperature for one to four hours.

For example: Double digest of pJG001 with BamH I and Xho I

10 µl dH_2O
2.0 µl DNA solution from standard plasmid preparation
1.5 µl React 3 Buffer
1.0 µl Xho I
0.5 µl BamH I
15 µl Total
Incubated four hours 37 °C
1.0 µl Loading buffer was added and mixed immediately prior to the running of the DNA gel.

Agarose gel electrophoresis

Restriction fragments were mapped on a 1% (w/v) agarose gel against a one kb ladder. 30 ml of boiling 1% agarose gel was cooled to ~50 °C and poured into a gel casting tray and the well comb inserted. The gel was allowed to set completely (about 30 minutes) before the comb was removed. The casting tray was then transferred into a gel tank containing electrophoresis TAE buffer. The gel was loaded with DNA samples (15 µl) mixed with loading dye (1 µl) containing DNA free RNAse. A DNA ladder was also loaded; 5 µl of the one kb ladder (Bio Rad; 4072, 3054, 2036, 1636, 1018). The gel was run at 60 V for two to three hours until the bromophenol blue band was nearing the end of the gel. The gel was stained with ethidium bromide (0.5 $mgml^{-1}$), and the DNA fragments were visualised on a UV transiluminator with a wavelength of 302 nm. The gel was then photographed under UV light.

B. Overexpression of the *dap A* gene

Transformation of pJG001 into *E. coli* XL-1 Blue

E. coli XL-1 Blue were transformed with pJG001 (derived from pBluescript by Grerrard[1]). Successful transformants were identified by conferred ampicillin resistance.

Restriction digest of pJG001

Plasmid preparation was carried out by the alkaline lysis method. Successful isolation of pJG001 was confirmed by restriction mapping: 4100 bp (Xho I), 4100 bp (BamH I), 3000 and 1100 bp (Xho I and BamH I double digest), and 3000 and 1100 bp (EcoR I and Hind III double digest).

C. Overexpression of the *dap B* gene

Transformation of pJK001 into *E.coli* XL-1 Blue

E. coli XL-1 Blue were transformed with pJK001 (derived from pBluescript by Kraunsoe[9]). Successful transformants were identified by conferred ampicillin resistance.

Restriction digest of pJK001

Plasmid preparation was carried out by the alkaline lysis method. Successful isolation of pJK001 was confirmed by restricion mapping: 3000 and 2300 bp (Xho I and BamH I double digest).

D. Biochemistry standard methods

Main Sources

R.K. Scopes *'Protein Purification. Principles and Practice'* 3rd ed., Springer Verlag, New York (1994).

E.L. Harris, S. Angal (Eds) *'Protein Purification. A practical approach'* IRL Press, Oxford (1989).

T.E. Creighton (Ed.) *'Protein Function. A practical approach'* IRL Press, Oxford (1989).

G.D. Fasman *'CRC Practical Handbook of Biochemistry and Molecular Biology'* CRC Press, Florida (1989).

Ion exchange

Pharmacia Product Information: *'Ion Exchange. Principles and Methods'* 3rd ed., Pharmacia LKB Biotechnology, Sweden (1991).

Gel Filtration

Pharmacia Product Information: *'Gel Filtration. Principles and Methods'* 5th ed., Pharmacia LKB Biotechnology, Sweden (1991).

Polyacrylamide Gel Electrophoresis (PAGE)

U.K. Laemmli *Nature* **227**, 680 (1970).

Product information Hoefer Scientific Sturdier Slab Gel Electrophoresis Unit.

B.D. Hames, D. Rickwood (Eds) *'Gel electrophoresis of proteins. A practical approach'* IRL Press, London (1981).

Ultrafiltration

Lida Ultrafiltration Product Information.

Preparation of Bradford Reagent[10]

Coomassie Brilliant Blue (100 mg) was dissolved in 95% (v/v) ethanol (50 ml) with vigorous agitation, then mixed with 85% (w/v) phosphoric acid (100 ml). The mixture was diluted to 1 litre with distilled water and filtered to remove the undissolved dye. The solution was stable at room temperature for several weeks. Each batch of Bradford reagent was calibrated against a series of Bovine Serum Albumin (BSA) standards of known concentration. A range of protein concentrations from 0.2 - 2.0 $mgml^{-1}$ was assayed and plotted on a graph to produce a calibration curve. Each measurement was performed in duplicate.

Standard Bradford assay[11,12]

The protein solution (0.05 ml) was added to the Bradford reagent (2.50 ml) and mixed thoroughly. The solution was allowed to stand for exactly 10 minutes, before the absorbance was measured at 595 nm against a blank solution (sample buffer (0.05 ml) and Bradford reagent (2.5 ml)). Protein concentrations were obtained from the calibration curve; however, since individual proteins interact with Coomassie Brillant Blue dye in a slightly different manner according to the amino acid compostion, only approximate protein concentrations were obtained.

Sodium dodecyl sulfate polyacrylamide gel electrophoresis (SDS-PAGE)

Stock solutions

Monomer solution	30% (w/v) Acrylamide
	2.7% (w/v) Bis-acrylamide
	Stored in a dark container at 4 °C
Resolving gel buffer	1.5 M Tris.HCl pH 8.8
Stacking gel buffer	0.5 M Tris.HCl pH 6.8
Electrophoresis tank buffer	0.125 M Tris.HCl pH 6.8
	200 mM Glycine
	4% SDS
1% Coomassie Brilliant Blue Stain	1% (w/v) Coomassie Brilliant Blue G 250
	Stirred vigorously and filtered
Coomassie Brilliant Blue Stain	0.125% 1% Stain stock
	50% Methanol
	10% Glacial acetic acid
Destain I	50% Methanol
	10% Glacial acetic acid
Destain II	5% Methanol
	7% Acetic acid

12.5% Resolving gel

Acrylamide monomer	12.5 ml
Resolving gel buffer	7.5 ml
Distilled water	9.5 ml
Degassed by swirling for 15 minutes under a water pump at room temperature	
10% SDS	300 µl
10% Ammonium persulfate	100 µl
TEMED (tetramethylethylenediamine)	25 µl

The acrylamide mixture was poured into the assembled slab gel plates which had been cleaned and dried thoroughly. Any air bubbles were removed by a heated nichrome wire. The surface of the gel was carefully overlayed with *n*-butanol to prevent drying out. The gel was allowed to set overnight.

4% Stacking gel

Acrylamide monomer	1.33 ml
Stacking gel bufer	2.5 ml
Distilled water	6.1 ml
Degassed by swirling for 15 minutes under a water pump at room temperature	
10% SDS	100 µl
10% Ammonium persulfate	50 µl
TEMED (tetramethylethylenediamine)	5 µl

n-Butanol was poured off the gel, and the stacking gel was then poured on. The gel comb was inserted on an angle to prevent the introduction of any air bubbles. The gel was allowed to set for about two hours before removing the comb, where it was then used immediately.

Running the gel

Samples were diluted to an approximate concentration (to allow the loading of ~20 µg of total protein) with TE buffer and then mixed with an equal volume of 2 x treatment buffer.

TE buffer	10 mM Tris.HCl pH 8.0
	1 mM EDTA
2 x Treatment buffer	0.125 M Tris.HCl pH 8.6
	4% SDS
	20% Glycerol
	10% 2-Mercaptoethanol
	0.25% Bromophenol blue
	Stored at -20 °C

The samples were centrifuged briefly and boiled for ~3 minutes before loading into the wells of the gel using a duckbill tip. A marker was also added, either 67, 60, 53, 46, 40, 34, 27, 15, 6.5 kDa; or 97.4, 66, 45, 31, 21.5, 14.5 kDa. The gel was electrophoresed at 4 °C at constant current (30 mA) through the stacking gel, then the ampage was increased to 40 mA until the bromophenol blue had run out the bottom of the resolving gel. The gel was then stained overnight, washed with destain I for ~4 hours, then washed with destain II overnight.

Preparation of dialysis tubing

Visking tubing was boiled for 10 minutes in a 2% (w/v) solution of sodium bicarbonate and 0.05% (w/v) EDTA. Care had to be taken to ensure the tubing remained submerged at all times. The tubing was then boiled for a further 10 minutes in deionised water, this was then repeated. The solution was cooled and the tubing stored at 4 °C in 0.1% (w/v) sodium azide for up to three months.

E. Overexpression and Purification of DHDPS

Growth of *E. coli* XL-1 Blue pJG001

E. coli XL-1 Blue pJG001 glycerol freeze was streaked out on LB agar and grown overnight at 37 °C. A single colony was selected and restreaked on LB agar, containing standard concentrations of both ampicillin and tetracycline, and incubated overnight at 37 °C. A single colony was then selected and used to innoculate 5 ml of LB broth, containing standard concentrations of both ampicillin and tetracycline, and incubated overnight (37 °C, 180 rpm). 1.0 ml of overnight culture was used to innoculate 200 ml of LB broth containing both ampicillin and tetracycline, and incubated overnight as above. The cells were chilled on ice for 30 minutes, then harvested by centrifugation (5000 rpm, 10 minutes). 10 l of LB broth gave ~50 g wet weight of cells.

Preparation of a crude cell free extract

Cells were harvested, as above, and washed by resuspending in 20 mM Tris.HCl pH 8.0 at 4 °C (30 ml), then gently pipetting the buffer and the cell pellet together. The cell suspension was centrifuged for (5000 rpm, 10 minutes). The supernatant was discarded and the cell pellet was resupended in an equal volume of 20 mM Tris.HCl pH 8.0 at 4 °C. The sample was then flash frozen in liquid nitrogen and stored at -20 °C.

To obtain the crude enzyme extract the cells were subjected to seven freeze thaw cycles; each cycle involved flash freezing the cells in liquid nitrogen (-196 °C) followed by slowly thawing on ice at 4 °C overnight. The crude extract was then obtained by centrifugation (5000 rpm, 10 minutes) to remove all the cell debris, the supernatant was collected (70 ml).

Purification

Ion exchange

The crude supernatant (35 ml) was loaded on to a Q-Sepharose ion exchange column (bed volume 70 ml, 15 x 2.6 cm) that had been pre-equilibrated with three bed volumes of 20 mM Tris.HCl pH 8.0 at 4 °C. The column was then washed with five bed volumes of the start buffer (20 mM Tris.HCl pH 8.0 at 4 °C) and the DHDPS was then eluted with a 0 to 1 M NaCl salt gradient in 20 mM Tris.HCl pH 8.0 at 4 °C. The column was then washed with three bed volumes of regeneration buffer (1 M NaCl in 20 mM Tris.HCl pH 8.0 at 4 °C). The eluted fractions were tested for DHDPS activity using the *o*-amino-benzaldehyde micro assay (see Part II). Active fractions eluted between 0.4 and 0.6 M NaCl, and were pooled (110 ml).

Dialysis

Dialysis buffer 20 mM Tris.HCl pH 8.0 at 4 °C
1 mM EDTA
1mM 2-Mercaptoethanol
1% Ammonium sulfate

Pooled material from the ion exchange (110 ml) was dialysed overnight in dialysis buffer (2 x 2 l). Dialysed sample was collected (100 ml).

Second ion exchange

(a) Small scale

A 1 ml Resource Q-Sepharose column (Pharmacia) was used in the final ion exchange step. 1.0 ml batches of dialysed sample were charged onto the 1 ml column, the column was then washed with five bed volumes of 20 mM Tris.HCl pH 8.0 at 4 °C. The column was then eluted with a linear gradient of 0 to 1 M NaCl in 20 mM Tris.HCl pH 8.0 at 4 °C. DHDPS eluted between 0.4 and 0.6 M NaCl; active fractions were pooled (5.0 ml).

(b) Large scale

For large amounts of DHDPS required for the coupled assay to measure the activity of DHDPR the second ion exchange was performed in an analogous way to the first ion exchange column. The supernatant (70 ml) was loaded on to a Q-Sepharose ion exchange column (bed volume 70 ml, 15 x 2.6 cm) that had been pre-equilibrated with three bed volumes of 20 mM Tris.HCl pH 8.0 at 4 °C. The column was then washed with five bed volumes of the start buffer (20 mM Tris.HCl pH 8.0 at 4 °C) and the DHDPS was then eluted with a 0 to 1 M NaCl salt gradient in 20 mM Tris.HCl pH 8.0 at 4 °C. The column was then washed with three bed volumes of regeneration buffer (1 M NaCl in 20 mM Tris.HCl pH 8.0 at 4 °C). The eluted fractions were tested for DHDPS

activity using the *o*-aminobenzaldehyde micro assay (see Part II). Active fractions eluted between 0.4 and 0.6 M NaCl, and were pooled (132 ml).

Purification

Purification step	Total protein ($mgml^{-1}$)	Activity ($\mu mol \cdot s^{-1}ml^{-1}$)	Specific activity ($\mu mol \cdot s^{-1}mg^{-1}$)
Crude supernatant	10.2	1.73×10^{-1}	1.70×10^{-2}
Ion exchange	2.4	1.35×10^{-2}	1.35×10^{-2}
Dialysis	1.6	5.18×10^{-2}	3.24×10^{-2}
Second ion exchange -Resource Q-Sepharose	4.0×10^{-2}	1.18×10^{-3}	4.70×10^{-1}
Second ion exchange -Q-Sepharose	8.0×10^{-2}	1.60×10^{-3}	2.00×10^{-1}

Attempted modifications to the DHDPS purification

Heat shock on the crude extract[6]

The crude supernatant (3.0 ml) was heat shocked at 70 °C for two minutes. Precipitated proteins were removed by centrifugation (5000 rpm, 10 minutes). The supernatant (2.5 ml) showed decreased DHDPS activity.

Gel filtration

A Sephacryl S-400 HR (bed volume 68 ml, 2.6 x 30 cm) column pre-equilibrated with 20 mM Tris.HCl pH 8.0 at 4 °C, was eluted at 2 $mlmin^{-1}$. An ion exchanged sample (4.2 ml) was loaded onto the column and eluted (104 ml), the bands were too diffuse for gel filtration to be of any practical use.

F: Over-Expression and Purification of DHDPR

Growth of *E. coli* XL-1 Blue pJK001

E. coli XL-1 Blue pJK001 glycerol freeze was streaked out on LB agar and grown overnight at 37 °C. A single colony was selected and restreaked on LB agar containing standard concentrations of both ampicillin and tetracycline, incubated overnight at 37 °C. A single colony was selected and used to innoculate 5 ml of LB broth containing both ampicillin and tetracycline, incubated overnight at 37 °C, 180 rpm. 1 ml of saturated overnight culture was used to innoculate 200 ml of LB broth containing both ampicillin and tetracycline, and incubated as above. The cells were chilled on ice for 30 minutes, then harvested by centrifugation (5000 rpm, 10 minutes).

Preparation of a crude cell free extract

Cells were harvested as above and washed by resuspending in 20 mM Tris.HCl pH 8.0 at 4 °C (30 ml), gently pipetting the buffer and the cell pellet together. The cell

suspension was centrifuged (5000 rpm, 10 minutes). The supernatant was discarded and the cell pellet resuspended in an equal volume of 20 mM Tris.HCl pH 8.0 at 4 °C, then flash frozen in liquid nitrogen and stored at -20 °C.

To obtain the crude extract the frozen cells were slowly thawed on ice at 4 °C overnight. The suspension was then ultrasonicated on ice, 4 microns, for 4 minutes in 15 second bursts with 15 seconds between each burst. The supernatant was then collected by centrifugation (5000 rpm, 10 minutes).

Purification

Heat shock

The supernatant was heat shocked in 1.0 ml aliquots at 70 °C for three minutes, followed immediately by cooling on ice. The precipitated proteins were removed by centrifugation (10 minutes, 5000 rpm), and the supernatant was collected (65 ml).

Ammonium sulfate precipitation

Solid ammonium sulfate was added to the supernatant, resulting from ultrasonication treatment, until 20% saturation was achieved (100% saturation of ammonium sulfate = 70 g/100 ml) and stirring was continued for 30 minutes. The mixture was centrifuged (10 minutes, 15 000 rpm). The supernatant was transferred to a fresh tube, solid ammonium sulfate was then added until 60% saturation was achieved, stirring was continued for 30 minutes. The supernatant was discarded, as was the first precipitate, while the second precipitate was dissolved in a volume of 20 mM Tris.HCl pH 8.0 at 4 °C equal to the volume of the crude extract.

Dialysis

Dialysis buffer — 20 mM Tris.HCl pH 8.0 at 4 °C
1 mM EDTA
1mM 2-Mercaptoethanol
1% Ammonium sulfate

The ammonium sulfate precipitate was dialysed against and 50 volumes of dialysis buffer overnight at 4 °C.

Ion exchange

The dialysed sample was loaded on to a Q-Sepharose ion exchange column (bed volume 70 ml, 15 x 2.6 cm) that had been pre-equilibrated with three bed volumes of 20 mM Tris.HCl pH 8.0 at 4 °C. The column was then washed with five bed volumes of the start buffer (20 mM Tris.HCl pH 8.0 at 4 °C) and the DHDPS was then eluted with a 0 to 1.0 M NaCl salt gradient in 20 mM Tris.HCl pH 8.0 at 4 °C. The column was then washed with three bed volumes of regeneration buffer (1 M NaCl in 20 mM Tris.HCl pH

8.0 at 4 °C). The eluted fractions were tested for DHDPR activity using the coupled assay. Active fractions eluted between 0.6 and 0.9 M NaCl, and were pooled.

Purification

Purification step	Total protein ($mgml^{-1}$)	Activity ($\mu mol \cdot s^{-1}ml^{-1}$)	Specific activity ($\mu mol \cdot s^{-1}mg^{-1}$)
Crude supernatant	9.0	7.10×10^{-3}	7.89×10^{-4}
Heat shocked supernatant	3.4	3.88×10^{-4}	1.14×10^{-4}
Ammonium sulfate precipiate	4.2	1.34×10^{-3}	3.18×10^{-4}
Dialysis	3.0	1.34×10^{-3}	4.45×10^{-4}
Ion exchange	1.0×10^{-2}	2.25×10^{-2}	2.25

References

1. J.A. Gerrard *'Studies on Dihydrodipicolinate Synthase'* D. Phil., Brasenose College, Oxford (1992).
2. N.F. Albertson *J. Am. Chem. Soc.* **68**, 450 (1946).
3. S. Black, N. Wright *J. Biol. Chem.* **213**, 39 (1955).
4. H.K. Chenault, J. Dahmer, G.M. Whitesides *J. Am. Chem. Soc.* **111**, 6354 (1989).
5. Aldrich Chemical Company Catalogue.
6. D.W. Tudor, T. Lewis, D.J. Robins *Synthesis* 1061 (1993).
7. R.L. Shriner, C.J. Hull *J. Org. Chem.* **10**, 228 (1945).
8. HMBC experiments were performed by J.W. Blunt.
9. J.A.E. Kraunsoe *'Studies in Lysine Biosynthesis'* Part II, Corpus Christi College, Oxford (1992).
10. R.K. Scopes *'Protein Purification: Principles and Practice'* 3rd ed., Springer Verlag, New York (1994).
11. M.M. Bradford *Anal. Biochem.* **72**, 248 (1976).
12. T. Spector *Anal. Biochem.* **86**, 142 (1978).

Experimental Part II

DHDPS and DHDPR Kinetics

o-Aminobenzaldehyde (55)[1]

Water (350 ml), ferrous sulfate heptahydrate (210 g), concentrated hydrochloric acid (1.0 ml), and *o*-nitrobenzaldehyde (12.0 g, 72.7 mmol) were added to a three-necked two litre round bottom flask. The mixture was stirred and heated under reflux. When the temperature reached 90 °C one portion of concentrated ammonia solution (50 ml) was added, followed by, at two minute intervals, two further portions (2 x 20 ml). Immediately after the addition of the last portion of ammonia solution heating under reflux was discontinued and the product was steam distilled. One 500 ml fraction of distillate was collected on ice (5 °C) and saturated with sodium chloride until precipitation appeared to be complete. The yellow solid was then dried under vacuum. The collected yellow crystalline solid was *o*-aminobenzaldehyde (55) with some dimerised material present.

The yield of *o*-aminobenzaldehyde (55) was 3.843 g (31.7 mmol, 39.6%)
Mp (decomposition) 38 - 40 °C, literature 38 - 40 °C.[2]
^{1}H NMR δ_H($CDCl_3$, 300 MHz) 6.12 (2H, bs, -N**H**$_2$), 6.66 (1H, d, J = 8.3 Hz, -C**H**=CNH$_2$), 6.75 (1H, t, J = 7.4 Hz, -C**H**=CHCCHO), 7.29 - 7.35 (1H, m, -C**H**CH=CNH$_2$), 7.49 (1H, d, J = 7.9 Hz, =C**H**-C-CHO), 9.88 (1H, s, -C**H**O) ppm.
IR ($CDCl_3$ solution) υ_{max} 3504 (N-H (m)), 3363 (N-H (m)), 1668 (CH=O (s)), 1619 (s), 1593 (m), 1557 (m), 1206 (m), 1159 (m) cm^{-1}.
MS m/z (EI) 224.1 (dimer), 121.0 (M^+, 60%), 93.0 ($MH\text{-}CHO^+$, 50%), 77.0 (Ph^+, 62%).

The *o*-aminobenzaldehyde assay (qualitative assay for DHDPS activity)[3]

Standard assay, semi-quantitative

Buffer (200 mM Tris.HCl pH 8.5 at 25 °C, 80 mM pyruvate)	500 µl
o-Aminobenzaldehyde (55) (50 mgml^{-1} in ethanol)	10 µl
Test solution	290 µl
(S)-Aspartate β-semialdehyde (11) (0.01 M) (added last)	200 µl
	1.00 ml

The mixture was incubated 30 °C for 30 minutes, then quenched by the addition of 10% (w/v) trichloroacetic acid (500 µl). *(S)*-Aspartate β-semialdehyde (11) was omitted from the blank; a control containing no enzyme was also included. A deep purple colour indicated the presence of DHDPS activity, in the absence of DHDPS a yellow colour resulted. Semi-quantitative measurements were made by measuring the increase in absorbance of the solution at 540 nm compared to the blank containing no *(S)*-aspartate β-semialdehyde (11).

Mini assay, semi-quantitative

Buffer (200 mM Tris.HCl pH 8.5 at 25 °C, 80 mM pyruvate)	500 µl
o-Aminobenzaldehyde (55) (50 $mgml^{-1}$ in ethanol)	10 µl
Test solution	29 µl
(S)-Aspartate β-semialdehyde (11) (0.01 M) (added last)	20 µl
	559 µl

The mixture was incubated 30 °C for 30 minutes, then quenched by the addition of 10% (w/v) trichloroacetic acid (500 µl). *(S)*-Aspartate β-semialdehyde (11) was omitted from the blank; a control containing no enzyme was also included. A deep purple colour indicated the presence of DHDPS activity, in the absence of DHDPS a yellow colour resulted. Semi-quantitative measurements were made by measuring the increase in absorbance of the solution at 540 nm compared to the blank containing no *(S)*-aspartate β-semialdehyde (11).

Micro assay, qualitative only

Buffer (200 mM Tris.HCl pH 8.5 at 25 °C, 80 mM pyruvate)	10 µl
o-Aminobenzaldehyde (55) (50 $mgml^{-1}$ in ethanol)	0.5 µl
Test solution	5 µl
(S)-Aspartate β-semialdehyde (11) (0.01 M) (added last)	5 µl
	20.5 µl

The mixture was incubated 30 °C for 30 minutes, then quenched by the addition of 10% (w/v) trichloroacetic acid (10 µl). *(S)*-Aspartate β-semialdehyde (11) was omitted from the blank; a control containing no enzyme was also included. A deep purple colour indicated the presence of DHDPS activity, in the absence of DHDPS a yellow colour resulted.

Test of whether dipicolinic acid (36) forms a purple complex with *o*-amino-benzaldehyde (55)

Standard assay

Buffer (200 mM Tris.HCl pH 8.5 at 25 °C, 80 mM pyruvate)	500 µl
o-Aminobenzaldehyde (55) (50 $mgml^{-1}$ in ethanol)	10 µl
Test solution (dipicolinic acid (36) 4.1 mM)	490 µl
	1.00 ml

The mixture was incubated 30 °C for 30 minutes, then quenched by the addition of 10% (w/v) trichloroacetic acid (500 µl). No colour changes were observed after 30 minutes, nor after the addition of 10% trichloroacetic acid (500 µl).

Mixtures of dipicolinic acid (36) (1 mM) and *o*-aminobenzaldehyde (55) (1 mM) (1.00 ml) were tested for the formation of a purple chromophore. Solutions were incubated at 30 °C for minutes. No colour changes were observed after this time nor after the addition of 0.50 ml of 10% trichloroacetic acid.

Dipicolinic acid (1 mM)	*o*-Amino-benzaldehyde (1mM)	Colour	λ_{max} (nm)	Absorbance (blanked against dH_2O)
99%	1%	clear	270	1.47
98%	2%	clear	214 270	0.14 1.43
90%	10%	clear	258	1.54
80%	20%	clear	260 364	1.74 0.21
50%	50%	yellow	264 368	2.23 1.05
20%	80%	yellow	266 370	2.33 2.24
10%	90%	yellow	266 370	2.38 2.56
2%	98%	yellow	266 370	2.39 2.74
1%	99%	yellow	266 368	2.39 2.75

Original quantitative DHDPS/DHDPR coupled assay (from Shedlarski and Gilvarg[4] and modified by Gerrard[5])

To test for DHDPS activity:

NADPH (54 mM in dH_2O)	3 µl
Buffer (1M Tris.HCl pH 8.5 at 25 °C, 80 mM pyruvate (17))	500 µl
dH_2O	337 µl
DHDPS (2.0×10^{-4} U, 4.8×10^{-4} mg)	10 µl
DHDPR (10 fold excess)	100 µl
(S)-ASA (11) (5 mM)	50 µl
	1.00 ml

Enzyme activity: 1 Unit = Δ[NADPH] = 1 $\mu mol \cdot ml^{-1}s^{-1}$

(Using 0.25 mM *(S)*-aspartate β-semialdehyde (11) at 30 °C, pH 7.2.)

The NADPH solution was viscous, requiring it to be added to the buffer and distilled water with vigorous mixing. The reaction was initiated in the cuvette by addition of freshly prepared *(S)*-aspartate β-semialdehyde (11), mixed by inversion of the cuvettte. ΔA_{340} was measured over 300 seconds at 30 °C, blanked against dH_2O. The control experiment contained no aspartate β-semialdehyde (11).

To test for DHDPR activity:

NADPH (54 mM in dH_2O)	3 µl
Buffer (1M Tris.HCl pH 8.5 at 25 °C, 80 mM pyruvate (17))	500 µl
dH_2O	337 µl
DHDPS (10 fold excess)	100 µl
(S)-ASA (11) (5 mM)	50 µl
DHDPR (2.25×10^{-4} U, 1.0×10^{-4} mg)	10 µl
	1.00 ml

Enzyme activity: 1 Unit (U) = Δ[NADPH] = 1 $\mu mol \cdot ml^{-1}s^{-1}$
(Using 0.25 mM *(S)*-aspartate β-semialdehyde (11), which converts to dihydrodipicolinate (18), at 30 °C, pH 7.2.)

The NADPH solution was viscous, requiring it to be added to the buffer and distilled water with vigorous mixing. The *(S)*-aspartate β-semialdehyde was added prior to initiation of the reaction to form the substrate. The reaction was then initiated in the cuvette by addition of DHDPR, mixed by inversion of the cuvettte. ΔA_{340} was measured over 300 seconds at 30 °C, blanked against dH_2O. The control experiment contained no aspartate β-semialdehyde (11).

During purification of the DHDPR the coupled assay was used to assess which fractions were active, thus containing DHDPR. This, at times, involved altering the volumes of reagents used, such as increasing the volume of DHDPR solution used.

Enzyme kinetics

Major sources

A. Cornish-Bowden *Biochem. J.* **137**, 143 (1974).

A. Cornish-Bowden, C.W. Wharton *'Enzyme Kinetics'* IRL Press, Oxford (1988).

M. Dixon *Biochem. J.* **55**, 170 (1953)

M. Dixon, E.C. Webb *'Enzymes'* 3rd edn, Academic Press (1979).

R. Eisenthal, M.J. Danson (Eds) *'Enzyme Assays. A practical approach'* IRL Press, Oxford (1992).

In the kinetic readings an outlier is denoted by an asterisk (*), and is then excluded from the calculations of K_m and V_{max}.

Buffer dependence of the coupled assay

Buffer	pK_a at 25 °C	buffering region[6]
Tris Tris(hydroxymethyl)methylamine	8.1	7.0 - 9.2
Hepes *N*-2-hydroxyethylpiperazine-*N'*-2-ethane-sulfonic acid	7.5	6.8 - 8.2
Mops 3-(*N*-Morpholino)propanesulfonic acid	7.2	6.4 - 7.9
Bis-Tris Bis(2-hydroxyethyl)iminotris(hydroxymethyl)methane	6.5	5.8 - 7.2
Mes 2-(*N*-Morpholino)ethanesulfonic acid	6.2 (20 °C)	5.5 - 6.8

Assay:

NADPH (54 mM in dH_2O)	3.0 µl
Buffer (200 mM buffer, pyruvate (17) 80 mM)	500 µl
dH_2O	337 µl
DHDPS (2.0×10^{-4} U, 4.8×10^{-4} mg)	10 µl
DHDPR (10 fold excess)	100 µl
(R,S)-ASA (11) (10.0 mM to 2.6 mM in dH_2O)	50 µl
	1.00 ml

The reaction was initiated in the cuvette by addition of freshly prepared *(S)*-aspartate β-semialdehyde (11), mixed by inversion of the cuvettte. ΔA_{340} was measured over 300 seconds at 30 °C, blanked against dH_2O.

DHDPS kinetics using 200 mM Tris pH 7.5 at 25 °C

[(*R,S*)-ASA] M x 10^{-4}	1/[(*R,S*)-ASA] M^{-1} x 10^{3}	Rate $\mu mol \cdot s^{-1} mg^{-1}$ x 10^{-1}	1/Rate $mg \cdot s \cdot \mu mol^{-1}$
5.00	2.00	2.00	4.99
5.00	2.00	2.75	3.64
2.50	4.00	2.17	4.60
2.50	4.00	1.88	5.31
1.70	5.88	1.84	5.44
1.70	5.88	1.94	5.15
1.30	7.69	1.82	5.50
1.30	7.69	1.77	5.64

V_{max} and K_m could not be estimated.

DHDPS kinetics using 200 mM Mops pH 7.5 at 25 °C

[(*R,S*)-ASA] M x 10^{-4}	1/[(*R,S*)-ASA] M^{-1} x 10^{3}	Rate $\mu mol \cdot s^{-1} mg^{-1}$ x 10^{-1}	1/Rate $mg \cdot s \cdot \mu mol^{-1}$
5.00	2.00	5.00	2.00
5.00	2.00	5.83	1.72
2.50	4.00	3.75	2.67
2.50	4.00	4.68	2.14
1.70	5.88	2.82	3.55
1.70	5.88	2.47	4.05
1.30	7.69	2.20	4.54
1.30	7.69	2.55	3.92

Lineweaver-Burk plot $V_{max} = 11.4 \times 10^{-1}$ $\mu mol \cdot s^{-1} mg^{-1}$ $K_m = 5.11 \times 10^{-4}$ M

DHDPS kinetics using 200 mM Mops pH 7.4 at 25 °C

[*(R,S)*-ASA] M x 10^{-4}	1/[*(R,S)*-ASA] M^{-1} x 10^{3}	Rate $\mu mol \cdot s^{-1} mg^{-1}$ x 10^{-1}	1/Rate $mg \cdot s \cdot \mu mol^{-1}$
5.00	2.00	4.66	2.14
5.00	2.00	5.55	1.80
2.50	4.00	3.33	3.00
2.50	4.00	3.61	2.77
1.70	5.88	3.00	3.33
1.70	5.88	2.92	3.42
1.30	7.69	2.39	4.18
1.30	7.69	2.58	3.88

Lineweaver-Burk plot V_{max} = 7.46 x 10^{-1} $\mu mol \cdot s^{-1} mg^{-1}$ K_m = 2.63 x 10^{-4} M

DHDPS kinetics using 200 mM Mops pH 7.3 at 25 °C

[*(R,S)*-ASA] M x 10^{-4}	1/[*(R,S)*-ASA] M^{-1} x 10^{3}	Rate $\mu mol \cdot s^{-1} mg^{-1}$ x 10^{-1}	1/Rate $mg \cdot s \cdot \mu mol^{-1}$
5.00	2.00	4.20	2.38
5.00	2.00	4.87	2.05
2.50	4.00	3.18	3.14
2.50	4.00	3.41	2.93
1.70	5.88	2.78	3.59
1.70	5.88	2.68	3.74
1.30	7.69	2.25	4.45
1.30	7.69	2.22	4.51

Lineweaver-Burk plot V_{max} = 6.98 x 10^{-1} $\mu mol \cdot s^{-1} mg^{-1}$ K_m = 2.73 x 10^{-4} M

DHDPS kinetics using 200 mM Mops pH 7.2 at 25 °C

[(*R,S*)-ASA] M x 10^{-4}	1/[(*R,S*)-ASA] M^{-1} x 10^{3}	Rate $\mu mol \cdot s^{-1} mg^{-1}$ x 10^{-1}	1/Rate $mg \cdot s \cdot \mu mol^{-1}$
5.00	2.00	4.28	2.34
5.00	2.00	4.29	2.33
2.50	4.00	3.42	2.93
2.50	4.00	4.33	2.31
1.70	5.88	2.86	3.50
1.70	5.88	2.45	4.08
1.30	7.69	1.60	6.24
1.30	7.69	1.44	6.93

Lineweaver-Burk plot $V_{max} = 3.67 \times 10^{-1}$ $\mu mol \cdot s^{-1} mg^{-1}$ $K_m = 2.67 \times 10^{-4}$ M

DHDPS kinetics using 200 mM Mops pH 7.1 at 25 °C

[(*R,S*)-ASA] M x 10^{-4}	1/[(*R,S*)-ASA] M^{-1} x 10^{3}	Rate $\mu mol \cdot s^{-1} mg^{-1}$ x 10^{-1}	1/Rate $mg \cdot s \cdot \mu mol^{-1}$
5.00	2.00	3.52	2.84
5.00	2.00	3.90	2.57
2.50	4.00	3.02	3.31
2.50	4.00	2.94	3.41
1.70	5.88	2.38	4.20
1.70	5.88	2.46	4.06
1.30	7.69	2.19	4.56
1.30	7.69	2.17	4.61

Lineweaver-Burk plot $V_{max} = 4.91 \times 10^{-1}$ $\mu mol \cdot s^{-1} mg^{-1}$ $K_m = 1.66 \times 10^{-4}$ M

DHDPS kinetics using 200 mM Mops pH 7.0 at 25 °C

[(*R,S*)-ASA] M x 10^{-4}	1/[(*R,S*)-ASA] M^{-1} x 10^{3}	Rate $\mu mol \cdot s^{-1} mg^{-1}$ x 10^{-1}	1/Rate $mg \cdot s \cdot \mu mol^{-1}$
5.00	2.00	3.05	3.28
5.00	2.00	2.43	4.12
2.50	4.00	2.62	3.82
2.50	4.00	2.12	4.72
1.70	5.88	2.01	4.97
1.70	5.88	1.99	5.02
1.30	7.69	1.62	6.19
1.30	7.69	1.52	6.56

Lineweaver-Burk plot V_{max} = 3.87 x 10^{-1} $\mu mol \cdot s^{-1} mg^{-1}$ K_m = 1.78 x 10^{-4} M

DHDPS kinetics using 200 mM Mops pH 6.9 at 25 °C

[(*R,S*)-ASA] M x 10^{-4}	1/[(*R,S*)-ASA] M^{-1} x 10^{3}	Rate $\mu mol \cdot s^{-1} mg^{-1}$ x 10^{-1}	1/Rate $mg \cdot s \cdot \mu mol^{-1}$
5.00	2.00	2.15	4.64
5.00	2.00	2.58	3.87
2.50	4.00	2.19	4.56
2.50	4.00	1.84	5.44
1.70	5.88	1.64	6.09
1.70	5.88	1.67	6.00
1.30	7.69	1.48	6.76
1.30	7.69	1.53	6.56

Lineweaver-Burk plot V_{max} = 2.98 x 10^{-1} $\mu mol \cdot s^{-1} mg^{-1}$ K_m = 1.30 x 10^{-4} M

DHDPS kinetics using 200 mM Mops pH 6.8 at 25 °C

[(*R,S*)-ASA] M x 10^{-4}	1/[(*R,S*)-ASA] M^{-1} x 10^{3}	Rate $\mu mol \cdot s^{-1} mg^{-1}$ x 10^{-1}	1/Rate $mg \cdot s \cdot \mu mol^{-1}$
5.00	2.00	1.68	5.95
5.00	2.00	1.90	5.26
2.50	4.00	1.65	6.06
2.50	4.00	1.58	6.33
1.70	5.88	1.28	7.82
1.70	5.88	1.38	7.26
1.30	7.69	1.24	8.05
1.30	7.69	1.16	8.60

Lineweaver-Burk plot V_{max} = 2.33 x 10^{-1} $\mu mol \cdot s^{-1} mg^{-1}$ K_m = 1.18 x 10^{-4} M

Enzyme kinetics of DHDPS

Kinetics of DHDPS with respect to* (S)-*aspartate β-semialdehyde (11)

Assay:

NADPH (54 mM in dH_2O)	3.0 µl
Buffer (200 mM Mops pH 7.2 at 25 °C, pyruvate (17) 80 mM)	500 µl
dH_2O	337 µl
DHDPS (2.0 x 10^{-4} U, 4.8 x 10^{-4} mg)	10 µl
DHDPR (10 fold excess)	100 µl
(S)-ASA (11) (5.0 mM to 1.2 mM in dH_2O)	50 µl
	1.00 ml

The reaction was initiated in the cuvette by addition of freshly prepared *(S)*-aspartate β-semialdehyde (11), mixed by inversion of the cuvettte. ΔA_{340} was measured over 300 seconds at 30 °C, blanked against dH_2O.

Run 1:

[(*S*)-ASA] M x 10^{-4}	1/[(*S*)-ASA] M^{-1} x 10^{3}	Rate $\mu mol \cdot s^{-1} mg^{-1}$ x 10^{-1}	1/Rate $mg \cdot s \cdot \mu mol^{-1}$	Rate/[(*S*)-ASA] $l \cdot s^{-1} mg^{-1}$ x 10^{-3}
2.50	4.00	4.17	2.40	1.67
2.50	4.00	4.71	2.12	1.88
1.50	6.67	3.86	2.59	2.57
1.50	6.67	2.50	4.00	1.67
1.00	10.0	3.03	3.30	3.03
1.00	10.0	2.91	3.44	2.91
0.80	12.5	2.52	3.97	3.15
0.80	12.5	2.55	3.92	3.19
0.60	16.7	2.06	4.85	3.44
0.60	16.7	2.10	4.76	3.51

Lineweaver-Burk plot V_{max} = 5.85 x 10^{-1} $\mu mol \cdot s^{-1} mg^{-1}$ K_m = 1.07 x 10^{-4} M
Eadie-Hofstee plot V_{max} = 5.42 x 10^{-1} $\mu mol \cdot s^{-1} mg^{-1}$ K_m = 0.882 x 10^{-4} M
Direct linear plot V_{max} = 6.92 x 10^{-1} $\mu mol \cdot s^{-1} mg^{-1}$ K_m = 1.40 x 10^{-4} M

Run 2:

[(*S*)-ASA] M x 10^{-4}	1/[(*S*)-ASA] M^{-1} x 10^{3}	Rate $\mu mol \cdot s^{-1} mg^{-1}$ x 10^{-1}	1/Rate $mg \cdot s \cdot \mu mol^{-1}$	Rate/[(*S*)-ASA] $l \cdot s^{-1} mg^{-1}$ x 10^{-3}
2.50	4.00	4.16	2.40	1.66
2.50	4.00	5.14	1.95	2.06
1.50	6.67	4.33	2.31	2.89
1.50	6.67	4.31	2.32	2.87
1.00	10.0	2.78	3.62	2.78
1.00	10.0	3.28	3.04	3.28
0.80	12.5	2.74	3.65	3.42
0.80	12.5	2.53	3.95	3.16
0.60	16.7	2.31	4.33	3.86
0.60	16.7	2.47	4.05	4.12

Lineweaver-Burk plot V_{max} = 7.08 x 10^{-1} $\mu mol \cdot s^{-1} mg^{-1}$ K_m = 1.24 x 10^{-4} M
Eadie-Hofstee plot V_{max} = 6.50 x 10^{-1} $\mu mol \cdot s^{-1} mg^{-1}$ K_m = 1.03 x 10^{-4} M
Direct linear plot V_{max} = 7.23 x 10^{-1} $\mu mol \cdot s^{-1} mg^{-1}$ K_m = 1.38 x 10^{-4} M

Kinetics of DHDPS with respect to pyruvate (17)

Assay:

NADPH (54 mM in dH_2O)	3.0 µl
Buffer (200 mM Mops pH 7.2 at 25 °C)	500 µl
dH_2O	87 µl
DHDPS (2.0×10^{-4} U, 4.8×10^{-4} mg)	10 µl
DHDPR (10 fold excess)	100 µl
Pyruvate (17) (2.0 mM to 0.20 mM in dH_2O)	250 µl
(S)-ASA (11) (50 mM in dH_2O)	50 µl
	1.00 ml

The reaction was initiated in the cuvette by addition of freshly prepared *(S)*-aspartate β-semialdehyde (11), mixed by inversion of the cuvettte. ΔA_{340} was measured over 300 seconds at 30 °C, blanked against dH_2O.

Run 1:

[Pyruvate] M x 10^{-4}	1/[Pyruvate] M^{-1} x 10^{3}	Rate $\mu mol \cdot s^{-1} mg^{-1}$ x 10^{-1}	1/Rate $mg \cdot s \cdot \mu mol^{-1}$	Rate/[Pyruvate] $l \cdot s^{-1} mg^{-1}$ x 10^{-3}
5.00	2.00	3.41	2.93	0.682
5.00	2.00	3.62	2.76	0.724
1.25	8.00	1.99	5.03	1.59
1.25	8.00	2.02	4.95	1.61
0.70	14.3	1.32	7.58	1.89
0.70	14.3	1.56	6.41	2.23
0.50	20.0	0.795	12.6	1.59
0.50	20.0	1.11	9.01	2.22

Lineweaver-Burk plot	$V_{max} = 5.99 \times 10^{-1}$ µmol·s^{-1}mg^{-1} $K_m = 2.56 \times 10^{-4}$ M
Eadie-Hofstee plot	$V_{max} = 4.35 \times 10^{-1}$ µmol·s^{-1}mg^{-1} $K_m = 1.51 \times 10^{-4}$ M
Direct linear plot	$V_{max} = 4.59 \times 10^{-1}$ µmol·s^{-1}mg^{-1} $K_m = 1.53 \times 10^{-4}$ M

Run 2:

[Pyruvate] M x 10^{-4}	1/[Pyruvate] M^{-1} x 10^{3}	Rate $\mu mol \cdot s^{-1} mg^{-1}$ x 10^{-1}	1/Rate $mg \cdot s \cdot \mu mol^{-1}$	Rate/[Pyruvate] $l \cdot s^{-1} mg^{-1}$ x 10^{-3}
5.00	2.00	3.80	2.63	0.760
5.00	2.00	4.86	2.06	0.972
1.25	8.00	1.97	5.08	1.58
1.25	8.00	2.70	3.70	2.16
0.70	14.3	1.97	5.08	2.82
0.70	14.3	1.72	5.81	2.46
0.50	20.0	1.33	7.52	2.66
0.50	20.0	1.65	6.06	3.30

Lineweaver-Burk plot V_{max} = 4.76 x 10^{-1} $\mu mol \cdot s^{-1} mg^{-1}$ K_m = 1.14 x 10^{-4} M

Eadie-Hofstee plot V_{max} = 4.85 x 10^{-1} $\mu mol \cdot s^{-1} mg^{-1}$ K_m = 1.12 x 10^{-4} M

Direct linear plot V_{max} = 5.49 x 10^{-1} $\mu mol \cdot s^{-1} mg^{-1}$ K_m = 1.34 x 10^{-4} M

Effect of high* (S)-*aspartate β-semialdehyde (11) concentration on DHDPS kinetics

Assay:

NADPH (54 mM in dH_2O)	3.0 µl
Buffer (200 mM Mops pH 7.2 at 25 °C)	500 µl
dH_2O	237 µl
DHDPS (2.0 x 10^{-4} U, 4.8 x 10^{-4} mg)	10 µl
DHDPR (10 fold excess)	100 µl
(S)-ASA (11) (200 mM to 2.5 mM in dH_2O)	50 µl
Pyruvate (17) (400 mM to 12.5 mM in dH_2O)	150 µl
	1.00 ml

The reaction was initiated in the cuvette by addition of freshly prepared *(S)*-aspartate β-semialdehyde (11), mixed by inversion of the cuvettte. ΔA_{340} was measured over 300 seconds at 30 °C, blanked against dH_2O.

Run 1:

[Pyruvate (17)] = 40 mM

[*(S)*-ASA] M x 10^{-3}	Rate $\mu mol \cdot s^{-1} mg^{-1}$ x 10^{-1}
0.25	4.85
0.25	4.21
0.50	6.38
0.50	7.39
0.75	6.14
0.75	6.50
1.00	7.27
1.00	8.01
1.25	6.76
1.25	8.85
1.50	8.21
1.50	8.05

Run 2:

[Pyruvate (17)] = 5.0 mM

[*(S)*-ASA] M x 10^{-3}	Rate $\mu mol \cdot s^{-1} mg^{-1}$ x 10^{-1}
1.00	6.27
1.00	4.54
1.50	6.82
1.50	6.27
2.00	7.66
2.00	5.46
2.50	6.58
2.50	7.46

Run 3:

[Pyruvate (17)] = 10.0 mM

[*(S)*-ASA] M x 10^{-3}	Rate $\mu mol \cdot s^{-1} mg^{-1}$ x 10^{-1}
1.00	7.89
1.00	6.65
1.50	7.78
1.50	6.81
2.00	7.53
2.00	7.01
2.50	7.68

Run 4:

[Pyruvate (17)] = 1.25 mM

[*(S)*-ASA] M x 10^{-3}	Rate $\mu mol \cdot s^{-1} mg^{-1}$ x 10^{-1}
0.125	2.72
0.125	2.39
0.250	2.61
0.250	2.56
0.500	2.84
0.500	3.91
1.00	4.13
1.00	4.62
1.50	4.14
1.50	3.93
2.00	4.42
2.00	4.22

Run 5:

[Pyruvate (17)] = 1.25 mM

[*(S)*-ASA] M x 10^{-3}	Rate $\mu mol \cdot s^{-1} mg^{-1}$ x 10^{-1}
1.00	4.56
1.00	4.96
2.50	8.17
2.50	10.0
5.00	11.4
6.00	11.6
10.0	9.92
10.0	12.1

Effect of* (S)*-lysine (12) on DHDPS kinetics with respect to* (S)*-aspartate β-semialdehyde (11)

Assay:

NADPH (54 mM in dH_2O)	3.0 µl
Buffer (200 mM Mops pH 7.2 at 25 °C, pyruvate (17) 80 mM)	500 µl
dH_2O	237 µl
DHDPS (2.0 x 10^{-4} U, 4.8 x 10^{-4} mg)	10 µl
DHDPR (10 fold excess)	100 µl
(S)-ASA (11) (5.0 mM to 1.3 mM in dH_2O)	50 µl
(S)-Lysine (12) (10.0 mM to 1.0 mM in dH_2O)	100 µl
	1.00 ml

The reaction was initiated in the cuvette by addition of freshly prepared *(S)*-aspartate β-semialdehyde (11), mixed by inversion of the cuvettte. ΔA_{340} was measured over 300 seconds at 30 °C, blanked against dH_2O.

Run 1:

[*(S)*-Lysine (12)] = 0 mM

[*(S)*-ASA] M x 10^{-4}	1/[*(S)*-ASA] M^{-1} x 10^{3}	Rate $\mu mol \cdot s^{-1} mg^{-1}$ x 10^{-1}	1/Rate $mg \cdot s \cdot \mu mol^{-1}$
2.50	4.00	4.04	2.48
2.50	4.00	4.19	2.39
1.25	8.00	4.13	2.42
1.25	8.00	4.30	2.32
0.85	11.8	3.35	2.98
0.85	11.8	3.59	2.79
0.65	15.4	2.70	3.70
0.65	15.4	2.80	3.60

Lineweaver-Burk plot V_{max} = 5.64 x 10^{-1} $\mu mol \cdot s^{-1} mg^{-1}$ K_m = 1.64 x 10^{-4} M

[*(S)*-Lysine (12)] = 0.10 mM

[*(S)*-ASA] M x 10^{-4}	1/[*(S)*-ASA] M^{-1} x 10^{3}	Rate $\mu mol \cdot s^{-1} mg^{-1}$ x 10^{-1}	1/Rate $mg \cdot s \cdot \mu mol^{-1}$
2.50	4.00	5.46	1.83
2.50	4.00	5.07	1.97
1.25	8.00	4.37	2.29
1.25	8.00	4.46	2.24
0.85	11.8	3.45	2.90
0.85	11.8	3.43	2.91
0.65	15.4	2.97	3.36
0.65	15.4	2.98	3.36

Lineweaver-Burk plot V_{max} = 7.61 x 10^{-1} $\mu mol \cdot s^{-1} mg^{-1}$ K_m = 0.997 x 10^{-4} M

[*(S)*-Lysine (12)] = 0.50 mM

[*(S)*-ASA] M x 10^{-4}	1/[*(S)*-ASA] M^{-1} x 10^{3}	Rate $\mu mol \cdot s^{-1} mg^{-1}$ x 10^{-1}	1/Rate $mg \cdot s \cdot \mu mol^{-1}$
2.50	4.00	3.00	3.33
2.50	4.00	3.01	3.32
1.25	8.00	2.44	4.10
1.25	8.00	2.49	4.02
0.85	11.8	1.73	5.76
0.85	11.8	1.83	5.45
0.65	15.4	1.18	8.44
0.65	15.4	1.40	7.14

Lineweaver-Burk plot V_{max} = 7.33 x 10^{-1} $\mu mol \cdot s^{-1} mg^{-1}$ K_m = 2.87 x 10^{-4} M

[*(S)*-Lysine (12)] = 1.0 mM

[*(S)*-ASA] M x 10^{-4}	1/[*(S)*-ASA] M^{-1} x 10^{3}	Rate $\mu mol \cdot s^{-1} mg^{-1}$ x 10^{-1}	1/Rate $mg \cdot s \cdot \mu mol^{-1}$
2.50	4.00	1.82	5.51
2.50	4.00	1.24	8.08
1.25	8.00	1.10	9.11
1.25	8.00	1.36	7.33
0.85	11.8	0.904	11.1
0.85	11.8	1.02	9.81
0.65	15.4	0.903	11.1
0.65	15.4	0.987	10.1

Lineweaver-Burk plot V_{max} = 1.82 x 10^{-1} $\mu mol \cdot s^{-1} mg^{-1}$ K_m = 0.658 x 10^{-4} M

Determination of K_i:

[(*S*)-ASA] M x 10^{-4}	[(*S*)-Lysine] M x 10^{-3}	1/Rate mg·s·μmol^{-1}		[(*S*)-ASA]/Rate s·mg·l^{-1} x 10^{2}	
2.50	0	2.48	2.39	6.20	5.98
2.50	0.10	1.83	1.97	4.58	4.93
2.50	0.50	3.33	3.32	8.33	8.30
2.50	1.0	5.51	8.08	13.8	20.2
1.25	0	2.42	2.32	3.03	2.90
1.25	0.10	2.29	2.24	2.86	2.80
1.25	0.50	4.10	4.02	5.13	5.03
1.25	1.0	9.11	7.33	11.4	9.16
0.85	0	2.98	2.79	2.53	2.37
0.85	0.10	2.90	2.91	2.47	2.47
0.85	0.50	5.76	5.45	4.90	4.63
0.85	1.0	11.1	9.81	9.44	8.34
0.65	0	3.70	3.60	2.41	2.34
0.65	0.10	12.1	7.71	2.18	2.18
0.65	0.50	8.44	7.14	5.49	4.64
0.65	1.0	11.1	10.1	7.22	6.57

Uncompetitive or mixed inhibition.

Assuming uncompetitive inhibition:

K_i' (Modified Dixon) 3.25 x 10^{-4} M

3.37 x 10^{-4} M

Assuming mixed inhibition:

K_i (Dixon) 1.90 x 10^{-4} M K_i' (Modified Dixon) 4.85 x 10^{-4} M

2.97 x 10^{-4} M 5.20 x 10^{-4} M

Run 2:

[(*S*)-Lysine (12)] = 0 mM

[(*S*)-ASA] M x 10^{-4}	1/[(*S*)-ASA] M^{-1} x 10^{3}	Rate $\mu mol \cdot s^{-1} mg^{-1}$ x 10^{-1}	1/Rate $mg \cdot s \cdot \mu mol^{-1}$
2.50	4.00	4.86	2.08
2.50	4.00	4.22	2.37
1.25	8.00	4.13	2.42
1.25	8.00	4.55	2.20
0.85	11.8	1.73	5.80
0.85	11.8	3.77	2.66
0.65	15.4	2.87	3.49
0.65	15.4	3.15	3.18

Lineweaver-Burk plot V_{max} = 6.03 x 10^{-1} $\mu mol \cdot s^{-1} mg^{-1}$ K_m = 1.19 x 10^{-4} M

[(*S*)-Lysine(12)] = 0.25 mM

[(*S*)-ASA] M x 10^{-4}	1/[(*S*)-ASA] M^{-1} x 10^{3}	Rate $\mu mol \cdot s^{-1} mg^{-1}$ x 10^{-1}	1/Rate $mg \cdot s \cdot \mu mol^{-1}$
2.50	4.00	4.42	2.26
2.50	4.00	4.68	2.14
1.25	8.00	3.23	3.10
1.25	8.00	1.54	6.51
0.85	11.8	2.99	3.34
0.85	11.8	2.98	3.36
0.65	15.4	2.34	4.28
0.65	15.4	1.94	5.16

Lineweaver-Burk plot V_{max} = 4.59 x 10^{-1} $\mu mol \cdot s^{-1} mg^{-1}$ K_m = 1.34 x 10^{-4} M

[*(S)*-Lysine (12)] = 0.50 mM

[*(S)*-ASA] M x 10^{-4}	1/[*(S)*-ASA] M^{-1} x 10^{3}	Rate $\mu mol \cdot s^{-1} mg^{-1}$ x 10^{-1}	1/Rate $mg \cdot s \cdot \mu mol^{-1}$
2.50	4.00	2.87	3.48
2.50	4.00	1.43*	6.99*
1.25	8.00	2.06	4.86
1.25	8.00	2.17	4.61
0.85	11.8	1.85	5.41
0.85	11.8	1.77	5.64
0.65	15.4	1.52	6.59
0.65	15.4	1.66	6.04

Lineweaver-Burk plot V_{max} = 3.70 x 10^{-1} $\mu mol \cdot s^{-1} mg^{-1}$ K_m = 1.13 x 10^{-4} M

[*(S)*-Lysine (12)] = 0.75 mM

[*(S)*-ASA] M x 10^{-4}	1/[*(S)*-ASA] M^{-1} x 10^{3}	Rate $\mu mol \cdot s^{-1} mg^{-1}$ x 10^{-1}	1/Rate $mg \cdot s \cdot \mu mol^{-1}$
2.50	4.00	2.36	4.24
2.50	4.00	2.03	4.93
1.25	8.00	1.62	6.19
1.25	8.00	1.75	5.71
0.85	11.8	1.40	7.15
0.85	11.8	1.43	7.01
0.65	15.4	1.19	8.40
0.65	15.4	1.14	8.78

Lineweaver-Burk plot V_{max} = 3.16 x 10^{-1} $\mu mol \cdot s^{-1} mg^{-1}$ K_m = 0.916 x 10^{-4} M

Determination of K_i:

[(*S*)-ASA] M x 10^{-4}	[(*S*)-Lysine] M x 10^{-3}	1/Rate mg·s·µmol^{-1}		[(*S*)-ASA]/Rate s·mg·l^{-1} x 10^{2}	
2.50	0	2.08	2.37	5.20	5.93
2.50	0.25	2.26	2.14	5.65	5.35
2.50	0.50	3.48	6.99*	8.70	1.75*
2.50	0.75	4.24	4.93	10.6	1.23
1.25	0	2.42	2.20	3.03	2.75
1.25	0.25	3.10	6.51	3.88	8.14
1.25	0.50	4.86	4.61	6.08	5.76
1.25	0.75	6.19	5.71	7.74	7.14
0.85	0	5.80	2.66	4.93	2.26
0.85	0.25	3.34	3.36	2.84	2.86
0.85	0.50	5.41	5.64	4.60	4.79
0.85	0.75	7.15	7.01	6.08	5.96
0.65	0	3.49	3.18	2.27	2.07
0.65	0.25	4.28	5.16	2.78	3.35
0.65	0.50	6.59	6.04	4.28	3.93
0.65	0.75	8.40	8.78	5.46	5.71

Uncompetitive inhibition:

K_i' (Modified Dixon) 3.43 x 10^{-4} M

3.73 x 10^{-4} M

3.91 x 10^{-4} M

Effect of* (S)-*lysine (12) on DHDPS kinetics with respect to pyruvate (17)

Assay:

NADPH (54 mM in dH_2O)	3.0 µl
Buffer (200 mM Mops pH 7.2 at 25 °C)	500 µl
dH_2O	12 µl
DHDPS (2.0 x 10^{-4} U, 4.8 x 10^{-4} mg)	10 µl
DHDPR (10 fold excess)	100 µl
Pyruvate (17) (2.0 mM to 0.20 mM in dH_2O)	250 µl
(S)-ASA (11) (50 mM in dH_2O)	50 µl
(S)-Lysine (12) (10 mM to 3.33 mM in dH_2O)	75 µl
	1.00 ml

The reaction was initiated in the cuvette by addition of freshly prepared *(S)*-aspartate β-semialdehyde (11), mixed by inversion of the cuvettte. ΔA_{340} was measured over 300 seconds at 30 °C, blanked against dH_2O.

Run 1:

[*(S)*-Lysine (12)] = 0 mM

[Pyruvate] M x 10^{-4}	1/[Pyruvate] M^{-1} x 10^{3}	Rate $\mu mol \cdot s^{-1} mg^{-1}$ x 10^{-1}	1/Rate $mg \cdot s \cdot \mu mol^{-1}$
5.00	2.00	5.31	1.88
5.00	2.00	6.74	1.48
1.25	8.00	3.12	3.20
1.25	8.00	3.30	3.03
0.70	14.3	1.94	5.16
0.70	14.3	1.98	5.06
0.50	20.0	1.44	6.96
0.50	20.0	1.67	5.99

Lineweaver-Burk plot V_{max} = 9.23 x 10^{-1} $\mu mol \cdot s^{-1} mg^{-1}$ K_m = 2.51 x 10^{-4} M

[*(S)*-Lysine (12)] = 0.25 mM

[Pyruvate] M x 10^{-4}	1/[Pyruvate] M^{-1} x 10^{3}	Rate $\mu mol \cdot s^{-1} mg^{-1}$ x 10^{-1}	1/Rate $mg \cdot s \cdot \mu mol^{-1}$
5.00	2.00	4.50	2.22
5.00	2.00	5.34	1.87
1.25	8.00	2.86	3.49
1.25	8.00	2.64	3.79
0.70	14.3	2.02	4.96
0.70	14.3	2.08	4.81
0.50	20.0	1.67	6.00
0.50	20.0	1.56	6.42

Lineweaver-Burk plot V_{max} = 5.98 x 10^{-1} $\mu mol \cdot s^{-1} mg^{-1}$ K_m = 1.36 x 10^{-4} M

[*(S)*-Lysine (12)] = 0.50 mM

[Pyruvate] M x 10^{-4}	1/[Pyruvate] M^{-1} x 10^{3}	Rate $\mu mol \cdot s^{-1} mg^{-1}$ x 10^{-1}	1/Rate $mg \cdot s \cdot \mu mol^{-1}$
5.00	2.00	4.07	2.45
5.00	2.00	3.77	2.65
1.25	8.00	2.82	3.55
1.25	8.00	2.30	4.35
0.70	14.3	1.75	5.71
0.70	14.3	1.75	5.72
0.50	20.0	1.54	6.48
0.50	20.0	1.46	6.85

Lineweaver-Burk plot $V_{max} = 4.71 \times 10^{-1}$ $\mu mol \cdot s^{-1} mg^{-1}$ $K_m = 0.906 \times 10^{-4}$ M

[*(S)*-Lysine (12)] = 0.75 mM

[Pyruvate] M x 10^{-4}	1/[Pyruvate] M^{-1} x 10^{3}	Rate $\mu mol \cdot s^{-1} mg^{-1}$ x 10^{-1}	1/Rate $mg \cdot s \cdot \mu mol^{-1}$
5.00	2.00	3.33	3.00
5.00	2.00	2.84	3.53
1.25	8.00	2.35	4.26
1.25	8.00	2.46	4.06
0.70	14.3	1.74	5.76
0.70	14.3	1.51	6.60
0.50	20.0	1.48	6.78
0.50	20.0	1.48	6.78

Lineweaver-Burk plot $V_{max} = 3.60 \times 10^{-1}$ $\mu mol \cdot s^{-1} mg^{-1}$ $K_m = 0.752 \times 10^{-4}$ M

Determination of K_i:

[Pyruvate] M x 10^{-4}	[*(S)*-Lysine] M x 10^{-3}	1/Rate mg·s·µmol^{-1}		[*(S)*-ASA]/Rate s·mg·l^{-1} x 10^{2}	
5.00	0	1.88	1.48	9.40	7.40
5.00	0.25	2.22	1.87	11.1	9.35
5.00	0.50	2.45	2.65	12.3	13.3
5.00	0.75	3.00	3.53	15.0	17.7
1.25	0	3.20	3.03	4.00	3.79
1.25	0.25	3.49	3.79	4.36	4.74
1.25	0.50	3.55	4.35	4.44	5.44
1.25	0.75	4.26	4.06	5.33	5.08
0.70	0	5.16	5.06	3.61	3.54
0.70	0.25	4.96	4.81	3.47	3.37
0.70	0.50	5.71	5.72	4.00	4.00
0.70	0.75	5.76	6.60	4.03	4.62
0.50	0	6.96	5.99	3.48	3.00
0.50	0.25	6.00	6.42	3.00	3.21
0.50	0.50	6.48	6.85	3.24	3.43
0.50	0.75	6.78	6.78	3.39	3.39

Uncompetitive inhibition:

K_i' (Modified Dixon) 4.50×10^{-4} M

4.68×10^{-4} M

4.85×10^{-4} M

5.73×10^{-4} M

Run 2:

[*(S)*-Lysine (12)] = 0 mM

[Pyruvate] M x 10^{-4}	1/[Pyruvate] M^{-1} x 10^{3}	Rate $\mu mol \cdot s^{-1} mg^{-1}$ x 10^{-1}	1/Rate $mg \cdot s \cdot \mu mol^{-1}$
5.00	2.00	4.17	2.40
5.00	2.00	5.64	1.77
1.25	8.00	3.66	2.73
1.25	8.00	3.68	2.72
0.70	14.3	2.32	4.32
0.70	14.3	2.51	3.99
0.50	20.0	1.93	5.19
0.50	20.0	1.82	5.49

Lineweaver-Burk plot V_{max} = 6.58 x 10^{-1} $\mu mol \cdot s^{-1} mg^{-1}$ K_m = 1.22 x 10^{-4} M

[*(S)*-Lysine (12)] = 0.25 mM

[Pyruvate] M x 10^{-4}	1/[Pyruvate] M^{-1} x 10^{3}	Rate $\mu mol \cdot s^{-1} mg^{-1}$ x 10^{-1}	1/Rate $mg \cdot s \cdot \mu mol^{-1}$
5.00	2.00	4.60	2.17
5.00	2.00	5.33	1.88
1.25	8.00	2.75	3.64
1.25	8.00	3.05	3.28
0.70	14.3	2.36	4.23
0.70	14.3	2.03	4.94
0.50	20.0	1.69	5.90
0.50	20.0	1.63	6.15

Lineweaver-Burk plot V_{max} = 6.19 x 10^{-1} $\mu mol \cdot s^{-1} mg^{-1}$ K_m = 1.34 x 10^{-4} M

[*(S)*-Lysine (12)] = 0.50 mM

[Pyruvate] M x 10^{-4}	1/[Pyruvate] M^{-1} x 10^{3}	Rate $\mu mol \cdot s^{-1} mg^{-1}$ x 10^{-1}	1/Rate $mg \cdot s \cdot \mu mol^{-1}$
5.00	2.00	2.99	3.35
5.00	2.00	3.56	2.81
1.25	8.00	2.68	3.73
1.25	8.00	2.76	3.63
0.70	14.3	2.20	4.54
0.70	14.3	2.18	4.59
0.50	20.0	1.69	5.92
0.50	20.0	1.66	6.03

Lineweaver-Burk plot V_{max} = 3.89 x 10^{-1} $\mu mol \cdot s^{-1} mg^{-1}$ K_m = 0.615 x 10^{-4} M

[*(S)*-Lysine (12)] = 0.75 mM

[Pyruvate] M x 10^{-4}	1/[Pyruvate] M^{-1} x 10^{3}	Rate $\mu mol \cdot s^{-1} mg^{-1}$ x 10^{-1}	1/Rate $mg \cdot s \cdot \mu mol^{-1}$
5.00	2.00	2.91	3.44
5.00	2.00	2.60	3.84
1.25	8.00	2.19	4.56
1.25	8.00	2.07	4.83
0.70	14.3	1.77	5.64
0.70	14.3	1.60	6.25
0.50	20.0	1.48	6.76
0.50	20.0	1.48	6.75

Lineweaver-Burk plot V_{max} = 3.02 x 10^{-1} $\mu mol \cdot s^{-1} mg^{-1}$ K_m = 0.531 x 10^{-4} M

Determination of K_i:

[Pyruvate] M x 10^{-4}	[*(S)*-Lysine] M x 10^{-3}	1/Rate mg·s·μmol^{-1}		[*(S)*-ASA]/Rate s·mg·l^{-1} x 10^2	
5.00	0	2.40	1.77	12.0	8.35
5.00	0.25	2.17	1.88	10.9	9.40
5.00	0.50	3.35	2.81	16.8	14.1
5.00	0.75	3.44	3.84	17.2	19.2
1.25	0	2.73	2.72	3.41	3.40
1.25	0.25	3.64	3.28	4.55	4.10
1.25	0.50	3.73	3.63	4.66	4.54
1.25	0.75	4.56	4.83	5.70	6.04
0.70	0	4.32	3.99	3.02	2.79
0.70	0.25	4.23	4.94	2.96	3.46
0.70	0.50	4.54	4.59	3.18	3.21
0.70	0.75	5.64	6.25	3.95	4.38
0.50	0	5.19	5.49	2.60	2.75
0.50	0.25	5.90	6.15	2.95	3.08
0.50	0.50	5.92	6.03	2.96	3.02
0.50	0.75	6.76	6.75	3.38	3.38

Uncompetitive inhibition:

K_i' (Modified Dixon) 3.13 x 10^{-4} M

3.81 x 10^{-4} M

DHDPR enzyme kinetics

Kinetics of DHDPR with respect to the substrate

Assay:

NADPH (54 mM in dH_2O)	3.0 μl
Buffer (200 mM Mops pH 7.2 at 25 °C, pyruvate (17) 80 mM)	500 μl
dH_2O	337 μl
DHDPS (10 fold excess)	100 μl
(S)-ASA (11) (6.0 mM to 1.0 mM in dH_2O)	50 μl
DHDPR (2.25 x 10^{-4} U, 1.0 x 10^{-4} mg)	10 μl
	1.00 ml

The *(S)*-aspartate β-semialdehyde was added prior to initiation of the reaction to form the substrate. The reaction was then initiated in the cuvette by addition of DHDPR, mixed by inversion of the cuvettte. ΔA_{340} was measured over 300 seconds at 30 °C, blanked against dH_2O.

Run 1:

[DHDPA] M x 10^{-4}	1/[DHDPA] M^{-1} x 10^{3}	Rate $\mu mol \cdot s^{-1} mg^{-1}$	1/Rate $mg \cdot s \cdot \mu mol^{-1}$	Rate/[DHDPA] $l \cdot s^{-1} mg^{-1}$ x 10^{-4}
2.50	4.00	1.60	0.627	6.40
2.50	4.00	1.99	0.503	7.96
1.50	6.67	1.30	0.766	8.66
1.50	6.67	1.32	0.758	8.13
1.00	10.0	0.851	1.18	8.51
1.00	10.0	0.845	1.18	8.45
0.65	15.4	0.621	1.61	9.56
0.65	15.4	0.551	1.81	8.49
0.50	20.0	0.420	2.38	8.40

Lineweaver-Burke plot V_{max} = 11.6 $\mu mol \cdot s^{-1} mg^{-1}$ K_m = 7.85 x 10^{-4} M
Eadie-Hofstee plot V_{max} = 4.12 $\mu mol \cdot s^{-1} mg^{-1}$ K_m = 3.71 x 10^{-4} M
Direct linear plot V_{max} = 6.52 $\mu mol \cdot s^{-1} mg^{-1}$ K_m = 6.59 x 10^{-4} M

Run 2:

[DHDPA] M x 10^{-4}	1/[DHDPA] M^{-1} x 10^{3}	Rate $\mu mol \cdot s^{-1} mg^{-1}$	1/Rate $mg \cdot s \cdot \mu mol^{-1}$	Rate/[DHDPA] $l \cdot s^{-1} mg^{-1}$ x 10^{-4}
3.00	3.33	1.97	0.507	6.56
3.00	3.33	2.12	0.471	7.06
2.50	4.00	1.94	0.517	7.76
2.50	4.00	1.83	0.546	7.32
2.00	5.00	1.55	0.646	7.75
2.00	5.00	1.46	0.685	7.30
1.50	6.66	1.27	0.787	8.46
1.50	6.66	1.25	0.798	8.33
1.00	10.0	0.825	1.21	8.25
1.00	10.0	0.823	1.21	8.23
0.50	20.0	0.486	2.06	9.72
0.50	20.0	0.499	2.00	9.98

Lineweaver-Burk plot V_{max} = 5.27 $\mu mol \cdot s^{-1} mg^{-1}$ K_m = 4.93 x 10^{-4} M
Eadie-Hofstee plot V_{max} = 5.39 $\mu mol \cdot s^{-1} mg^{-1}$ K_m = 5.04 x 10^{-4} M
Direct linear plot V_{max} = 5.71 $\mu mol \cdot s^{-1} mg^{-1}$ K_m = 5.29 x 10^{-4} M

Kinetics of DHDPR with respect to the cofactor NADPH

Assay:

NADPH (13.5 to 3.43 mM in dH_2O)	3.0 µl
Buffer (200 mM Mops pH 7.2 at 25 °C, pyruvate (17) 80 mM)	500 µl
dH_2O	337 µl
DHDPS (10 fold excess)	100 µl
(S)-ASA (11) (5 mM in dH_2O)	50 µl
DHDPR (2.25×10^{-4} U, 1.0×10^{-4} mg)	10 µl
	1.00 ml

The *(S)*-aspartate β-semialdehyde was added prior to initiation of the reaction to form the substrate. The reaction was then initiated in the cuvette by addition of DHDPR, mixed by inversion of the cuvettte. ΔA_{340} was measured over 300 seconds at 30 °C, blanked against dH_2O.

Run 1:

[NADPH] M x 10^{-5}	1/[NADPH] M^{-1} x 10^{4}	Rate $\mu mol \cdot s^{-1} mg^{-1}$	1/Rate $mg \cdot s \cdot \mu mol^{-1}$ x 10^{-1}	Rate/[NADPH] $l \cdot s^{-1} mg^{-1}$ x 10^{-3}
4.05	2.47	2.84	3.52	7.02
4.05	2.47	2.87	3.48	7.09
2.70	3.70	2.64	3.78	9.77
2.70	3.70	2.70	3.70	9.99
1.35	7.41	1.70	5.87	12.6
1.35	7.41	1.25	7.99	9.26
1.08	9.26	1.61	6.22	14.9
1.08	9.26	1.68	5.94	15.6

Lineweaver-Burk plot	$V_{max} = 4.34\ \mu mol \cdot s^{-1} mg^{-1}$ $K_m = 2.10 \times 10^{-5}$ M
Eadie-Hofstee plot	$V_{max} = 3.62\ \mu mol \cdot s^{-1} mg^{-1}$ $K_m = 1.35 \times 10^{-5}$ M
Direct linear plot	$V_{max} = 3.90\ \mu mol \cdot s^{-1} mg^{-1}$ $K_m = 1.49 \times 10^{-5}$ M

Run 2:

[NADPH] M x 10^{-5}	1/[NADPH] M^{-1} x 10^{4}	Rate $\mu mol \cdot s^{-1} mg^{-1}$	1/Rate $mg \cdot s \cdot \mu mol^{-1}$ x 10^{-1}	Rate/[NADPH] $l \cdot s^{-1} mg^{-1}$ x 10^{-3}
4.05	2.47	2.58	3.88	6.37
2.00	4.00	2.23	4.49	8.92
2.00	4.00	2.51	3.99	10.0
1.35	7.41	1.77	5.65	13.1
1.35	7.41	1.77	5.65	13.1
1.03	9.71	1.28	7.82	12.4
1.03	9.71	1.51	6.63	14.7

Lineweaver-Burk plot V_{max} = 4.14 $\mu mol \cdot s^{-1} mg^{-1}$ K_m = 1.96 x 10^{-5} M
Eadie-Hofstee plot V_{max} = 3.58 $\mu mol \cdot s^{-1} mg^{-1}$ K_m = 1.45 x 10^{-5} M
Direct linear plot V_{max} = 3.63 $\mu mol \cdot s^{-1} mg^{-1}$ K_m = 1.65 x 10^{-5} M

Kinetics of DHDPR with respect to the cofactor NADH

Assay:

NADH (10.7 to 1.33 mM in dH_2O)	3.0 µl
Buffer (200 mM Mops pH 7.2 at 25 °C, pyruvate (17) 80 mM)	500 µl
dH_2O	337 µl
DHDPS (10 fold excess)	100 µl
(S)-ASA (11) (5 mM in dH_2O)	50 µl
DHDPR (2.25 x 10^{-4} U, 1.0 x 10^{-4} mg)	10 µl
	1.00 ml

The *(S)*-aspartate β-semialdehyde was added prior to initiation of the reaction toform the substrate. The reaction was then initiated in the cuvette by addition of DHDPR, mixed by inversion of the cuvettte. ΔA_{340} was measured over 300 seconds at 30 °C, blanked against dH_2O.

Run 1:

[NADH] M x 10^{-5}	1/[NADH] M^{-1} x 10^{4}	Rate $\mu mol \cdot s^{-1} mg^{-1}$	1/Rate $mg \cdot s \cdot \mu mol^{-1}$ x 10^{-1}	Rate/[NADH]] $l \cdot s^{-1} mg^{-1}$ x 10^{-3}
3.20	3.13	1.52	6.59	4.76
3.20	3.13	1.32	7.57	4.13
1.60	6.25	1.55	6.47	9.69
1.60	6.25	1.27	7.89	7.94
1.10	9.09	1.27	7.86	11.5
1.10	9.09	1.23	8.10	11.2
0.800	12.5	0.985	10.2	12.3

Lineweaver-Burk plot V_{max} = 1.74 $\mu mol \cdot s^{-1} mg^{-1}$ K_m = 5.09 x 10^{-6} M
Eadie-Hofstee plot V_{max} = 1.58 $\mu mol \cdot s^{-1} mg^{-1}$ K_m = 3.21 x 10^{-6} M
Direct linear plot V_{max} = 1.96 $\mu mol \cdot s^{-1} mg^{-1}$ K_m = 6.27 x 10^{-6} M

Run 2:

[NADH] M x 10^{-5}	1/[NADH] M^{-1} x 10^{4}	Rate $\mu mol \cdot s^{-1} mg^{-1}$	1/Rate $mg \cdot s \cdot \mu mol^{-1}$ x 10^{-1}	Rate/[NADH]] $l \cdot s^{-1} mg^{-1}$ x 10^{-3}
3.20	3.13	2.11	4.74	6.60
3.20	3.13	1.81	5.54	5.67
1.60	6.25	1.55	6.44	9.69
1.60	6.25	1.40	7.12	8.75
0.800	12.5	1.21	8.30	15.1
0.800	12.5	0.826	12.1	10.3
0.400	25.0	1.00	9.97	25.0
0.400	25.0	0.789	12.7	19.7

Lineweaver-Burk plot V_{max} = 1.95 $\mu mol \cdot s^{-1} mg^{-1}$ K_m = 5.36 x 10^{-6} M
Eadie-Hofstee plot V_{max} = 1.96 $\mu mol \cdot s^{-1} mg^{-1}$ K_m = 4.95 x 10^{-6} M
Direct linear plot V_{max} = 2.36 $\mu mol \cdot s^{-1} mg^{-1}$ K_m = 6.56 x 10^{-6} M

References

1. L.I. Smith, J.W. Opie *Organic Synthesis* Coll. Vol. **III** 56 (1955).
2. Aldrich Chemical Company Catalogue.
3. J.G. Shedlarski *Meth. Enz.,* **17b**, 129 (1971).
4. Y. Yugari, C.Gilvarg *J. Biol. Chem*, **240**, 4710 (1965).
5. J.A. Gerrard *'Studies on Dihydrodipicolinate Synthase'* D.Phil., Brasenose College, Oxford (1992).
6. Sigma Chemical Company Catalogue.

Experimental Part III

The Structure of (S)-*Aspartate β-Semialdehyde*

Stability of homoserine lactone (31) (2-amino-4-butyrolactone)

NMR studies, including HMBC and nOe experiments, were performed on homoserine lactone (31) (15 mg) in D_2O at pH = 1. Infra-red studies were also performed, in aqueous solution and in potassium bromide.

Homoserine lactone (31)

^{1}H NMR (300 MHz, D_2O) δ_H 2.13 - 2.28 (1H, m, -C**H**$_2$CHNH$_2$ (pro-R); nOe to δ_H 4.2, 4.4), 2.51 - 2.61 (1H, m, -C**H**$_2$CHNH$_2$ (pro-S); nOe to δ_H 4.2), 4.16 - 4.26 (2H, m, -C**H**$_2$CH$_2$CHNH$_2$), 4.33 - 4.40 (1H, m, -C**H**NH$_2$) ppm.

^{13}C NMR (75 MHz, D_2O) δ_C 27.9 (t, -**C**H$_2$CH$_2$O-), 46.9 (d, -**C**HNH$_3$), 68.7 (t, -**C**H$_2$O-), 173 (-**C**=O).

HMBC:[1] δ_H *ca.* 2.2, coupling to δ_C 46.9, and 68.7; δ_H *ca.* 2.6, coupling to δ_C 46.9, and 173; δ_H *ca.* 4.2, coupling to δ_C 27.9, and 173; δ_H *ca.* 4.4 coupling to δ_C 27.9, 46.9, and 173.

IR (KBr disc) υ_{max} 3448 (N-H (w)), 2976 (C-H (s)), 1774 (C=O (s)), 1490 (w), 1216 (w), 1188 (w), 1026 (w) cm^{-1}.

IR (H_2O) υ_{max} 1748 cm^{-1}.

Homoserine lactone (31) was found to hydrolyse to homoserine (64).

Homoserine (64)

^{1}H NMR (300 MHz, D_2O) δ_H 1.88 - 2.03 (2H, m, -C**H**$_2$CHNH$_2$), 3.54 - 3.58 (2H, m, -C**H**$_2$CH$_2$CHNH$_2$), 3.97 - 4.01 (1H, m, -C**H**NH$_2$)ppm.

Stability at pH 8.0

Homoserine lactone (31) (1 mg) in phosphate buffer (KH_2PO_4/K_2HPO_4), in D_2O, (150 μl) followed by ^{1}H NMR.

Homoserine lactone (%)	Homoserine (%)	Time
100	0	0 mins
90	10	37 mins
77	23	47 mins
69	31	57 mins
38	62	4 hrs
0	100	22 hrs

Stability at pH 7.5

Homoserine lactone (31) (1 mg) in phosphate buffer, in D_2O, (150 µl) followed by ^1H NMR.

Homoserine lactone (%)	Homoserine (%)	Time
100	0	0 mins
80	20	36 mins
75	25	42 mins
0	100	22 hrs

Stability at pH 7.0

Homoserine lactone (31) (1 mg) in phosphate buffer, in D_2O, (150 µl) followed by ^1H NMR.

Homoserine lactone (%)	Homoserine (%)	Time
100	0	0 mins
87	13	39 mins
83	17	44 mins
75	25	53 mins
0	100	22 hrs

Stability in Mops buffer at pH 7.2

Homoserine lactone (31) (1 mg) in 200 mM Mops buffer, pH 7.2 at 25 °C in D_2O, (150 µl) followed by ^1H NMR.

Homoserine lactone (%)	Homoserine (%)	Time
100	0	0 mins
93.9	6.1	6 mins
89.4	10.6	13 mins
86.6	13.4	22 mins
81.0	19.0	30 mins
71.1	28.9	40 mins
66.2	33.8	49 mins
0	100	24 hrs

Effect of homoserine lactone (31) on DHDPS kinetics respect to *(S)*-aspartate β-semialdehyde (11)

Assay:

NADPH (54 mM in dH_2O)	3.0 µl
Buffer (200 mM Mops pH 7.2 at 25 °C, pyruvate (17) 80 mM)	500 µl
dH_2O	257 µl
DHDPS (2.0×10^{-4} U, 4.8×10^{-4} mg)	10 µl
DHDPR (10 fold excess)	100 µl
(S)-ASA (11) (5.0 mM to 1.2 mM in dH_2O)	50 µl
Homoserine lactone (31)	
(1.0 M to 0.5 M in 0.5 M Mops pH 3.5 at 25 °C)	80 µl
	1.00 ml

The reaction was initiated in the cuvette by the addition of freshly prepared *(S)*-aspartate β-semialdehyde (11), mixed by inversion of the cuvette. ΔA_{340} was measured over 300 seconds at 30 °C, blanked against dH_2O.

Run 1:

[Homoserine lactone (31)] = 0 mM

[*(S)*-ASA] M x 10^{-4}	1/[*(S)*-ASA] M^{-1} x 10^{3}	Rate µmol·$s^{-1}$$mg^{-1}$ x 10^{-1}	1/Rate mg·s·μmol^{-1}
2.50	4.00	4.17	2.40
2.50	4.00	4.71	2.12
1.50	6.67	3.86	2.59
1.50	6.67	2.50	4.00
1.00	10.0	3.03	3.30
1.00	10.0	2.91	3.44
0.80	12.5	3.03	3.97
0.80	12.5	2.55	3.92
0.60	16.7	2.06	4.85
0.60	16.7	2.10	4.76

Lineweaver-Burk plot $V_{max} = 5.85 \times 10^{-1}$ µmol·$s^{-1}$$mg^{-1}$ $K_m = 1.07 \times 10^{-4}$ M

[Homoserine lactone (31)] = 40 mM

[(*S*)-ASA] M x 10^{-4}	1/[(*S*)-ASA] M^{-1} x 10^{3}	Rate $\mu mol \cdot s^{-1} mg^{-1}$ x 10^{-1}	1/Rate $mg \cdot s \cdot \mu mol^{-1}$
2.50	4.00	2.16	4.63
2.50	4.00	1.84	5.42
1.50	6.67	1.47	6.78
1.50	6.67	1.63	6.14
1.00	10.0	1.36	7.38
1.00	10.0	1.32	7.60
0.80	12.5	1.18	8.46
0.80	12.5	1.20	8.33
0.60	16.7	1.00	10.0
0.60	16.7	1.07	9.37

Lineweaver-Burk plot V_{max} = 2.60 x 10^{-1} $\mu mol \cdot s^{-1} mg^{-1}$ K_m = 0.933 x 10^{-4} M

[Homoserine lactone (31)] = 60 mM

[(*S*)-ASA] M x 10^{-4}	1/[(*S*)-ASA] M^{-1} x 10^{3}	Rate $\mu mol \cdot s^{-1} mg^{-1}$ x 10^{-1}	1/Rate $mg \cdot s \cdot \mu mol^{-1}$
2.50	4.00	1.25	7.97
2.50	4.00	1.25	7.99
1.50	6.67	1.22	8.22
1.50	6.67	1.45	6.90
1.00	10.0	0.846	11.8
1.00	10.0	0.801	12.5
0.80	12.5	0.770	13.0
0.80	12.5	0.800	12.5
0.60	16.7	0.616	16.2
0.60	16.7	0.743	13.5

Lineweaver-Burk plot V_{max} = 2.00 x 10^{-1} $\mu mol \cdot s^{-1} mg^{-1}$ K_m = 1.22 x 10^{-4} M

[Homoserine lactone (31)] = 80 mM

[(*S*)-ASA] M x 10^{-4}	1/[(*S*)-ASA] M^{-1} x 10^{3}	Rate $\mu mol \cdot s^{-1} mg^{-1}$ x 10^{-1}	1/Rate $mg \cdot s \cdot \mu mol^{-1}$
2.50	4.00	0.901	11.1
2.50	4.00	0.910	11.0
1.50	6.67	0.741	13.4
1.50	6.67	0.769	13.0
1.00	10.0	0.668	15.0
1.00	10.0	0.542	18.5
0.80	12.5	0.388	25.8
0.80	12.5	0.537	18.6
0.60	16.7	0.496	20.2
0.60	16.7	0.503	19.9

Lineweaver-Burk plot $V_{max} = 1.20 \times 10^{-1}$ $\mu mol \cdot s^{-1} mg^{-1}$ $K_m = 0.997 \times 10^{-4}$ M

Determination of K_i:

[(*S*)-ASA] M x 10^{-4}	[Homoserine lactone] M x 10^{-3}	1/Rate mg·s·µmol^{-1}		[(*S*)-ASA]/Rate s·mg·l^{-1} x 10^2	
2.50	0	2.40	2.12	6.00	5.31
2.50	40	4.63	5.42	11.6	13.6
2.50	60	7.97	7.99	20.0	20.0
2.50	80	11.1	11.0	27.7	27.5
1.50	0	2.59	4.00	3.89	6.00
1.50	40	6.78	6.14	10.2	9.20
1.50	60	8.22	6.90	12.3	10.3
1.50	80	13.4	13.0	20.2	19.5
1.00	0	3.30	3.44	3.30	3.44
1.00	40	7.38	7.60	7.38	7.60
1.00	60	11.8	12.5	11.8	12.5
1.00	80	15.0	18.5	15.0	18.5
0.80	0	3.97	3.92	3.17	3.14
0.80	40	8.46	8.33	6.78	6.67
0.80	60	13.0	12.5	10.4	10.0
0.80	80	25.8	18.6	20.6	14.9
0.60	0	4.85	4.76	2.91	2.86
0.60	40	10.0	9.37	6.00	5.61
0.60	60	16.2	13.5	9.74	8.08
0.60	80	20.2	19.9	12.1	11.9

Noncompetitive inhibition:

K_i (Dixon)	1.03 x 10^{-2} M	K_i' (Modified Dixon)	1.03 x 10^{-2} M
	1.50 x 10^{-2} M		1.50 x 10^{-2} M
	1.56 x 10^{-2} M		1.57 x 10^{-2} M
	2.05 x 10^{-2} M		2.06 x 10^{-2} M
	2.26 x 10^{-2} M		2.25 x 10^{-2} M

Run 2:

[Homoserine lactone (31)] = 0 mM

[(*S*)-ASA] M x 10^{-4}	1/[(*S*)-ASA] M^{-1} x 10^{3}	Rate $\mu mol \cdot s^{-1} mg^{-1}$ x 10^{-1}	1/Rate $mg \cdot s \cdot \mu mol^{-1}$
2.50	4.00	4.16	2.40
2.50	4.00	5.14	1.95
1.50	6.67	4.33	2.31
1.50	6.67	4.31	2.32
1.00	10.0	2.78	3.62
1.00	10.0	3.28	3.05
0.80	12.5	2.74	3.65
0.80	12.5	2.53	3.95
0.60	16.7	2.31	4.33
0.60	16.7	2.47	4.05

Lineweaver-Burk plot V_{max} = 7.08 x 10^{-1} $\mu mol \cdot s^{-1} mg^{-1}$ K_m = 1.24 x 10^{-4} M

[Homoserine lactone (31)] = 40 mM

[(*S*)-ASA] M x 10^{-4}	1/[(*S*)-ASA] M^{-1} x 10^{3}	Rate $\mu mol \cdot s^{-1} mg^{-1}$ x 10^{-1}	1/Rate $mg \cdot s \cdot \mu mol^{-1}$
2.50	4.00	1.90	5.26
2.50	4.00	2.07	4.83
1.50	6.67	1.84	5.43
1.50	6.67	1.56	6.41
1.00	10.0	1.75	5.71
1.00	10.0	1.36	7.35
0.80	12.5	1.19	8.40
0.60	16.7	1.05	9.52
0.60	16.7	1.02	9.80

Lineweaver-Burk plot V_{max} = 2.94 x 10^{-1} $\mu mol \cdot s^{-1} mg^{-1}$ K_m = 1.08 x 10^{-4} M

[Homoserine lactone (31)] = 60 mM

[(*S*)-ASA] M x 10^{-4}	1/[(*S*)-ASA] M^{-1} x 10^{3}	Rate $\mu mol \cdot s^{-1} mg^{-1}$ x 10^{-1}	1/Rate $mg \cdot s \cdot \mu mol^{-1}$
2.50	4.00	1.23	8.15
2.50	4.00	1.34	7.45
1.50	6.67	1.12	8.93
1.50	6.67	1.05	9.54
1.00	10.0	0.872	11.5
1.00	10.0	0.870	11.5
0.80	12.5	0.803	12.5
0.80	12.5	0.708	14.1
0.60	16.7	0.766	13.0
0.60	16.7	0.701	14.3

Lineweaver-Burk plot V_{max} = 1.63 x 10^{-1} $\mu mol \cdot s^{-1} mg^{-1}$ K_m = 0.803 x 10^{-4} M

[Homoserine lactone (31)] = 80 mM

[(*S*)-ASA] M x 10^{-4}	1/[(*S*)-ASA] M^{-1} x 10^{3}	Rate $\mu mol \cdot s^{-1} mg^{-1}$ x 10^{-1}	1/Rate $mg \cdot s \cdot \mu mol^{-1}$
2.50	4.00	0.929	10.8
2.50	4.00	0.942	10.6
1.50	6.67	0.911	11.0
1.50	6.67	0.772	13.0
1.00	10.0	0.586	17.1
1.00	10.0	0.569	17.6
0.80	12.5	0.579	17.3
0.80	12.5	0.649	15.0
0.60	16.7	0.456	21.9
0.60	16.7	0.587	17.0

Lineweaver-Burk plot V_{max} = 1.22 x 10^{-1} $\mu mol \cdot s^{-1} mg^{-1}$ K_m = 0.853 x 10^{-4} M

Determination of K_i:

[(*S*)-ASA] M x 10^{-4}	[Homoserine lactone] M x 10^{-3}	1/Rate mg·s·μmol^{-1}		[(*S*)-ASA]/Rate s·mg·l^{-1} x 10^2	
2.50	0	2.40	1.95	6.01	4.86
2.50	40	5.26	4.83	13.2	12.1
2.50	60	8.15	7.45	20.3	18.7
2.50	80	10.8	10.6	26.9	26.5
1.50	0	2.31	2.32	3.46	3.48
1.50	40	5.43	6.41	8.15	9.62
1.50	60	8.93	9.54	13.4	14.3
1.50	80	11.0	13.0	16.5	19.4
1.00	0	3.62	3.04	3.60	3.05
1.00	40	5.71	7.35	5.71	7.35
1.00	60	11.5	11.5	11.5	11.5
1.00	80	17.1	17.6	17.1	17.6
0.80	0	3.65	3.95	2.92	3.16
0.80	40	8.40		6.72	
0.80	60	12.5	14.1	10.0	11.3
0.80	80	17.3	15.0	13.8	12.3
0.60	0	4.33	4.05	2.60	2.43
0.60	40	9.52	9.80	5.71	5.88
0.60	60	13.0	14.3	7.83	8.56
0.60	80	21.9	17.0	13.2	10.2

Noncompetitive inhibition:

K_i (Dixon)	K_i' (Modified Dixon)
1.17 x 10^{-2} M	1.17 x 10^{-2} M
1.57 x 10^{-2} M	1.58 x 10^{-2} M
1.61 x 10^{-2} M	1.62 x 10^{-2} M
1.83 x 10^{-2} M	1.82 x 10^{-2} M
2.11 x 10^{-2} M	2.22 x 10^{-2} M

Effect of homoserine lactone (31) on DHDPS kinetics with respect to pyruvate (17)

Assay:

NADPH (54 mM in dH_2O)	3.0 µl
Buffer (200 mM Mops pH 7.2 at 25 °C)	500 µl
dH_2O	7 µl
DHDPS (2.0×10^{-4} U, 4.8×10^{-4} mg)	10 µl
DHDPR (10 fold excess)	100 µl
Pyruvate (17) (2.0 mM to 0.20 mM in dH_2O)	250 µl
(S)-ASA (11) (50 mM in dH_2O)	50 µl
Homoserine lactone (31)	
(1.0 M to 0.50 M in 0.5 M Mops pH 3.5 at 25 °C)	80 µl
	1.00 ml

The reaction was initiated in the cuvette by the addition of freshly prepared *(S)*-aspartate β-semialdehyde (11), mixed by inversion of the cuvette. ΔA_{340} was measured over 300 seconds at 30 °C, blanked against dH_2O.

Run 1:

[Homoserine lactone (31)] = 0 mM

[Pyruvate] M x 10^{-4}	1/[Pyruvate] M^{-1} x 10^{3}	Rate µmol·$s^{-1}$$mg^{-1}$ x 10^{-1}	1/Rate mg·s·$µmol^{-1}$
5.00	2.00	3.41	2.93
5.00	2.00	3.62	2.76
1.25	8.00	1.99	5.03
1.25	8.00	2.02	4.95
0.70	14.3	1.32	7.58
0.70	14.3	1.56	6.41
0.50	20.0	0.795	12.6
0.50	20.0	1.11	9.01

Lineweaver-Burk plot $V_{max} = 5.99 \times 10^{-1}$ µmol·$s^{-1}$$mg^{-1}$ $K_m = 2.56 \times 10^{-4}$ M

[Homoserine lactone (31)] = 40 mM

[Pyruvate] M x 10^{-4}	1/[Pyruvate] M^{-1} x 10^{3}	Rate $\mu mol \cdot s^{-1} mg^{-1}$ x 10^{-1}	1/Rate $mg \cdot s \cdot \mu mol^{-1}$
5.00	2.00	1.93	5.18
5.00	2.00	2.24	4.47
1.25	8.00	1.18	8.45
1.25	8.00	1.16	8.59
0.70	14.3	0.775	12.9
0.70	14.3	0.498	20.1
0.50	20.0	0.666	15.0
0.50	20.0	0.605	16.5

Lineweaver-Burk plot $V_{max} = 2.59 \times 10^{-1}$ $\mu mol \cdot s^{-1} mg^{-1}$ $K_m = 1.76 \times 10^{-4}$ M

[Homoserine lactone (31)] = 60 mM

[Pyruvate] M x 10^{-4}	1/[Pyruvate] M^{-1} x 10^{3}	Rate $\mu mol \cdot s^{-1} mg^{-1}$ x 10^{-1}	1/Rate $mg \cdot s \cdot \mu mol^{-1}$
5.00	2.00	1.39	7.20
5.00	2.00	1.60	6.26
1.25	8.00	0.790	12.7
1.25	8.00	0.859	11.6
0.70	14.3	0.603	16.6
0.70	14.3	0.584	17.1
0.50	20.0	0.459	21.8
0.50	20.0	0.430	23.2

Lineweaver-Burk plot $V_{max} = 1.99 \times 10^{-1}$ $\mu mol \cdot s^{-1} mg^{-1}$ $K_m = 1.72 \times 10^{-4}$ M

[Homoserine lactone (31)] = 80 mM

[Pyruvate] M x 10^{-4}	1/[Pyruvate] M^{-1} x 10^{3}	Rate $\mu mol \cdot s^{-1} mg^{-1}$ x 10^{-1}	1/Rate $mg \cdot s \cdot \mu mol^{-1}$
1.25	8.00	0.375	26.1
1.25	8.00	0.552	18.1
0.70	14.3	0.409	24.4
0.70	14.3	0.440	22.7
0.50	20.0	0.289	34.6

Lineweaver-Burk plot $V_{max} = 0.719 \times 10^{-1}$ $\mu mol \cdot s^{-1} mg^{-1}$ $K_m = 0.632 \times 10^{-4}$ M

Determination of K_i:

[Pyruvate] M x 10^{-4}	[Homoserine lactone] M x 10^{-3}	1/Rate $mg \cdot s \cdot \mu mol^{-1}$		[Pyruvate]/Rate $s \cdot mg \cdot l^{-1}$ x 10^{2}	
5.00	0	2.93	2.76	14.7	13.8
5.00	40	5.18	4.47	25.9	22.3
5.00	60	7.20	6.26	36.0	31.3
1.25	0	5.03	4.95	6.28	6.34
1.25	40	8.45	8.59	10.6	10.8
1.25	60	12.7	11.6	15.8	14.6
1.25	80	26.6	18.1	33.3	22.6
0.70	0	7.58	6.41	5.30	4.49
0.70	40	12.9	20.1	9.03	14.1
0.70	60	16.6	17.1	11.6	12.0
0.70	80	24.4	22.7	17.1	15.9
0.50	0	12.6	9.01	6.29	4.50
0.50	40	15.0	16.5	7.51	8.26
0.50	60	21.8	23.2	10.9	11.6
0.50	80	34.6		17.3	

Noncompetitive inhibition:

K_i (Dixon)	3.48 x 10^{-2} M	K_i' (Modified Dixon)	3.47 x 10^{-2} M
	3.73 x 10^{-2} M		3.72 x 10^{-2} M
	4.34 x 10^{-2} M		4.36 x 10^{-2} M

Run 2:

[Homoserine lactone (31)] = 0 mM

[Pyruvate] M x 10^{-4}	1/[Pyruvate] M^{-1} x 10^{3}	Rate $\mu mol \cdot s^{-1} mg^{-1}$ x 10^{-1}	1/Rate $mg \cdot s \cdot \mu mol^{-1}$
5.00	2.00	3.80	2.63
5.00	2.00	4.86	2.06
1.25	8.00	1.97	5.08
1.25	8.00	2.70	3.70
0.70	14.3	1.97	5.08
0.70	14.3	1.72	5.81
0.50	20.0	1.33	7.52
0.50	20.0	1.65	6.06

Lineweaver-Burk plot V_{max} = 4.76 x 10^{-1} $\mu mol \cdot s^{-1} mg^{-1}$ K_m = 1.14 x 10^{-4} M

[Homoserine lactone (31)] = 40 mM

[Pyruvate] M x 10^{-4}	1/[Pyruvate] M^{-1} x 10^{3}	Rate $\mu mol \cdot s^{-1} mg^{-1}$ x 10^{-1}	1/Rate $mg \cdot s \cdot \mu mol^{-1}$
5.00	2.00	1.46	6.83
5.00	2.00	1.63	6.12
1.25	8.00	1.05	9.55
1.25	8.00	1.02	9.78
0.70	14.3	0.605	16.5
0.70	14.3	0.709	14.1
0.50	20.0	0.650	15.4
0.50	20.0	0.604	16.6

Lineweaver-Burk plot V_{max} = 1.80 x 10^{-1} $\mu mol \cdot s^{-1} mg^{-1}$ K_m = 0.973 x 10^{-4} M

[Homoserine lactone (31)] = 60 mM

[Pyruvate] M x 10^{-4}	1/[Pyruvate] M^{-1} x 10^{3}	Rate $\mu mol \cdot s^{-1} mg^{-1}$ x 10^{-1}	1/Rate $mg \cdot s \cdot \mu mol^{-1}$
5.00	2.00	1.43	6.99
5.00	2.00	1.21	8.27
1.25	8.00	0.710	14.1
1.25	8.00	0.731	13.7
0.70	14.3	0.596	16.8
0.70	14.3	0.427	23.4
0.50	20.0	0.642	15.6
0.50	20.0	0.599	16.7

Lineweaver-Burk plot V_{max} = 1.17 x 10^{-1} $\mu mol \cdot s^{-1} mg^{-1}$ K_m = 0.624 x 10^{-4} M

[Homoserine lactone (31)] = 80 mM

[Pyruvate] M x 10^{-4}	1/[Pyruvate] M^{-1} x 10^{3}	Rate $\mu mol \cdot s^{-1} mg^{-1}$ x 10^{-1}	1/Rate $mg \cdot s \cdot \mu mol^{-1}$
5.00	2.00	0.611	16.4
5.00	2.00	0.696	14.4
1.25	8.00	0.141*	71.1*
1.25	8.00	0.418	23.9
0.70	14.3	0.389	25.7
0.70	14.3	0.215	46.6
0.50	20.0	0.221	45.2
0.50	20.0	0.255	39.2

Lineweaver-Burk plot V_{max} = 0.796 x 10^{-1} $\mu mol \cdot s^{-1} mg^{-1}$ K_m = 1.22 x 10^{-4} M

Determination of K_i:

[Pyruvate] M x 10^{-4}	[Homoserine lactone] M x 10^{-3}	1/Rate mg·s·μmol^{-1}		[Pyruvate]/Rate s·mg·l^{-1} x 10^2	
5.00	0	2.63	2.06	13.8	10.3
5.00	40	6.83	6.12	34.2	3.07
5.00	60	6.99	8.27	35.0	41.3
5.00	60	16.4	14.4	81.8	71.8
1.25	0	5.08	3.70	6.35	4.63
1.25	40	9.55	9.78	11.9	12.3
1.25	60	14.1	13.7	17.6	17.1
1.25	80	71.1*	23.4	88.7*	29.9
0.70	0	5.08	5.81	3.55	4.07
0.70	40	16.5	14.1	11.6	9.87
0.70	60	16.8	23.4	11.7	16.4
0.70	80	25.7	46.6	18.0	32.6
0.50	0	7.52	6.06	3.76	3.03
0.50	40	15.4	16.6	7.69	8.28
0.50	60	15.6	16.7	7.79	8.35
0.50	80	45.2	39.2	22.6	19.6

Noncompetitive inhibition:

K_i (Dixon)	8.23 x 10^{-3} M	K_i' (Modified Dixon)	8.21 x 10^{-3} M
	9.06 x 10^{-3} M		9.13 x 10^{-3} M
	9.10 x 10^{-3} M		9.59 x 10^{-3} M
	15.0 x 10^{-3} M		15.0 x 10^{-3} M

Effect of *(S)*-homoserine lactone (31) on DHDPS kinetics with respect to *(S)*-aspartate β-semialdehyde (11)

Assay:

NADPH (54 mM in dH_2O)	3.0 μl
Buffer (200 mM Mops pH 7.2 at 25 °C, pyruvate (17) 80 mM)	500 μl
dH_2O	257 μl
DHDPS (2.0 x 10^{-4} U, 4.8 x 10^{-4} mg)	10 μl
DHDPR (10 fold excess)	100 μl
(S)-ASA (11) (5.0 mM to 1.3 mM in dH_2O)	50 μl
(S)-Homoserine lactone (31)	
(0.875 M to 0.5 M in 0.5 M Mops pH 3.5 at 25 °C)	80 μl
	1.00 ml

The reaction was initiated in the cuvette by the addition of freshly prepared *(S)*-aspartate β-semialdehyde (11), mixed by inversion of the cuvette. ΔA_{340} was measured over 300 seconds at 30 °C, blanked against dH_2O.

[*(S)*-Homoserine lactone (31)] = 0 mM

[*(S)*-ASA] M x 10^{-4}	1/[*(S)*-ASA] M^{-1} x 10^{3}	Rate $\mu mol \cdot s^{-1} mg^{-1}$ x 10^{-1}	1/Rate $mg \cdot s \cdot \mu mol^{-1}$
2.50	4.00	4.33	2.31
2.50	4.00	5.64	1.77
1.25	8.00	4.23	2.36
1.25	8.00	4.27	2.34
0.85	11.8	3.39	2.95
0.85	11.8	3.19	3.13
0.65	15.4	2.63	3.80
0.65	15.4	2.76	3.62

Lineweaver-Burk plot $V_{max} = 7.57 \times 10^{-1}$ $\mu mol \cdot s^{-1} mg^{-1}$ $K_m = 1.13 \times 10^{-4}$ M

[*(S)*-Homoserine lactone (31)] = 40 mM

[*(S)*-ASA] M x 10^{-4}	1/[*(S)*-ASA] M^{-1} x 10^{3}	Rate $\mu mol \cdot s^{-1} mg^{-1}$ x 10^{-1}	1/Rate $mg \cdot s \cdot \mu mol^{-1}$
2.50	4.00	1.11*	8.98*
2.50	4.00	2.00	5.00
1.25	8.00	0.970*	10.3*
1.25	8.00	1.92	5.20
0.85	11.8	1.80	5.56
0.85	11.8	1.64	6.10
0.65	15.4	1.40	7.12
0.65	15.4	1.51	6.62

Lineweaver-Burk plot $V_{max} = 2.48 \times 10^{-1}$ $\mu mol \cdot s^{-1} mg^{-1}$ $K_m = 0.425 \times 10^{-4}$ M

[*(S)*-Homoserine lactone (31)] = 60 mM

[*(S)*-ASA] M x 10^{-4}	1/[*(S)*-ASA] M^{-1} x 10^{3}	Rate $\mu mol \cdot s^{-1} mg^{-1}$ x 10^{-1}	1/Rate $mg \cdot s \cdot \mu mol^{-1}$
2.50	4.00	2.16	4.63
2.50	4.00	2.34	4.27
1.25	8.00	1.55	6.45
1.25	8.00	1.70	5.88
0.85	11.8	1.38	7.25
0.85	11.8	1.30	7.69
0.65	15.4	1.00	10.0
0.65	15.4	1.10	9.09

Lineweaver-Burk plot V_{max} = 3.79 x 10^{-1} $\mu mol \cdot s^{-1} mg^{-1}$ K_m = 1.65 x 10^{-4} M

[*(S)*-Homoserine lactone (31)] = 70 mM

[*(S)*-ASA] M x 10^{-4}	1/[*(S)*-ASA] M^{-1} x 10^{3}	Rate $\mu mol \cdot s^{-1} mg^{-1}$ x 10^{-1}	1/Rate $mg \cdot s \cdot \mu mol^{-1}$
2.50	4.00	1.60	6.26
2.50	4.00	1.46	6.86
1.25	8.00	1.27	7.88
1.25	8.00	0.627*	14.9*
0.85	11.8	1.04	9.63
0.85	11.8	1.05	9.51
0.65	15.4	0.899	11.1
0.65	15.4	1.02	9.79

Lineweaver-Burk plot V_{max} = 1.92 x 10^{-1} $\mu mol \cdot s^{-1} mg^{-1}$ K_m = 0.674 x 10^{-4} M

Determination of K_i:

[(*S*)-ASA] M x 10^{-4}	[(*S*)-Homo-serine lactone] M x 10^{-3}	1/Rate mg·s·μmol^{-1}		[(*S*)-ASA]/Rate s·mg·l^{-1} x 10^2	
2.50	0	2.31	1.77	5.77	4.43
2.50	40	8.98*	5.00	22.5*	12.5
2.50	60	4.63	4.27	11.6	10.7
2.50	70	6.26	6.86	15.6	17.1
1.25	0	2.36	2.34	2.96	2.93
1.25	40	10.3*	5.20	12.9*	6.51
1.25	60	6.45	5.88	8.06	7.35
1.25	70	7.88	14.9*	9.84	18.6*
0.85	0	2.95	3.13	2.51	2.66
0.85	40	5.56	6.10	4.72	5.18
0.85	60	7.25	7.69	6.16	6.54
0.85	70	9.63	9.51	8.17	8.10
0.65	0	3.80	3.62	2.47	2.36
0.65	40	7.12	6.62	4.64	4.30
0.65	60	10.0	9.09	6.50	5.91
0.65	70	11.1	9.79	7.23	6.37

Noncompetitive inhibition:

K_i (Dixon)	3.20 x 10^{-2} M	K_i' (Modified Dixon)	3.19 x 10^{-2} M
	3.27 x 10^{-2} M		3.28 x 10^{-2} M
	3.61 x 10^{-2} M		3.61 x 10^{-2} M
	3.70 x 10^{-2} M		3.71 x 10^{-2} M

Ethyl *(S)*-α,γ-diaminobutyrate dihydrochloride (66)[2,3]

(S)-α,γ-Diaminobutyric acid hydrochloride (65) (99.8 mg, 0.646 mmol) was suspended in dry ethanol (6.0 ml). Dry hydrogen chloride gas was passed through the mixture, while being heated under reflux, until a clear solution was obtained (two to three hours). The solution was then heated under reflux overnight to remove any excess dissolved hydrogen chloride gas. The ethanol was then removed *in vacuo*, and any remaining residual solvent was removed by azeotroping with ethanol (2.0 ml) and toluene (1.0 ml). ^{1}H NMR showed there was a mixture of product (two parts) and starting material (one part). The material was re-reacted in dry ethanol (6.0 ml). Dry hydrogen chloride gas was passed through the solution, while being heated under reflux, for two hours. The ethanol was removed *in vacuo* and any residual solvents were removed by azeotroping with ethanol (2.0 ml) and toluene (1.0 ml), the solvents were removed *in*

vauo. Ethyl *(S)*-α,γ-diaminobutyrate dihydrochloride (66) was obtained as a white viscous solid.

The yield of ethyl *(S)*-α,γ-diaminobutyrate dihydrochloride (66) was 121 mg (0.554 mol, 85.8%).
Mp (decomposition) 170 °C (literature 172 °C[3]).
^{1}H NMR (300 MHz, D_2O) δ_H 1.21 (3H, t, J = 7.3 Hz, $-OCH_2\mathbf{CH_3}$), 2.07 - 2.34 (2H, m, $-\mathbf{CH_2}CH_2NH_2$), 3.05 - 3.23 (2H, m, $-\mathbf{CH_2}NH_2$), 4.12 - 4.17 (1H, m, $-\mathbf{CH}NH_2$), 4.24 (2H, q, J = 6.9 Hz, $-O\mathbf{CH_2}CH_3$) ppm.
IR (KBr disc) υ_{max} 3426 (C-H (m)), 3001 (m), 1742 (C=O (s)), 1618 (m), 1501 (m), 1237 (m) cm^{-1}.
MS m/z (FAB (gly)) 147 (MH^+, 100%), 132 ($MH\text{-}CH_3^+$, 100%), 93 (100%), 75 (100%).

(S)-3-Aminopyrrolid-2-one (62)[2,3]

Ethyl *(S)*-α,γ-diaminobutyrate dihydrochloride (66) (92.8 mg, 0.423 mmol) was dissolved in dry ethanol (0.66 ml) and cooled to -5 °C, in an atmosphere of dry nitrogen. A solution of sodium ethoxide, sodium (19 mg, 0.826 mmol) in dry ethanol (0.33 ml), was added with vigorous stirring. After two minutes the mixture was diluted with dry diethyl ether (1.99 ml). Sodium chloride immediately precipitated out and was removed by centrifugation (5 minutes, 15 000 rpm). The yellow supernatant was evaporated *in vacuo* to give *(S)*-3-aminopyrrolid-2-one (62) as a brownish yellow solid.

The yield of *(S)*-3-aminopyrrolid-2-one (62) was 18.5 mg (0.136 mmol, 32.2%).
Mp 95 - 97 °C (literature 98 - 99 °C[3]).
^{1}H NMR (300 MHz, D_2O) δ_H 1.55 - 1.80 (m), 2.31 - 2.41 (2H, m, $-C\mathbf{H_2}NH$-) 2.56 - 2.61 (m), 3.15 - 3.27 (2H, m, $-CH_2C\mathbf{H_2}NH$-), 3.45 - 3.47 (1H, m, $-C\mathbf{H}CH_2CH_2NH$-) ppm.
IR (KBr disc) υ_{max} 3196 (N-H (s)), 2878 (C-H (s)), 1682 (C=O (s)), 1574 (s), 1408 (w), 1294 (w), 1051 (w) cm^{-1}.
MS m/z (FAB (gly)) 101 (M^+, 22%).

Effect of *(S)*-3-aminopyrrolid-2-one (62) on DHDPS kinetics with respect to *(S)*-aspartate β-semialdehyde (11)

Assay:

NADPH (54 mM in dH_2O)	3.0 µl
Buffer (200 mM Mops pH 7.2 at 25 °C, pyruvate (17) 80 mM)	500 µl
dH_2O	257 µl
DHDPS (2.0×10^{-4} U, 4.8×10^{-4} mg)	10 µl
DHDPR (10 fold excess)	100 µl
(S)-ASA (11) (5.0 mM)	50 µl
(S)-3-Aminopyrrolid-2-one (62) (0.525 M to 0.25 M in dH_2O)	80 µl
	1.00 ml

The reaction was initiated in the cuvette by the addition of freshly prepared *(S)*-aspartate β-semialdehyde (11), mixed by inversion of the cuvette. ΔA_{340} was measured over 300 seconds at 30 °C, blanked against dH_2O. *(S)*-Aspartate β-semialdehyde (11) was present at a concentration of 0.25 mM. The activity is the rate of reaction with inhibitor present relative to the rate of reaction in the absence of the inhibitor.

Compound	Concentration mM	Activity %
(S)-3-aminopyrrolid-2-one (62)	20	100
	40	85.0
	42	100

Cyclopentanone oxime (68)[4,5]

Cyclopentanone (67) (8.88 ml, 0.10 mol) was stirred in a 250 ml round bottom flask fitted with a double surface reflux condenser and a thermometer. A solution of hydroxylamine hydrochloride (8.7g, 0.125 mol) in water (15.0 ml) was added as the mixture was stirred vigorously. A solution of anhydrous sodium carbonate (6.7 g, 63.0 mmol) in water (25.0 ml) was added dropwise, via a separating funnel fitted to the reflux condenser, at such a rate that the temperature did not rise above 45 °C. The reaction was stirred for a further hour. The oxime solidified out of the aqueous layer, and was recrystallised from warm (40 °C) water. The white crystals of the oxime were collected over a sintered glass funnel.

The yield of cyclopentanone oxime (68) was 6.58 g (66.4 mmol, 66.4%).
Mp 55 - 56 °C.
^1H NMR (300 MHz, $CDCl_3$) δ_H 1.70 - 1.83 (4H, m, 2x -CH_2C=NOH), 2.34 - 2.39 (2H, m, 2x -CH_2CH_2C=NOH), 2.43 - 2.48 (2H, m, 2x -CH_2CH_2C=NOH) ppm.

IR ($CDCl_3$ solution) υ_{max} 2962 (C-H (s)), 2857 (w), 1540 (s), 1447 (s), 1261 (s), 1097 (s), 1016 (s) cm^{-1}.
MS m/z (EI) 99 (M^+)

Aminocyclopentane (69)[4,6]

Cyclopentanone oxime (68) (6.0 g, 60.1 mmol) in dry ethanol (35 ml) was heated under reflux on a water bath whilst sodium metal (9.0 g, 0.39 mol) was added. Additional ethanol (60 ml) was added to maintain a vigorous reaction and ensure all of the sodium had dissolved. The reaction was cooled and water (30 ml) was added, this was distilled off, over an oil bath, until the boiling point reached 80 °C. Additional water (30 ml) was added and distillation was continued until the boiling point reached 92 °C. Most of the amine remained as a layer in the strongly alkaline solution and was extracted with diethyl ether (100ml, 2 x 50 ml). Some of the amine had distilled over into the ethanol layer; this was then fractionally distilled, the amine layer being extracted with diethyl ether (40 ml, 2 x 20ml). The ether layers were combined and dried over sodium hydroxide. The solvent was removed under vaccum and the residue was then fractionally distilled under reduced pressure (~20 mm Hg); aminocyclopentane (69) was collected at 23 - 29 °C as a yellow oil.

The yield of aminocyclopentane (69) was 2.01g (23.7 mmol, 38.9%).
Bp 23 - 29 °C (~20 mm Hg).
^1H NMR (300 MHz, $CDCl_3$) δ_H 1.24 (4H, t, J = 7.4 Hz, 2x -C**H**$_2$CH$_2$CHNH$_2$), 1.54 (2H, bs, -N**H**$_2$), 1.60 - 1.75 (1H, m, -C**H**$_2$CHNH$_2$), 1.78 - 1.87 (1H, m, -C**H**$_2$CHNH$_2$), 3.32 (1H, qu, J = 6.4 Hz, -C**H**NH$_2$), 3.71 (2H, q, J = 7.3 Hz, -CH$_2$CHNH$_2$) ppm.
IR ($CDCl_3$ solution) υ_{max} 3619 (N-H (m)), 2960 (s), 2872 (w), 1602 (w), 1449 (w), 1255 (w) cm^{-1}.
MS m/z (E.I.) 85 (M^+, 8%), 69 (M-NH_2^+, 9%), 56 ($CH_2CH_2CH_2CH_2^+$, 37%), 40 (100%).

***tert*-Butyl hypochlorite (70)**[7]

Sodium hypochlorite bleach solution (6.25%, 250 ml) was cooled to below 10 °C and a solution of *tert*-butyl alcohol (71) (18.5 ml, 0.195 mol) and glacial acetic acid (12.3 ml, 0.215 mol) were added, in a dark environment, to the rapidly stirring solution. Stirring was then continued for a further three minutes. The aqueous layer was discarded, and the organic layer was washed with 10% aqueous sodium carbonate (25 ml) followed by water (25 ml). The resulting *tert*-butyl hypochlorite (70) was dried over calcium chloride (0.5 g), and filtered. The *tert*-butyl hypochlorite (70) was collected as a yellow liquid, and stored over calcium chloride, away from light, at -20 °C.
The yield of *tert*-butyl hypochlorite (70) was 12.1 g (0.112 mol, 60.5%).

2-Aminocyclopentanone (63)[8,9]

In a dry 100 ml three necked flask fitted with a magnetic stirrer, a dropping funnel, a calcium chloride drying tube, and a thermometer was placed aminocyclopentane (69) (1.00 ml, 0.857 g, 10.1 mmol) in dry toluene (2.5 ml). The solution was stirred and cooled to 5 °C in an ice-salt bath. A solution of *tert*-butyl hypochlorite (70) (2.53 ml, 20.7 mmol) in dry toluene (2.5 ml) was added dropwise at such a rate so as to maintain the temperature below 10 °C. The reaction was then stirred for 2.5 hours at room temperature. The drying tube was replaced with a reflux condenser, again fitted with a drying tube. Freshly prepared sodium (0.697 g, 30.3 mmol) in anhydrous methanol (7.1 ml), see note 1, was added to the toluene solution dropwise so as to maintain a gentle reflux. The reaction was then heated under reflux (bath temperature 94 °C) for one hour whereupon a test with starch-iodide paper was negative, see note 2.

The reaction mixture was then cooled in an ice bath, and the precipitated sodium chloride was removed by filtration through a sintered glass funnel. The filter cake was washed with three portions of dry toluene (3 x 1.25 ml), and the combined filtrates were then added very slowly, with stirring, to 2 M hydrochloric acid (7.6 ml) in a 50 ml beaker. The organic layer was removed *in vacuo*, and the remaining aqueous layer was then extracted with diethyl ether (2 x 20 ml). The dark brown aquous layer was evaporated to dryness *in vacuo* at a temperature not greater than 40 °C. The residue, in a 500 ml round bottom flask, was heated under reflux for 30 minutes in a solution of isopropyl alcohol, concentrated hydrochloric acid (99:1) (20.2 ml), then filtered, hot, through a sintered glass funnel. The residual solid, mainly sodium chloride, was re-extracted with a solution of isopropyl alcohol and concentrated hydrochloric acid (99:1) (7.6 ml). The two extracts were cooled separately at room temperature and then placed at 4 °C overnight.

Black micro-crystals had formed overnight, these were collected over a Buchner funnel and washed with dry diethyl ether (2.5 ml each). Each of the filtrates were then diluted with an equal volume of dry diethyl ether (20.2 ml and 7.6 ml respectively) and placed at 4 °C overnight. Large brown fern-crystals formed, these were recrystallised from hot isopropyl alcohol. The 2-aminocyclopentanone (63) was obtained as a brownish white crystalline product.

The yield of 2-aminocyclopentanone (63) was 151 mg (1.12 mmol, 11.0%).
Mp 142 °C (literature 146 -147 °C[8]).
^{1}H NMR (300 MHz, D_2O) δ_H 1.46 - 1.78 (4H, m, -C**H**$_2$C**H**$_2$CHNH$_3^+$), 1.93 - 1.97 (2H, m, -C**H**$_2$C=O), 3.52 - 3.59 (1H, m, -C**H**NH$_2$) ppm.
IR (thin film) υ_{max} 3431(N-H (m)), 2937 (C-H (s)), 1751 (C=O (s)), 1597, 1491, 1153, 1059 cm^{-1}.

HRMS m/z (FAB(gly) 100.07601 ($M^{+\cdot}$, 100% ($C_5H_{10}NO$ requires 100.07624)).
MS m/z (FAB(gly) 100 ($M^{+\cdot}$, 100%), 93 (22%), 82 (10%), 73 (56%), 61 (36%), 57 (14%).

Note 1: Anhydrous methanol was prepared by refluxing methanol (100 ml) over magnesium (1.0 g) for four hours. Inverse addition procedure was used for the preparation of the sodium methoxide, that is methanol was added dropwise to the sodium metal.
Note 2: To perform a starch-iodide test, starch-iodide paper is moistened with 2 M hydrochloric acid. A positive test is indicated by the immediate formation of a dark violet/black spot, while a faint beige colour is a negative result.

Effect of 2-aminocyclopentanone (63) on DHDPS kinetics with respect to *(S)*-aspartate β-semialdehyde (11)

Assay:

NADPH (54 mM in dH_2O)	3.0 µl
Buffer (200 mM Mops pH 7.2 at 25 °C, pyruvate (17) (80 mM)	500 µl
dH_2O	257 µl
DHDPS (2.0×10^{-4} U, 4.8×10^{-4} mg)	10 µl
DHDPR (10 fold excess)	100 µl
(S)-ASA (11) (5.0 mM)	50 µl
2-Aminocyclopentanone (63) (1.0 M to 0.50 M in dH_2O)	80 µl
	1.00 ml

The reaction was initiated in the cuvette by the addition of freshly prepared *(S)*-aspartate β-semialdehyde (11), mixed by inversion of the cuvette. ΔA_{340} was measured over 300 seconds at 30 °C, blanked against dH_2O.

[2-Aminocyclopentanone (63)] = 0 mM

[*(S)*-ASA] M x 10^{-4}	1/[*(S)*-ASA] M^{-1} x 10^{3}	Rate $\mu mol \cdot s^{-1} mg^{-1}$ x 10^{-1}	1/Rate $mg \cdot s \cdot \mu mol^{-1}$
2.50	4.00	3.69	2.71
2.50	4.00	4.13	2.42
1.25	8.00	3.27	3.06
1.25	8.00	2.53	2.83
0.85	11.8	2.93	3.41
0.85	11.8	1.48*	6.78*
0.65	15.4	2.21	4.53
0.65	15.4	2.69	3.72

Lineweaver-Burk plot V_{max} = 5.16 x 10^{-1} $\mu mol \cdot s^{-1} mg^{-1}$ K_m = 0.706 x 10^{-4} M

[2-Aminocyclopentanone (63)] = 40 mM

[*(S)*-ASA] M x 10^{-4}	1/[*(S)*-ASA] M^{-1} x 10^{3}	Rate $\mu mol \cdot s^{-1} mg^{-1}$ x 10^{-1}	1/Rate $mg \cdot s \cdot \mu mol^{-1}$
2.50	4.00	2.93	3.41
2.50	4.00	5.45*	1.83*
1.25	8.00	2.64	3.78
1.25	8.00	2.35	4.26
0.85	11.8	1.39	7.19
0.85	11.8	1.11	8.97
0.65	15.4	0.825	12.1
0.65	15.4	1.30	7.71

Lineweaver-Burk plot V_{max} and K_m were not able to be estimated accurately.

[2-Aminocyclopentanone (63)] = 60 mM

[(*S*)-ASA] M x 10^{-4}	1/[(*S*)-ASA] M^{-1} x 10^{3}	Rate $\mu mol \cdot s^{-1} mg^{-1}$ x 10^{-1}	1/Rate $mg \cdot s \cdot \mu mol^{-1}$
2.50	4.00	3.20	3.13
2.50	4.00	3.64	2.74
1.25	8.00	2.65	3.77
1.25	8.00	2.60	3.85
0.85	11.8	2.05	4.88
0.85	11.8	2.44	4.09
0.65	15.4	1.78	5.60
0.65	15.4	1.92	5.20

Lineweaver-Burk plot V_{max} = 4.81 x 10^{-1} $\mu mol \cdot s^{-1} mg^{-1}$ K_m = 1.02 x 10^{-4} M

[2-Aminocyclopentanone (63)] = 80 mM

[(*S*)-ASA] M x 10^{-4}	1/[(*S*)-ASA] M^{-1} x 10^{3}	Rate $\mu mol \cdot s^{-1} mg^{-1}$ x 10^{-1}	1/Rate $mg \cdot s \cdot \mu mol^{-1}$
2.50	4.00	2.50	4.00
2.50	4.00	2.58	3.88
1.25	8.00	1.91	5.22
1.25	8.00	2.02	4.96
0.85	11.8	1.67	5.97
0.85	11.8	1.64	6.09
0.65	15.4	1.28	7.80

Lineweaver-Burk plot V_{max} = 3.86 x 10^{-1} $\mu mol \cdot s^{-1} mg^{-1}$ K_m = 1.21 x 10^{-4} M

Determination of K_i:

[(*S*)-ASA] M x 10^{-4}	[2-Amino cyclo-pentanone] M x 10^{-3}	1/Rate mg·s·μmol^{-1}		[(*S*)-ASA]/Rate s·mg·l^{-1} x 10^{2}	
2.50	0	2.71	2.42	6.78	6.05
2.50	40	3.41	1.83*	8.53	4.59*
2.50	60	3.13	2.74	7.81	6.87
2.50	80	4.00	3.88	10.0	9.69
1.25	0	3.06	2.83	3.82	3.54
1.25	40	3.78	4.26	4.73	5.32
1.25	60	3.77	3.85	4.72	4.81
1.25	80	5.22	4.96	6.54	6.19
0.85	0	3.41	6.78*	2.90	5.74*
0.85	40	7.19	8.97	6.12	7.66
0.85	60	4.88	4.09	4.15	3.48
0.85	80	5.97	6.09	5.09	5.18
0.65	0	4.53	3.72	2.94	2.42
0.65	40	12.1	7.71	7.88	5.00
0.65	60	5.60	5.20	3.65	3.39
0.65	80	7.80		3.96	

Noncompetitive inhibition:

K_i (Dixon)	1.23 x 10^{-1} M	K_i' (Modified Dixon)	1.23 x 10^{-1} M
	1.49 x 10^{-1} M		1.77 x 10^{-1} M
	1.76 x 10^{-1} M		2.36 x 10^{-1} M

Picryl chloride (73) (1-chloro-2,4,6,-trinitrobenzene)[2,10,11]

1-Chloro-2,4-dinitrobenzene (72) (23.9 g, 0.118 mol) was dissolved in concentrated sulfuric acid (98%, 185 ml) and stirred for three hours in a 500 ml round bottomed flask stoppered with glass wool. Fuming concentrated nitric acid (30 ml) was then added dropwise, the solution became yellow brown in colour. The reaction was heated, in an oil bath, to 135 °C with an air condenser attached, again stoppered with glass wool. The reaction turned a deep orange and was heated under reflux for 21 hours. The reaction was cooled for 15 minutes, turning a clear pale yellow, and added slowly to 2.0 l of distilled water in a 3 l beaker. A yellowish green liquid formed; this was left for 72 hours where upon a yellow precipitate had formed. The yellow 1-chloro-2,4,6, trinitrobenzene (73) was removed via suction through a sintered glass funnel.

The yield of picryl chloride (73) was 27.3 g (0.110 mol, 93.3 %).
Mp 75 - 76 °C.
^{1}H NMR (300 MHz, $CDCl_3$) δ_H 8.86 (2H, s, aryl) ppm.
IR ($CDCl_3$ solution) υ_{max} 3092 (C-H (s)), 1606 (s), 1546 (N-O_2 (s)), 1340 (s) cm^{-1}.
MS m/z (EI) 247 (M^+, 100%), 149 (65%), 109 (M-3NO_2^+, 65%), 74 (M-(3NO_2+Cl)$^+$, 65%), 40 (65%).

Sodium picrylsulfonate (74)[2,11,12]

Sodium bisulfite (0.246 mol), were added to absolute ethanol (20 ml). This mixture was then added to picryl chloride (73) (25.1 g, 0.102 mol) suspended in absolute ethanol (300 ml) and heated under reflux for six hours (bath temperature 110 °C). The reaction was cooled to 0 °C where the crude sodium picrylsulfonate (74) precipitated, this was filtered off and stirred into distilled water (50 ml). The aqueous suspension was heated under reflux until all the solid had dissolved, approximately ten hours. During this time the solution lightened from deep red to pale orange. The hot solution was filtered, and the filtrate cooled to 0 °C. The sodium picrylsulfonate (74) immediately crystallised, where it was recrystallised once from boiling water, and once from 50% ethanol in 50% water. The sodium picrylsulfonate (74) was collected as fine pale yellow crystals.

The yield of sodium picrylsulfonate (74) was 2.83 g (9.05 mmol, 8.8%).
Mp >215 °C.
^{1}H NMR (300 MHz, D_2O) δ_H 8.82 (2H, s, aryl) ppm.
IR (KBr disc) υ_{max} 3096 (C-H (s)), 1542 (N-O_2 (s)), 1355 (s), 1270 (s), 1236 (s) cm^{-1}.

Picrylsulfonic acid (75)[2,11,12]

Sodium picrylsulfonate (74) (2.50 g, 7.99 mmol) was dissolved in propanone (25 ml), and filtered through decolourising charcoal. Concentrated hydrochloric acid (1.25 ml) was added to the filtrate and the precipitated sodium chloride was filtered off. The

filtrate was then concentrated *in vacuo* to 7.5 ml, and the further precipitated sodium chloride was filtered off. The filtrate was then concentrated to dryness, *in vacuo*, the residue being recrystallised from a hot solution of ethanol (2.5 ml), water (1.5 ml), and concentrated hydrochloric acid (3.5 ml). The picryl sulfonic acid (75) formed pale yellow crystals which were collected over a sintered glass funnel.

The yield of picryl sulfonic acid (75) was 891 mg (3.04 mmol, 38.1%).
Mp (decomposition) 172 - 176 °C, literature 190 °C.[13]
^{1}H NMR (300 MHz, D_2O) δ_H 8.77 (2H, s, aryl) ppm.
IR (KBr disc) υ_{max} 3489 (m), 3095 (C-H (w)), 1652 (w), 1609 (w), 1550 (N-O_2, (s)), 1355 (s), 1271 (s), 1235 (s) cm^{-1}.
MS m/z (E.I.) 293 (M^+, 1%), 213 (M-SO_3H^+, 100%), 167 (25%), 120 (40%), 75 (90%).

(*S*)-Aspartate β-semialdehyde hydrate picrylsulfonate[2]

Picrylsulfonic acid (75) (41.9 mg, 133 μmol, 2.3 equivalents) was dissolved in water (1.5 ml) and then added to the *(S)-N-tert*-butoxycarbonylaspartic acid β-semialdehyde *p*-methoxybenzyl ester (53) (19.6 mg, 58 μmol) and anisole (6.3 μl, 58 μmol, 1.0 equivalent), flushed with nitrogen, and left to react for three hours. The water was removed *in vacuo* yielding an oily white solid. Further water (2 x 1.5 ml) was added and removed *in vacuo* yielding an impure sample of the above named product. Attempts to crystallise the above product in water, water and dioxane, water and acetonitrile, ethanol, and diethyl ether all failed.

The yield of the impure *(S)*-aspartic acid β-semialdehyde hydrate picrylsulfonate was 56.0 mg.
^{1}H NMR (300 MHz, D_2O) δ_H 2.06 - 2.15 (2H, m, -C**H**$_2$CHNH$_2$), 4.17 - 4.18 (1H, m, -C**H**NH$_2$), 5.11 - 5.10 (1H, m, -C**H**(OH)$_2$), 8.81 (2H, s, aryl, picrylsulfonate) ppm.
IR (thin film) υ_{max} 3445(O-H, C-H (s)), 1636 (w), 1542 (m), 1355 (m) cm^{-1}.
MS m/z (FAB(gly)) 277 (20%), 185 (90%), 93 (100%).

Stability of* (S)-*aspartate β-semialdehyde hydrate trifluoroacetate (11b) at pH = 7 in D_2O.

After 24 hours the signal at δ_H 1.97 - 2.21 (m, -C**H**$_2$CHNH$_2$) is reduced in intensity. After 96 hours this signal has disappeared.

^{1}H NMR of* (S)*-aspartate β-semialdehyde hydrate trifluoroacetate (11b) as a function of pH.

pH = 1.

^{1}H NMR (300 MHz D_2O) δ_H 1.98 - 2.20 (2H, m, -C**H**$_2$CHNH$_2$), 4.00 -4.04 (1H, m, -C**H**NH$_2$), 5.19 - 5.22 (1H, m, -C**H**(OH)$_2$) ppm.

pH = 4.

^{1}H NMR (300 MHz D_2O) δ_H 1.96 - 2.16 (2H, m, -C**H**$_2$CHNH$_2$), 3.85 - 3.89 (1H, m, -C**H**NH$_2$), 5.16 - 5.20 (1H, m, -C**H**(OH)$_2$) ppm.

pH = 7.

^{1}H NMR (300 MHz D_2O) δ_H 1.91 (2H, m, -C**H**$_2$CHNH$_2$), 3.55 (1H, m, -C**H**NH$_2$), 5.12 (1H, m, -C**H**(OH)$_2$) 9.58 (1H, s, -C**H**O) ppm.

pH = 9.

^{1}H NMR (300 MHz D_2O) δ_H 1.80 (2H, m, -C**H**$_2$CHNH$_2$), 3.39 (1H, m, -C**H**NH$_2$), 5.10 (1H, m, -C**H**(OH)$_2$) 9.58 (1H, s, -C**H**O) ppm.

Attempts to prepare aldehyde derivatives of *(S)*-aspartate β-semialdehyde trifluoroacetate (11)[4]

Using semi-carbazide

Stock solution — 1 g semi-carbazide hydrochloride
1.5 g crystallised sodium acetate

(S)-Aspartate β-semialdehyde (11) (pH = 7, in phosphate buffer (KH_2PO_4/K_2HPO_4), 2 mg) and reagent (0.02 ml) gave no crystalline semi-carbazone.

Using 2,4-dinitrophenylhydrazine

Stock solution — 0.25 g 2,4-dinitrophenylhydrazine suspended in 5.0 ml methanol
0.5 ml concentrated sulfuric acid
The solution was then filtered

(S)-Aspartate β-semialdehyde (11) (pH = 7, in phosphate buffer, 2 mg) and reagent (0.05 ml) gave no crystalline hydrazone.

Using hydroxylamine

Stock solution 1.0 g hydroxylamine hydrochloride
2.0 g crystallised sodium acetate
8 - 10 ml water

(S)-Aspartate β-semialdehyde (11) (pH = 7, in phosphate buffer, 2 mg) and reagent (0.04 ml) heated on a water bath for 10 minutes failed to give a crystalline oxime.

Using benzaldehyde

(S)-Aspartate β-semialdehyde (11) (pH = 7, in phosphate buffer, 2mg), benzaldehyde (2.1 mg, 2 μl), ethanol (0.02 ml), and 5 M NaOH (1 μl) gave no isolable derivative.

Using dimedone

Stock solution Saturated aqueous dimedone solution

(S)-Aspartate β-semialdehyde (11) (pH = 7, in phosphate buffer, 2 mg) added to reagent gave no isolable derivative.

Preparation *S*-methyl *(R)*-cysteine sulfoxide (77)[14]

30% Hydrogen peroxide (1.48 ml, approximately 14.8 mmol) was added dropwise to a stirred solution of *S*-methyl *(R)*-cysteine (76) (1.00 g, 7.40 mmol) in water (37 ml). After three hours at room temperature methanol (18.5 ml) and propanone (148 ml) were added and the solution was left overnight, during which time the sulfoxide (77) precipitated as a white solid (a mixture of the two diasteroisomers).

The yield of *S*-methyl *(R)*-cysteine sulfoxide (77) was 260 mg (1.72 mmol, 23.2%).
Mp (decomposition) 150 - 155 °C.
^{1}H NMR (300 MHz, D_2O) δ_H 2.75 (3H, s, -SC**H**$_3$), 3.12 - 3.19 (1H, m, -C**H**$_2$SCH$_3$), 3.29 - 3.45 (1H, m, -C**H**$_2$SCH$_3$), 4.11 - 4.21 (1H, m, -C**H**NH$_2$) ppm.
^{13}C NMR (75 MHz, D_2O) δ_C 39.33 (-S**C**H$_3$); 40.27 (-S**C**H$_3$); 52.30, 53.09, 54.23, and 55.08 (2 x -**C**H$_2$**C**HNH$_2$), 118.24 (-**C**=O), 173.44 (-**C**=O) ppm.
IR (KBr disc) υ_{max} 3431 (N-H (s)), 2918 (C-H (m)), 1630 (C=O (s)), 1385 (m), 1022 (S=O (s)) cm^{-1}.
HRMS m/z (FAB (gly)) 152.03796 (MH^+, 100% ($C_4H_{10}O_3N^{32}S$ requires 152.03814)).
MS m/z (FAB (gly)) 152 (MH^+, 100%), 136 (M-CH_3^+, 46%), 119 (20%), 110 (20%).

Preparation of *S*-methyl *(R)*-cysteine sulfone (78)[15]

Ammonium molybdate (91 mg, 73.6 μmol) was added to water (2.7 ml), followed by the addition of 70% perchloric acid (0.63 ml, 73.0 μmol). The solution was boiled for five minutes, then filtered and left to cool. *S*-Methyl *(R)*-cysteine (76) (1.00 g, 7.4 mmol) was added to 0.738 ml of the solution prepared above in a 25 ml round bottom flask. Additional water (0.6 ml) was added and the resulting thick slurry was stirred at 0 °C. 30% Hydrogen peroxide solution (1.29 ml, 12.6 μmol) was added in 0.1 ml portions while maintaining the reaction at 0 °C. After addition of the hydrogen peroxide was complete the temperature was allowed to rise, and the reaction was stirred overnight at room temperature. The product precipitated out as a yellow solid and was collected by filtration followed by washing with water (25 ml), ethanol (25 ml), and diethyl ether (25 ml). The *S*-methyl *(R)*-cysteine sulfone (78) formed a yellowish white powder.

The yield of *S*-methyl *(R)*-cysteine sulfone (78) was 349 mg (2.09 mmol, 28.2%).
Mp 174 - 178 °C.
^{1}H NMR (300 MHz, D_2O) δ_H 3.17 (3H, s, -SC**H**$_3$), 3.64 - 3.72 (2H, m, -C**H**NH_2), 3.90 (1H, d, J = 15.5 Hz, -C**H**$_2$CHNH_2), 4.23 (1H, d, J = 9.5 Hz, -C**H**$_2$CHNH_2) ppm.
^{13}C NMR (75 MHz, D_2O) δ_C 43.03 (-S**C**H_3), 51.00 (-**C**H_2-), 55.74 (-**C**H-), 172.43 (-**C**OOH) ppm.
IR (KBr disc) υ_{max} 3225 (N-H (w)), 2880 (C-H (m)), 1558 (C=O (s)), 1410 (S=O (m)) 1387 (S=O (m)), 1356 (m), 1281 (m), 1207 (m), 1119 (m) cm^{-1}.
HRMS m/z (FAB (gly)) 168.03270 (MH^+, 78% ($C_4H_{10}NO_4{}^{32}S$ requires 168.03306)).
MS m/z (FAB (gly)) 168 (MH^+, 78%), 122 (10%), 110 (8%).

Effect of *(S)*-aspartate β-semialdehyde hydrate (11b) mimics on DHDPS kinetics

Assay:

NADPH (54 mM in dH_2O)	3.0 μl
Buffer (200 mM Mops pH 7.2 at 25 °C, pyruvate (17) 80 mM)	500 μl
dH_2O	137 μl
DHDPS (2.0 x 10^{-4} U, 4.8 x 10^{-4} mg)	10 μl
DHDPR (10 fold excess)	100 μl
(S)-ASA (11) (5.0 mM)	50 μl
Inhibitor (appropriate concentration)	200 μl
	1.00 ml

The reaction was initiated in the cuvette by the addition of freshly prepared *(S)*-aspartate β-semialdehyde (11), mixed by inversion of the cuvette. ΔA_{340} was measured over 300 seconds at 30 °C, blanked against dH_2O. *(S)*-Aspartate β-semialdehyde was

present at a concentration of 0.25 mM. The activity is the rate of reaction with inhibitor present relative to the rate of reaction in the absence of the inhibitor.

Compound	Concentration mM	Activity %
S-Methyl *(R)*-cysteine (76)	50	119
S-Methyl *(R)*-cysteine sulfoxide (77)	50	112
S-Methyl *(R)*-cysteine sulfone (78)	50	96.1
(R)-Cysteine sulfinic acid (79)	50	11.0
	10	62.8
	5.0	94.2
(S)-Aspartic acid (9)	50	29.1
	30	45.2
	5.0	95.5
(S)-Asparagine (80)	50	109
(S)-Glutamic acid (81)	50	12.4
	10	83.0
	5.0	119

Effect of *(R)*-cysteine sulfinic acid (79) on DHDPS kinetics with respect to *(S)*-aspartate β-semialdehyde (11)

Assay:

NADPH (54 mM in dH_2O)	3.0 µl
Buffer (200 mM Mops pH 7.2 at 25 °C, pyruvate (17) 80 mM)	500 µl
dH_2O	137 µl
DHDPS (2.0 x 10^{-4} U, 4.8 x 10^{-4} mg)	10 µl
DHDPR (10 fold excess)	100 µl
(S)-ASA (11) (5.0 mM to 1.30 mM in dH_2O)	50 µl
(R)-Cysteine sulfinic acid (79) (150 mM to 40 mM in dH_2O)	200 µl
	1.00 ml

The reaction was initiated in the cuvette by the addition of freshly prepared *(S)*-aspartate β-semialdehyde (11), mixed by inversion of the cuvette. ΔA_{340} was measured over 300 seconds at 30 °C, blanked against dH_2O.

Run 1:

[*(R)*-Cysteine sulfinic acid (79)] = 0 mM

[*(S)*-ASA] M x 10^{-4}	1/[*(S)*-ASA] M^{-1} x 10^{3}	Rate $\mu mol \cdot s^{-1} mg^{-1}$ x 10^{-1}	1/Rate $mg \cdot s \cdot \mu mol^{-1}$
2.50	4.00	3.66	2.73
2.50	4.00	4.21	2.37
1.25	8.00	2.96	3.38
1.25	8.00	2.62	3.81
0.85	11.8	2.35	4.25
0.85	11.8	2.10	4.77
0.65	15.4	1.73	5.78
0.65	15.4	1.99	5.02

Lineweaver-Burk plot V_{max} = 6.36 x 10^{-1} $\mu mol \cdot s^{-1} mg^{-1}$ K_m = 1.58 x 10^{-4} M

[*(R)*-Cysteine sulfinic acid (79)] = 8 mM

[*(S)*-ASA] M x 10^{-4}	1/[*(S)*-ASA] M^{-1} x 10^{3}	Rate $\mu mol \cdot s^{-1} mg^{-1}$ x 10^{-1}	1/Rate $mg \cdot s \cdot \mu mol^{-1}$
2.50	4.00	3.53	2.83
2.50	4.00	3.51	2.85
1.25	8.00	2.72	3.68
1.25	8.00	2.69	3.72
0.85	11.8	2.00	5.01
0.85	11.8	2.36	4.24
0.65	15.4	2.01	4.98
0.65	15.4	1.91	5.24

Lineweaver-Burk plot V_{max} = 4.83 x 10^{-1} $\mu mol \cdot s^{-1} mg^{-1}$ K_m = 0.985 x 10^{-4} M

[*(R)*-Cysteine sulfinic acid (79)] = 15 mM

[*(S)*-ASA] M x 10^{-4}	1/[*(S)*-ASA] M^{-1} x 10^{3}	Rate $\mu mol \cdot s^{-1} mg^{-1}$ x 10^{-1}	1/Rate $mg \cdot s \cdot \mu mol^{-1}$
2.50	4.00	2.90	3.45
2.50	4.00	2.96	3.38
1.25	8.00	1.78	5.60
1.25	8.00	1.97	5.07
0.85	11.8	1.91	5.23
0.85	11.8	1.84	5.43
0.65	15.4	1.32	7.56
0.65	15.4	1.21	8.24

Lineweaver-Burk plot $V_{max} = 4.91 \times 10^{-1}$ $\mu mol \cdot s^{-1} mg^{-1}$ $K_m = 1.73 \times 10^{-4}$ M

[*(R)*-Cysteine sulfinic acid (79)] = 25 mM

[*(S)*-ASA] M x 10^{-4}	1/[*(S)*-ASA] M^{-1} x 10^{3}	Rate $\mu mol \cdot s^{-1} mg^{-1}$ x 10^{-1}	1/Rate $mg \cdot s \cdot \mu mol^{-1}$
2.50	4.00	1.65	6.05
2.50	4.00	1.76	5.68
1.25	8.00	1.15	8.72
1.25	8.00	1.11	9.04
0.85	11.8	1.08	9.28
0.85	11.8	1.01	9.91
0.65	15.4	0.928	10.8

Lineweaver-Burk plot $V_{max} = 2.15 \times 10^{-1}$ $\mu mol \cdot s^{-1} mg^{-1}$ $K_m = 0.919 \times 10^{-4}$ M

Determination of K_i:

[(*S*)-ASA] M x 10^{-4}	[(*R*)-Cysteine sulfinic acid] M x 10^{-3}	1/Rate $mg \cdot s \cdot \mu mol^{-1}$		[(*S*)-ASA]/Rate $s \cdot mg \cdot l^{-1}$ x 10^{2}	
2.50	0	2.73	2.37	6.83	5.93
2.50	8.0	2.83	2.85	7.08	7.13
2.50	15	3.45	3.38	8.63	8.45
2.50	25	6.05	5.68	15.1	14.2
1.25	0	3.38	3.81	4.23	4.76
1.25	8.0	3.68	3.72	4.60	4.65
1.25	15	5.60	5.07	7.00	6.34
1.25	25	8.72	9.04	10.9	11.3
0.85	0	4.25	4.77	3.61	4.05
0.85	8.0	5.01	4.24	4.26	3.60
0.85	15	5.23	5.43	4.45	4.62
0.85	25	9.28	9.91	7.89	8.42
0.65	0	5.78	5.02	3.76	3.26
0.65	8.0	4.98	5.24	3.24	3.41
0.65	15	7.56	8.24	4.91	5.36
0.65	25	10.8		7.02	

Uncompetitive inhibition:

K_i' (Modified Dixon) 2.62 x 10^{-3} M

3.72 x 10^{-3} M

4.04 x 10^{-3} M

12.1 x 10^{-3} M

13.9 x 10^{-3} M

Run 2:

[*(R)*-Cysteine sulfinic acid (79)] = 0 mM

[*(S)*-ASA] M x 10^{-4}	1/[*(S)*-ASA] M^{-1} x 10^{3}	Rate $\mu mol \cdot s^{-1} mg^{-1}$ x 10^{-1}	1/Rate $mg \cdot s \cdot \mu mol^{-1}$
2.50	4.00	3.66	2.73
2.50	4.00	4.21	2.37
1.25	8.00	2.96	3.38
1.25	8.00	2.62	3.81
0.85	11.8	2.35	4.25
0.85	11.8	3.30	3.03
0.65	15.4	1.73	5.78
0.65	15.4	1.68	5.94

Lineweaver-Burk plot $V_{max} = 7.37 \times 10^{-1}$ $\mu mol \cdot s^{-1} mg^{-1}$ $K_m = 1.92 \times 10^{-4}$ M

[*(R)*-Cysteine sulfinic acid (79)] = 10 mM

[*(S)*-ASA] M x 10^{-4}	1/[*(S)*-ASA] M^{-1} x 10^{3}	Rate $\mu mol \cdot s^{-1} mg^{-1}$ x 10^{-1}	1/Rate $mg \cdot s \cdot \mu mol^{-1}$
2.50	4.00	2.64	3.78
2.50	4.00	2.86	3.50
1.25	8.00	0.810*	12.3
1.25	8.00	2.14	4.67
0.85	11.8	1.91	5.23
0.85	11.8	2.24	4.46
0.65	15.4	1.88	5.32
0.65	15.4	1.68	5.94

Lineweaver-Burk plot $V_{max} = 3.30 \times 10^{-1}$ $\mu mol \cdot s^{-1} mg^{-1}$ $K_m = 0.547 \times 10^{-4}$ M

[*(R)*-Cysteine sulfinic acid (79)] = 20 mM

[*(S)*-ASA] M x 10^{-4}	1/[*(S)*-ASA] M^{-1} x 10^{3}	Rate $\mu mol \cdot s^{-1} mg^{-1}$ x 10^{-1}	1/Rate $mg \cdot s \cdot \mu mol^{-1}$
2.50	4.00	2.09	4.79
2.50	4.00	2.02	4.95
1.25	8.00	1.80	5.57
1.25	8.00	1.50	6.66
0.85	11.8	2.03	4.93
0.85	11.8	1.48	6.75
0.65	15.4	1.17	8.51
0.65	15.4	1.26	7.92

Lineweaver-Burk plot V_{max} = 2.66 x 10^{-1} $\mu mol \cdot s^{-1} mg^{-1}$ K_m = 0.679 x 10^{-4} M

[*(R)*-Cysteine sulfinic acid (79)] = 30 mM

[*(S)*-ASA] M x 10^{-4}	1/[*(S)*-ASA] M^{-1} x 10^{3}	Rate $\mu mol \cdot s^{-1} mg^{-1}$ x 10^{-1}	1/Rate $mg \cdot s \cdot \mu mol^{-1}$
2.50	4.00	1.16	8.62
2.50	4.00	1.36	7.37
1.25	8.00	0.923	10.8
1.25	8.00	1.30	7.70
0.85	11.8	0.741	13.5
0.85	11.8	0.894	11.2
0.65	15.4	0.902	11.1
0.65	15.4	0.831	12.0

Lineweaver-Burk plot V_{max} = 1.49 x 10^{-1} $\mu mol \cdot s^{-1} mg^{-1}$ K_m = 0.543 x 10^{-4} M

Determination of K_i:

[*(S)*-ASA] M x 10^{-4}	[*(R)*-Cysteine sulfinic acid] M x 10^{-3}	1/Rate $mg \cdot s \cdot \mu mol^{-1}$		[*(S)*-ASA]/Rate $s \cdot mg \cdot l^{-1}$ x 10^{2}	
2.50	0	2.73	2.37	6.83	5.93
2.50	10	3.78	3.50	9.45	8.75
2.50	20	4.79	4.95	12.0	12.4
2.50	30	8.62	7.37	21.6	18.4
1.25	0	3.38	3.81	4.23	4.76
1.25	10	12.3*	4.67	15.4*	5.84
1.25	20	5.57	6.66	6.96	8.33
1.25	30	10.8	7.70	13.5	9.63
0.85	0	4.25	3.03	3.61	2.58
0.85	10	5.23	4.46	4.44	3.79
0.85	20	4.93	6.75	4.19	5.74
0.85	30	13.5	11.2	11.5	9.52
0.65	0	5.78	5.94	3.76	3.86
0.65	10	5.32	5.94	3.46	3.86
0.65	20	8.51	7.92	5.53	5.15
0.65	30	11.1	12.0	7.22	7.80

Uncompetitive inhibition

K_i' (Modified Dixon) 6.13 x 10^{-3} M

6.84 x 10^{-3} M

8.64 x 10^{-3} M

Effect of *(S)*-aspartic acid (9) on DHDPS kinetics with respect to *(S)*-aspartate β-semialdehyde (11)

Assay:

NADPH (54 mM in dH_2O)	3.0 µl
Buffer (200 mM Mops pH 7.2 at 25 °C, pyruvate (17) 80 mM)	500 µl
dH_2O	137 µl
DHDPS (2.0 x 10^{-4} U, 4.8 x 10^{-4} mg)	10 µl
DHDPR (10 fold excess)	100 µl
(S)-ASA (11) (5.0 mM to 1.30 mM in dH_2O)	50 µl
(S)-Aspartic acid (9) (150 mM to 50 mM in dH_2O)	200 µl
	1.00 ml

The reaction was initiated in the cuvette by the addition of freshly prepared *(S)*-aspartate β-semialdehyde (11), mixed by inversion of the cuvette. ΔA_{340} was measured over 300 seconds at 30 °C, blanked against dH_2O.

Run 1:

[*(S)*-Aspartic acid (9)] = 0 mM

[*(S)*-ASA] M x 10^{-4}	1/[*(S)*-ASA] M^{-1} x 10^{3}	Rate $\mu mol \cdot s^{-1} mg^{-1}$ x 10^{-1}	1/Rate $mg \cdot s \cdot \mu mol^{-1}$
2.50	4.00	3.60	2.78
2.50	4.00	3.92	2.55
1.25	8.00	2.27	4.41
1.25	8.00	3.01	3.32
0.85	11.8	2.22	4.51
0.85	11.8	2.21	4.52
0.65	15.4	1.88	5.32
0.65	15.4	1.60	6.25

Lineweaver-Burk plot V_{max} = 6.14 x 10^{-1} $\mu mol \cdot s^{-1} mg^{-1}$ K_m = 1.62 x 10^{-4} M

[*(S)*-Aspartic acid (9)] = 10 mM

[*(S)*-ASA] M x 10^{-4}	1/[*(S)*-ASA] M^{-1} x 10^{3}	Rate $\mu mol \cdot s^{-1} mg^{-1}$ x 10^{-1}	1/Rate $mg \cdot s \cdot \mu mol^{-1}$
2.50	4.00	1.95	5.12
2.50	4.00	2.22	4.51
1.25	8.00	1.57	6.39
1.25	8.00	1.33	7.55
0.85	11.8	1.84	5.43
0.85	11.8	1.01	9.86
0.65	15.4	0.943	10.6
0.65	15.4	1.06	9.42

Lineweaver-Burk plot V_{max} = 3.15 x 10^{-1} $\mu mol \cdot s^{-1} mg^{-1}$ K_m = 1.35 x 10^{-4} M

[*(S)*-Aspartic acid (9)] = 20 mM

[*(S)*-ASA] M x 10^{-4}	1/[*(S)*-ASA] M^{-1} x 10^{3}	Rate $\mu mol \cdot s^{-1} mg^{-1}$ x 10^{-1}	1/Rate $mg \cdot s \cdot \mu mol^{-1}$
2.50	4.00	2.61	3.83
2.50	4.00	2.71	3.68
1.25	8.00	1.99	5.01
1.25	8.00	1.32	7.59
0.85	11.8	0.898	11.1
0.85	11.8	0.727	13.8
0.65	15.4	1.01	9.90
0.65	15.4	0.765	13.1

Lineweaver-Burk plot V_{max} = 11.4 x 10^{-1} $\mu mol \cdot s^{-1} mg^{-1}$ K_m = 8.84 x 10^{-4} M

[*(S)*-Aspartic acid (9)] = 30 mM

[*(S)*-ASA] M x 10^{-4}	1/[*(S)*-ASA] M^{-1} x 10^{3}	Rate $\mu mol \cdot s^{-1} mg^{-1}$ x 10^{-1}	1/Rate $mg \cdot s \cdot \mu mol^{-1}$
2.50	4.00	1.47	6.79
2.50	4.00	2.39	4.19
1.25	8.00	1.61	6.22
1.25	8.00	1.51	6.62
0.85	11.8	1.34	7.46
0.85	11.8	0.855	11.7
0.65	15.4	1.06	9.47
0.65	15.4	0.805	12.4

Lineweaver-Burk plot V_{max} = 3.24 x 10^{-1} $\mu mol \cdot s^{-1} mg^{-1}$ K_m = 1.66 x 10^{-4} M

Determination of K_i:

[(*S*)-ASA] M x 10^{-4}	[(*S*)-Aspartic acid] M x 10^{-3}	1/Rate $mg \cdot s \cdot \mu mol^{-1}$		[(*S*)-ASA]/Rate $s \cdot mg \cdot l^{-1}$ x 10^{2}	
2.50	0	2.78	2.55	6.95	6.38
2.50	10	5.12	4.51	12.8	11.3
2.50	20	3.83	3.68	9.58	9.20
2.50	30	6.79	4.19	17.0	10.5
1.25	0	4.41	3.32	5.51	4.15
1.25	10	6.39	7.55	7.99	9.44
1.25	20	5.01	7.59	6.26	9.49
1.25	30	6.22	6.62	7.78	8.29
0.85	0	4.51	4.52	3.83	3.84
0.85	10	5.43	9.89	4.62	8.41
0.85	20	11.1	13.8	9.44	11.8
0.85	30	7.46	11.7	6.34	9.95
0.65	0	5.32	6.25	3.46	4.06
0.65	10	10.6	9.42	6.89	6.12
0.65	20	9.90	13.1	6.44	8.52
0.65	30	9.47	12.4	6.16	8.06

The type of inhibition could not be determined unambiguously.

Run 2:

[*(S)*-Aspartic acid (9)] = 0 mM

[*(S)*-ASA] M x 10^{-4}	1/[*(S)*-ASA] M^{-1} x 10^{3}	Rate $\mu mol \cdot s^{-1} mg^{-1}$ x 10^{-1}	1/Rate $mg \cdot s \cdot \mu mol^{-1}$
2.50	4.00	3.93	2.55
2.50	4.00	4.23	2.36
1.25	8.00	3.01	3.32
1.25	8.00	2.70	3.70
0.85	11.8	2.41	4.15
0.85	11.8	2.38	4.20
0.65	15.4	1.99	5.03
0.65	15.4	1.89	5.28

Lineweaver-Burk plot V_{max} = 6.40 x 10^{-1} $\mu mol \cdot s^{-1} mg^{-1}$ K_m = 1.48 x 10^{-4} M

[*(S)*-Aspartic acid (9)] = 10 mM

[*(S)*-ASA] M x 10^{-4}	1/[*(S)*-ASA] M^{-1} x 10^{3}	Rate $\mu mol \cdot s^{-1} mg^{-1}$ x 10^{-1}	1/Rate $mg \cdot s \cdot \mu mol^{-1}$
2.50	4.00	3.12	3.21
2.50	4.00	3.72	2.69
1.25	8.00	2.72	3.68
1.25	8.00	2.59	3.86
0.85	11.8	1.97	5.07
0.85	11.8	2.09	4.79
0.65	15.4	1.88	5.33
0.65	15.4	1.60	6.27

Lineweaver-Burk plot V_{max} = 5.38 x 10^{-1} $\mu mol \cdot s^{-1} mg^{-1}$ K_m = 1.37 x 10^{-4} M

[(*S*)-Aspartic acid (9)] = 20 mM

[(*S*)-ASA] M x 10^{-4}	1/[(*S*)-ASA] M^{-1} x 10^{3}	Rate $\mu mol \cdot s^{-1} mg^{-1}$ x 10^{-1}	1/Rate $mg \cdot s \cdot \mu mol^{-1}$
2.50	4.00	2.18	4.58
2.50	4.00	2.41	4.16
1.25	8.00	1.73	5.78
1.25	8.00	1.19	8.43
0.85	11.8	1.45	6.89
0.85	11.8	1.57	6.39
0.65	15.4	1.35	7.43
0.65	15.4	1.32	7.60

Lineweaver-Burk plot V_{max} = 2.46 x 10^{-1} $\mu mol \cdot s^{-1} mg^{-1}$ K_m = 0.586 x 10^{-4} M

[(*S*)-Aspartic acid (9)] = 30 mM

[(*S*)-ASA] M x 10^{-4}	1/[(*S*)-ASA] M^{-1} x 10^{3}	Rate $\mu mol \cdot s^{-1} mg^{-1}$ x 10^{-1}	1/Rate $mg \cdot s \cdot \mu mol^{-1}$
2.50	4.00	1.84	5.43
2.50	4.00	1.81	5.53
1.25	8.00	1.33	7.53
1.25	8.00	1.14	8.77
0.85	11.8	0.895	11.2
0.85	11.8	0.975	10.3
0.65	15.4	0.766	13.1
0.65	15.4	0.744	13.4

Lineweaver-Burke plot V_{max} = 3.67 x 10^{-1} $\mu mol \cdot s^{-1} mg^{-1}$ K_m = 2.50 x 10^{-4} M

Determination of K_i:

[(*S*)-ASA] M x 10^{-4}	[(*S*)-Aspartic acid] M x 10^{-3}	1/Rate mg·s·μmol^{-1}		[(*S*)-ASA]/Rate s·mg·l^{-1} x 10^{2}	
2.50	0	2.55	2.36	6.38	5.90
2.50	10	3.21	2.69	8.03	6.73
2.50	20	4.58	4.16	11.5	10.4
2.50	30	5.43	5.53	13.6	13.8
1.25	0	3.32	3.70	4.15	4.63
1.25	10	3.68	3.86	4.60	4.83
1.25	20	5.78	8.43	7.23	10.5
1.25	30	7.53	8.77	9.41	11.0
0.85	0	4.15	4.20	3.53	3.57
0.85	10	5.07	4.79	4.31	4.07
0.85	20	6.89	6.39	5.86	5.43
0.85	30	11.2	10.3	9.52	8.76
0.65	0	5.03	5.28	3.27	3.43
0.65	10	5.33	6.27	3.46	4.08
0.65	20	7.43	7.60	4.83	4.94
0.65	30	13.1	13.4	8.52	8.71

Mixed inhibition:

K_i (Dixon)	0.868 x 10^{-2} M	K_i' (Modified Dixon)	2.12 x 10^{-2} M
	1.07 x 10^{-2} M		2.53 x 10^{-2} M
	1.13 x 10^{-2} M		2.69 x 10^{-2} M
	1.15 x 10^{-2} M		3.20 x 10^{-2} M
	1.19 x 10^{-2} M		3.37 x 10^{-2} M
	1.36 x 10^{-2} M		3.87 x 10^{-2} M

Effect of *(S)*-glutamic acid (81) on DHDPS kinetics with respect to *(S)*-aspartate β-semialdehyde (11)

Assay:

NADPH (54 mM in dH_2O)	3.0 µl
Buffer (200 mM Mops pH 7.2 at 25 °C, pyruvate (17) 80 mM)	500 µl
dH_2O	137 µl
DHDPS (2.0×10^{-4} U, 4.8×10^{-4} mg)	10 µl
DHDPR (10 fold excess)	100 µl
(S)-ASA (11) (5.0 mM to 1.30 mM in dH_2O)	50 µl
(S)-Glutamic acid (81) (150 mM to 50 mM in dH_2O)	200 µl
	1.00 ml

The reaction was initiated in the cuvette by the addition of freshly prepared *(S)*-aspartate β-semialdehyde (11), mixed by inversion of the cuvette. ΔA_{340} was measured over 300 seconds at 30 °C, blanked against dH_2O.

Run 1:

[*(S)*-Glutamic acid (81)] = 0 mM

[*(S)*-ASA] M x 10^{-4}	1/[*(S)*-ASA] M^{-1} x 10^{3}	Rate $\mu mol \cdot s^{-1} mg^{-1}$ x 10^{-1}	1/Rate $mg \cdot s \cdot \mu mol^{-1}$
2.50	4.00	3.42	2.92
2.50	4.00	3.06	3.27
1.25	8.00	2.13	4.70
1.25	8.00	2.92	3.43
0.85	11.8	1.77	5.66
0.85	11.8	2.19	4.57
0.65	15.4	1.69	5.90
0.65	15.4	1.63	6.15

Lineweaver-Burk plot $V_{max} = 4.91 \times 10^{-1}$ $\mu mol \cdot s^{-1} mg^{-1}$ $K_m = 1.27 \times 10^{-4}$ M

[(*S*)-Glutamic acid (81)] = 10 mM

[(*S*)-ASA] M x 10^{-4}	1/[(*S*)-ASA] M^{-1} x 10^{3}	Rate $\mu mol \cdot s^{-1} mg^{-1}$ x 10^{-1}	1/Rate $mg \cdot s \cdot \mu mol^{-1}$
2.50	4.00	2.56	3.91
2.50	4.00	3.48	2.87
1.25	8.00	2.20	4.54
1.25	8.00	2.39	4.19
0.85	11.8	1.75	5.72
0.85	11.8	1.89	5.30
0.65	15.4	1.49	6.72
0.65	15.4	2.03	4.94

Lineweaver-Burk plot V_{max} = 3.87 x 10^{-1} $\mu mol \cdot s^{-1} mg^{-1}$ K_m = 0.865 x 10^{-4} M

[(*S*)-Glutamic acid (81)] = 20 mM

[(*S*)-ASA] M x 10^{-4}	1/[(*S*)-ASA] M^{-1} x 10^{3}	Rate $\mu mol \cdot s^{-1} mg^{-1}$ x 10^{-1}	1/Rate $mg \cdot s \cdot \mu mol^{-1}$
2.50	4.00	2.16	4.62
2.50	4.00	3.24	3.09
1.25	8.00	2.26	4.43
1.25	8.00	2.14	4.66
0.85	11.8	1.60	6.25
0.85	11.8	1.60	6.23
0.65	15.4	1.37	7.31
0.65	15.4	1.31	7.62

Lineweaver-Burk plot V_{max} = 4.34 x 10^{-1} $\mu mol \cdot s^{-1} mg^{-1}$ K_m = 1.43 x 10^{-4} M

[(*S*)-Glutamic acid (81)] = 30 mM

[(*S*)-ASA] M x 10^{-4}	1/[(*S*)-ASA] M^{-1} x 10^{3}	Rate $\mu mol \cdot s^{-1} mg^{-1}$ x 10^{-1}	1/Rate $mg \cdot s \cdot \mu mol^{-1}$
2.50	4.00	0.947	10.6
2.50	4.00	1.03	9.73
1.25	8.00	1.31	7.66
1.25	8.00	1.37	7.31
0.85	11.8	0.734	13.6
0.85	11.8	0.813	12.3
0.65	15.4	0.923	10.8
0.65	15.4	0.811	12.3

Lineweaver-Burk plot V_{max} = 1.24 x 10^{-1} $\mu mol \cdot s^{-1} mg^{-1}$ K_m = 0.311 x 10^{-4} M

Determination of K_i:

[(*S*)-ASA] M x 10^{-4}	[(*S*)-Glutamic acid] M x 10^{-3}	1/Rate $mg \cdot s \cdot \mu mol^{-1}$		[(*S*)-ASA]/Rate $s \cdot mg \cdot l^{-1}$ x 10^{2}	
2.50	0	2.92	3.27	7.30	8.18
2.50	10	3.91	2.87	9.78	7.18
2.50	20	4.62	3.09	11.6	7.73
2.50	30	10.6	9.73	26.5	24.3
1.25	0	4.70	3.43	5.88	4.29
1.25	10	4.54	4.19	5.68	5.24
1.25	20	4.43	4.66	5.54	5.83
1.25	30	7.66	7.31	9.58	9.14
0.85	0	5.66	4.57	4.81	3.38
0.85	10	5.72	5.30	4.86	4.51
0.85	20	6.25	6.23	5.31	5.30
0.85	30	13.6	12.3	11.6	10.5
0.65	0	5.90	6.15	3.84	4.00
0.65	10	6.72	4.94	4.37	3.21
0.65	20	7.31	7.62	4.75	4.95
0.65	30	12.3	12.3	7.02	8.00

Uncompetitive inhibition:

K_i' (Modified Dixon) 4.37 x 10^{-3} M

4.35 x 10^{-3} M

Run 2:

[*(S)*-Glutamic acid (81)] = 0 mM

[*(S)*-ASA] M x 10^{-4}	1/[*(S)*-ASA] M^{-1} x 10^{3}	Rate $\mu mol \cdot s^{-1} mg^{-1}$ x 10^{-1}	1/Rate $mg \cdot s \cdot \mu mol^{-1}$
2.50	4.00	3.72	2.69
2.50	4.00	3.71	2.70
1.25	8.00	2.55	3.93
1.25	8.00	2.56	3.91
0.85	11.8	1.91	5.23
0.85	11.8	1.92	5.22
0.65	15.4	1.74	5.76
0.65	15.4	1.59	6.27

Lineweaver-Burk plot V_{max} = 6.43 x 10^{-1} $\mu mol \cdot s^{-1} mg^{-1}$ K_m = 1.91 x 10^{-4} M

[*(S)*-Glutamic acid (81)] = 10 mM

[*(S)*-ASA] M x 10^{-4}	1/[*(S)*-ASA] M^{-1} x 10^{3}	Rate $\mu mol \cdot s^{-1} mg^{-1}$ x 10^{-1}	1/Rate $mg \cdot s \cdot \mu mol^{-1}$
2.50	4.00	2.91	3.44
2.50	4.00	3.25	3.07
1.25	8.00	1.97	5.08
1.25	8.00	2.07	4.84
0.85	11.8	1.73	5.79
0.85	11.8	1.75	5.71
0.65	15.4	1.29	7.78
0.65	15.4	1.51	6.64

Lineweaver-Burk plot V_{max} = 4.93 x 10^{-1} $\mu mol \cdot s^{-1} mg^{-1}$ K_m = 6.09 x 10^{-4} M

[(*S*)-Glutamic acid (81)] = 20 mM

[(*S*)-ASA] M x 10^{-4}	1/[(*S*)-ASA] M^{-1} x 10^{3}	Rate $\mu mol \cdot s^{-1} mg^{-1}$ x 10^{-1}	1/Rate $mg \cdot s \cdot \mu mol^{-1}$
2.50	4.00	2.13	4.69
2.50	4.00	2.36	4.24
1.25	8.00	1.65	6.06
1.25	8.00	1.53	6.54
0.85	11.8	1.38	7.25
0.85	11.8	1.40	7.17
0.65	15.4	1.19	8.40
0.65	15.4	1.15	8.73

Lineweaver-Burk plot V_{max} = 3.05 x 10^{-1} $\mu mol \cdot s^{-1} mg^{-1}$ K_m = 1.05 x 10^{-4} M

[(*S*)-Glutamic acid (81)] = 25 mM

[(*S*)-ASA] M x 10^{-4}	1/[(*S*)-ASA] M^{-1} x 10^{3}	Rate $\mu mol \cdot s^{-1} mg^{-1}$ x 10^{-1}	1/Rate $mg \cdot s \cdot \mu mol^{-1}$
2.50	4.00	1.80	5.55
2.50	4.00	1.66	6.04
1.25	8.00	1.24	8.06
1.25	8.00	1.10	9.07
0.85	11.8	0.957	10.4
0.85	11.8	0.863	11.5
0.65	15.4	0.942	10.6
0.65	15.4	0.844	11.8

Lineweaver-Burk plot V_{max} = 2.20 x 10^{-1} $\mu mol \cdot s^{-1} mg^{-1}$ K_m = 0.997 x 10^{-4} M

Determination of K_i:

[(*S*)-ASA] M x 10^{-4}	[(*S*)-Glutamic acid] M x 10^{-3}	1/Rate mg·s·μmol^{-1}		[(*S*)-ASA]/Rate s·mg·l^{-1} x 10^{2}	
2.50	0	2.69	2.70	6.73	6.35
2.50	10	3.44	3.07	8.60	7.68
2.50	20	4.69	4.24	11.7	10.6
2.50	25	5.55	6.04	13.9	15.1
1.25	0	3.93	3.91	4.91	4.89
1.25	10	5.08	4.84	6.35	6.05
1.25	20	6.06	6.54	7.58	8.18
1.25	25	8.06	9.07	10.1	11.3
0.85	0	5.23	5.22	4.45	4.44
0.85	10	5.79	5.71	4.92	4.85
0.85	20	7.25	7.17	6.16	6.09
0.85	25	10.4	11.5	8.84	9.78
0.65	0	5.76	6.27	3.74	4.08
0.65	10	7.78	6.64	5.06	4.32
0.65	20	8.40	8.73	5.46	5.67
0.65	25	10.6	11.8	6.89	7.67

Uncompetitive inhibition:

K_i' (Modified Dixon) 0.88 x 10^{-2} M

1.22 x 10^{-2} M

1.56 x 10^{-2} M

1.57 x 10^{-2} M

1.57 x 10^{-2} M

References

1. HMBC experiments were performed by J.W. Blunt.
2. S.J. Thomas *'Studies of Lysine Biosynthesis'* M.Sc., University of Canterbury (1994).
3. S. Wilkinson *J. Chem. Soc.* **154**, 104 (1951).
4. A.I. Vogel *'A Textbook of Practical Organic Chemistry'* 3rd ed., Longman, London, (1956).
5. *'Dictionary of Organic Compound'* 5th ed., C-03623 (1982).
6. *'Dictionary of Organic Compound'* 5th ed., C-03681 (1982).
7. M.J. Mintz, C. Walling *Org. Synth.* Coll. Vol. **V**, 184 (1973).
8. H.E. Baumgarten, J.M. Petersen *Org. Synth.* Coll. Vol. **V**, 909 (1973).
9. *'Dictionary of Organic Compound'* 5th ed., A-01343 (1982).
10. *Chemical Abstracts, Am. Chem. Soc.* **14**, 3068 (1920).
11. P.F. Frankland, F.H. Gardner *J. Soc. Chem. Ind.* **89**, 257 (1920).
12. C. Golumbic, J.S. Fruton, M. Bergmann *J. Org. Chem.* **11**, 518 (1946).
13. Aldrich Chemical Company Catalogue.
14. C.R. Johnson, M.P. Westrick *Meth. Enz.* **143**, 281 (1987).
15. O.W. Griffith *Meth. Enz.* **143**, 274 (1987).

Experimental Part IV

Analogues of Dipicolinate Species

DHDPS activity at high *(S)*-aspartate β-semialdehyde (11) and high pyruvate (17) concentrations

Assay:

NADPH (54 mM in dH_2O)	3.0 µl
Buffer (200 mM Mops pH 7.2 at 25 °C)	500 µl
dH_2O	287 µl
DHDPS (2.0×10^{-4} U, 4.8×10^{-4} mg)	10 µl
DHDPR (10 fold excess)	100 µl
(S)-ASA (11) (100 mM to 10 mM in dH_2O)	100 µl
Pyruvate (17) (100 mM to 10 mM in dH_2O)	100 µl
	1.00 ml

The reaction was initiated in the cuvette by addition of freshly prepared *(S)*-aspartate β-semialdehyde (11), mixed by inversion of the cuvettte. ΔA_{340} was measured over 300 seconds at 30 °C, blanked against dH_2O.

[*(S)*-ASA] = [Pyruvate] M x 10^{-3}	Rate µmol·$s^{-1}mg^{-1}$ x 10^{-1}
1.00	6.55
1.00	9.40
2.50	9.34
2.50	9.87
5.00	11.8
5.00	13.4
10.0	13.7

Comparison of Mops and phosphate buffers

Assay:

NADPH (54 mM in dH_2O)	3 µl
Buffer (1M Tris.HCl pH 8.5 at 25 °C, 80 mM pyruvate (17))	500 µl
dH_2O	337 µl
DHDPS (2.0×10^{-4} U, 4.8×10^{-4} mg)	10 µl
DHDPR (10 fold excess)	100 µl
(S)-ASA (11) (5.0 mM)	50 µl
	1.00 ml

The reaction was initiated in the cuvette by addition of freshly prepared *(S)*-aspartate β-semialdehyde (11), mixed by inversion of the cuvettte. ΔA_{340} was measured over 300 seconds at 30 °C, blanked against dH_2O.

DHDPS kinetics using 200 mM Mops pH 7.2 at 25 °C

[*(S)*-ASA] M x 10^{-4}	1/[*(S)*-ASA] M^{-1} x 10^{3}	Rate $\mu mol \cdot s^{-1} mg^{-1}$ x 10^{-1}	1/Rate $mg \cdot s \cdot \mu mol^{-1}$
2.50	4.00	4.16	2.40
2.50	4.00	5.14	1.95
1.50	6.67	4.33	2.31
1.50	6.67	4.31	2.32
1.00	10.0	2.78	3.62
1.00	10.0	3.28	3.04
0.80	12.5	2.74	3.65
0.80	12.5	2.53	3.95
0.60	16.7	2.31	4.33
0.60	16.7	2.47	4.05

Lineweaver-Burk plot $V_{max} = 7.08 \times 10^{-1}$ $\mu mol \cdot s^{-1} mg^{-1}$ $K_m = 1.24 \times 10^{-4}$ M

DHDPS kinetics using 200 mM Phosphate buffer pH 7.2 at 25 °C

[*(S)*-ASA] M x 10^{-4}	1/[*(S)*-ASA] M^{-1} x 10^{3}	Rate $\mu mol \cdot s^{-1} mg^{-1}$ x 10^{-1}	1/Rate $mg \cdot s \cdot \mu mol^{-1}$
2.50	4.00	9.05	1.10
2.50	4.00	4.11	2.43
1.25	8.00	3.56	2.81
1.25	8.00	3.33	3.00
0.85	11.8	3.33	3.00
0.85	11.8	2.95	3.39
0.65	15.4	2.63	3.80
0.65	15.4	2.56	3.91

Lineweaver-Burk plot $V_{max} = 8.11 \times 10^{-1}$ $\mu mol \cdot s^{-1} mg^{-1}$ $K_m = 1.41 \times 10^{-4}$ M

NMR studies on the enzymatic reaction of DHDPS

General method

(S)-Aspartate β-semialdehyde (11) and pyruvate (17) in 500 mM phosphate buffer pH 7.2 at 25 °C were analysed by ^{1}H NMR. The phosphate buffer was made up at pH 7.4 which dropped to pH 7.2 on the addition of the *(S)*-aspartate β-semialdehyde (11) which was present as the trifluoroacetate salt. DHDPS enzyme was then added and the reaction followed by ^{1}H NMR (300 MHz, D_2O).

Run 1

(S)-Aspartate β-semialdehyde (11) (10 μmol, 2.5 mg)
Pyruvate (17) (10 μmol, 1.1 mg)
500 mM phosphate buffer pH 7.2 at 25 °C (180 μl in D_2O)
DHDPS enzyme (20 μl, concentration of 1.2 $mgml^{-1}$) was added.

Time	Substrates	New resonaces	Colour
10 mins	*(S)*-ASA and pyruvate present	δ_H 5.92, 7.15 ppm	Clear
40 mins	*(S)*-ASA and pyruvate present	δ_H 5.92, 7.15, 7.69 - 7.87 (m), 8.27 - 8.49 (m) ppm	Clear
170 mins	No *(S)*-ASA Pyruvate present	δ_H 5.92, 7.15, 7.69 - 7.87 (m), 8.27 - 8.49 (m) ppm	Light red

Run 2

(S)-Aspartate β-semialdehyde (11) (10 μmol, 2.5 mg).
Pyruvate (17) (10 μmol, 1.1 mg).
500 mM phosphate buffer pH 7.2 at 25 °C (170 μl in D_2O).
DHDPS enzyme (30 μl, dialysed into D_2O) was added.
Performed under nitrogen.
Changes occurred in the reaction and in the control.

Time	Substrates	New resonaces	Colour
10 mins	*(S)*-ASA and pyruvate present	δ_H 7.8 - 8.6 ppm	Clear
15 mins	*(S)*-ASA -C**H**$_2$CHNH$_2$ peaks have decreased Pyruvate present	δ_H 7.8 - 8.6 ppm	Clear
85 mins	*(S)*-ASA -C**H**$_2$CHNH$_2$ peaks have decreased Pyruvate present	δ_H 7.5 - 8.0 (m), 8.25 - 8.4 (m), 8.4 - 8.55 (m) ppm	Light red
24 hours	No *(S)*-ASA or pyruvate present	δ_H 7.5 - 8.0 (m), 8.25 - 8.4 (m), 8.4 - 8.55 (m) ppm	Red

Run 3

(S)-Aspartate β-semialdehyde (11) (10 μmol, 2.5 mg)

Pyruvate (17) (10 μmol, 1.1 mg)

500 mM phosphate buffer pH 7.2 at 25 °C (170 μl in D_2O)

DHDPS enzyme (30 μl, concentration of 0.201 $mgml^{-1}$)

Time	Substrates	ΔA_{340} from the coupled assay
5 mins	*(S)*-ASA and pyruvate present	5.26 x 10^{-3} Aus^{-1}
15 mins	*(S)*-ASA present Pyruvate resonace has decreased	2.12 x 10^{-3} Aus^{-1}
25 mins	*(S)*-ASA -C**H**(OH)$_2$ have disappeared Pyruvate resonace has decreased	0 Aus^{-1}
40 mins	*(S)*-ASA -C**H**(OH)$_2$ have disappeared Pyruvate resonace has decreased	0 Aus^{-1}
60 mins	*(S)*-ASA -C**H**(OH)$_2$ have disappeared Pyruvate resonace has decreased	0 Aus^{-1} Purple (semi-quantitative) assay gave a negative result

Run 4

(S)-Aspartate β-semialdehyde (11) (20 μmol, 5.0 mg)
Pyruvate (17) (20 μmol, 2.2 mg)
500 mM phosphate buffer pH 7.2 at 25 °C (340 μl in D_2O).
DHDPS enzyme (60 μl) was added.

Time	Substrates	New resonances	Purple assay
1 min	*(S)*-ASA and pyruvate present		Positive
10 mins	*(S)*-ASA and pyruvate are disappearing		Positive
20 mins	*(S)*-ASA and pyruvate are disappearing	δ_H 3.4 - 4.2 ppm	Positive
40 mins	*(S)*-ASA and pyruvate are disappearing	δ_H 1.6 - 2.6, 3.4 - 4.4 ppm	Positive
6 hrs	*(S)*-ASA is disappearing No pyruvate	δ_H 1.6 - 2.6, 3.4 - 4.4 ppm	Positive

Inhibiton of DHDPS by cyclic compounds

Assay:

NADPH (54 mM in dH_2O)	3.0 μl
Buffer (200 mM Mops pH 7.2 at 25 °C, pyruvate (17) 80 mM)	500 μl
dH_2O	237 μl
DHDPS (2.0×10^{-4} U, 4.8×10^{-4} mg)	10 μl
DHDPR (10 fold excess)	100 μl
(S)-ASA (11) (5.0 mM in dH_2O)	50 μl
Inhibitor (appropriate concentration, in methanol if required)	100 μl
	1.00 ml

The reaction was initiated in the cuvette by addition of freshly prepared *(S)*-aspartate β-semialdehyde (11), mixed by inversion of the cuvettte. ΔA_{340} was measured over 300 seconds at 30 °C, blanked against dH_2O, containing 10% methanol if required. *(S)*-Aspartate β-semialdehyde was present in a concentration of 0.25 mM. The activity is the rate of reaction with inhibitor present relative to the rate of reaction in the absence of the inhibitor.

Compound	Concentration mM	Activity %
2-Aminoacetophenone (94)	10	0
in 10% methanol	1.0	1.4
	0.1	92.8
Benzoic acid (93)	50	14.7
in 10% methanol	10	61.1
	1.0	95.0
Dipicolinic acid (36)	2.5	83.6
	1.0	97.8
Isophthalic acid (41)	10	72.2
	5.0	94.8
2-Methylpyridine (90)	100	100
Morpholine (98)	100	100
Nicotinic acid (91)	50	14.2
	10	100
Phthalic acid (96)	12.5	5.1
in 10% methanol	10	29.5
	1.0	100
Phthalimide (95)	1.0	77.0
in 10% methanol	0.1	88.2
Picolinic acid (42)	100	9.4
	50	20.0
	10	95.0
	1.0	100
Piperidine (97)	100	0
	10	100
Pyridine (89)	100	100
Pyridoxal 5-phosphate (92)	2.5	5.1
	1.0	47.2
	0.1	100

Inhibition of DHDPR by cyclic compounds

Assay:

NADPH (54 mM in dH_2O)	3.0 µl
Buffer (200 mM Mops pH 7.2 at 25 °C, pyruvate (17) 80 mM)	500 µl
dH_2O	237 µl
DHDPS (10 fold excess)	100 µl
(S)-ASA (11) (5.0 mM in dH_2O)	50 µl
DHDPR (2.25×10^{-4} U, 1.0×10^{-4} mg)	10 µl
Inhibitor (appropriate concentration, in methanol if required)	100 µl
	1.00 ml

The *(S)*-aspartate β-semialdehyde was added prior to initiation of the reaction to form the substrate. The reaction was then initiated in the cuvette by addition of DHDPR, mixed by inversion of the cuvettte. ΔA_{340} was measured over 300 seconds at 30 °C, blanked against dH_2O, containing 10% methanol if required. The activity is the rate of reaction with inhibitor present relative to the rate of reaction in the absence of the inhibitor.

Compound	Concentration mM	Activity %
2-Aminoacetophenone (94)	10	19.7
in 10% methanol	1.0	17.1
	0.1	100
Benzoic acid (93)	50	0
in 10% methanol	10	100
Dipicolinic acid (36)	2.5	19.7
	1.0	25.1
	0.1	90.1
	0.01	100
Isophthalic acid (41)	2.5	78.8
in 10% methanol	1.0	100
2-Methylpyridine (90)	100	100
Morpholine (98)	100	15.7
	50	55.2
	25	77.4
	1.0	100

Compound	Concentration mM	Activity %
Nicotinic acid (91)	50	45.0
	10	77.5
	1.0	100
Phthalic acid (96) in 10% methanol	10	28.3
	1.0	69.9
	0.1	100
Phthalimide (95) in 10% methanol	1.0	100
Picolinic acid (42)	100	39.7
	50	78.1
	10	100
Piperidine (97)	100	0
	50	11.5
	10	53.5
	1.0	100
Pyridine (89)	100	100
Pyridoxal 5-phosphate (92)	2.5	0
	1.0	10.8
	0.1	100

Effect of dipicolinic acid (36) on DHDPR kinetics with respect the substrate

Assay:

NADPH (54 mM in dH_2O)	3.0 µl
Buffer (200 mM Mops pH 7.2 at 25 °C, pyruvate (17) 80 mM)	500 µl
dH_2O	237 µl
DHDPS (10 fold excess)	100 µl
(R,S)-ASA (11) (3.0 mM to 10 mM in dH_2O)	50 µl
DHDPR (2.25×10^{-4} U, 1.0×10^{-4} mg)	10 µl
Dipicolinic acid (36) (1.0 mM to 10 mM in dH_2O)	100 µl
	1.00 ml

The *(R,S)*-aspartate β-semialdehyde was added prior to initiation of the reaction to form the substrate. The reaction was then initiated in the cuvette by addition of DHDPR, mixed by inversion of the cuvettte. ΔA_{340} was measured over 300 seconds at 30 °C, blanked against dH_2O.

Run 1:

[Dipicolinic acid (36)] = 0 mM

[DHDPA] M x 10^{-4}	1/[DHDPA] M^{-1} x 10^{3}	Rate $\mu mol \cdot s^{-1} mg^{-1}$	1/Rate $mg \cdot s \cdot \mu mol^{-1}$
2.50	4.00	2.09	0.478
2.50	4.00	2.42	0.412
1.50	6.67	1.12	0.895
1.50	6.67	2.12	0.472
1.00	10.0	1.65	0.672
1.00	10.0	1.25	0.798
0.75	13.3	1.14	0.876
0.75	13.3	1.09	0.916

Lineweaver-Burk plot V_{max} = 3.20 $\mu mol \cdot s^{-1} mg^{-1}$ K_m = 1.41 x 10^{-4} M

[Dipicolinic acid (36)] = 0.10 mM

[DHDPA] M x 10^{-4}	1/[DHDPA] M^{-1} x 10^{3}	Rate $\mu mol \cdot s^{-1} mg^{-1}$	1/Rate $mg \cdot s \cdot \mu mol^{-1}$
2.50	4.00	2.50	0.400
2.50	4.00	2.03	0.493
1.50	6.67	1.69	0.593
1.50	6.67	1.66	0.602
1.00	10.0	1.29	0.773
1.00	10.0	1.13	0.884
0.75	13.3	1.08	0.926
0.75	13.3	0.753	1.33

Lineweaver-Burk plot V_{max} = 7.77 $\mu mol \cdot s^{-1} mg^{-1}$ K_m = 5.68 x 10^{-4} M

[Dipicolinic acid (36)] = 0.40 mM

[DHDPA] M x 10^{-4}	1/[DHDPA] M^{-1} x 10^{3}	Rate $\mu mol \cdot s^{-1} mg^{-1}$	1/Rate $mg \cdot s \cdot \mu mol^{-1}$
2.50	4.00	1.41	0.711
2.50	4.00	2.01	0.498
1.50	6.67	1.50	0.667
1.50	6.67	1.49	0.671
1.00	10.0	0.804	1.24
1.00	10.0	0.838	1.19
0.75	13.3	0.583	1.72
0.75	13.3	0.920	1.09

Lineweaver-Burk plot V_{max} = 6.05 $\mu mol \cdot s^{-1} mg^{-1}$ K_m = 5.75 x 10^{-4} M

[Dipicolinic acid (36)] = 0.80 mM

[DHDPA] M x 10^{-4}	1/[DHDPA] M^{-1} x 10^{3}	Rate $\mu mol \cdot s^{-1} mg^{-1}$	1/Rate $mg \cdot s \cdot \mu mol^{-1}$
2.50	4.00	1.14	0.880
2.50	4.00	1.56	0.640
1.50	6.67	1.14	0.874
1.50	6.67	1.11	0.905
1.00	10.0	0.690	1.45
1.00	10.0	0.576	1.74
0.75	13.3	0.308*	3.25*
0.75	13.3	0.499	2.00

Lineweaver-Burk plot V_{max} = 10.1 $\mu mol \cdot s^{-1} mg^{-1}$ K_m = 14.4 x 10^{-4} M

Determination of K_i:

[DHDPA] M x 10^{-4}	[Dipicolinic acid] M x 10^{-3}	1/Rate $mg \cdot s \cdot \mu mol^{-1}$		[DHDPA]/Rate $s \cdot mg \cdot l^{-1}$ x 10^2	
2.50	0	0.478	0.412	1.20	1.03
2.50	0.10	0.400	0.493	1.00	1.23
2.50	0.40	0.711	0.498	1.78	1.25
2.50	0.80	0.880	0.640	2.20	1.60
1.50	0	0.895	0.472	1.34	0.708
1.50	0.10	0.583	0.602	0.890	0.903
1.50	0.40	0.667	0.671	1.00	1.01
1.50	0.80	0.874	0.905	1.31	1.36
1.00	0	0.672	0.798	0.672	0.798
1.00	0.10	0.773	0.884	0.773	0.884
1.00	0.40	1.24	1.19	1.24	1.19
1.00	0.80	1.45	1.74	1.45	1.74
0.75	0	0.876	0.916	0.657	0.687
0.75	0.10	0.926	1.33	0.695	0.998
0.75	0.40	1.72	1.09	1.29	0.818
0.75	0.80	3.25*	2.00	2.44*	1.50

Competitive inhibition:

K_i (Dixon) 3.19 x 10^{-4} M

4.57 x 10^{-4} M

5.69 x 10^{-4} M

Run 2:

[Dipicolinic acid (36)] = 0 mM

[DHDPA] M x 10^{-4}	1/[DHDPA] M^{-1} x 10^{3}	Rate $\mu mol \cdot s^{-1} mg^{-1}$	1/Rate $mg \cdot s \cdot \mu mol^{-1}$
2.50	4.00	1.32	0.755
2.50	4.00	1.82	0.550
1.50	6.67	1.49	0.670
1.50	6.67	1.73	0.577
1.00	10.0	1.39	0.719
1.00	10.0	1.23	0.813
0.75	13.3	0.974	1.03
0.75	13.3	1.63*	0.615*

Lineweaver-Burk plot V_{max} = 2.26 $\mu mol \cdot s^{-1} mg^{-1}$ K_m = 0.837 x 10^{-4} M

[Dipicolinic aicd (36)] = 0.10 mM

[DHDPA] M x 10^{-4}	1/[DHDPA] M^{-1} x 10^{3}	Rate $\mu mol \cdot s^{-1} mg^{-1}$	1/Rate $mg \cdot s \cdot \mu mol^{-1}$
2.50	4.00	2.15	0.465
2.50	4.00	1.77	0.563
1.50	6.67	1.28	0.783
1.50	6.67	1.40	0.712
1.00	10.0	0.909	1.10
1.00	10.0	0.777	1.29
0.75	13.3	0.667	1.50
0.75	13.3	0.840	1.19

Lineweaver-Burk plot V_{max} = 6.54 $\mu mol \cdot s^{-1} mg^{-1}$ K_m = 6.14 x 10^{-4} M

[Dipicolinic acid (36)] = 0.50 mM

[DHDPA] M x 10^{-4}	1/[DHDPA] M^{-1} x 10^{3}	Rate $\mu mol \cdot s^{-1} mg^{-1}$	1/Rate $mg \cdot s \cdot \mu mol^{-1}$
2.50	4.00	1.50	0.665
2.50	4.00	1.49	0.669
1.50	6.67	1.11	0.903
1.50	6.67	0.950	1.05
1.00	10.0	0.555	1.80
1.00	10.0	0.880	1.14
0.75	13.3	0.675	1.48
0.75	13.3	0.388	2.58

Lineweaver-Burk plot V_{max} = 41.7 $\mu mol \cdot s^{-1} mg^{-1}$ K_m = 28.3 x 10^{-4} M

[Dipicolinic acid (36)] = 1.0 mM

[DHDPA] M x 10^{-4}	1/[DHDPA] M^{-1} x 10^{3}	Rate $\mu mol \cdot s^{-1} mg^{-1}$	1/Rate $mg \cdot s \cdot \mu mol^{-1}$
2.50	4.00	0.628*	1.59*
2.50	4.00	1.06	0.941
1.50	6.67	0.823	1.22
1.50	6.67	0.839	1.19
1.00	10.0	0.504	1.98
1.00	10.0	0.483	2.07
0.75	13.3	0.472	2.12
0.75	13.3	0.403	2.48

Lineweaver-Burk plot V_{max} = 3.85 $\mu mol \cdot s^{-1} mg^{-1}$ K_m = 6.13 x 10^{-4} M

Determination of K_i:

[DHDPA] M x 10^{-4}	[Dipicolinic acid] M x 10^{-3}	1/Rate mg·s·µmol^{-1}		[DHDPA]/Rate s·mg·l^{-1} x 10^{2}	
2.50	0	0.755	0.550	1.89	1.38
2.50	0.10	0.465	0.565	1.16	1.41
2.50	0.50	0.665	0.669	1.66	1.67
2.50	1.0	1.59*	0.941	3.98*	2.35
1.50	0	0.670	0.577	1.01	0.866
1.50	0.10	0.783	0.712	1.17	1.07
1.50	0.50	0.903	1.05	1.35	1.58
1.50	1.0	1.22	1.19	1.83	1.79
1.00	0	0.719	0.813	0.719	0.813
1.00	0.10	1.10	1.29	1.10	1.29
1.00	0.50	1.80	1.14	1.80	1.14
1.00	1.0	1.98	2.07	1.98	2.07
0.75	0	1.03	0.615*	0.773	0.461*
0.75	0.10	1.50	1.19	1.13	0.893
0.75	0.50	1.48	2.58	1.11	1.94
0.75	1.0	2.12	2.48	1.59	1.86

Competitive inhibition:

K_i (Dixon) 4.32 x 10^{-4} M
4.39 x 10^{-4} M
4.43 x 10^{-4} M

Effect of isophthalic acid (41) on DHDPR kinetics with respect to the substrate

Assay:

NADPH (54 mM in dH_2O)	3.0 µl
Buffer (200 mM Mops pH 7.2 at 25 °C, pyruvate (17) 80 mM)	500 µl
dH_2O	237 µl
DHDPS (10 fold excess)	100 µl
(R,S)-ASA (11) (3.0 mM to 10 mM in dH_2O)	50 µl
DHDPR (2.25 x 10^{-4} U, 1.0 x 10^{-4} mg)	10 µl
Isophthalic acid (41) (25 mM to 75 mM in dH_2O)	100 µl
	1.00 ml

The *(R,S)*-aspartate β-semialdehyde was added prior to initiation of the reaction to form the substrate. The reaction was then initiated in the cuvette by addition of DHDPR, mixed by inversion of the cuvettte. ΔA_{340} was measured over 300 seconds at 30 °C, blanked against dH_2O.

Run 1:

[Isophthalic acid (41)] = 0 mM

[DHDPA] M x 10^{-4}	1/[DHDPA] M^{-1} x 10^3	Rate $\mu mol \cdot s^{-1} mg^{-1}$	1/Rate $mg \cdot s \cdot \mu mol^{-1}$
2.50	4.00	2.07	0.483
2.50	4.00	2.02	0.495
1.50	6.67	1.91	0.523
1.50	6.67	1.81	0.553
1.00	10.0	1.65	0.605
1.00	10.0	1.28	0.782
0.75	13.3	0.968	1.03
0.75	13.3	0.943	1.06

Lineweaver-Burk plot V_{max} = 5.29 $\mu mol \cdot s^{-1} mg^{-1}$ K_m = 3.13 x 10^{-4} M

[Isophthalic acid (41)] =2.5 mM

[DHDPA] M x 10^{-4}	1/[DHDPA] M^{-1} x 10^3	Rate $\mu mol \cdot s^{-1} mg^{-1}$	1/Rate $mg \cdot s \cdot \mu mol^{-1}$
2.50	4.00	1.90	0.525
2.50	4.00	2.11	0.475
1.50	6.67	1.52	0.657
1.50	6.67	1.40	0.716
1.00	10.0	0.895	1.12
1.00	10.0	1.05	0.949
0.75	13.3	0.801	1.25
0.75	13.3	0.789	1.27

Lineweaver-Burk plot V_{max} = 6.47 $\mu mol \cdot s^{-1} mg^{-1}$ K_m = 5.45 x 10^{-4} M

[Isophthalic acid (41)] = 5.0 mM

[DHDPA] M x 10^{-4}	1/[DHDPA] M^{-1} x 10^{3}	Rate $\mu mol \cdot s^{-1} mg^{-1}$	1/Rate $mg \cdot s \cdot \mu mol^{-1}$
2.50	4.00	1.73	0.579
2.50	4.00	1.68	0.594
1.50	6.67	1.22	0.823
1.50	6.67	1.03	0.970
1.00	10.0	0.803	1.25
1.00	10.0	0.880	1.14
0.75	13.3	0.415*	2.41*
0.75	13.3	0.341*	2.94*

Lineweaver-Burk plot V_{max} = 5.07 $\mu mol \cdot s^{-1} mg^{-1}$ K_m = 5.12 x 10^{-4} M

[Isophthalic acid (41)] = 6.5 mM

[DHDPA] M x 10^{-4}	1/[DHDPA] M^{-1} x 10^{3}	Rate $\mu mol \cdot s^{-1} mg^{-1}$	1/Rate $mg \cdot s \cdot \mu mol^{-1}$
2.50	4.00	1.98	0.505
2.50	4.00	1.78	0.562
1.50	6.67	1.28	0.783
1.50	6.67	0.955	1.05
1.00	10.0	0.823	1.22
1.00	10.0	0.554	1.81
0.75	13.3	0.761	1.31
0.75	13.3	0.534	1.87

Lineweaver-Burk plot V_{max} = 8.27 $\mu mol \cdot s^{-1} mg^{-1}$ K_m = 9.93 x 10^{-4} M

Determination of K_i:

[DHDPA] M x 10^{-4}	[Isophthalic acid] M x 10^{-3}	1/Rate $mg \cdot s \cdot \mu mol^{-1}$		[DHDPA]/Rate $s \cdot mg \cdot l^{-1}$ x 10^2	
2.50	0	0.483	0.495	1.21	1.24
2.50	2.5	0.525	0.475	1.31	1.19
2.50	5.0	0.579	0.594	1.45	1.49
2.50	6.5	0.505	0.562	1.26	1.41
1.50	0	0.523	0.553	0.785	0.830
1.50	2.5	0.657	0.716	0.986	1.07
1.50	5.0	0.823	0.970	1.23	1.46
1.50	6.5	0.783	1.05	1.17	1.58
1.00	0	0.605	0.782	0.605	0.782
1.00	2.5	1.12	0.949	1.12	0.949
1.00	5.0	1.25	1.14	1.25	1.14
1.00	6.5	1.22	1.81	1.22	1.81
0.75	0	1.03	1.06	0.773	0.795
0.75	2.5	1.25	1.27	0.938	0.953
0.75	5.0	2.41*	2.94*	1.81*	2.21*
0.75	6.5	1.31	1.87	0.983	1.40

Competitive inhibition:

K_i (Dixon) 1.03 x 10^{-3} M

1.97 x 10^{-3} M

2.85 x 10^{-3} M

Run 2:

[Isophthalic acid (41)] = 0 mM

[DHDPA] M x 10^{-4}	1/[DHDPA] M^{-1} x 10^{3}	Rate $\mu mol \cdot s^{-1} mg^{-1}$	1/Rate $mg \cdot s \cdot \mu mol^{-1}$
2.50	4.00	2.28	0.439
2.50	4.00	2.20	0.454
1.50	6.67	2.52	0.397
1.50	6.67	2.25	0.445
1.00	10.0	1.55	0.644
1.00	10.0	1.28	0.780
0.75	13.3	0.906	1.10
0.75	13.3	0.960	1.04

Lineweaver-Burk plot V_{max} = 15.6 $\mu mol \cdot s^{-1} mg^{-1}$ K_m = 11.0 x 10^{-4} M

[Isophthalic acid (41)] =2.5 mM

[DHDPA] M x 10^{-4}	1/[DHDPA] M^{-1} x 10^{3}	Rate $\mu mol \cdot s^{-1} mg^{-1}$	1/Rate $mg \cdot s \cdot \mu mol^{-1}$
2.50	4.00	2.06	0.484
2.50	4.00	1.80	0.557
1.50	6.67	1.28	0.779
1.50	6.67	1.52	0.656
1.00	10.0	0.978	1.02
1.00	10.0	0.923	1.08
0.75	13.3	0.780	1.28
0.75	13.3	0.655	1.53

Lineweaver-Burk plot V_{max} = 9.23 $\mu mol \cdot s^{-1} mg^{-1}$ K_m = 8.86 x 10^{-4} M

[Isophthalic acid (41)] = 5.0 mM

[DHDPA] M x 10^{-4}	1/[DHDPA] M^{-1} x 10^{3}	Rate $\mu mol \cdot s^{-1} mg^{-1}$	1/Rate $mg \cdot s \cdot \mu mol^{-1}$
2.50	4.00	1.67	0.600
2.50	4.00	1.56	0.642
1.50	6.67	1.91	0.524
1.50	6.67	1.75	0.570
1.00	10.0	1.46	0.685
1.00	10.0	1.03	0.970
0.75	13.3	0.793	1.26
0.75	13.3	0.781	1.28

Lineweaver-Burk plot V_{max} = 5.08 $\mu mol \cdot s^{-1} mg^{-1}$ K_m = 3.71 x 10^{-4} M

[Isophthalic acid (41)] = 7.5 mM

[DHDPA] M x 10^{-4}	1/[DHDPA] M^{-1} x 10^{3}	Rate $\mu mol \cdot s^{-1} mg^{-1}$	1/Rate $mg \cdot s \cdot \mu mol^{-1}$
2.50	4.00	1.55	0.650
2.50	4.00	1.65	0.605
1.50	6.67	1.30	0.767
1.50	6.67	1.40	0.713
1.00	10.0	0.720	1.39
1.00	10.0	0.712	1.40
0.75	13.3	0.597	1.68
0.75	13.3	0.691	1.45

Lineweaver-Burk plot V_{max} = 7.49 $\mu mol \cdot s^{-1} mg^{-1}$ K_m = 8.36 x 10^{-4} M

Determination of K_i:

[DHDPA] M x 10^{-4}	[Isophthalic acid] M x 10^{-3}	1/Rate $mg \cdot s \cdot \mu mol^{-1}$		[DHDPA]/Rate $s \cdot mg \cdot l^{-1}$ x 10^{2}	
2.50	0	0.439	0.454	1.10	1.14
2.50	2.5	0.484	0.557	1.21	1.39
2.50	5.0	0.600	0.642	1.50	1.61
2.50	7.5	0.650	0.605	1.63	1.51
1.50	0	0.397	0.445	0.596	0.668
1.50	2.5	0.779	0.656	1.17	0.984
1.50	5.0	0.524	0.570	0.786	0.855
1.50	7.5	0.767	0.713	1.15	1.07
1.00	0	0.644	0.780	0.644	0.780
1.00	2.5	1.02	1.08	1.02	1.08
1.00	5.0	0.685	0.970	0.685	0.970
1.00	7.5	1.39	1.40	1.39	1.40
0.75	0	1.10	1.04	0.825	0.780
0.75	2.5	1.28	1.53	0.960	1.15
0.75	5.0	1.26	1.28	0.945	0.960
0.75	7.5	1.68	1.45	1.26	1.09

Competitive inhibition:

K_i (Dixon) 5.43 x 10^{-3} M

5.60 x 10^{-3} M

5.62 x 10^{-3} M

Δ^3-Tetrahydroisophthalic acid (99)[1]

Isophthalic acid (41) (2.08 g, 12.5 mmol) was dissolved in a slight excess of sodium carbonate (1.43 g, 13.5 mmol) in distilled water (16.0 ml). To this solution was added sodium amalgam 3.5 % (130 g).[2] The solution was heated to 70 °C and stirred for 48 hours. The reaction progress was monitored by ^{1}H NMR; a small aliquot was removed and the water removed *in vacuo*. When it appeared that all the isophthalic acid (41) had reacted, and all the sodium had been consumed, the reaction was cooled to room temperature. To aid in the removal of the mercury from the gelatinous reaction mixture further distilled water (16.0 ml) was added. The liquid was decanted off the mercury, and then acidified to pH 3 by the addition of concentrated hydrochloric acid (~10 ml). The resulting grey precipitate was removed by filtration over a Buchner funnel; the precipitate contained mainly sodium salts. The resulting yellow solid was purified by fractional crystallisation during which a considerable amount of isophthalic acid (41) was recovered. Δ^3-Tetrahydroisophthalic acid (99) was obtained as a fine white powder.

The yield of Δ^3-tetrahydroisophthalic acid (99) was 100 mg (0.589 mmol, 4.7%).
Mp 212 -217 °C, literature 237 - 240 °C.[1]
^{1}H NMR (300 MHz, CD_3OD) δ_H 1.35 - 1.48 (1H, m, -C**H**$_2$-), 1.76 - 1.80 (1H, m, -C**H**$_2$-), 2.00 - 2.08 (2H, m, -C**H**$_2$C=), 2.08 - 2.17 (1H, m, -C**H**COOH), 2.29 - 2.37 (2H, m, -C**H**$_2$C=), 6.76 (1H, s, =C**H**-) ppm.
^{13}C NMR (75 MHz, D_2O) δ_C 25.53 (-**C**H$_2$CH$_2$CH=), 26.25 (-**C**HCOOH), 27.92 (-**C**H$_2$CH=), 40.32 (-**C**H$_2$CCOOH), 135.17 (-**C**HCOOH), 140.64 (=**C**H-) ppm.
IR (KBr disc) υ_{max} 3400 (O-H (w)), 2876 (=C-H (m)), 2552 (C-H (w)), 1695 (C=O (s)), 1647 (C=C (w)), 1420 (s), 1279 (s), 953 (s) cm^{-1}.
HRMS m/z (FAB(NOBA)) 171.06529 (MH^+, 100% ($C_8H_{11}O_4$ requires 171.06573)).
MS m/z (FAB(NOBA)) 171 (MH^+, 30%), 154 ($M\text{-}OH^+$, 100%), 136 (98%).

Δ^2-, Δ^3-, Δ^4-Tetrahydroisophthalic acid (100, 99, 101)[1]

Isophthalic acid (41) (5.60 g, 33.7 mmol) was dissolved in a slight excess of sodium carbonate (3.93 g, 37.1 mmol) in distilled water (150 ml). To this solution was added sodium amalgam 3.5 % (250 g).[2] The solution was heated to 45 °C and stirred for 48 hours under a steady flow of carbon dioxide. The supernatant was then decanted off the mercury, and acidified with concentrated hydrochloric acid (~50 ml). The precipitated sodium salts were then filtered off. The aqueous layer was extracted with diethyl ether (3 x 150 ml), the ethereal layer being dried over calcium chloride and concentrated to dryness *in vacuo*, yielding a yellow solid (2.82 g). Repeated attempts at fractional crystallisation gave a pale yellow solid.

The yield of reduced material was 1.99 g.
^{1}H NMR (300 MHz CD_3OD) δ_H 1.64 - 1.90 (m), 2.09 - 2.39 (m), 2.54 - 2.65 (m), 3.18 - 3.29 (m), 5.79 (bs/m) ppm.

Cyclohexanone cyanohydrin (103)[3]

Potassium cyanide (38.5 g, 0.591 mol) and water (173 ml) were stirred in a flask fitted with a thermometer and a pressure equalising dropping funnnel. Cyclohexanone (102) (50.0 g, 0.509 mol) in diethyl ether (208 ml) was then added. Over four hours concentrated sulfuric acid (150 ml) was added dropwise while maintaning the temperature below 15 - 20 °C. The reaction was then stirred for a further hour, and left overnight. Water (100ml) was added to the supernatant which had been decanted off the precipitated salts. The organic and aqueous layers were then separated The ethereal layer was dried over sodium sulfate then concentrated *in vacuo* to a brown oil.

The yield of cyclohexanone cyanohydrin (103) was 42.2 g (0.337 mol, 66.3%).
^{1}H NMR (300 MHz, $CDCl_3$) δ_H 1.19 - 1.31 (1H, m), 1.46 - 1.67 (5H, m), 1.70 - 1.87 (2H, m), 2.04 - 2.09 (2H, m) ppm.

2-Cyano-1-cyclohexene (104)[3]

Cyclohexanone cyanohydrin (103) (42.2 g, 0.337 mol) was dissolved in toluene (100 ml) and then dried with sodium sulfate. The solution was filtered into a two-necked round bottom flask fitted with a thermometer and a pressure equalising dropping funnel. Thionyl chloride (100 g, 61.3 ml, 0.841 mol) was then added dropwise to the solution stirred in an ice-salt bath overnight. The material was then fractionally distilled under vacuum, initially at ~20 mm Hg to remove the toluene and thionyl chloride, followed by distillation at ~1.5 mm Hg. Two fractions of product were obtained, the first containing the product and toluene, the second being pure product.

The yield of the pure 2-cyano-1-cyclohexene (104) was 6.83 g (63.8 mmol, 18.9%).
^{1}H NMR (300 MHz, $CDCl_3$) δ_H 1.63 - 1.70 (4H, m, 2 x -$\mathbf{CH_2}CH_2CH$=), 2.17 - 2.21 (4H, m, 2 x-$\mathbf{CH_2}$C=), 6.62 (1H, bs, =C**H**-) ppm.
IR (thin film) υ_{max} 2937 (=C-H (s)), 2864 (C-H (s)), 2214 (C=N (s)), 1638 (C=C (s)), 1448 (m), 1437 (s), 1425 (m) cm^{-1}.
HRMS m/z (EI) 107.07340 (M^+, 79% (C_7H_9N requires 107.07350)).
GCMS m/z (EI) 107 (M^+, 79%), 92 (100%), 79 (90%), 67 (39%).

Ethyl tetrahydrobenzoate (105)[4]

In a 50 ml round bottom flask fitted with a reflux condenser were mixed 2-cyano-1-cyclohexene (104) (3.83 g, 35.8 mmol), ethanol (6.79 g, 8.5 ml), and concentrated sulfuric acid (6.97 g, 3.8 ml). The mixture was stirred and heated under reflux overnight in an oil bath at 120 °C. The reaction was cooled to room temperature and partitioned between water (18.5 ml) and diethyl ether (2 x 18.5 ml). The ethereal layers were combined and washed with a saturated aqueous sodium carbonate solution (10 ml), then dried with magnesium sulfate. The solvent was removed *in vacuo* yielding the titled product as a yellow oil. Further product was extracted from the aqueous layer with ethyl acetate (2 x 18.5 ml) after the addition of sodium chloride. This material was obtained as a yellow semi-solid oil.

The yield of the ethyl tetrahydrobenzoate (105) as an oil was 2.31 g (15.0 mmol, 41.9%), while the yield of the semi-solid oil was 0.819 g (5.31 mmol, 14.8%).
TLC (pet ether and diethyl ether (1:1)) R_f 0.63.
^{1}H NMR (300 MHz, $CDCl_3$) δ_H 1.24 (3H, t, J = 7.0 Hz, -C**H**$_3$), 1.54 - 1.63 (4H, m, 2 x -C**H**$_2$CH$_2$C=), 2.13 - 2.15 (2H, m, -C**H**$_2$C=), 2.15 - 2.57 (2H, m, -C**H**$_2$C=), 4.14 (2H, q, J = 7.0 Hz, -CO$_2$C**H**$_2$CH$_3$), 6.93 (1H, s, =C**H**-) ppm.
^{13}C NMR (75 MHz, $CDCl_3$) δ_H 13.65 (-CH$_2$**C**H$_3$), 20.86, 21.47, 23.86, 25.12, 59.52 (-**C**H$_2$CH$_3$), 129.84 (=**C**CO$_2$CH$_2$CH$_3$), 138.79 (=**C**H-), 167.03 (-**C**O$_2$-) ppm.
IR (KBr disc) υ_{max} 2980 (=C-H (w)), 2937 (C-H (s)), 2862 (w), 1713 (C=O (s)), 1649 (C=C (s)), 1275 (s), 1236 (m), 1089 (m), 1045 (m) cm^{-1}.
HRMS m/z (EI) 154.09924 (M^+, 31% ($C_9H_{14}O_2$ requires 154.09938)).
GCMS m/z (EI) 154 (M^+, 31%), 126 (12%), 109 (40%), 81.07255 (100%), 53 (23%).

Ethyl 3-carbethoxy-Δ^2-cyclohexeneglyoxalate (107)[5]

A mixture of ethyl tetrahydrobenzoate (105) (1.00 g, 6.49 mmol) and diethyl oxalate (106) (1.00 g, 6.90 mmol) was added to an ice-cold solution of sodium (0.15 g, 6.52 mmol, 1.0 equivalent) in ethanol (4.0 ml) with constant stirring. The reaction turned bright yellow in colour and was stirred in an ice bath at 4 °C overnight. To the resulting solid was added water (10 ml), followed by 5% sulfuric acid (3 ml). The organic layer was then extracted with ether (10 ml), washed with water (10 ml), dried over magnesium sulfate, and concentrated *in vacuo* to a yellow oil, 1.01 g. No product was obtained.

Ethyl dicarboxypimelate (110)[5,6]

To a 500 ml three-necked round bottom flask fitted with a reflux condenser and a thermometer was added dry ethanol (215 ml) and sodium (9.84 g, 0.428 mmol). Diethyl malonate (109) (68.6 g, 0.428 mmol) was added dropwise via a dropping funnel while the reaction vessel was maintained at ~60 °C over an oil bath. 1,3-Dibromopropane (108) (43.2 g, 0.214 mmol) was then added dropwise, again while maintaining the reaction vessel at ~60 °C. The reaction was then heated under reflux for three and a half hours, pH 7. The ethanol was removed *in vacuo*, and the residue diluted with water (100 ml) and brought to pH 3 by the addition of 5% sulfuric acid (15 ml). The organic material was extracted with ethyl acetate (250 ml, 2 x 100 ml). The ethyl acetate layers were combined and dried over magnesium sulfate, the solvent was then removed *in vacuo* to yield a yellow solution. This material was fractionally distilled under vacuum, with the titled product distilling at 160 - 185 °C (~1.5 mm Hg).

The yield of the ethyl dicarboxypimelate (110) was 16.6 g (46.0 mmol, 21.5%).
Bp 160 -185 °C (~1.5 mm Hg).
^{1}H NMR (300 MHz, $CDCl_3$) δ_H 1.26 (12H, t, J = 7.3 Hz, 4 x -$CO_2CH_2C\mathbf{H}_3$), 1.29 - 1.38 (2H, m, -$CH_2C\mathbf{H}_2CH_2$-), 1.92 (4H, q, J = 8.3 Hz, 2 x -$C\mathbf{H}_2$CH-), 3.31 (2H, t, J = 7.3 Hz, 2x -C**H**-), 4.19 (8H, q, J = 7.8 Hz, 4 x -$CO_2C\mathbf{H}_2CH_3$) ppm.
^{13}C NMR (75 MHz, $CDCl_3$) δ_C 13.96 (-**C**H_3), 24.97 (-$CH_2\mathbf{C}H_2CH_2$-), 28.19 (-$\mathbf{C}H_2$CH-), 51.60 (-**C**H-), 61.27 (-$O\mathbf{C}H_2CH_3$), 169.1 (-**C**=O) ppm.
IR (thin film) υ_{max} 2984 (C-H (s)), 1732 (C=O (s)), 1464 (m), 1369(m), 1246 (s), 1151 (s), 1097 (m), 1028 (m), 862 (m) cm^{-1}.
HRMS m/z (EI) 315.14441 (M-$OCH_2CH_3^+$, 7% ($C_{15}H_{23}O_7$ requires 315.14438)).
MS m/z (EI) 315 (M-$OCH_2CH_3^+$, 7%), 269 (10%), 235 (29%), 201 (68%), 173 (100%), 109 (56%).

Ethyl cyclohexanone-2,6-dicarboxylate (111)[5]

Ethyl dicarboxypimelate (110) (4.98 g, 13.8 mmol) was added to sodium (0.58 g, 25.2 mmol) in dry ethanol (10.0 ml) and heated under reflux for three hours (bath tempertaure 135 °C). Further sodium (0.60 g, 26.1 mmol) in dry ethanol (10.0 ml) was added, the reaction was heated under reflux for a further 16 hours. The ethyl carbonate and ethanol were then removed *in vacuo*. The residue was diluted with water (8.3 ml), and acidified to pH 3 by the addition of 20% sulfuric acid while being maintained at 0 °C. Further water (40 ml) was added and the organic material was extracted with diethyl ether (2 x 40 ml). The combined ethereal layers were dried over magnesium sulfate and the solvent removed *in vacuo*, yielding a yellow oil. The product was purified by radial chromatography (4 mm silica plate). The solvent was removed *in vacuo* to yield the ethyl cyclohexanone-2,6-dicarboxylate (111) as a clear oil.

The yield of ethyl cyclohexanone-2,6-dicarboxylate (111) was 1.26 g (5.18 mmol, 37.5%).

^{1}H NMR (300 MHz, $CDCl_3$) δ_H 1.26 - 1.28 (6H, m, 2 x -OCH_2CH_3), 1.55 - 1.60 (1H, m, -$CH_2CH_2CH_2$-), 1.60 - 1.77 (1H, m, -$CH_2CH_2CH_2$-), 2.20 - 2.29 (4H, m, 2 x -CH_2CHC=O), 3.31 - 3.35 (2H, m, 2 x -CHC=O), 4.17 4.26 (4H, m, 2 x -OCH_2CH_3); enol form 1.26 - 1.28 (6H, m, 2 x -OCH_2CH_3), 1.55 - 1.60 (1H, m, -$CH_2CH_2CH_2$-), 1.60 - 1.77 (1H, m, -$CH_2CH_2CH_2$-), 1.93 - 1.95 (2H, m, -CH_2CHC=), 2.20 - 2.29 (2H, m, -CH_2C=), 3.35 - 3.41 (1H, m, -CHC=), 4.17 - 4.26 (4H, m, 2 x -OCH_2CH_3) ppm.

^{13}C NMR (75 MHz, $CDCl_3$) δ_C 14.2 (-OCH_2CH_3), 20.6 (-$CH_2CH_2CH_2$-), 30.0 (-CH_2CHC=O), 57.5 (-CHC=O), 61.2 (-OCH_2CH_3), 155.7 (-CHC=OCH-), 166.7 (-C=O), 169.0 (-C=O); enol form 14.2 (-OCH_2CH_3), 20.6 (-$CH_2CH_2CH_2$-), 22.2 (-CH_2C=), 26.3 (-CH_2CHC=), 45.7 (-CHC=), 61.2 (-OCH_2CH_3), 99.8 (=COH), 166.7 (-C=O), 169.0 (-C=O) ppm.

IR ($CHCl_3$) υ_{max} 2943 (C-H (w)), 1730 (HOC=O (s)), 1657 (C=O (s)), 1620 (w), 1400 (w), 1379 (w), 1298 (m), 1269 (m), 1256 (m), 1198 (m), 1178 (m) cm^{-1}.

HRMS m/z (EI) 242.11567 (M^+, 21% ($C_{12}H_{18}O_5$ requires 242.11542)).

MS m/z (EI) 242 (M^+, 21%), 196 (50%), 168 (100%), 140 (39%), 123 (30%), 95 (32%).

Ethyl cyclohexanol-2,6-dicarboxylate (112)[5]

Ethyl cyclohexanone-2,6-dicarboxylate (111) (4.13 g, 17.0 mmol) in ethanol (95%) (33.0 ml), ferrous chloride solution (0.13 gl^{-1}) (165 µl), and platinum oxide catalyst (330 mg) were stirred vigorously in a hydrogen atmosphere. After 20 hours the catalyst was reactivated by stirring in air for one hour. The reaction was then stirred in hydrogen for a further 20 hours. The catalyst was removed by filtration and the solvent removed *in vacuo* to yield a clear oil. The product was purified by radial chromatography (4 mm silica plate). The solvent was removed *in vacuo* to yield the ethyl cyclohexanol-2,6-dicarboxylate (112) as a clear oil.

The yield of ethyl cyclohexanol-2,6-dicarboxylate (112) was 3.84 g (15.7 mmol, 92.4%).

^{1}H NMR (300 MHz, $CDCl_3$) δ_H 1.21 - 1.35 (6H, m, 2 x -OCH_2CH_3), 1.43 - 1.55 (1H, m, -$CH_2CH_2CH_2$-), 1.58 - 1.69 (1H, m, -$CH_2CH_2CH_2$-), 1.76 - 1.91 (2H, m, 2 x -$CH_2CHCHOH$), 2.33 - 2.39 (2H, m, 2 x -$CH_2CHCHOH$), 2.85 - 2.94 (2H, m, 2x -CHCHOH), 4.14 - 4.23 (4H, m, 2 x -OCH_2CH_3), 4.63 (1H, bs, -CHOH) ppm.

^{13}C NMR (75 MHz, $CDCl_3$) δ_C 14.1 (-OCH_2CH_3), 21.6 (-$CH_2CH_2CH_2$-), 24.3 (-$CH_2CHCHOH$), 46.9 (-CHCHOH), 60.7 (-OCH_2CH_3), 66.6 (-CHOH), 174.2 (-C=O) ppm.

IR (thin film) υ_{max} 3512 (O-H (m)), 2941 (C-H (s)), 1728 (HOC=O (s)), 1448 (m),

1375 (m), 1310 (m), 1180 (s), 1036 (m), 982 (w) cm^{-1}.
GCMS m/z (EI) 244 (M^+, 1%), 181 (100%), 152 (48%), 124 (47%), 101 (38%), 73 (50%), 55 (53%); 244 (M^+, 7%), 181 (100%), 152 (65%), 125 (68%), 101 (58%), 73 (75%), 55 (66%).

Ethyl Δ^2-tetrahydroisophthalic acid (113)[5,7]

Thionyl chloride (2.36 g, 19.9 mmol) was added dropwise to ethyl cyclohexanol-2,6-dicarboxylate (112) (49.7 mg, 0.203 mmol) in pyridine (709 mg, 8.96 mmol), whilst stirring at 0°C. The reaction was stirred for 30 minutes while slowly warming from to 0°C room temperature, then stirred for a further hour. The reaction was added to water (2.18 ml) at 0°C, and extracted with diethyl ether (2 x 5.0 ml). The combined ethereal layers were dried over magnesium sulfate, then the solvent removed *in vacuo* to yield a yellow oil. The product was purified by radial chromatography (2 mm silica plate). The solvent was removed *in vacuo* to yield the ethyl Δ^2-tetrahydroisophthalic acid (113) as a clear oil.

The yield of the ethyl Δ^2-tetrahydroisophthalic acid (113) was 16.4 mg (0.072 mmol, 35.7%).
^{1}H NMR (300 MHz, $CDCl_3$) δ_H 1.26 - 1.32 (6H, m, 2 x-OCH_2CH_3), 1.59 - 1.65 (2H, m, -$CH_2CH_2CH_2$-), 1.80 - 1.93 (2H, m, -CH_2CHCH=), 2.24 - 2.30 (2H, m, -CH_2C=), 3.20 - 3.26 (1H, m, -CHCH=), 4.17 - 4.21 (4H, m, 2 x -OCH_2CH_3), 7.00 (1H, bs, =CH-) ppm.
^{13}C NMR (75 MHz, $CDCl_3$) δ_C 14.1 (-OCH_2CH_3), 14.2 (-OCH_2CH_3), 20.6 (-$CH_2CH_2CH_2$-), 23.9 (-CH_2C=), 24.4 (-CH_2CHC=), 41.9 (-CHCH=), 60.5 (-OCH_2CH_3), 60.9 (-OCH_2CH_3), 132.4 (=C-), 135.2 (=CH-) ppm.
IR (thin film) υ_{max} 2941 (C-H (s)), 2361 (s), 1713 (C=O (s)), 1651 (m), 1448 (m), 1367 (m), 1238 (s), 1174 (s), 1087 (m), 1030 (m), 922 (m), 748 (m) cm^{-1}.
GCMS m/z (EI) 226 (M^+, 2%), 180 (61%), 152 (65%), 79 (100%).

Δ^2-Tetrahydroisophthalic acid (100)[5,8]

Ethyl Δ^2-tetrahydroisophthalate (113) (560 mg, 2.48 mmol) and potassium carbonate (686 mg, 4.96 mmol) were heated under reflux in methanol (62 ml) and water (6.2 ml) for 20 hours. The methanol was removed *in vacuo*, following which water (24.8 ml) and 10% aqueous hydrochloric acid (124 ml) were added. The water was removed *in vacuo* to yield a white solid. The organic soluble components were taken up in methanol (50 ml). The methanol was then removed *in vacuo*. The residue was dissolved in aqueous sodium hydroxide (15 ml), pH >10, and extracted with diethyl ether (15 ml). Aqueous hydrochloric acid was added, pH 7, and the solution was again extracted with diethyl ether (15 ml). Further aqueous hydrochloric acid was added, pH <3, and the solution

was extracted with diethyl ether (2 x 15 ml). The final ethereal layer was dried over magnesium sulfate and the solvent removed *in vauco* to a white solid.

The yield of Δ^2-tetrahydroisophthalate (100) was 201 mg (1.18 mmol, 47.5%).
Mp 171 - 174 °C.
^{1}H NMR (300 MHz, CD_3OD) δ_H 1.60 - 1.65 (2H, m, -CH_2**C**$H_2$$CH_2$-), 1.72 - 1.93 (2H, m, -**C**H_2CHC=), 2.19 - 2.24 (2H, m, -**C**H_2C=), 3.23 - 3.25 (1H, m, -**C**HCH=), 7.02 - 7.03 (1H, bs, -**C**H=) ppm.
^{13}C NMR (75 MHz, CD_3OD) δ_C 22.1 (-CH_2**C**$H_2$$CH_2$-), 25.3 (-**C**$H_2$C=), 25.9 (-**C**$H_2$CHC=), 43.1 (-**C**HCH=), 133.4 (=**C**-), 137.8 (=**C**H-), 170.8 (-**C**=O), 176.8 (-**C**=O) ppm.
IR (KBr disc) υ_{max} 2945 (C-H (m)), 1686 (C=O (s)), 1265 (w), 1094 (w), 953 (m), 797 (w) cm^{-1}.
HRMS m/z (EI) 152.04738 (M-H_2O^+, 20% ($C_8H_8O_3$ requires 152.04734)).
MS m/z (EI) 152 (M-H_2O^+, 23%),124 (51%), 97 (5%), 79 (100%), 53 (17%).

Δ^2-Tetrahydroisophthalic acid (100) and Δ^3-tetrahydroisophthalic acid (99) inhibition of DHDPS and DHDPR

DHDPS
Assay:

NADPH (54 mM in dH_2O)	3.0 µl
Buffer (200 mM Mops pH 7.2 at 25 °C, pyruvate (17) 80 mM)	500 µl
dH_2O	237 µl
DHDPS (2.0 x 10^{-4} U, 4.8 x 10^{-4} mg)	10 µl
DHDPR (10 fold excess)	100 µl
(S)-ASA (11) (5.0 mM in dH_2O)	50 µl
Inhibitor (appropriate concentration, in methanol if required)	100 µl
	1.00 ml

The reaction was initiated in the cuvette by addition of freshly prepared *(S)*-aspartate β-semialdehyde (11), mixed by inversion of the cuvettte. ΔA_{340} was measured over 300 seconds at 30 °C, blanked against dH_2O, containing 10% methanol if required. *(S)*-Aspartate β-semialdehyde was present in a concentration of 0.25 mM. The activity is the rate of reaction with inhibitor present relative to the rate of reaction in the absence of the inhibitor.

Compound	Concentration mM	Activity %
Δ^2-Tetrahydroisophthalic acid (100)	40	76.7
	20	82.5
	10	87.0
	5	85.0
Δ^3-Tetrahydroisophthalic acid (99) (in methanol)	30	9.23
	10	61.3
	5.0	77.9

IC_{50} (Δ^3-tetrahydroisophthalic acid (99)) ~1.5 x 10^{-2} M.

DHDPR

Assay:

NADPH (54 mM in dH_2O)	3.0 µl
Buffer (200 mM Mops pH 7.2 at 25 °C, pyruvate (17) 80 mM)	500 µl
dH_2O	237 µl
DHDPS (10 fold excess)	100 µl
(S)-ASA (11) (5.0 mM in dH_2O, gives DHDPA)	50 µl
DHDPR (2.25 x 10^{-4} U, 1.0 x 10^{-4} mg)	10 µl
Inhibitor (appropriate concentration, in methanol if required)	100 µl
	1.00 ml

The *(S)*-aspartate β-semialdehyde was added prior to initiation of the reaction to form the substrate. The reaction was then initiated in the cuvette by addition of DHDPR, mixed by inversion of the cuvettte. ΔA_{340} was measured over 300 seconds at 30 °C, blanked against dH_2O, containing 10% methanol if required. The activity is the rate of reaction with inhibitor present relative to the rate of reaction in the absence of the inhibitor.

Compound	Concentration mM	Activity %
Δ^2-Tetrahydroisophthalic acid (100)	40	79.8
	20	83.6
	10	91.1
	5	78.0
Δ^3-Tetrahydroiophthalic acid (99)	30	15.7
	10	34.0
	5.0	41.7
	1.0	100

IC_{50} (Δ^3-tetrahydroisophthalic acid (99)) ~4 x 10^{-3} M.

References

1. W.H. Perkin, S.S. Pickles *J. Chem. Soc.* **87**, 293 (1905).
2. B.S. Furniss, A.J. Hannaford, P.W.G. Smith, A.R. Tatchell (Eds) *'Vogel's Textbook of Practical Organic Chemistry'* 5th ed., Longman Scientific, England (1989).
3. von L. Ruzika, W. Brugger *Helv. Chem. Acta* **9**, 399 (1926).
4. R. Adams, A.F. Thal *Org. Synth.* Coll. Vol. **I**, 270 (1941).
5. G.A.R. Kon, B.L. Nandi *J. Chem. Soc.* **136**, 1628 (1933).
6. R. Adams, R.M. Kamm *Org. Synth.* Coll. Vol. **I**, 250 (1941).
7. A. Schwartz, P. Madan *J. Org. Chem.* **51**, 5463 (1986).
8. A.D. Abell, M. Brandt, M.A. Levy, D.A. Holt *J. Chem. Soc. Perkin Trans. I* 1663 (1997).

Appendix

Appendix

Enzyme Kinetics and Inhibition

Enzyme kinetics

Major sources

A. Cornish-Bowden *Biochem. J.* **137**, 143 (1974).

A. Cornish-Bowden, C.W. Wharton *'Enzyme Kinetics'* IRL Press, Oxford (1988).

M. Dixon *Biochem. J.* **55**, 170 (1953)

M. Dixon, E.C. Webb *'Enzymes'* 3rd edn, Academic Press (1979).

R. Eisenthal, M.J.Danson (Eds) *'Enzyme Assays. A practical approach'* IRL Press, Oxford (1992).

Enzyme catalysed reaction

The enzyme catalysed reaction converting the substrate to the product is shown in figure A-1.

Figure A-1: Enzyme catalysed reaction

$$E + S \underset{k_{-1}}{\overset{k_1}{\rightleftharpoons}} ES \underset{k_{-2}}{\overset{k_2}{\rightleftharpoons}} E + P$$

fast slow

Steady state occurs when the enzyme is operating at maximum efficiency, that is at enzyme saturation where there is no free enzyme available, see figure A-2.

Figure A-2: Substrate curve

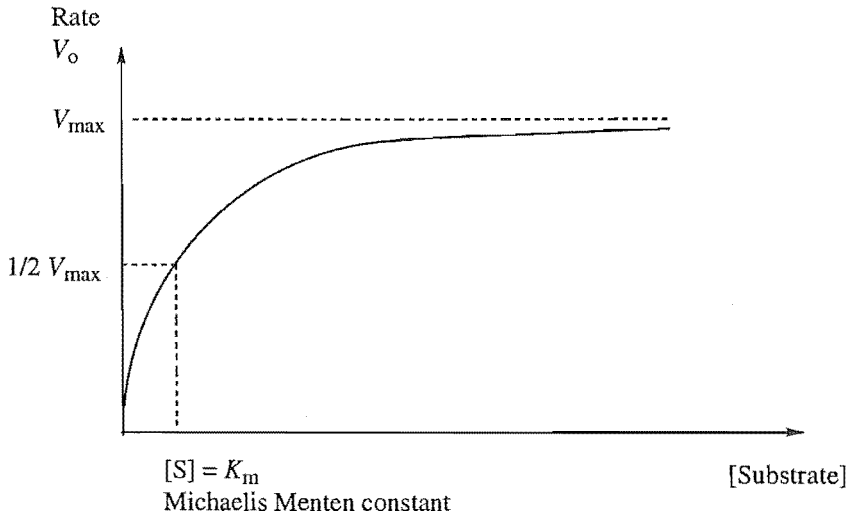

Michaelis-Menten equation

k_{-2} is assumed to be zero.

Rate of formation of ES = k_1[E][S]

$[E]_T$ = total concentration of enzyme

[E] = free enzyme

$[E] = [E]_T - [ES]$

At saturation $V_o = V_{max}$, and there is no free enzyme, [E] = 0

$[E]_T = [ES]$

$[E]_T << [S]$ if there is a very large amount of substrate compared to the amount of enzyme.

Rate of formation of ES = $k_1([E]_T - [ES])[S]$

Rate of breakdown of ES = $k_{-1}[ES] + k_2[ES]$

At steady state the rate of formation of equal to the rate of breakdown.

$k_1([E]_T - [ES])[S] = k_{-1}[ES] + k_2[ES]$

$k_1[E]_T[S] - k_1[ES][S] = k_{-1}[ES] + k_2[ES]$

$[ES](k_{-1} + k_2 + k_1[S]) = k_1[E]_T[S]$

$[ES] = (k_1[E]_T[S])/(k_1[S] + k_{-1} + k_2)$

$[ES] = ([E]_T[S])/([S] + (k_{-1} + k_2)/k_1)$

$k_2[ES] = (k_2[E]_T[S])/([S] + (k_{-1} + k_2)/k_1)$

The conversion of the enzyme substrate complex, ES, to the product and regenerated enzyme, E + P, is the rate determining step.

$V_o = k_2[ES]$

$V_{max} = k_2[E]_T$

$K_m = (k_{-1} + k_2)/k_1$

Michaelis-Menten equation $V_o = (V_{max}[S])/([S] + K_m)$

When rate is half V_{max} ($V_o = 1/2\ V_{max}$)

$1/2\ V_{max} = (V_{max}[S])/([S] + K_m)$

$1/2 = [S]/([S] + K_m)$

$[S] + K_m = 2[S]$

$K_m = [S]$

That is K_m is the substrate concentration when V_o is half V_{max}.

When the substrate concentration is very large the rate is approximately equal to V_{max}.

$V_o = (V_{max}[\text{large S}])/([\text{large S}] + K_m)$

$V_o \simeq (V_{max}[\text{large S}])/[\text{large S}]$

$V_o \simeq V_{max}$

Lineweaver-Burk plot

$V_o = (V_{max}[S])/([S] + K_m)$ Michaelis-Menten equation

$1/V_o = [S]/(V_{max}[S]) + K_m/(V_{max}[S])$

$1/V_o = 1/V_{max} + K_m/(V_{max}[S])$

$1/V_o = (K_m/V_{max})(1/[S]) + 1/V_{max}$

Plot of $1/V_o$ against 1/[S] gives a slope of K_m/V_{max} and a y-intercept of $1/V_{max}$, see figure A-3.

When [S] is very large then $K_m/(V_{max}[S]) \simeq 0$

$1/V_o = 1/V_{max}$

When V_o is very large $1/V_o \simeq 0$

$0 = (K_m/V_{max})(1/[S]) + 1/V_{max}$

$(K_m/V_{max})(1/[S]) = -1/V_{max}$

$1/[S] = -1/K_m$

The x-intercept = $-1/K_m$

Figure A-3: Lineweaver-Burk plot

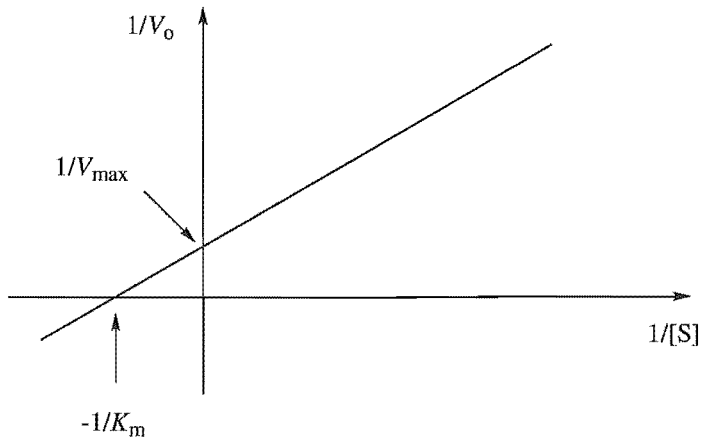

Eadie-Hofstee plot

$1/V_o = (K_m/V_{max})(1/[S]) + 1/V_{max}$ from above

$[S]/V_o = K_m/V_{max} + [S]/V_{max}$

$[S]/V_o = (K_m + [S])/V_{max}$

$V_{max} = V_o/[S](K_m + [S])$

$V_{max} = K_m(V_o/[S]) + V_o$

$V_o = V_{max} - K_m(V_o/[S])$

Plot of V_o against $V_o/[S]$ gives a slope of $-K_m$, the y-intercept is V_{max}, and the x-intercept is V_{max}/K_m, see figure A-4.

Figure A-4: Eadie-Hofstee plot

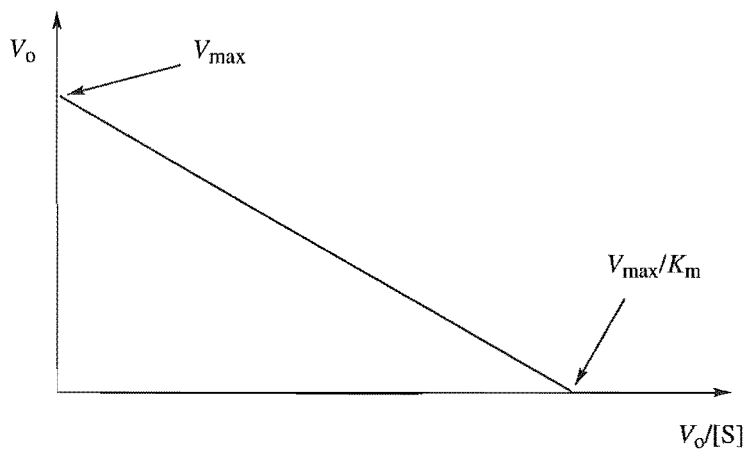

Direct linear plot

$V_o = V_{max} - K_m(V_o/[S])$ from above

$V_{max} = V_o + (V_o/[S])K_m$

V_{max} and K_m are treated as variables and V_o and [S] are treated as constants, so a family of lines is obtained. The line is all possible pairs of K_m and V_{max} that satisfy an observed rate V_o at substrate concetration [S].

V_o is plotted against -[S], the x-intercept is K_m, while the y-intercept is V_{max}.

Each point of intersection provides an estimate of K_m and V_{max}, of which the median is normally quoted, see figure A-5.

Figure A-5: Direct linear plot

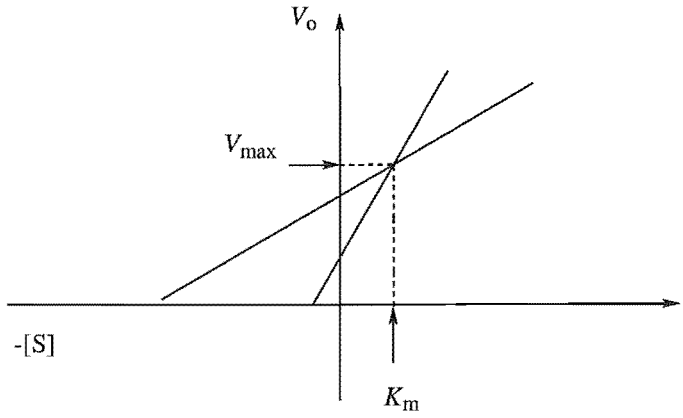

Inhibition kinetics

Irreversible inhibition normally occurs when a covalent bond is formed between the enzyme and the inhibitor, thus altering the kinetics. It also includes mechanism-based inhibitors (so called suicide inhibitors), and transition state analogues.

The other type of inhibition is reversible and is normally divided into four catergories, competitive, noncompetitive, uncompetitive, and mixed inhibition. These catergories are greatly simplified, as true examples are rarely just one type of inhibition.

(i) Competitive inhibition

The inhibitor competes with the substrate to bind to the active site, see figure A-6. The inhibitor can be 'washed out' by increasing the concentration of the substrate. Thus V_{max} stays the same while K_m increases with increasing concentration of the inhibitor. A Dixon plot gives K_i, the dissociation constant of EI, see figure A-9.

Figure A-6: Competitive inhibition

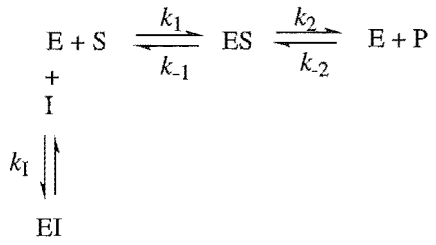

(ii) Noncompetitive inhibition

The inhibitor binds to a site on the enzyme away from the active site altering catalysis but not substrate binding, see figure A-7. Some enzymologists do not include this as a distinct class, as binding at a second site must affect the binding of the substrate, even if this is a very small effect. With noncompetitive inhibition V_{max} decreases while K_m stays constant with increasing inhibitor concentration. Both a Dixon plot and a modified Dixon plot will give K_i, the dissociation constant of EI, which is equal to K_i', the dissociation constant of EIS, see figure A-9.

Figure A-7: Noncompetitive inhibition

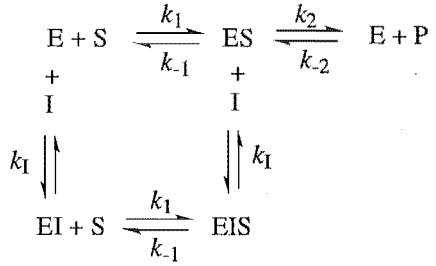

(iii) Uncompetitive inhibition

The inhibitor binds only to the enzyme-substrate complex, see figure A-8. V_{max} decreases with increasing inhibitor concentration, as the enzyme is less catalytically effective. K_m also decreases with increasing inhibitor concentraion, as the inhibitor removes some of the enzyme substrate complex. A modified Dixon plot will give K_i', see figure A-9.

Figure A-8: Uncompetitive inhibition

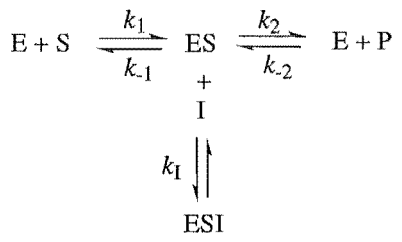

(iv) Mixed inhibition

The inhibitor binds to both the free enzyme and the enzyme substrate complex. The binding of the inhibitor may affect both V_{max} and K_m; V_{max} may decrease and K_m may also decrease, stay the same, or increase. Mixed inhibition is often said to show competitive and uncompetitive effects simultaneously. A Dixon plot will give K_i, the dissociation constant of the EI complex, and a modified Dixon plot will give K_i', the dissociation constant of the EIS complex, where K_i does not necessarily equal K_i', see figure A-9.

Dixon plots and modified Dixon plots for enzyme inhibition

$V_o = (V_{max})/((K_m(1 + ([I]/K_i)) + [S](1 + ([I]/K_i')))$

K_i = the dissociation constant of the EI complex

K_i' = the dissociation constant of the EIS complex

Plotting $1/V_o$ against [I] gives a Dixon plot that estimates K_i.

$[S]/V_o = (K_m/V_{max})(1 + [I]/K_i) + ([S]/V_{max})(1 + [I]/K_i')$

Plotting $[S]/V_o$ aganst [I] gives a modified Dixon plot that estimates K_i'.

Figure A-9: Dixon and modified Dixon plots

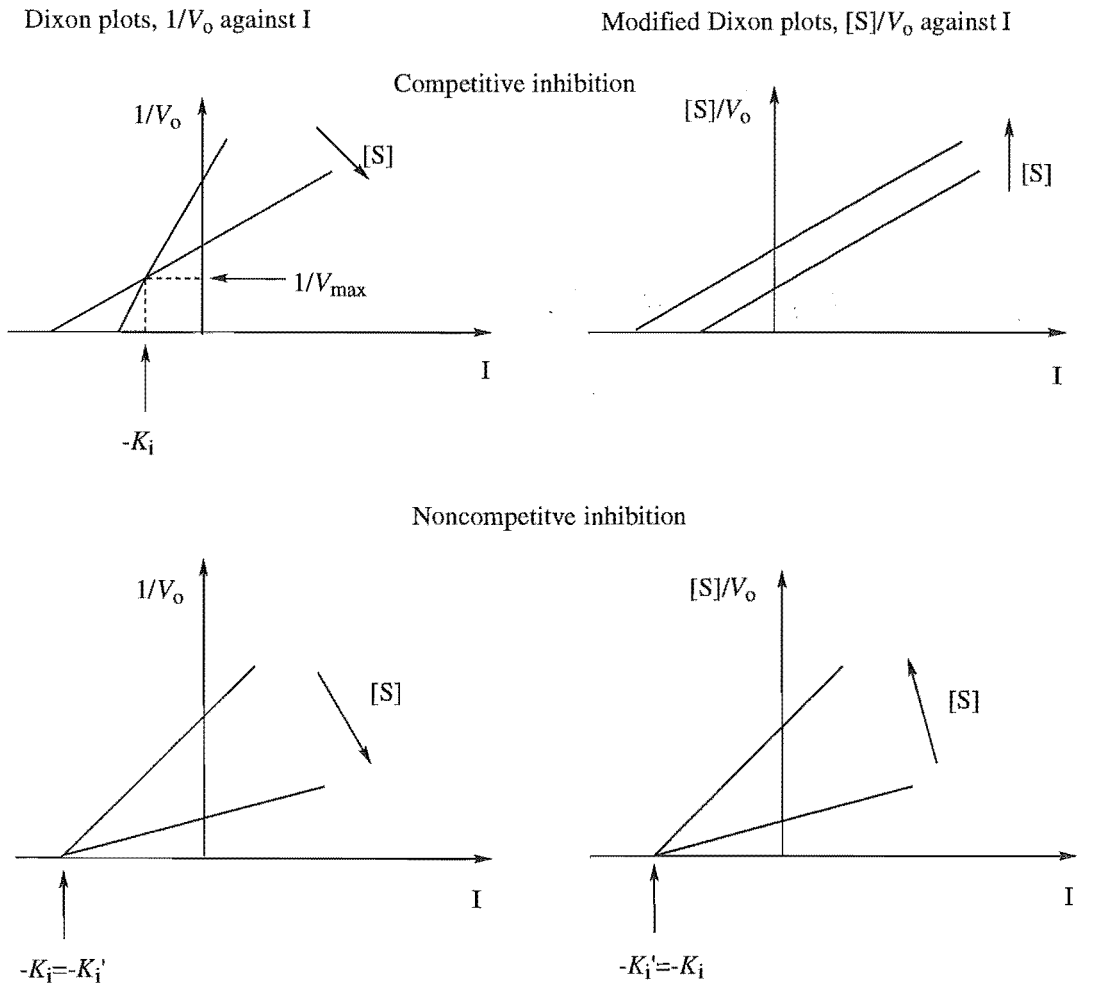

Figure A-9: Dixon and modified Dixon plots, continued

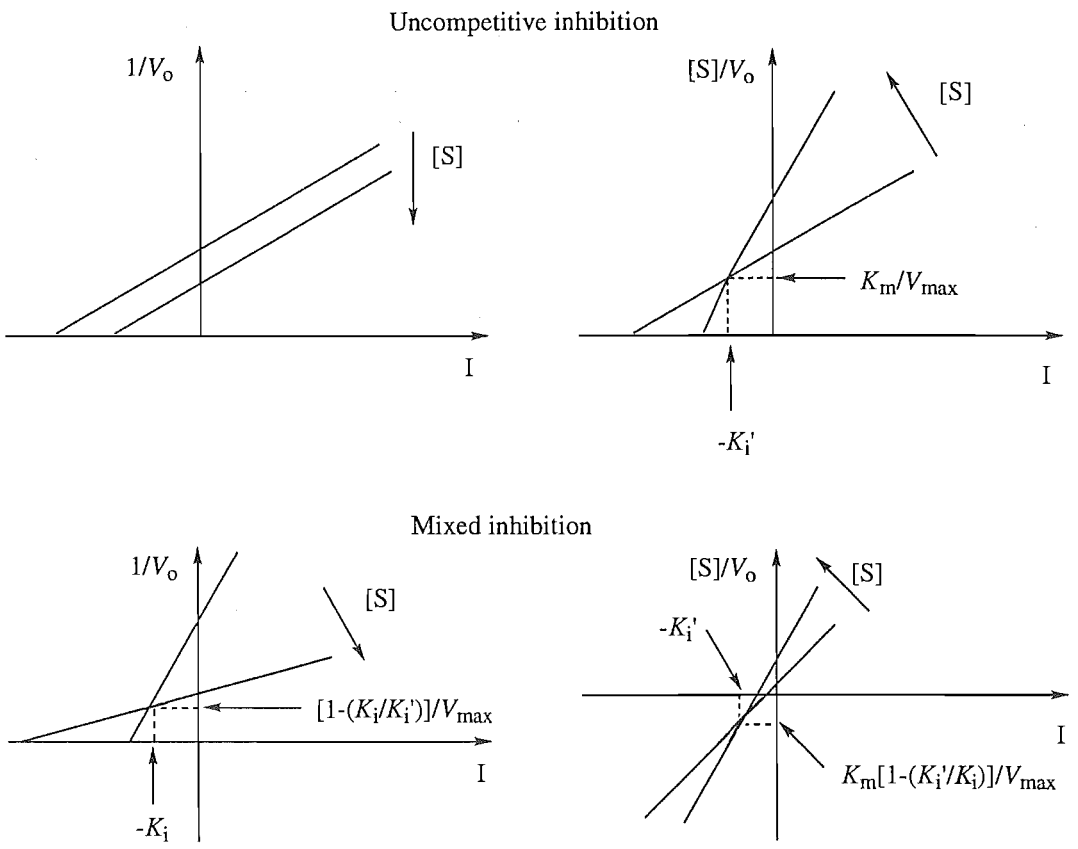

Units used in the kinetic plots

Lineweaver-Burk plot

The substrate concentration is given in M ($mol \cdot l^{-1}$), giving the inverse of the substrate concentration in M^{-1} ($l \cdot mol^{-1}$). The rate is given in $\mu mol \cdot s^{-1} mg^{-1}$, that is the micromoles of substrate turned over per second per milligram of protein. Thus, the inverse of the rate is $mg \cdot s \cdot \mu mol^{-1}$.

Eadie-Hofstee plot

The rate is given in $\mu mol \cdot s^{-1} mg^{-1}$. The rate/substrate concentration has the units of $l \cdot s^{-1} mg^{-1}$. These units come from the rate, in $\mu mol \cdot s^{-1} mg^{-1}$, being divided by the substrate concentration, in M ($mol \cdot l^{-1}$), where the moles cancel leaving $l \cdot s^{-1} mg^{-1}$.

Direct linear plot

For the direct linear plots the rate is given in $\mu mol \cdot s^{-1} mg^{-1}$ and the substrate concentration is given in M ($mol \cdot l^{-1}$).

Dixon plot

The rate is given in $\mu mol \cdot s^{-1} mg^{-1}$, while the inhibitor concentration is given in mM ($mmol \cdot l^{-1}$).

Modified Dixon plot

The rate substrate concentration/rate is given in $s \cdot mg \cdot l^{-1}$, this comes from the substrate concentration, in M ($mol \cdot l^{-1}$), being divided by the rate, in $\mu mol \cdot s^{-1} mg^{-1}$, where the moles cancel leaving $s \cdot mg \cdot l^{-1}$. The inhibitor concentration is given in mM ($mmol \cdot l^{-1}$).